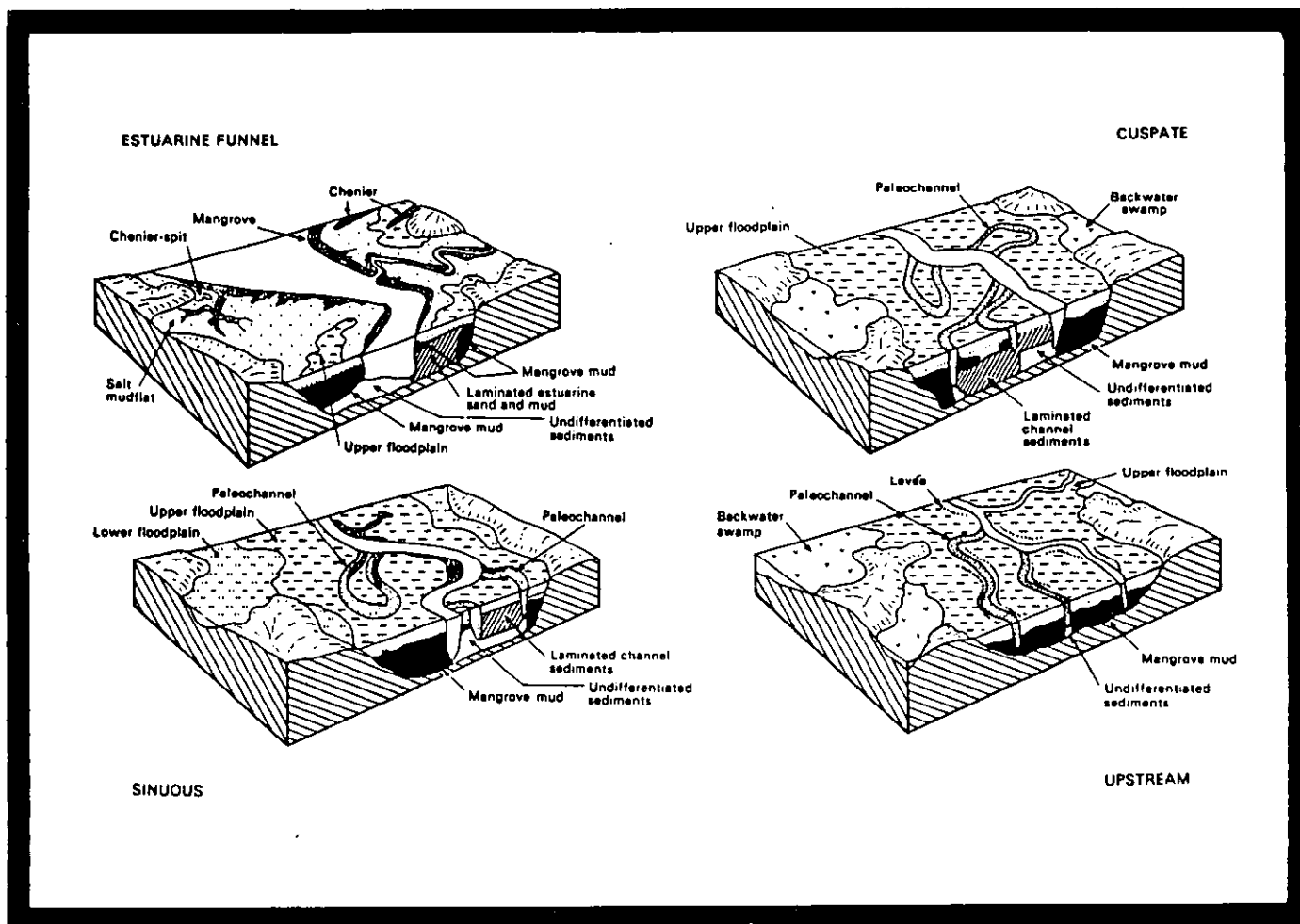
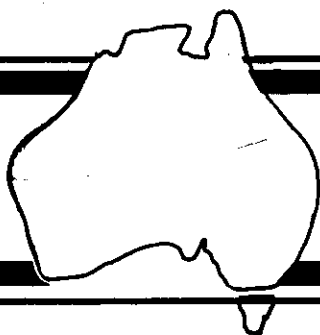




GEOMORPHOLOGICAL DYNAMICS AND EVOLUTION OF THE SOUTH ALLIGATOR TIDAL RIVER AND PLAINS, NORTHERN TERRITORY



C.D. Woodroffe, J.M.A. Chappell, B.G. Thom and E. Wallensky



Australian National University North Australia Research Unit
Mangrove Monograph No. 3
Darwin 1986

DISPLAY COPY

GEOMORPHOLOGICAL DYNAMICS AND EVOLUTION OF THE SOUTH ALLIGATOR TIDAL RIVER AND PLAINS, NORTHERN TERRITORY

C.D. Woodroffe¹, J.M.A. Chappell²,
B.G. Thom³, E. Wallensky²

¹ North Australia Research Unit, Australian National University

² Department of Biogeography & Geomorphology, Australian National University

³ Department of Geography, University of Sydney

Australian National University
North Australia Research Unit
Mangrove Monograph No. 3

First published in Australia 1986

Printed in Australia by the Australian National University

© Australian National University North Australia Research Unit

This book is copyright. Apart from any fair dealing for the purpose of private study, research, criticism or review, as permitted under the Copyright Act, no part may be reproduced by any process without written permission. Inquiries should be directed to the publisher, North Australian Research Unit, Casuarina NT 5792, Australia

National Library of Australia
Cataloguing-in-publication entry

Geomorphological dynamics and evolution of the South
Alligator tidal river and plains, Northern Territory.

Bibliography.
ISBN 0 86784 917 7.

1. Geomorphology - Northern Territory - South
Alligator River Region. I. Woodroffe, Colin D. II.
Australian National University. North Australia
Research Unit. (Series: Mangrove monograph; no. 3).

551.4'5'0994295

ACKNOWLEDGEMENTS

The stratigraphic drilling and geomorphology on which this study is based was funded by the Australian National Parks and Wildlife Service, and has been carried out as part of the larger 'tidal rivers and mangroves' program at NARU supported by a special allocation from the Commonwealth Tertiary Education Commission. Other sources have supported some of the work reported here. The water chemistry surveys are part of a larger component of the NARU program which is funded by a research grant from the NT Commercial Fisherman's Association Trust Fund, and pollen analyses used herein are part of an AMSTAC Marine Sciences and Technologies Grants-supported project into mangrove history in Northern Territory.

We are grateful to Peter Loveday, Field Director, and the staff of the North Australia Research Unit for administrative support and for giving every consideration to needs of the project, and to Jim Toner and Jann King for support from NASS. We also thank the Department of Biogeography and Geomorphology, RSPacS, ANU, for continued support with laboratory services and field equipment. The logistics of field operations were made immeasurably simpler by the use of the CSIRO research facility at Kapalga and we thank Mike Ridpath and Pat Werner for permission to use this and Peter Pan Quee for his help at Kapalga. Dan Gillespie provided access to information collected by ANPWS. We are grateful to the traditional owners of land in the study area for permission to undertake investigations, and to Mick Alderson and Dave Lindner for information on environmental change. We are grateful to the Australian Survey Office, particularly to Tom Reid, for surveys they undertook for us.

Our study would not have been as detailed or as accurate without the expertise of Karl Shaw of Australian Defence Forces Academy in the operation of the drill rig. We are grateful to Kristin Bardsley, NARU, for her help at all stages of planning, data collection, and drafting. PhD scholars in the Department of Biogeography and Geomorphology, John Grindrod and Rob Vertessy, were involved in fieldwork as part of more detailed studies of their own, and we wish to thank them for data that they have made available to us. Jim Davie and Marilyn Ball of NARU were involved in vegetation studies in conjunction with our geomorphological work and have contributed in the field and in discussion to our study. For assistance in the field we thank David Mills, Rob Kazmarek, Jenny Hutson, Rob Mueller, Peter Hartney, Peter Ward, Colin Holbert, Damien Kelleher, David Corp, Janet Harrison, Darren McArley. For laboratory analyses we thank Ian Prosser, Keith Fitchett and Jim Caldwell. Pollen analysis was undertaken by Joan Guppy and Janet Williams.

A major contribution has been made through radiocarbon dating done by the ANU Radiocarbon Dating Laboratory, and we are particularly grateful to John Head, Henry Polach, and Steve Robertson. The results of this study would not have been produced without their work, which represents a large commitment by the laboratory.

The figures in this volume were drawn by Ian Hayward, and the geomorphological map sheets were drawn by Nigel Duffey. The large task of typing and editing drafts and the final manuscript was undertaken by Janet Sincock.

CONTENTS

Acknowledgements	iii
List of Tables	viii
List of Figures	ix
Two Coloured Maps	Loose, unbound
1. Environmental Setting	3
1.1 Geology	3
1.2 Topography	3
1.3 Climate and Hydrology	6
1.4 Vegetation and Soils	12
1.5 Late Quaternary Depositional Context	17
2. Estuarine Morphodynamics	25
2.1 Nearshore Wave Regime	25
2.2 Tidal Behaviour, Dry and Wet Seasons	28
2.3 Yearly Cycles of Salinity and Water Chemistry	32
2.4 Sediment Movement in the Tidal River	40
2.5 Bank and Creek Stability	43
3. Geomorphology	49
3.1 Methods	49
3.2 Morphologic Patterns	49
3.2.1 Coastal Plain	52
3.2.2 Deltaic-estuarine Plain	54
3.2.3 Alluvial Plain	65
3.3 Morphologic Processes and Change	66

4.	Stratigraphy	75
4.1	Methodology	75
4.1.1	Field Methods	75
4.1.2	Laboratory Methods	75
4.2	Stratigraphic and Morphostratigraphic Concepts	78
4.3	Stratigraphic and Morphostratigraphic Units	79
4.3.1	Morphostratigraphic Group	81
4.3.2	Stratigraphic Group	83
4.4	Stratigraphic Patterns	84
4.4.1	General Pattern	84
4.4.2	Stratigraphy of the Coastal Plain	85
4.4.3	Stratigraphy of the Estuarine Funnel	87
4.4.4	Stratigraphy of the Sinuous Meandering Segment	90
4.4.5	Stratigraphy of the Cuspate Meandering Segment	96
4.4.6	Stratigraphy of the Upstream Segment	104
4.4.7	Summary	113
5.	Depositional History and Evolutionary Model	117
5.1	Models of Tidal River and Plains Evolution	117
5.1.1	Alternative Models for Holocene Development of Deltaic-estuarine Plains	117
5.1.2	Alternative Models for Channel Change	119
5.2	Transgressive Phase, 8000-7000 years B.P.	122
5.2.1	Sea-level rise relative to South Alligator area	125
5.3	Big Swamp Phase, 6800-5300 years B.P.	127
5.3.1	Mangrove Succession in Big Swamp Times	127
5.4	The Sinuous River Phase, 4000-2500 years B.P.	130
5.5	The Cuspate River Phase	139

6.	Morphodynamics over the last 6000 years	143
6.1	Comparison of the South Alligator and other rivers	143
6.2	Tidal changes during evolution of the South Alligator	146
6.3	Changing patterns of sedimentation	149
7.	Summary and Conclusions	157
7.1	Concluding review	157
7.2	Recommendations	158
	References	161
	Appendices	
A1	Estimation of South Alligator floodwater discharge	171
A2	Tide modelling	173
A3	Seasonal salinity modelling	176
A4	Particle size analysis of selected samples	178
A5	Salt concentration (KCl equivalents), parts per thousand (sediment dry weight)	180
A6	Pollen analysis of mangrove history	181
A7	Carbonate content of selected samples as a percentage of sediment dry weight	182
A8	Radiocarbon dates	183
A9	Details of depth, elevation with respect to AHD and age of samples used for sea-level plot (Figure 69)	190

List of Tables

1	Vegetation communities in the Alligator Rivers region and the terms used to describe them by several authors	13
2	Significant winds and predicted waves	26
3	Dry season mean tidal parameters spring tides \pm 3 days	29
4	Principal morphologic units of coastal, deltaic- estuarine and alluvial plains	58
5	Comparison of Morphologic units with CSIRO land systems and geological map equivalents	61
6	Main characteristics of stratigraphic and morphostratigraphic units	80
7	Big swamp fossil stump sites; species recorded and their age	129
8	Composition and age of middens on South Alligator plains	135
9	Comparisons between South Alligator, Adelaide and Daly rivers	145
10	Comparisons of present and paleo South Alligator Rivers and Adelaide River, tidal parameters	147
11	Sedimentation during different phases of the South Alligator system	153

List of Figures

1	Geology of the Alligator Rivers Region	4
2	Topography of the South Alligator River catchment	5
3	Denudational surfaces and their relation to topography of the South Alligator River	6
4	Annual rainfall at Oenpelli	6
5 a	Pattern of summer rainfall across North Australia	8
b	Pattern of rainfall within the South Alligator River catchment	8
6 a	Mean monthly Rainfall at Oenpelli (P)	9
b	Mean monthly water balance, at Oenpelli	9
c	Mean monthly soil moisture storage at Oenpelli	9
7	Return period and excedence probabilities versus discharge Daly River and South Alligator River	10
8 a	Monthly runoff characteristics of the Daly River	11
b	February and March total discharges in relation to gross rainfall, Daly River	11
9	Soil and vegetation catenary sequence from lateritic uplands to estuarine plains	12
10	Vegetation communities in the South Alligator River region	14
11	Distribution and composition of mangrove communities along the South Alligator River	16
12	Reconstruction of the prior valley of the South Alligator	18
13	Sea-level characteristics from eastern Australia, for the last 20,000 years	20
14 a	Summary of climatic trends in North Australia during the late Quaternary	21
b	Approximate location of shoreline 18,000 and 10,000 years ago	22
c	Maximum hypothesized rainfall isohyets, 18,000 years ago	22
15	Bathymetry of van Diemen Gulf	27
16	Map of South Alligator River channel and width relationships with distance from the mouth	30
17	Observations on tidal height and current velocity at three stations on the South Alligator River	31
18	Cross-sectional velocity structure during flood and ebb maximum velocities at 47 and 63km from the river mouth	33
19	Longitudinal discharge profile, South Alligator River	34
20	Salinity change in the South Alligator River through the dry season	35

21	Inorganic water chemistry, South Alligator River: wet season	36
22	Wet and dry season vertical circulation and mixing in the South Alligator River	38
23 a	Organic water chemistry, South Alligator River: wet season	39
b	Organic water chemistry, South Alligator River: dry season, 1984	39
24	Particle size characteristics of river bed samples and overbank sediments	40
25	Observations of suspended sediment along the South Alligator River	41
26	Detailed survey of morphology and bedforms of a mid-channel shoal, South Alligator River	42
27 a	Eroding, accreting and neutral (or indeterminate) banks of the South Alligator River	44
b	Bank erosion or accretion from aerial photographs	44
28	Definition of Australian Height Datum and its relation to surveys along the South Alligator River	50
29	Morphologic provinces of the South Alligator River	51
30	Coastal plain on the east side of the South Alligator River mouth	53
31	Schematic tidal river of the Northern Territory type showing characteristics of different river segments	55
32	Cross-sectional traverses showing relationships between morphologic units and elevation at various points along the river	57
33	Detail of Lower and Upper Floodplain units on west bank of South Alligator River, about 15km upstream from mouth	63
34	Detail of sinuous river bend 47 km upstream from mouth	64
35	Detail of morphologic units at Bullocky Point about about 60 km upstream of river mouth	64
36	Transition from tidal river (deltaic-estuarine province) to alluvial plain	65
37 a	The elevational range of Upper and Lower Floodplain along the South Alligator River	67
b	The elevational range of mangroves along the South Alligator River	68
38	Map of recent channel changes and tidal creek extension from aerial photography	71
39	The location of drillholes SAH 1 to SAH 131, the numbering of transects, and the location of short cores, South Alligator River	76

40	Particle size characteristics of laminated channel sediments, channel fill and mangrove mud	82
41	Stratigraphy of Transect 1, Coastal plain and tentative isochrons of coastal progradation	86
42	Stratigraphy of Transect 2, estuarine funnel	88
43	Stratigraphy of Transect 3, estuarine funnel and tentative isochrons of coastal progradation	89
44	Schematic stratigraphy of Transect 4, sinuous meandering segment	91
45	Stratigraphy of Transect 5, sinuous meandering segment	92
46	Stratigraphy of Transect 6A, sinuous meandering segment	93
47	Stratigraphy of Transect 6B, sinuous meandering segment	94
48	Block diagram showing stratigraphic relationships in the Apple Tree Bend and Rookery Bend region of the sinuous meandering segment	95
49	Detailed map of morphostratigraphic units and drillholes in the Bullocky Point area	96
50	Stratigraphy of Transect 7, Bullocky Point, cusate meandering segment	97
51	Stratigraphy of Transect 8A, Bullocky Point, cusate meandering segment, and tentative isochrons of channel migration	98
52	Block diagram showing schematic interpretation of channel migration in the Bullocky Point area	100
53	Stratigraphy of transect 8B, opposite Bullocky Point, cusate meandering segment	101
54	Stratigraphy of Transect 9A, cusate meandering segment	102
55	Stratigraphy of Transect 9B, cusate meandering segment	103
56	Stratigraphy of Transect 10, cusate meandering segment	104
57	Stratigraphy of Transect 11, upstream segment	105
58	Stratigraphy of Transect 12A, upstream segment	106
59	Stratigraphy of Transect 12B, upstream segment	107
60	Stratigraphy of Transect 13A, upstream segment	108
61	Stratigraphy of Transect 13B, upstream segment	109
62	Stratigraphy of Transect 14, Leichhardt Billabong, Alluvial plain	110

63	Block diagram showing interpretation of stratigraphic relationships in the vicinity of Transect 10	111
64	Block diagrams summarising morphologic and stratigraphic relationships in the estuarine funnel, sinuous meandering, cusped meandering and upstream sections of the river	112
65	Three alternative models of Holocene estuarine sedimentation	118
66	Location of samples and radiocarbon dates on buried mid-Holocene mangrove facies recorded in drillholes and river bank exposures	120
67	Two models of channel migration on the deltaic estuarine plains	121
68	Distribution and radiocarbon dates on channel fill and laminated channel sediments in the deltaic-estuarine plains	123
69	Age-depth plot of radiocarbon dates on mangrove material, indicating relative sea-level change, South Alligator River	124
70	Map of the distribution of environments recorded (and inferred) 7000 years B.P.	126
71	Map of the distribution of environments recorded and inferred) 6500-6000 years B.P., during the big swamp phase	128
72	Pollen diagram of core SAH 40	131
73	Pollen diagram of drillhole SAH 67	132
74	Distribution and age of middens on the South Alligator plains	134
75	Bullocky Point, distribution of shallow subsurface sediments and radiocarbon dates	136
76	Paleochannels and radiocarbon ages of their margin and fill deposits	137
77	Paleochannels in the deltaic-estuarine plains of the South Alligator River, and their width/depth relationship	138
78	Shallow stratigraphy revealed in bank exposures, and radiocarbon ages of deposits cut or adjacent to banks of present river	140
79	Channel segments of Adelaide, South Alligator and Daly Rivers	144
80	High spring tide and mean water levels along the South Alligator, Adelaide and paleo South Alligator rivers	148
81	Reconstruction of isochrons of coastal progradation in the estuarine funnel of the South Alligator River	150

Chapter 1

Environmental Setting

- 1.1 Geology
- 1.2 Topography
- 1.3 Climate and Hydrology
- 1.4 Vegetation and Soils
- 1.5 Late Quaternary Depositional Context

1. ENVIRONMENTAL SETTING

1.1 Geology

The South Alligator River drainage system conforms to a pre-Tertiary structural basin, termed the South Alligator trough, a secondary tectonic depression associated with the Lower Proterozoic Pine Creek Geosyncline. It probably has not changed its overall drainage pattern significantly since the Tertiary (Williams 1969a; 1969b). The valley occupied by the lower course of the river is filled with Holocene sediments, forming a broad floodplain (Figure 1).

The general geology is described by Dunn (1962), Needham et al. (1973); Galloway (1976) and Needham (1984). As noted by Galloway (1976), Lower Proterozoic rocks intruded by granite and dolerite occupy the western and north-eastern parts of the drainage area. Middle Proterozoic sandstone with interbedded volcanics form the rugged Arnhem Land plateau in the east. Patches of Mesozoic sediments occur in the south. Cainozoic sand, alluvium and deep weathering zones cover much of the older rocks in the west and north (Figure 1).

1.2 Topography

The north and northwestern coast of Australia has a number of large river systems draining the hinterland and dissecting the northern lateritic plains (Christian and Stewart, 1953). The South Alligator River system is one of the larger of these rivers with a catchment area of about 9000 km². The low gradient of the lateritic plains, coupled with the large tidal range, 5-6 m at springs in the Alligator Rivers region, causes the tidal influence to penetrate approximately 105 km up the river system. Due to pronounced seasonality of climate, the hydrology of the river is entirely different between the dry season and wet season. In the dry season the freshwater discharge is low, becoming less as the season advances, until in August or September it ceases to flow. The tidal reach of the river becomes well-mixed and increasingly saline during the dry season. In the wet season commencing December, the river experiences freshwater discharges rising to peak flow of about 400-700 cumecs (see section 1.3) and extensive flooding occurs over the adjacent plains. A salt wedge develops in the estuary which becomes floodwater-dominated until March or April.

Most of the catchment is drained by the South Alligator River plus its major right-bank tributaries Fisher Creek, Koolpin Creek, Barramundi Creek, Jim Jim Creek and Nourlangie and Deaf Adder Creek (Figure 2). The upper reaches of these rivers flow across the Arnhem Land plateau in either shallow valleys or deep gorges; there are numerous waterfalls and little or no alluvium. The middle reaches cross the western lowlands in braided channels with extensive freshwater swamps, numerous waterholes and sandy levées (Galloway, 1976). The lower reaches are tidal with single wide meandering channels flowing across clay plains. Regional topography is shown in Figure 2.

Williams (1969b) and Galloway (1976) have discussed the geomorphic history of the landscape in the drainage basin of the South Alligator River and other rivers flowing into van Diemen Gulf. Several stages are recognised in the formation of the landscape including:

- (a) Formation of the sub-Cretaceous land surface;
- (b) Formation of the older weathered land surface which essentially is restricted to headwater areas of Cretaceous rocks;

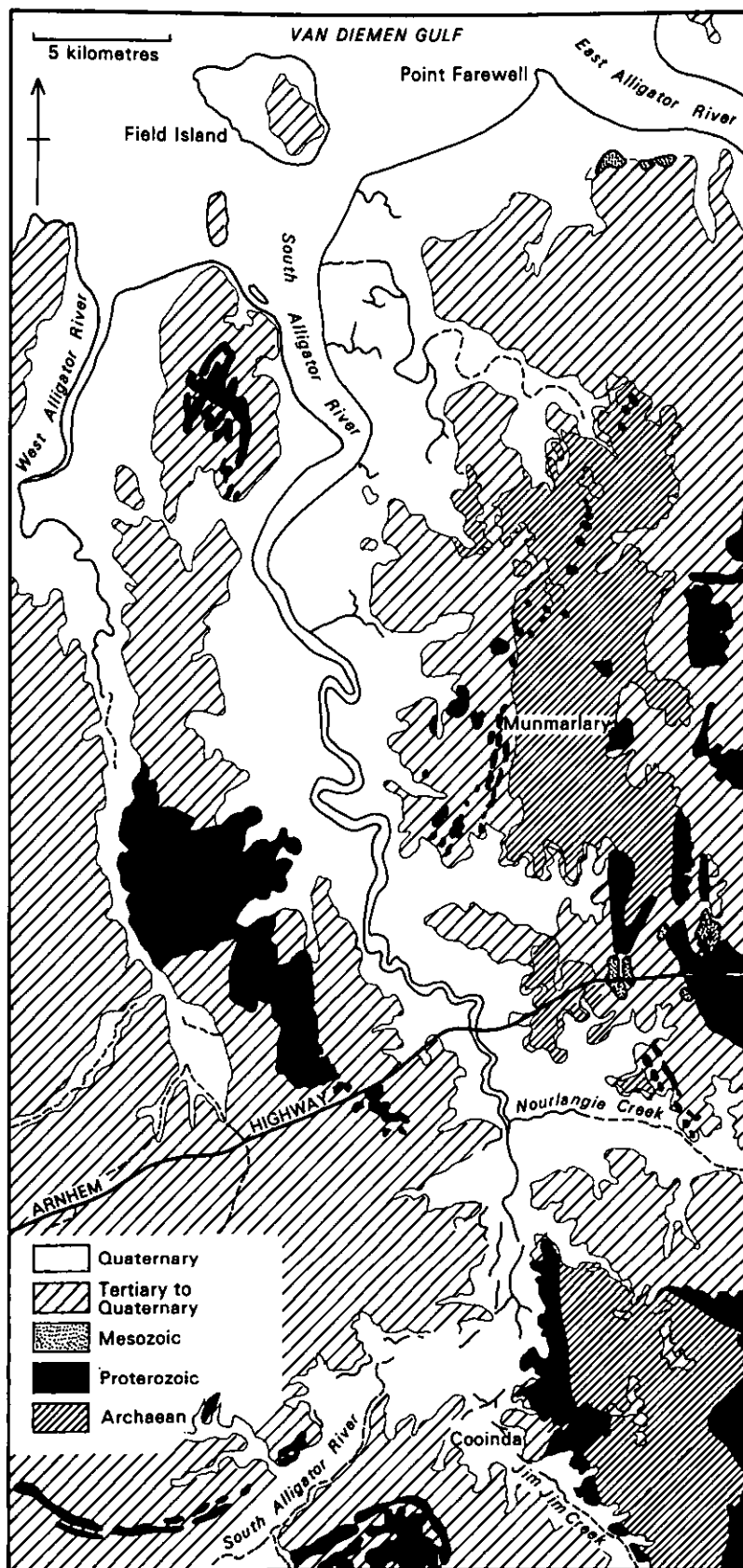


Figure 1: Geology of the lower South Alligator River. Most of the land marked as Quaternary has Holocene sedimentary cover

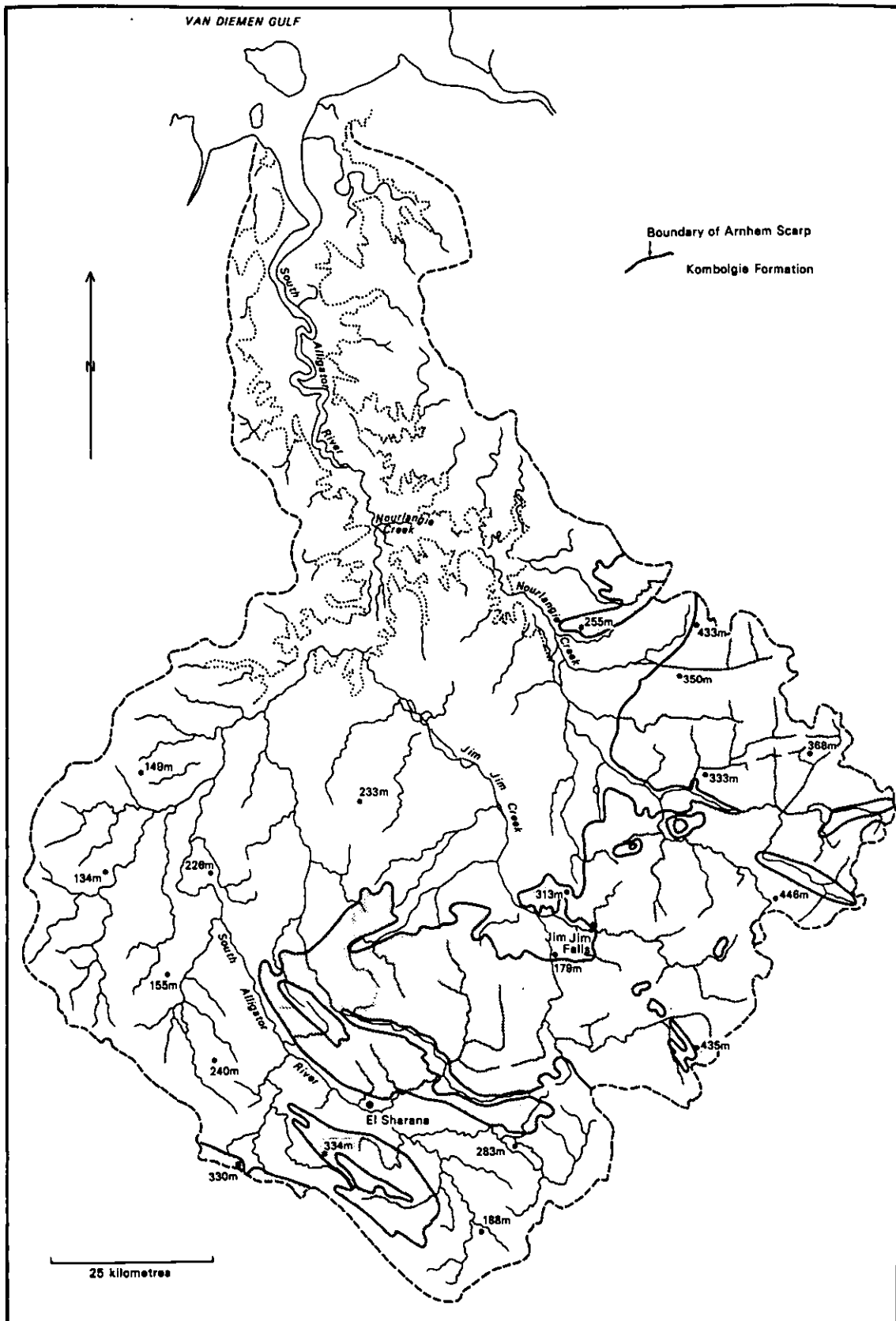


Figure 2: Topography of the South Alligator catchment, showing the main tributaries. The plains are outlined by a dotted line.

- (c) Dissection of the older weathered surface and formation of the younger weathered land surface, which extends over much of the plateau hinterland;
- (d) Late Tertiary dissection to produce the bedrock land surface of the present catchment;
- (e) Quaternary alluviation in lower reaches of the valleys and along the coast.

This report is focussed on the late Quaternary deposits of the tidal reach of the South Alligator River, which are described in detail in Chapters 3 and 4. However, for contextual reasons, the surfaces associated with these older stages of landscape history are shown schematically in Figure 3.

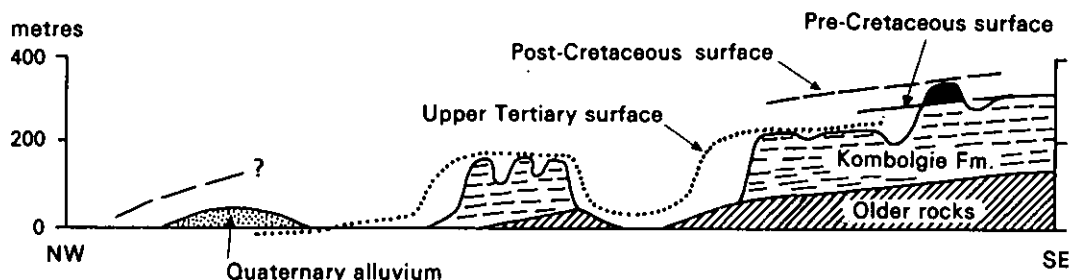


Figure 3: Denudational surfaces and their relation to topography of the South Alligator River, indicating older stages of landscape history (Sources: Williams 1969b and Galloway, 1976).

1.3 Climate and Hydrology

The climate of the Alligator Rivers area of the Northern Territory has been previously described within a broad regional context by Christian and Stewart (1953), Anon. (1961) and McAlpine (1969, 1976). Oenpelli, with 75 years of rainfall and temperature records, is taken as the best station to represent the lower South Alligator region.

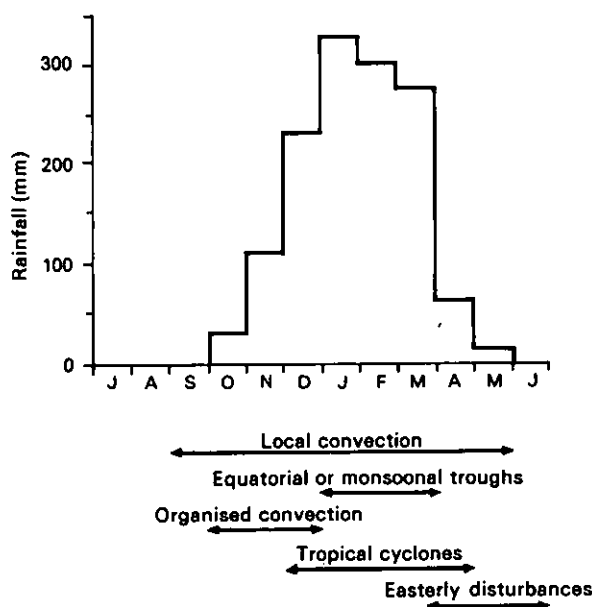


Figure 4: Annual rainfall at Oenpelli, and the five categories of rainfall-producing system (after Southern, 1966)

Two distinct seasons occur in the area, an almost rainless dry season from May to September and a wet season from November to March. Southern (1966), in discussing rainfall types, differentiates between organised rainfall, typified by monsoonal or cyclonic weather and widespread convection, and non-organised rainfall, typified by apparent random or mesoscale convection. He distinguishes five categories of rain-producing systems, i.e., local convection, organised convection, monsoonal troughs, tropical cyclones, and easterly disturbances. The occurrence of these types through the year is shown in Figure 4. The climax of the wet season, December to March, is the period when monsoonal troughs and tropical cyclones are important.

The rainfall regime of the area has three major characteristics: it is highly seasonal, it is reliable (on the basis of annual or even monthly totals) and in average terms does not appear to vary greatly in seasonality or amount from place to place (McAlpine, 1976; Taylor and Tulloch, 1985). The coefficient of variation, being the standard deviation of the rainfall over a series of years divided by the mean, is a measure of rainfall reliability (the lower the figure the greater the reliability). On an annual basis, coefficient values of 0.21 at Oenpelli (McAlpine 1976) and around 0.26 for other stations including Katherine (Chappell and Bardsley, 1985) indicate fair reliability. The lowest decile value at Oenpelli (1007 mm) is more than half the highest (1749 mm; McAlpine 1976). The annual rainfall pattern over north Australia, and within the catchment of the South Alligator River are shown in Figure 5. Variation is high on a daily basis, however, both at and between stations. Data given by McAlpine (1976) show that 41 per cent of the days through the wettest months at Oenpelli (January through March) have zero rain, while 1.7 per cent of the days receive more than 75 mm. The correlation between daily falls at stations near the catchment (Katherine and Douglas-Daly) is insignificant and is low even on a monthly basis (Chappell and Bardsley, 1985).

Temperature and wind data are given in detail by McAlpine (1976). Mean monthly temperature varies from 24.6°C in July to 30.2°C in November. Extremes typically are as much as 10°C higher and more than 10°C lower than the means (Oenpelli data). Wind data from Jabiru show strong easterly flow during the winter months and less strong east to north winds during the wet season. Wind data are summarised in Table 2 (next chapter), in conjunction with nearshore wave climate.

The annual cycle of rainfall, temperature and evaporation combine to yield the water balance relationship which is critical to our understanding of wet season growth and dry season desiccation. Figure 6 summarises the water balance data. Mean monthly rainfall (P) at Oenpelli given by McAlpine (1976) is shown in Figure 6a. Estimates of mean monthly evaporation (E), calculated by McAlpine (1976) using the method of Fitzpatrick (1963), are subtracted from P to give the figures for P-E graphed in Figure 6b, showing that an excess of rainfall over evaporation exists only from December to March. September is the month with the highest water deficit, of -240mm. The cumulative water balance, being the running sum of P-E starting from the first positive month (December), is shown in Figure 6c. The cumulative balance has its peak near the end of March and reaches its greatest deficit in November. Soil moisture storage, calculated from Oenpelli data by McAlpine (1976), is also shown in Figure 6c and resembles the mean monthly P-E figures more closely than the cumulative data.

On the basis of the soil moisture curve, McAlpine (1976) estimates that the average duration of useful 'pasture' growth (e.g. grasses) is about 25 weeks, and may range from 17 weeks in the driest year to 39 weeks in the wettest. The cumulative P-E curve indicates that open water bodies will go to net loss from about June.

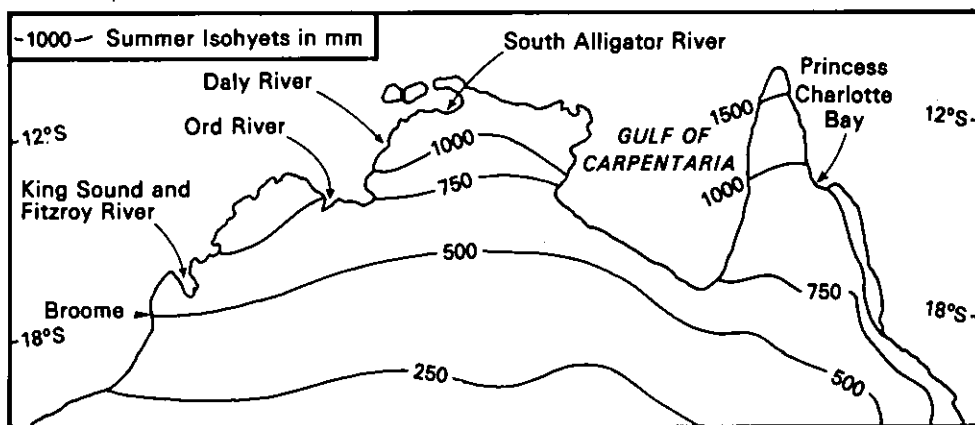


Figure 5a: Pattern of summer rainfall across North Australia

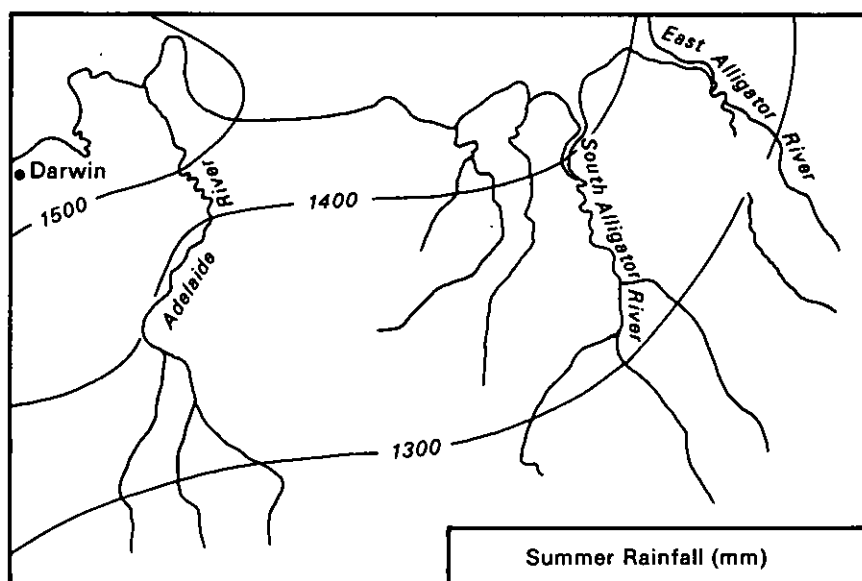


Figure 5b: Pattern of rainfall within the South Alligator River catchment (Sources: Anon 1961, McAlpine 1969).

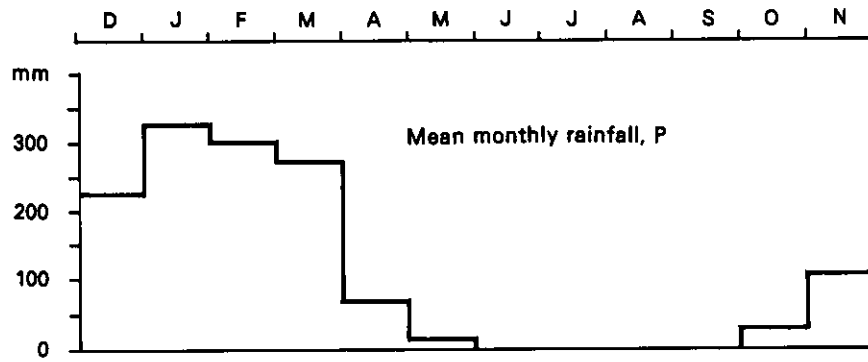


Figure 6a: Mean monthly rainfall at Oenpelli (P)

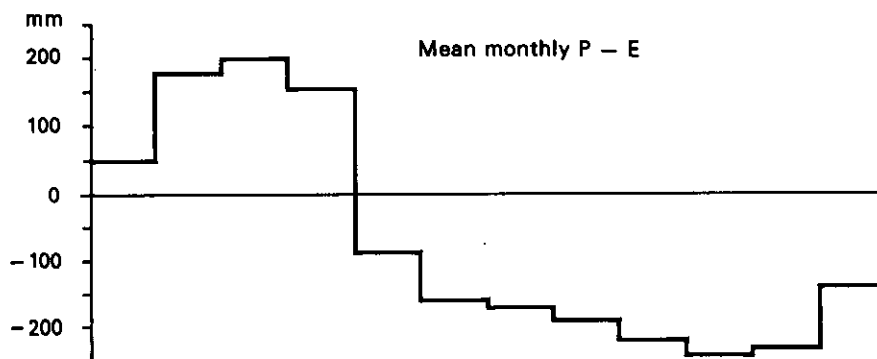


Figure 6b Mean monthly water balance, P-E (evaporation; Fitzpatrick method; see McAlpine, 1976) at Oenpelli

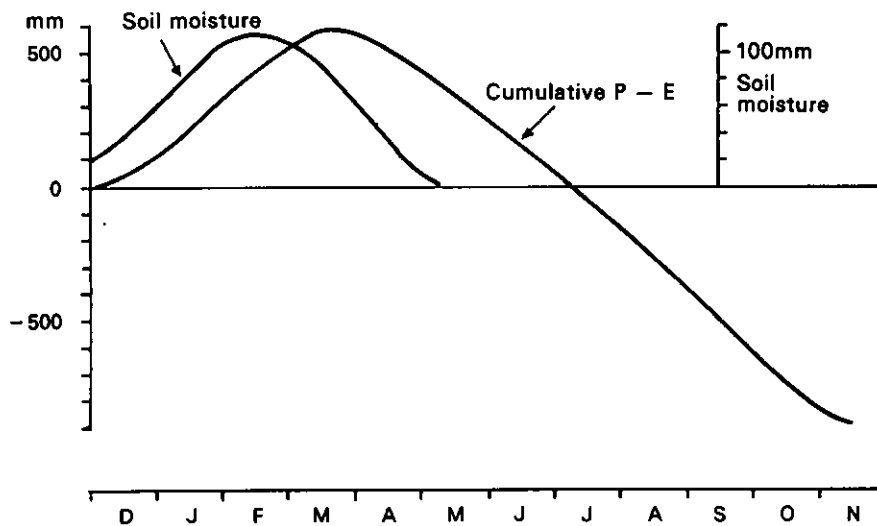


Figure 6c: Mean monthly soil moisture storage at Oenpelli (McAlpine, 1976), and cumulative P-E curve

Hydrology of the lower South Alligator River cannot be estimated directly as the numerous tributaries entering through plains and wetlands (Figure 2) make gauging impracticable. Freshwater flow develops during the wet season and virtually ceases by June. Flood discharges are estimated here using the Daly River as an analogue. The Daly River draws on a roughly similar, though much larger, catchment and is accurately gauged at Mt. Nancar (N.T. Water Division gauge 814040). The rainfall regime is similar to that of the South Alligator River. Flood discharge to recurrence interval relationships at Mt Nancar for 28 years are given by Power *et al.* (1983) and Chappell and Bardsley (1985). Using the methods given in Appendix A1, the Daly River results are scaled down to the South Alligator catchment, and are plotted on a log-Pearson type III graph in Figure 7. Due to uncertainties introduced by scaling, Figure 7 should be taken as a guide only. The graph shows, for example, that flows between 400 and 700 cubic metres/second (cumecs) have a likely return period of 2 years, while 1100 to 2000 cumecs has an average return period around 10 years.

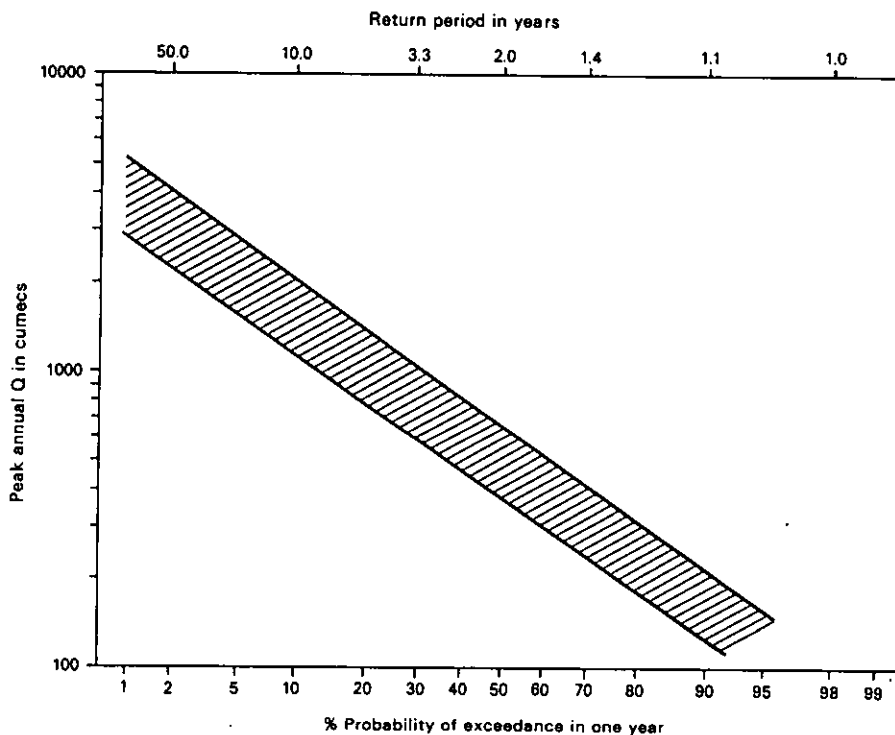


Figure 7: Return period and exceedence probabilities versus discharge, estimated for the South Alligator River by rescaling Daly River data (see Appendix A1).

Runoff efficiency increases through the wet season, apparently as the soil moisture and cumulative P-E indices increase. Total water balance data for Daly river show runoff increasing from about 2 per cent of rainfall in December to about 30 per cent in March (Figure 8). The South Alligator catchment is expected to behave similarly. Additionally, the quantity of runoff increases faster than total wet season rainfall. Figure

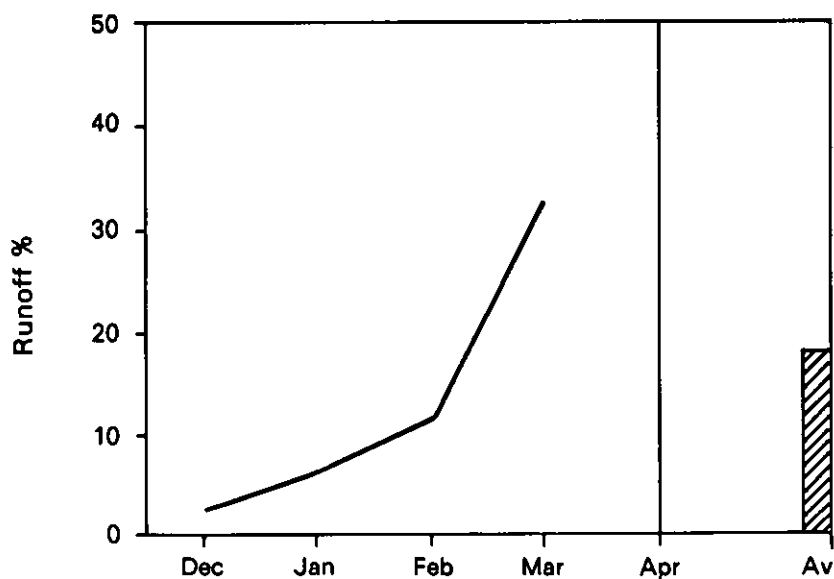


Figure 8a: Monthly runoff characteristics of the Daly River (after Chappell and Bardsley, 1985)

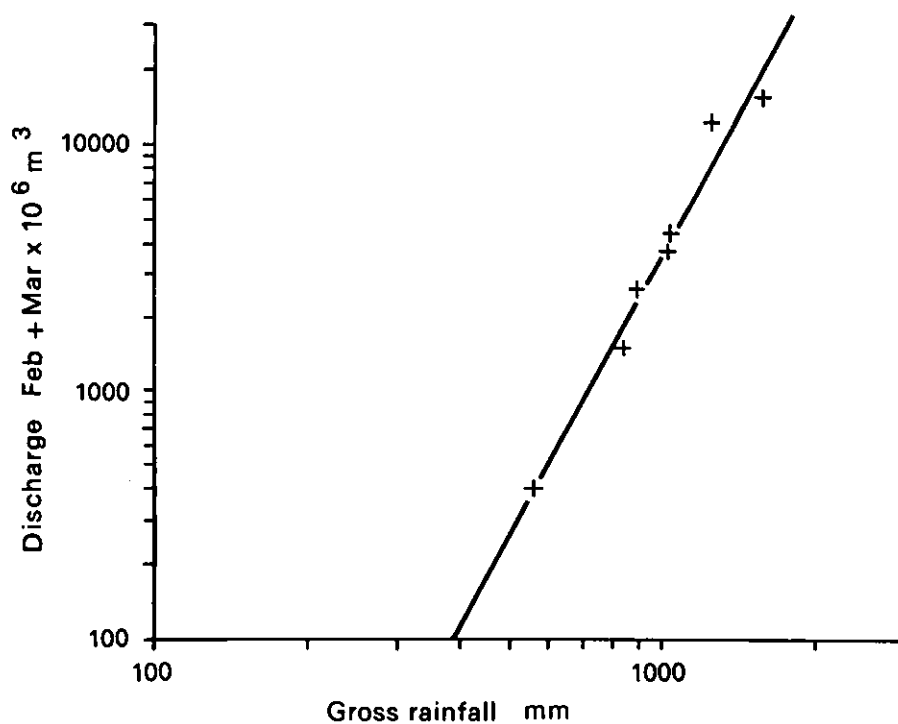


Figure 8b: February and March total discharges in relation to gross rainfall, Daly River (7 sample years, after Chappell and Bardsley, 1985)

8 plots wet season rainfall (P) against total discharge for February and March (Q_{FM}) for the Daly River, for 7 years with complete records. The relationship is

$$Q_{FM} = 1.63 \times 10^{-8} P^{3.78},$$

showing that discharge increases nearly as the fourth power of rainfall, presumably because greater soil and shallow groundwater storage in wet years facilitates much higher runoff efficiencies than in dry years (Chappell and Bardsley, 1985). It is noted that this relationship cannot be true for very high rainfalls because the fourth power relationship implies some level beyond which discharge exceeds rainfall input. It is expected that the relationship changes when runoff efficiency is high, approaching Q_{FM} proportional to P. However, these results show that flood discharge is inherently much more variable than rainfall.

1.4 Vegetation and Soils

Vegetation and soils of the area have been mapped during CSIRO studies of land systems of the region (Story et al., 1969; Story et al., 1976). Figure 9 depicts the general vegetation-soil types adjacent to and on the floodplain of the South Alligator River (Aldrick, 1976). This catenary sequence occurs widely in the study area crossing several of the land systems defined by Story et al. Our morphologic units expand on the CSIRO land systems and comparisons are described fully in section 3. Table 1 includes a list of CSIRO land systems which occur in the floodplain/coastal region. Figure 10 shows the distribution of major vegetation types in the study area. Different authors have used different terms to describe vegetation communities and their descriptive terminology is summarised in Table 1.

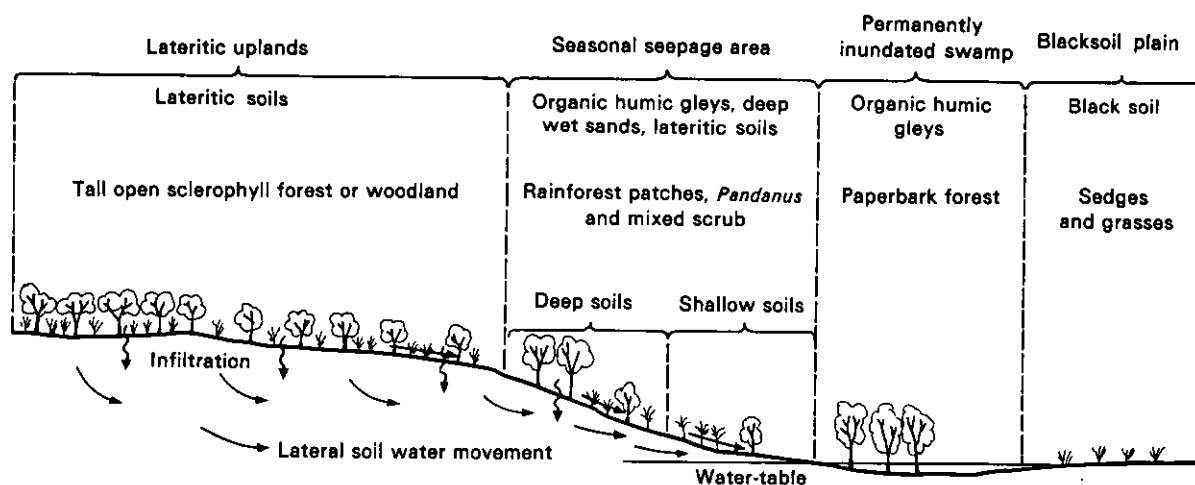


Figure 9: Soil and vegetation catenary sequence from lateritic uplands to estuarine plains (after Aldrick 1976)

Much of the northern lateritic country (Koolpinyah Land System) is covered by tall open eucalypt forest or eucalypt woodland. Two species, *Eucalyptus tetrodonta* and *E. miniata* are dominant; particular stands of tall open forest or woodland being dominated by one or other of the species more often than by a mixture of the two species. Open eucalypt forest and eucalypt woodland are not distinct in their floristic compositions, and ordination techniques have not always distinguished them unambiguously (Burgman and Thompson, 1982; Rice and Westoby, 1985). In Figure 10 mapping

Table 1

Vegetation communities in the Alligator rivers region
and the terms used to describe them by several authors

Story, 1969, 1976	CSIRO Land Systems typically containing vegetation communities (Story et al. 1969, 1976)	Williams, 1979	Burgman and Thompson, 1982	Taylor and Dunlop, 1985	In this study (Figure 10)
Tall/Mixed Open forest	Jay, Kay, Knifehandle Kysto, Queue	-	<u>Eucalyptus miniata</u> types/mixed eucalypt 3	<u>Eucalyptus</u> forest	Tall open forest
Woodland/Stunted woodland	Baker, Bend, Jay, Knifehandle, Kysto, Queue	-	Mixed eucalypt 1 and 2	<u>Eucalyptus</u> woodland	Woodland
Rainforest/ Semi-deciduous forest	Kosher	-	-	Lowland monsoon forest	Lowland monsoon forest (mapped as woodland)
Pandanus scrub/ Mixed fringing communities	Kosher	-	Upper floodplain fringe	Margin woodland	Margin woodland (mapped as woodland)
-	Kosher	Grassland	Floodplain fringe	Lawn	Lawn (not mapped)
Paperbark forest	Effington, Pinwinkle	Forest	Floodplain fringe	<u>Melaleuca</u> swamp	Paperbark swamp Back- water Swamp
-	Copeman, Cyperus	Freshwater lagoon/ perennial swamp	-	-	Freshwater lagoon Swamp
Herbaceous swamp	Copeman, Cyperus	Annual swamp	Floodplain macrophyte	<u>Eleocharis</u> swamp	(mapped as grassland sedgeland and saltflat)
Herbaceous swamp Sedgeland	Copeman, Cyperus Cyperus	Mixed herbfield	Floodplain macrophyte -	<u>Oryza</u> swamp <u>Pimbristylis</u> sedgeland	
Samphire	Littoral	-	-	-	-
Mangrove Scrub	Littoral	-	-	-	Mangrove



Figure 10: Vegetation communities in the South Alligator River region (based on Story 1969, 1976)

of forest and woodland follows Story (1969), with extensive areas shown as mixed forest and woodland. The canopy reaches up to 13 m above ground level, and occasionally Ironwood, Erythrophleum chlorostachys is an important element. Smaller trees include the palm Livistona benthamii, Acacia sp., Terminalia ferdinandiana, Xanthostemon paradoxus, Planchonia careya, Petalostigma quadriloculare and Buchanania obovata (Story 1969, 1976).

The less well drained soils at the foot of the slope contain several other vegetation types. In a few localised pockets there are dense luxuriant evergreen stands of lowland monsoon forest, termed rain forest by Story (1976). In these Ficus virens is often a prominent component; full species lists are provided by Russell-Smith (1985a) and Taylor and Dunlop (1985).

Around the edges of the South Alligator plains margin woodland of Eucalyptus papuana, with ground cover of the exotic weeds Hyptis suaveolens and Cassia sp., frequently occurs. A grassy 'lawn' up to 20 m wide dominated by Pseudoraphis spinescens, extensively routed by pigs, often separates the marginal woodland from the floodplain surface. Scrub of Pandanus spiralis also forms stands in this slope foot location.

Paperbark swamps, dominated by Melaleuca leucadendra, occur within reentrants into the uplands. Open water bodies in these areas, termed 'ponded floodplains' by Christian and Aldrick (1977) and 'freshwater lagoons' by Galloway (1976) and freshwater lagoons and perennial swamps by Williams (1979), are included by us in our term backwater swamps. Where paperbark swamps occur these are generally monospecific; their distribution is shown in Figure 10. Barringtonia acutangula is occasionally found along channel margins.

Within backwater swamps, and between stands of paperbark are areas of annual or perennial swamp in which Hymenachne acutigluma or Nelumbo nucifera are common (Williams, 1979).

The floodplains themselves, and the coastal plains, are described by Story (1969, 1976) as characterised by sedgeland, and in the wetter areas, herbaceous swamp vegetation. Vegetation types within these categories are expanded by Taylor and Dunlop (1985). Much of the plains close to the river is on what they term a levee, where the sedgeland is dominated by Fimbristylis tristachya. Further from the rivers, there are Eleocharis and Oryza swamps dominated by Eleocharis dulcis and the wild rice Oryza meridionalis respectively. Scattered patches of Sesbania cannabina, Cassia sp. and Cathormion umbellatum occur across the plains, the latter especially in the upstream reaches.

Species composition varies across the deltaic-estuarine plains according to depth of flooding and length of inundation, and can show considerable year to year variation (Taylor, unpubl. results). The Eleocharis swamp subject to flooding to depths of 1.0-1.5m in the wet season is the least diverse community (Taylor and Dunlop, 1985). Many of the species dry out beyond recognition in the dry season. In addition to the sedges described above, the grasses Hymenachne acutigluma, Oryza meridionalis and Pseudoraphis spinescens are extensive. Also found are Commelina lanceolata, Ludwigia adscendens, Nymphoides indica, Paspalum scrobiculatum, Phylidrum lanuginosum, Scleria sp. and Utricularia fulva. Slightly drier locations have Phyla nodiflora, Echinochloa colona, Elytrophorus spicatus, Euphorbia sp., Ipomoea aquatica, Panicum spp. and Sporobolus virginicus (Story, 1969, 1976).

The intertidal zone is occupied by mangroves forming a low to medium forest fringe up to 300 metres wide at the coast and lower estuary. On salt mudflats there is a sporadic cover of samphires Tecticornia australasica and Halosarcia indica. Mangroves form narrow to sparse

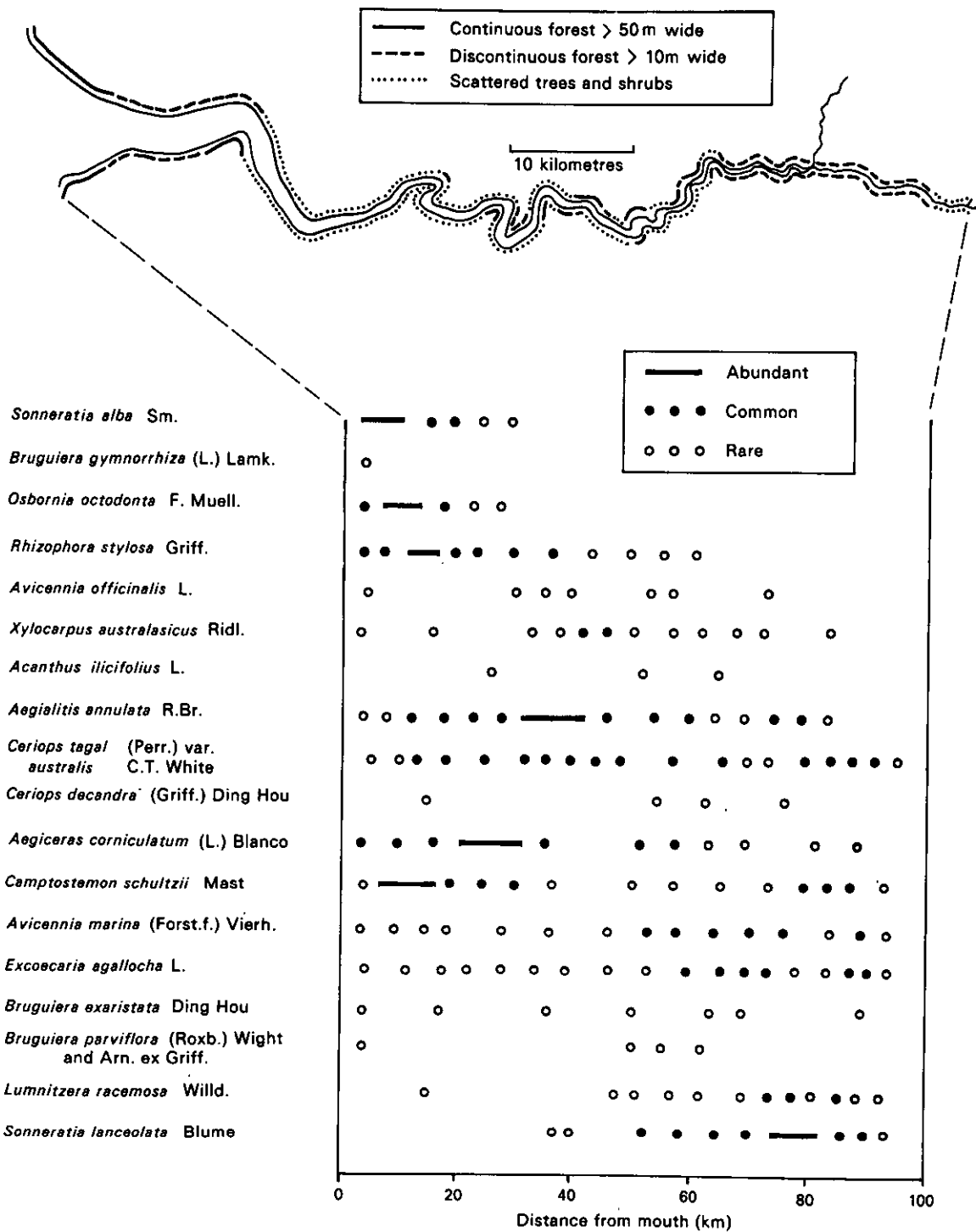


Figure 11: Distribution and composition of mangrove communities along the South Alligator River; (based on Wells, 1984; supplemented from Messel *et al.*, 1979; Davie, 1985; M. Ball, pers. comm.)

fringes along the river banks along the tidal river with a few local exceptions where patches of forest up to a few hundred metres wide extend along the banks generally for no more than a kilometre. Mangroves also line tidal creeks running off the main channel. There is often a height gradient away from the creek with small trees and shrubs, many of which are dead, extending into the sedges of the plains. The distribution of mangroves along the main channel is outlined in Figure 11 (based on Wells, 1984; supplemented from Messel et al., 1979; Davie, 1985; M. Ball pers. comm.).

Eighteen species of mangroves occur along the South Alligator River. The greatest diversity occurs within the lower estuary and on the adjacent muddy coast, where Sonneratia alba and Rhizophora stylosa are dominants in the taller, seaward or riverside zone of the forest. Ceriops tagal var. australis is typical of the upper tidal levels in the lower estuary. Avicennia marina occurs towards the higher tidal zone of the mangrove fringe, throughout the tidal river. Sonneratia lanceolata has not been noted less than 30 km from the sea and extends to the tidal limit. Figure 11 summarises the distribution of the main mangrove constituents along the river, and also shows the average width of the fringe. The width and character of the mangrove fringe varies with depositional or erosional conditions on the river banks, and this is reviewed in more detail in Chapter 2.5.

Soils of the lowlands of Koolpinyah land surface are generally shallow and gravelly and developed over lateritised surfaces. Within the Kosher land system, marginal to the floodplains, there are coarse-textured colluvial soils, yellow sandy, and red loamy soils developed on laterite (Hooper, 1969). Much of the surface has a sand cover, or a layer of ferruginous nodules. Skeletal soils are most common, and soils have been classed in the Koolpinyah and Murrabibbi families.

The soils of the riverine and coastal plains are uniform fine-textured soils which crack seasonally into smooth-faced soil peds. The two soil families which cover most of the plains are the Wildman family of black, massive clays formed to depths of about 90 cm over older, alkaline saline estuarine clays, and the Carmor family, found in wetter parts of the plains, which consists of massive or weakly self-mulching clays over estuarine mud, and with amorphous calcium carbonate (Aldrick, 1976).

The bare salt mudflats are underlain by saline clays, and the mangroves are underlain by juvenile clay soils or similar saline muds. These soils belong to the Carpentaria family of soils (Hooper, 1969).

1.5 Late Quaternary Depositional Context

The coastal lowlands and floodplains of the South Alligator River, in common with those elsewhere, have formed during a period when sea level and climate have changed substantially. Late Quaternary sea-level rise, associated with retreat of the northern hemisphere icecaps of the last ice age, commenced about 18,000 years ago from a level about 150 m lower than present relative to Northern Australia (van Andel et al., 1967; Jongsma, 1970). The sea reached approximately its present level around 6500 years ago (Thom and Chappell, 1975; Thom and Roy, 1983). Valleys which had been cut across the previously exposed continental shelves thus were flooded during the rising sea-level phase. Since sea level stabilised around 6500 to 6000 years ago, valley infill by sedimentation created the present floodplains. The exact history of valley drowning and floodplain development depends on several factors, including geometry of the prior valley, sediment input, and interaction between seasonal floodwaters, the tide and waves. The exact course of sea-level change over the last 6000 years, which is known to vary between different parts of Australia (Chappell et al., 1982) may also affect floodplain and tidal river development.

The general form of the South Alligator River valley, prior to flooding by rising sea level, is known from our drilling studies (Woodroffe *et al.* 1985a, 1985b). We have drilled 130 stratigraphic holes through the sediments which infilled the valley since sea-level rise; these are described in Chapter 4. The prior topography is known from the depths at which many of the drillholes intersect basal soils and alluvial/colluvial deposits of the pre-flooding ground surface. As described in Chapter 4, these are characteristically clayey or sandy, strongly weathered, mottled, or leached. Figure 12 maps the prior valley surface, based on the drill-hole data. The map, and the inset histogram, show that the prior valley had a rather flat floor about 10-12m below AHD (Australian Height Datum, approximately mean sea level, see Chapter 3, Figure 28) up as far as Nourlangie Creek. Deeper points near the axis of the valley (inset sections, Figure 12) show positions of the prior river channel. Flooding of the valley as a whole would have commenced when rising sea level reached 10m or so below present.

Figure 13 shows sea-level changes relative to the northeast Australian coast, over the last 10,000 years. These are expected to apply quite closely to the South Alligator area, although our results show certain differences in detail, which are described in Chapter 5. Figure 13 is used as the sea-level 'baseline' for interpreting geomorphologic and stratigraphic data in Chapters 3 and 4. The basis for Figure 13 is as follows:

- (i) Thom and Roy (1983, 1985) summarise evidence for rising sea level from a large number of radiocarbon-dated drillholes in coastal southeast Australia. These results are shown as an envelope defined by the two solid lines in Figure 13b.
- (ii) Grindrod and Rhodes (1984) describe dated mangrove deposits at the bases of 19 drillholes at Hinchinbrook Island, North Queensland. These deposits directly overlie the land surface which was drowned by rising sea level. The ages and depths of each occurrence are plotted as crosses in Figure 13b; lengths of the crossed lines indicate standard errors. Most of these results lie within or close to the southeast Australian envelope.
- (iii) Chappell (1982), Chappell *et al.* (1983) and Chappell and Grindrod (1984) describe dated coral microatolls occurring in 12 surveyed fringing reefs at northern Great Barrier Reef sites. These data are plotted in Figure 13a, and are the basis of the solid line showing a steady fall of sea level by 1 metre over the last 6000 years in that region.

Figure 13 shows that sea level passed through -10 m between 8500 and 8000 years B.P. This is the time when widespread drowning of the South Alligator valley is expected to have begun. Our drilling and dating results (Chapter 4) are broadly consistent with this.

Climate has also changed during the last 20,000 years. At the height of the last ice age, 18,000 years ago, climates were about 5 to 7°C cooler in Australia and Papua New Guinea (CLIMANZ, 1983). Conditions were substantially drier than present from 18,000 to about 10,000 years ago in much of southern Australia as well as in the Atherton region in north Queensland (CLIMANZ, 1983). Analysis of sediments from the Timor shelf suggests that a similar arid period was experienced in north Australia (van Andel *et al.*, 1967). It has been suggested that sea surface temperatures were more than 2°C cooler, that the trade winds were cooler and that the general climate of the area was drier than in equivalent coastal environments at present (Webster and Streten, 1978). In addition to these general factors, the Alligator Rivers region was more continental in climate, 18,000 years ago, as the coast at the time lay about 300 km northwest of its present position. Although there are no paleoclimatic studies from the area, as yet, it can be inferred that climate in the Alligator Rivers

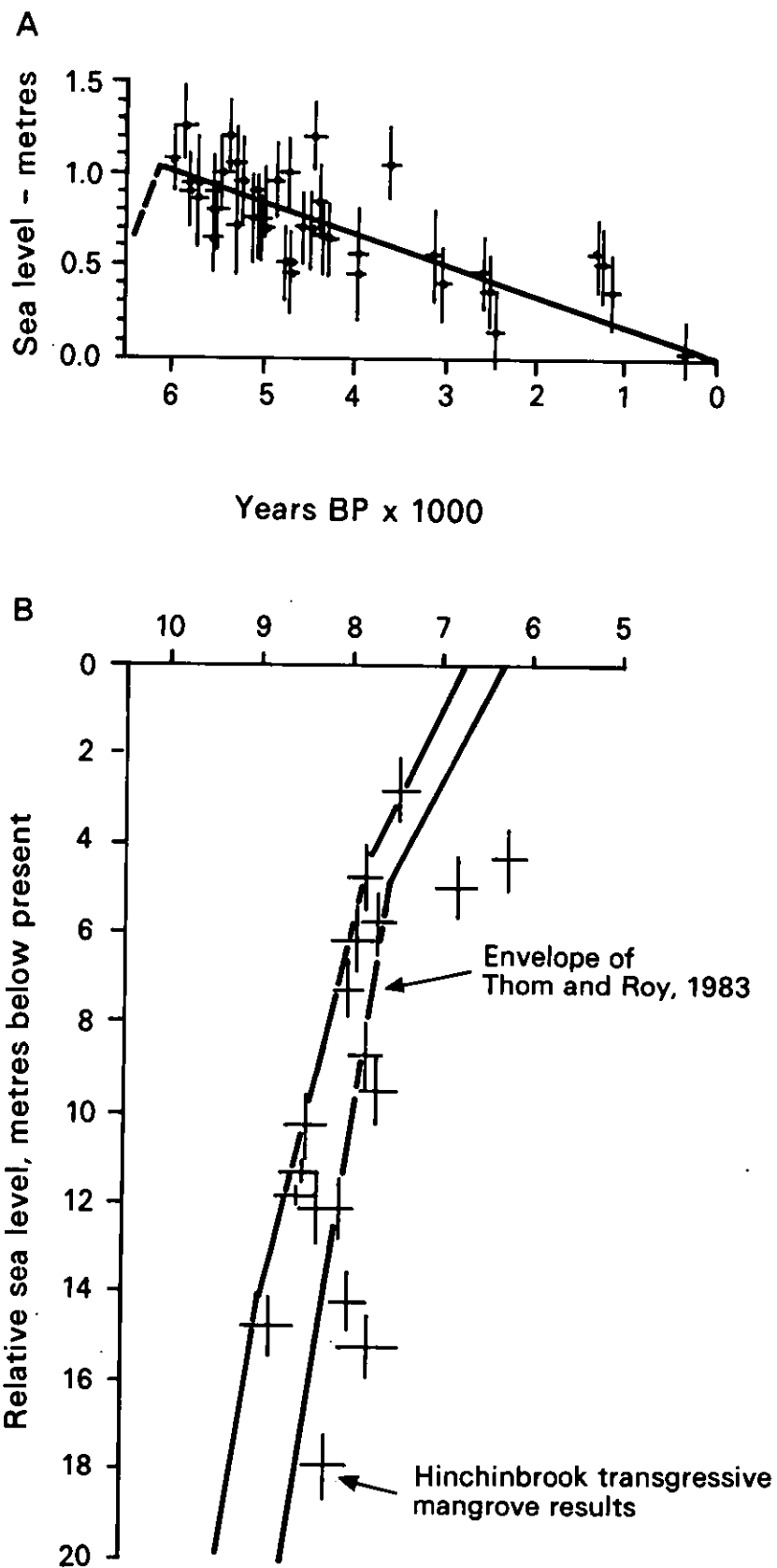


Figure 13: Sea-level characteristics from eastern Australia, for the last 20,000 years (references given in text)

catchments was similar to that which occurs today in the region between Katherine and Tennant Creek (Figure 14). Weathering and slope denudation in the catchments are likely to have differed from those processes active today, perhaps with relatively higher production of sand and coarser material, and less effective transport through the lower river systems.

Climate was warming rapidly, 10,000 years ago, and appears to have become similar to present by the time when drowning of the South Alligator valley began, 8500-8000 years ago. However, there is some evidence of climatic variation in the last 8000 years in northern Australia, particularly from the Atherton Tableland (Kershaw, 1983). Figure 14a summarises interpretations of climate during this period, from CLIMANZ (1983). Differences between results from different regions make it uncertain whether any of the variations shown in Figure 14a extended into the northern parts of Northern Territory.

The sea-level changes and possible climatic fluctuations shown in Figures 13 and 14 are the boundary conditions under which the present South Alligator tidal river and plains have developed, and in light of which we later interpret stratigraphic and geomorphologic data.

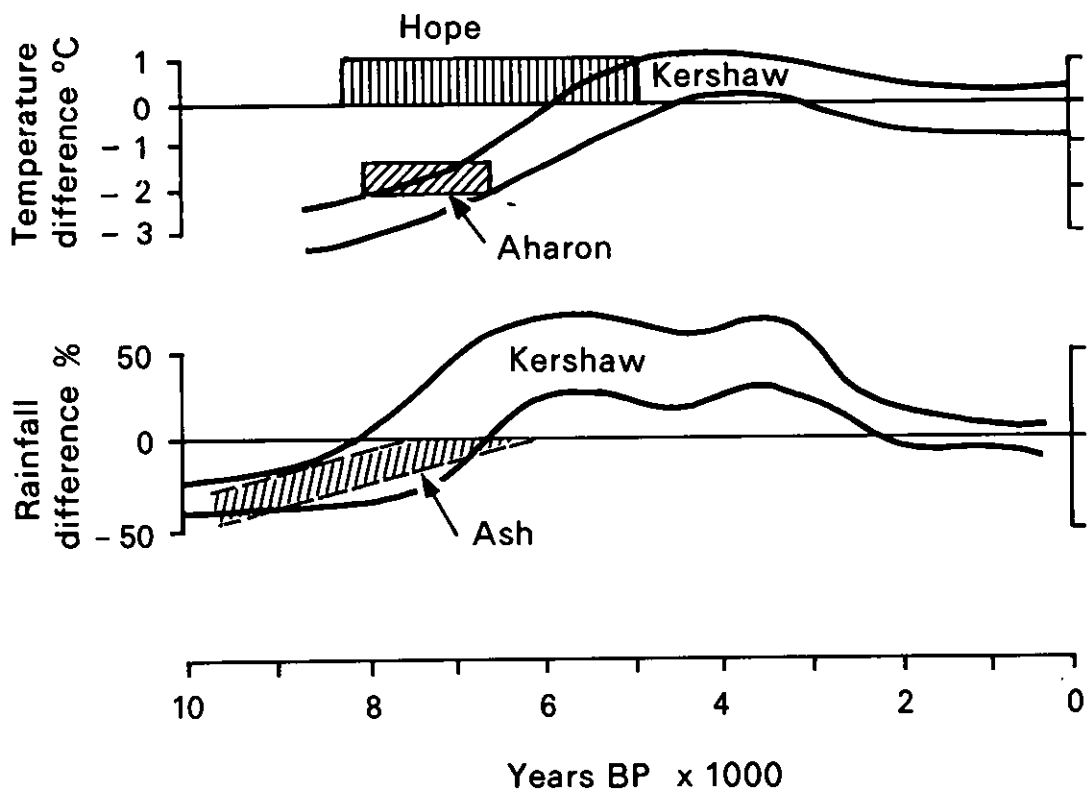


Figure 14a: Summary of climatic trends in North Australia during the late Quaternary (Source: CLIMANZ 1983)

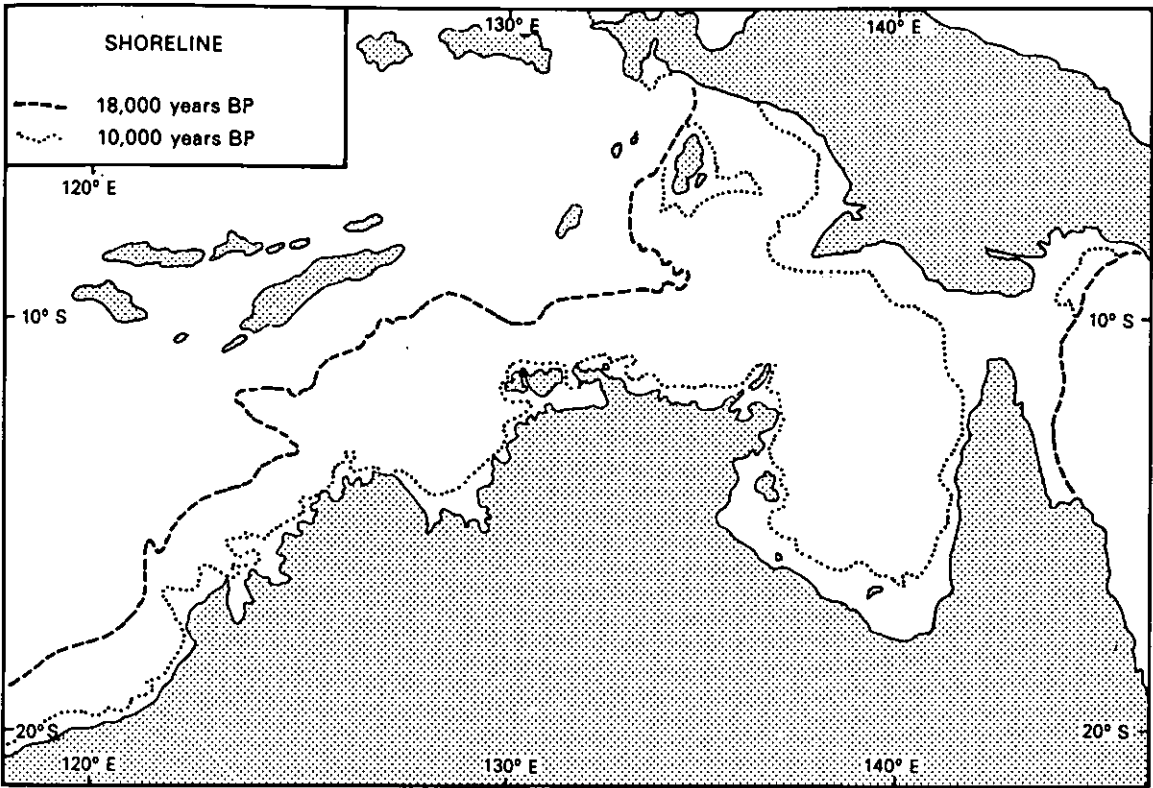


Figure 14b: Approximate location of shoreline 18,000 and 10,000 years ago

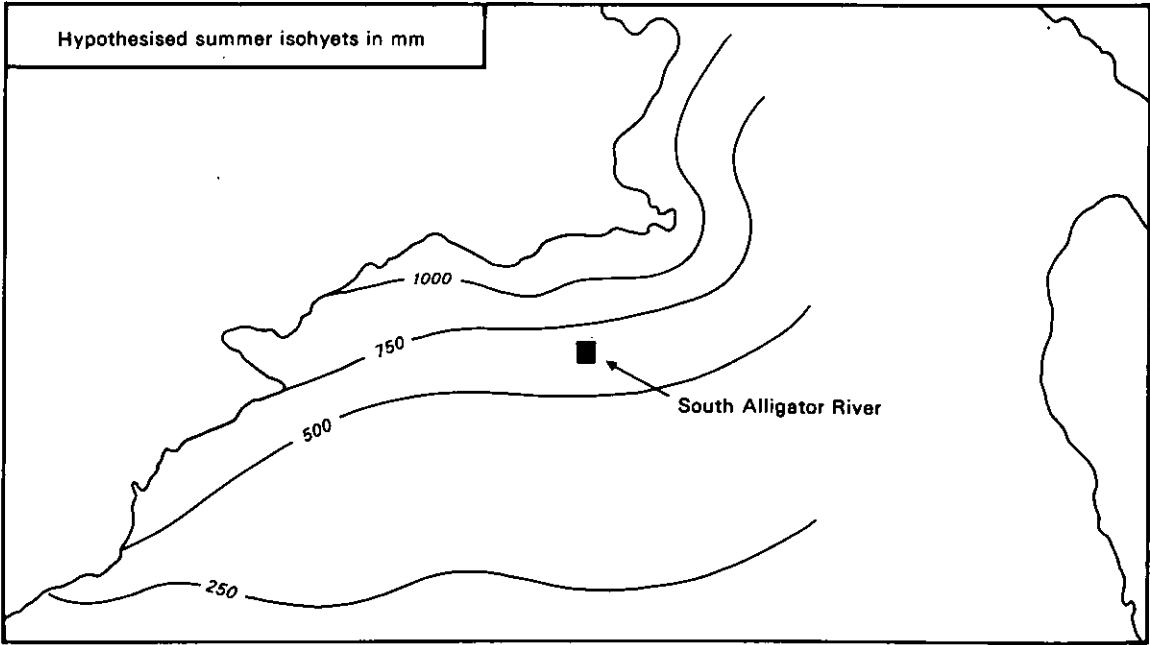


Figure 14c: Maximum hypothesized rainfall isohyets, 18,000 years ago

Chapter 2

Estuarine Morphodynamics

- 2.1 Nearshore Wave Regime
- 2.2 Tidal Behaviour, Dry and Wet Seasons
- 2.3 Yearly Cycles of Salinity and Water Chemistry
- 2.4 Sediment Movement in the Tidal River
- 2.5 Bank and Creek Stability

2. ESTUARINE MORPHODYNAMICS

The concept of interaction between process and form has been strongly developed in Australian coastal geomorphology. We refer to the concept as coastal morphodynamics. Although this concept did not originate in Australia, it nonetheless has received considerable emphasis in various studies here and has provided the conceptual framework for many empirical studies (e.g. Wright *et al.*, 1979). In a sense, the morphodynamic approach represents an application of systems thinking with the identification of spatial and temporal systems at specified scales. Within each system the emphasis is on understanding the interaction of process, material and form, all of which are continually adjusting over time in response to external and internal forces (see Wright and Thom, 1977). In this section we discuss geomorphic processes operating at the present time in the South Alligator River region and the relationship of these processes to the movement of sediment and the formation of morphological features.

2.1 Nearshore Wave Regime

The nearshore wave regime is significant for sediment movements at the coast and in the mouth of the South Alligator River. We are not aware of any measurements of wave climate in the area. Hence, the prediction methods of the U.S. Army Coastal Engineers, summarised by Komar (1976) are used. Input data are fetch lengths along principal compass sectors to Field Island measured from the maps of van Diemen Gulf (Figure 15). Summer (October to March) and winter (April to September) wind data are summarised in Table 2.

Predicted waves in each sector from west through north to southeast, for each of the two seasons, are given in Table 2. Only three wind classes are listed, i.e. 2.5 to 5 m/s, 5 to 10 m/s, and >10 m/s. In the two lower classes, waves are for the upper limit winds, i.e. 5 and 10 m/s respectively. In the third class, $U > 10$ m/s, waves are for 20 m/s (i.e. 40 knot) winds. Hence, the percent frequencies of occurrence in each wind class and sector are likely to exceed real frequencies of occurrence (%) of the given waves.

The waves in Table 2 are estimated on the basis of there being no shoaling effects. Bathymetric data for van Diemen Gulf are relatively few (Figure 15). However, available soundings indicate that even the largest of the predicted waves (1.7 m, 5.5 seconds, NW sector, summer season) will not be inhibited by bottom effects through most of the Gulf. As the waves approach the shore their height will increase by shoaling, up to the point at which they break. Using the method of Komar and Gaughan (1973), the height gain factor ranges from about 1.0 for the smallest waves in Table 2, to 1.08 for the largest. Hence, the 1.7 m waves from the NW will increase to about 1.85 m before breaking. In addition to shoaling, wave height will be altered by refraction effects, but this cannot be estimated as bathymetric data are too sparse around Field Island and the South Alligator mouth.

In summary, waves from the north to north-west sector dominate in the October-March season, and may exceed 1.5 m for 1 to 2 per cent of the time. The most common height is expected to be between 0.4 and 0.7 m, occurring for roughly 25 per cent of the time. During the April-September season, waves may exceed 0.6 m for 2 to 3 per cent of the time, and waves around 0.5 m are expected for about 10 per cent of the time. All waves up to the largest predicted in Table 2 have heights substantially less than the tidal range, which means that all the waves listed in Table 2 may break within the front of the coastal mangrove forest at high spring tide. (Waves break when water depth is about 1.25 times wave height). The energetic process of wave breaking within the mangrove front may have some effect on mangrove recruitment.

Table 2
Significant winds and predicted waves

A. April-September

Sector	U=2.5-5m/s			U=5-10m/s			U>10m/s		
	%	H(m)	T(s)	%	H(m)	T(s)	%	H(m)	T(s)
N	7	0.3	2.3	1	0.6	3.2			
NE	4	0.25	2.0	1	0.5	2.5			
E	25	-	-	6	0.4	2.3	2	0.8	3.7
SE	15	-	-	2	0.3	2.3	1	0.6	3.0

B. October-March

Sector	U=2.5-5m/s			U=5-10m/s			U>10m/s		
	%	H(m)	T(s)	%	H(m)	T(s)	%	H(m)	T(s)
W	10	0.4	2.5	1	0.7	3.3			
NW	12	0.4	2.5	1	0.7	3.3	1	1.7	5.5
N	12	0.3	2.3	3	0.6	3.2	1	1.5	5.0
NE	3	0.25	2.0	1	0.5	2.5			
E	3	-	-	2	0.3	2.3	1	0.8	3.7

Notes: U (wind velocity in m/s) given in 3 classes shown. Predicted waves for each class correspond to velocities of 5, 10, and 20 m/s, respectively. Frequency of occurrence of winds in each class and sector shown as percentage (%) of time in 6 month season.
H = wave height; T = wave period.

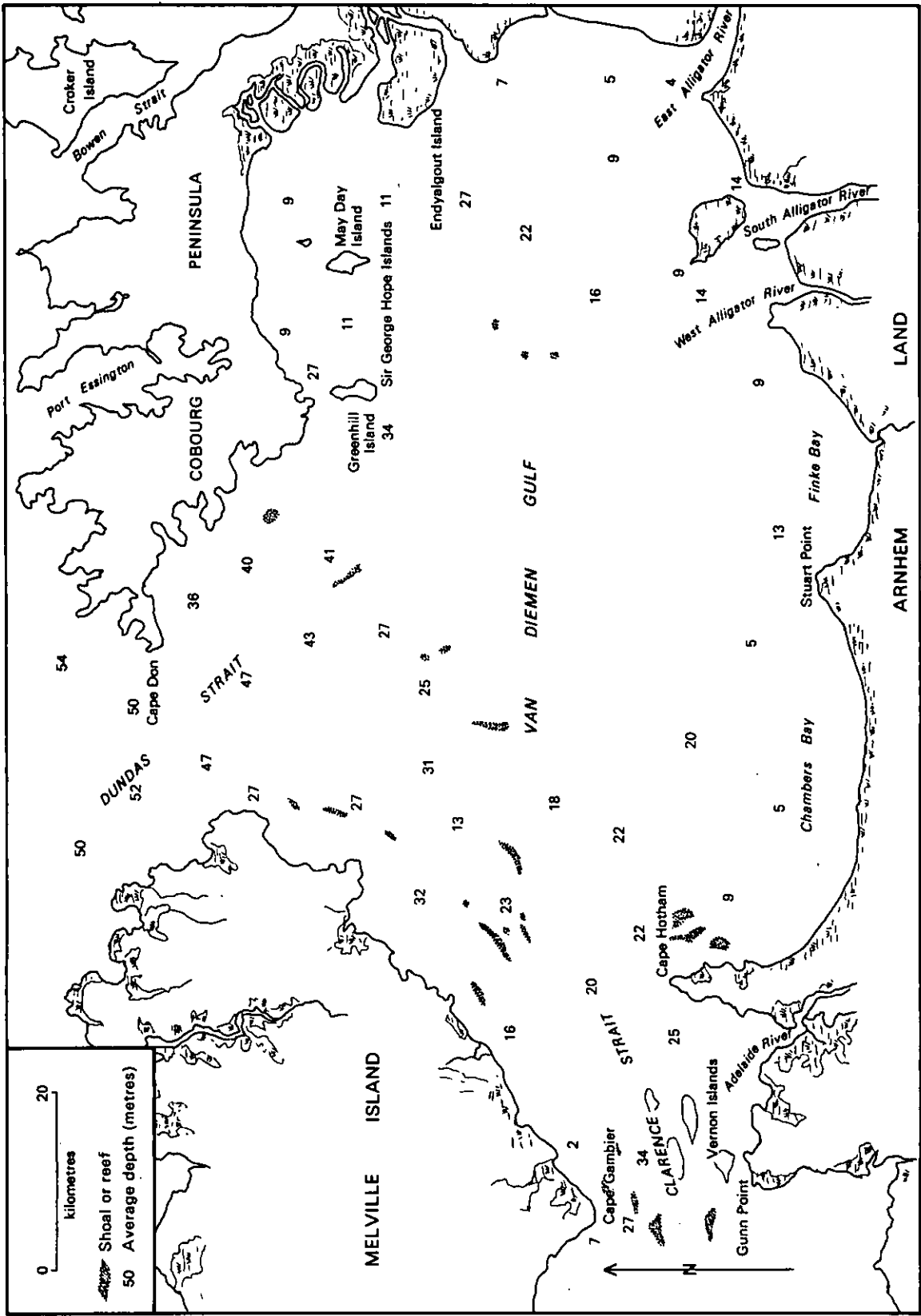


Figure 15: Bathymetry of van Diemen Gulf. Average depths derived from chart Aus308.

The potential for waves to cause sediment drift cannot be estimated with any confidence, as the bathymetry near the South Alligator mouth is insufficiently known. Refraction around Field Island up the deeper water of the Cunningham Channel (location, Figure 15) is likely, and we have frequently observed waves in the lower estuary which are significantly higher than those outside. Fine sediment is seen held in suspension by waves and tidal currents in the estuary and nearby eastern shore. According to Wu (1975), wave/wind surface drift amounts to about 4 per cent of wind velocity. With winds from the north to east occurring frequently (Table 2), there is a significant potential for nearshore suspended sediment to be held near the river mouth, and returned to the estuary when the tide is flooding.

The final factor in the wave climate is the occurrence of cyclones. Hopley and Harvey (1979) estimate that the 5° square centered on Arnhem Land and van Diemen Gulf may be affected by about 1.4 cyclones per year, on average. The actual frequency of direct cyclone effects on any given part of the coast is much lower, of course. For example, Whittingham (1964) estimates that extreme gusts of 45 m/s (about 160 km/hour) will occur every fifty years, on average, at any point on this coast, and that 60 m/s gusts have a return period around 100 years. Cyclone crossings probably follow similar patterns.

As far as cyclone effects are concerned, the combined wave and storm surge effects have to be estimated. Due to the relatively shallow depth of southeastern van Diemen Gulf (8 to 10 m), waves are unlikely to reach the sizes possible in open ocean. A limiting size of 2.5 to 3 m seems likely. Depending on the degree of surge elevation and tidal height, these waves will propagate more or less freely onto the coast and coastal plains, where not impeded by mangroves. Highest water levels occur when storm surge coincides with high spring tide. Hopley and Harvey (1979), using historical records and taking tidal and other factors into consideration, estimate surge height recurrence intervals for main points around north Australia, including Darwin. Surges are likely to be greater in the semi-closed van Diemen Gulf than at Darwin which therefore provides conservative estimates for the South Alligator mouth. The height/recurrence interval curve for Darwin estimated by Hopley and Harvey indicates that surges exceeding highest spring tide level by 0.5 m or more are likely to occur every 100-150 years, on average. Waves around 2.5 m are likely to break well within the mangrove fringe under these conditions at times of high tide.

2.2 Tidal Behaviour

Tides of the northern coasts of Northern Territory are semidiurnal and have spring ranges to over 6 m. Spring range at the mouth of the South Alligator River is around 6 m. Darwin tide tables are a reasonable guide to range at the river mouth but not to tide times. In order to assess tides within the river, systematic surveys of tidal stage and current velocity profiles were made at several stations along the river, using portable tide gauges, stage boards, and the fixed recorder at the Arnhem Highway bridge which is operated by the N.T. Water Division. Table 3 lists the observation stations and their distances from the river mouth.

Measurement of tidal stage through several tide cycles at different stations allows calculation of other parameters such as velocity and discharge, which can be checked against direct measurements. We used a tide model, outlined in Appendix A 2, to simulate the tidal river. In addition to records of tidal stage, other input data include channel width and depth data along the river. These are shown in Figure 16, based on 1:25,000 aerial photos and echogram profiles. Figure 16 shows that the width-distance data divides into three segments fitted by negative-exponential regression lines. From the mouth, these are referred to as the

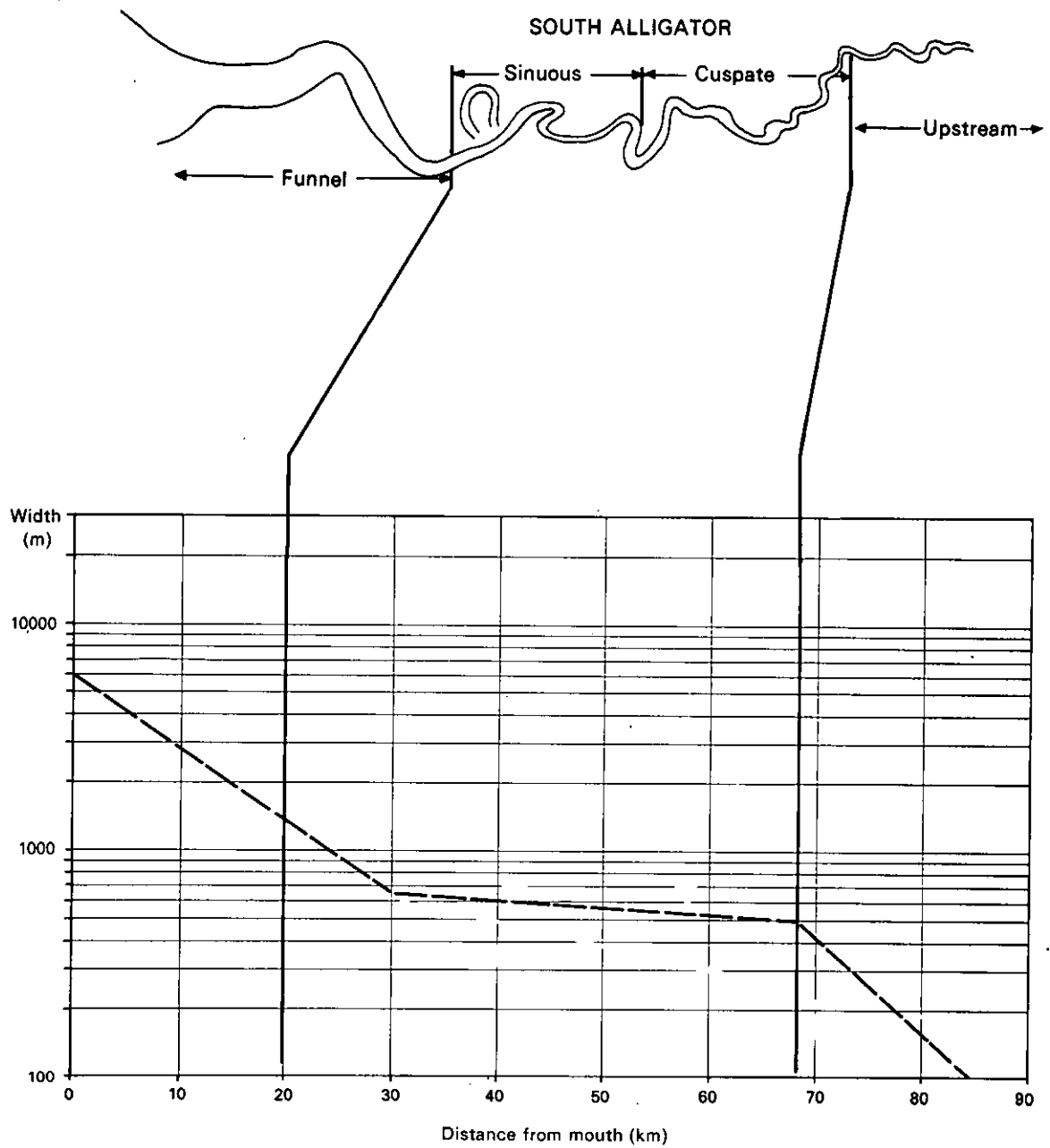


Figure 16: Map of South Alligator River channel and width relationships with distance from the mouth

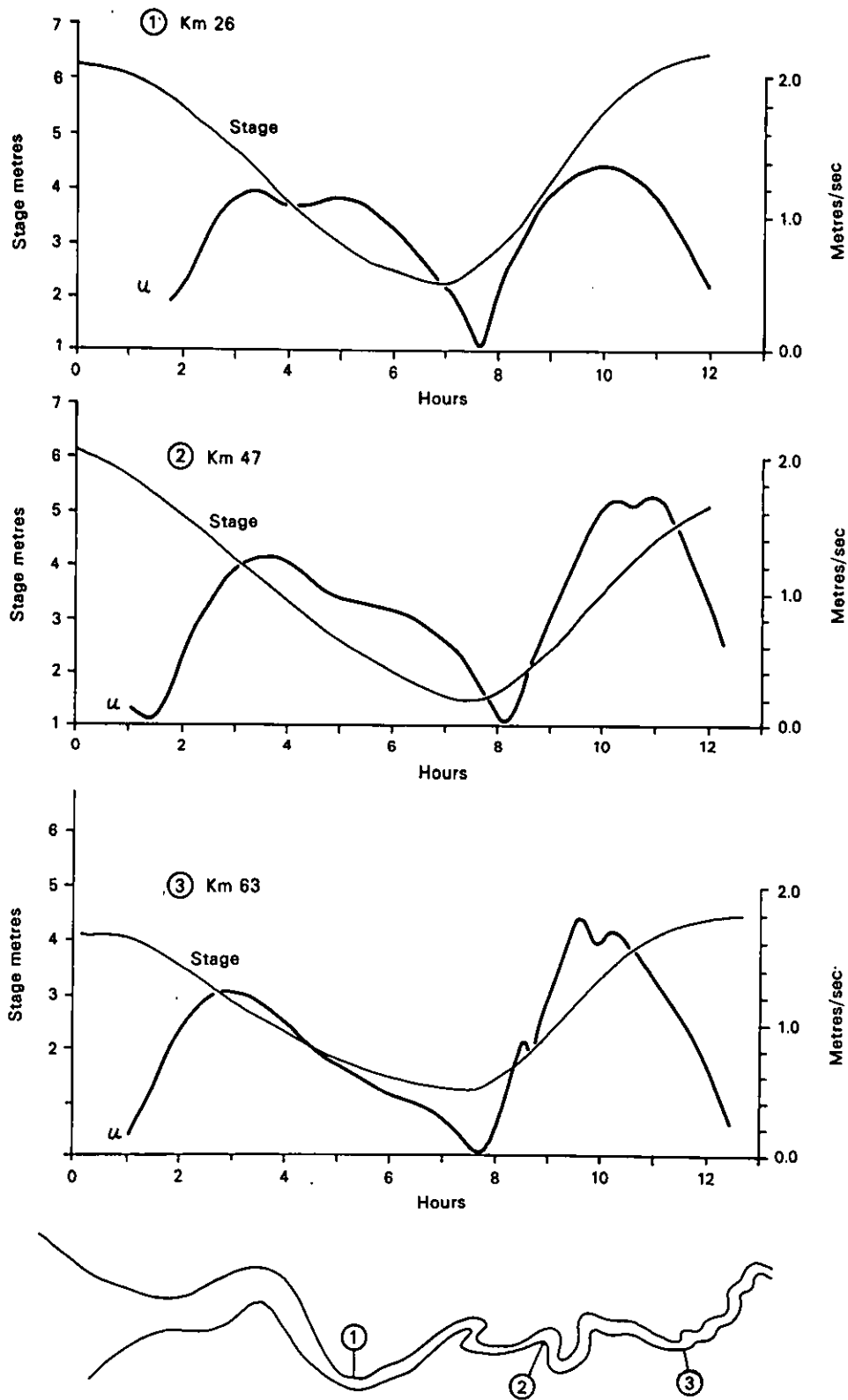


Figure 17: Observations on tidal height and current velocity (u) close to spring tide at three stations on the South Alligator River, July 1983

The tide model (Appendix A2) is based on sinusoidal solutions to the tide equations (Ippen, 1966). Observations show that tidal stage and currents do not vary sinusoidally. Figure 17 shows stage and mid-channel velocity curves measured through tide cycles at three stations (26, 47 and 63 km from the mouth). Flood tide velocities exceed ebb velocities, their duration is shorter, and patterns are not sinusoidal. Flood and ebb can both show more than one peak. The differences between flood and ebb may have some effects on channel development, discussed later and in Chapter 6. The cross-channel velocity structure can also differ between flood and ebb. Figure 18 shows velocity structures at three cross sections, based on current metering at several stations and depths across the channel at each site. Shear is greater during flood than ebb, and flow is not symmetrically placed in the channel. These results are referred to in later discussion of channel form and process.

Tidal discharge for the dry season and mean velocity throughout the river, graphed in Figure 19, are calculated from the tide model with parameters given in Appendix A2. Direct observations of mean velocity and discharge, based on Figures 17 and 18 and similar gaugings, plot close to predicted values in Figure 19.

Tidal flows in the wet season are modified by fresh water flood discharges, which have the effect of lengthening the duration of ebb tidal flows and reducing the duration and velocity of flood tidal flows. There is a point in the channel where upstream flow during rising tide is prevented by the freshwater discharge. We refer to this as the limit of tide reversal. Upstream of this point the flow is continuously seawards, although the water surface rises and falls tidally, up to the tide limit. The position of the limit of tide reversal is closer to the mouth for large freshwater flows than for smaller ones. The levels of high and low tide water surfaces are higher throughout the river than in the dry season.

We have no tide gauge records through wet season floods, other than from the Arnhem Highway bridge. Annual records of daily high and low tide water level at the bridge, from dry through wet and back to dry season show peak water levels in February and March more than 1 m above dry season spring tide levels; at this stage overbank flooding occurs.

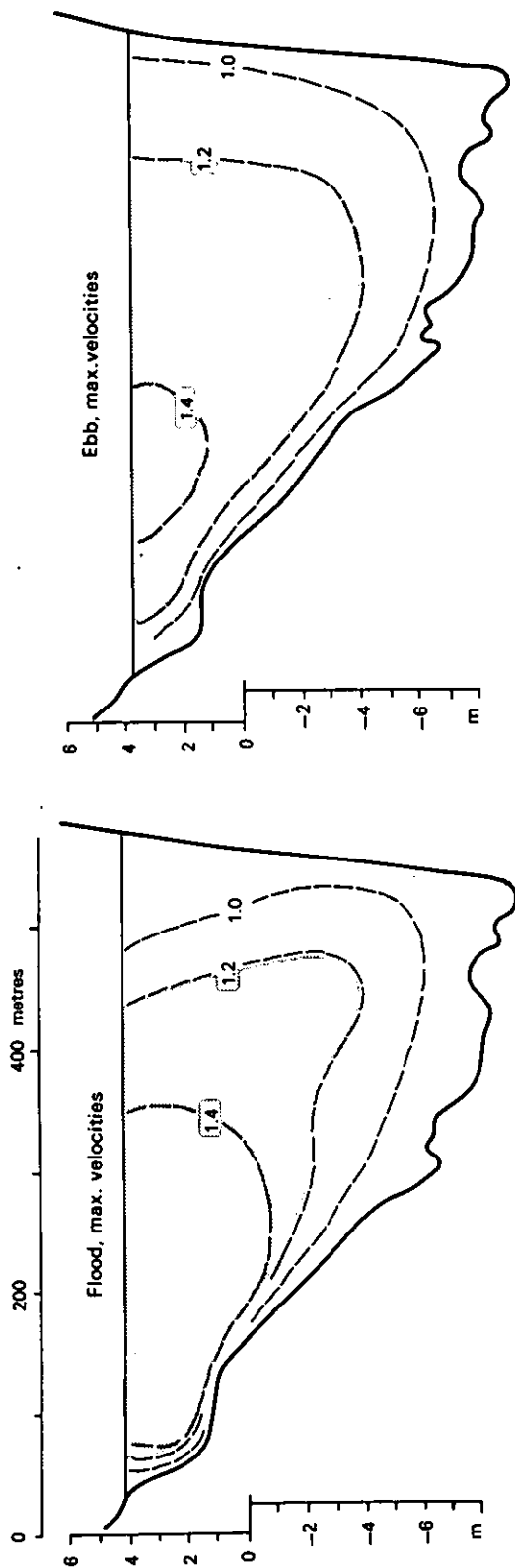
We have some observations of current velocities and the limit of tide reversal, made during the floods of March 1984. Mid-channel gauging near the bridge at mid-ebb tide stages (non-reversing flow) demonstrated a mean discharge of 800 cumecs, i.e. about 60% greater than mean dry season tidal flow (cf. Figure 19). The non-tidal component of this flow probably was about 300 to 500 cumecs, on the basis of observations around the 90 km points in Nourlangie Creek and the main channel. The limit of tide reversal at the time was near the 70 km point, where the mean dry season tidal flow is about 1000 cumecs (Figure 19). These figures suggest that the limit of tide reversal occurs where freshwater flood input is about half the mean dry season tidal flow. Observations during the same 1984 flood in the Daly River showed similar relationships.

2.3 Yearly Cycles of Salinity and Water Chemistry

The salinity regime of the South Alligator River is dominated by seasonal contrasts in rainfall and river discharge. Salinity and water chemistry profiles from river mouth to 90 km upstream have been observed regularly from July 1983 to July 1985, and two salinity profiles were reported previously by Messel *et al.* (1979).

The dominant factor affecting dry season water chemistry is progressive mixing, by turbulent diffusion, of salt water migrating in the upstream direction. Both tidal and wet season flood flows are highly turbulent, mixing the water vertically through most of the river. Upstream diffusion of salt commences as floods recede at the end of the wet season.

APPLETREE BEND (KM 47)



OLD KAPALGA (KM 63)

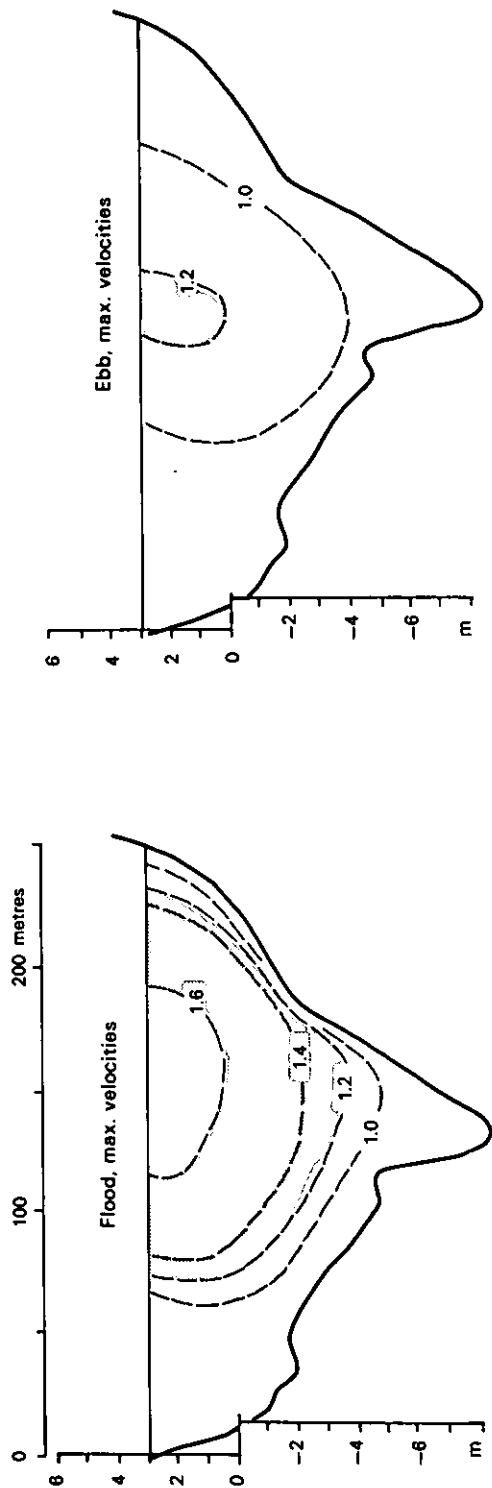


Figure 18: Cross-sectional velocity structure during flood and ebb maximum velocities at 47 and 63 km from the river mouth (location 2 and 3 respectively on Figure 17), July 1983.

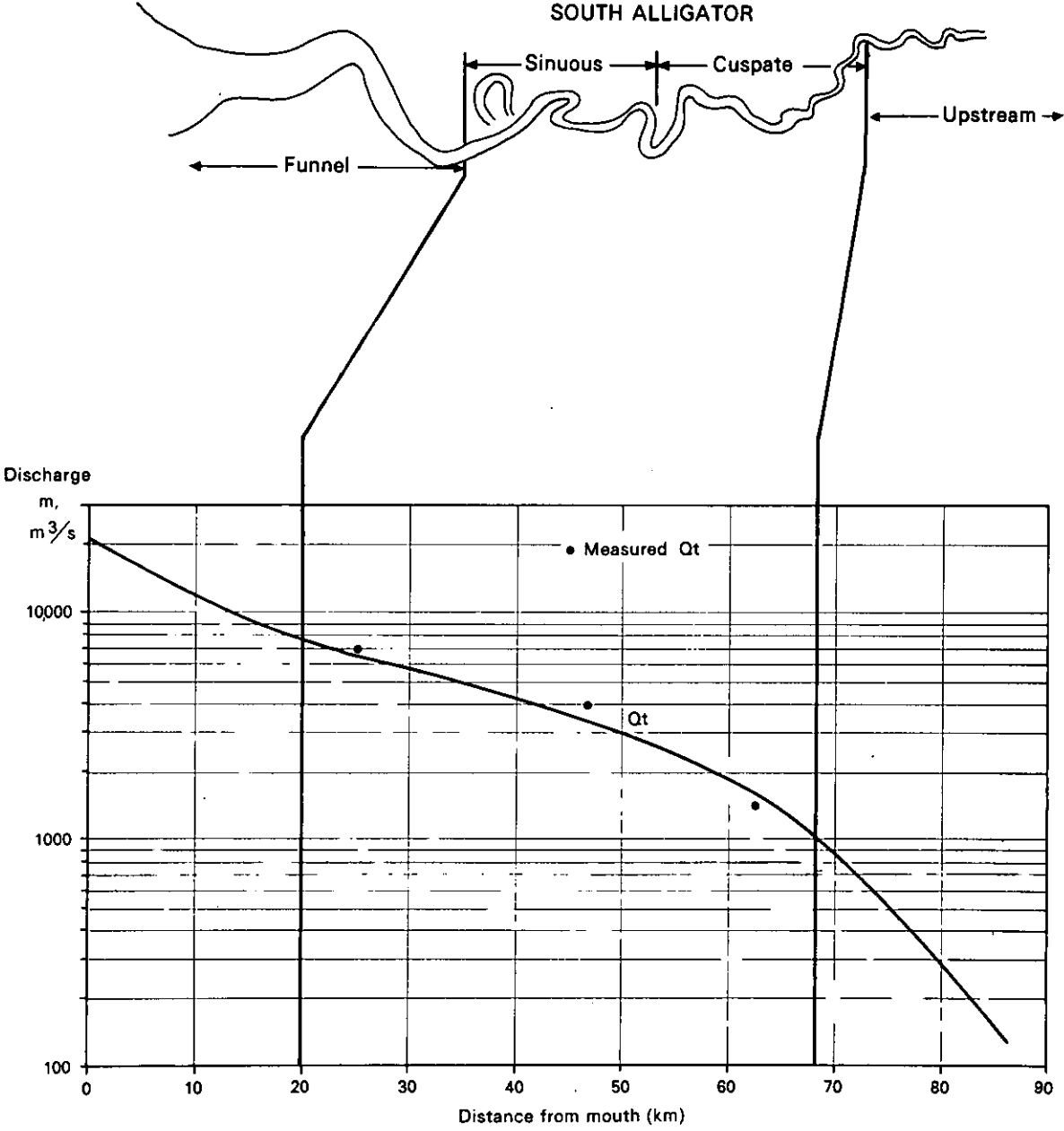


Figure 19: Longitudinal discharge profile, South Alligator River

The to and fro excursion of water through dry season spring tidal cycles has been measured (current metering and salinometry) as ranging between 8 and 15 km throughout the lower 75 km. As the tidal excursion distance is small relative to the length of tidal river, diffusive in-mixing of seawater is relatively slow. This process has been successfully modelled by turbulent diffusion, using methods outlined in Appendix A3.

Figure 20 shows predicted and observed salinity profiles from termination of the wet through to the end of the dry. Observations and predictions agree reasonably well. The model assumes that freshwater discharge ceases at the end of the wet season. This is not exactly true, but observation suggests that freshwater flow declines so rapidly that it is negligible relative to tidal flow by early June at the latest.

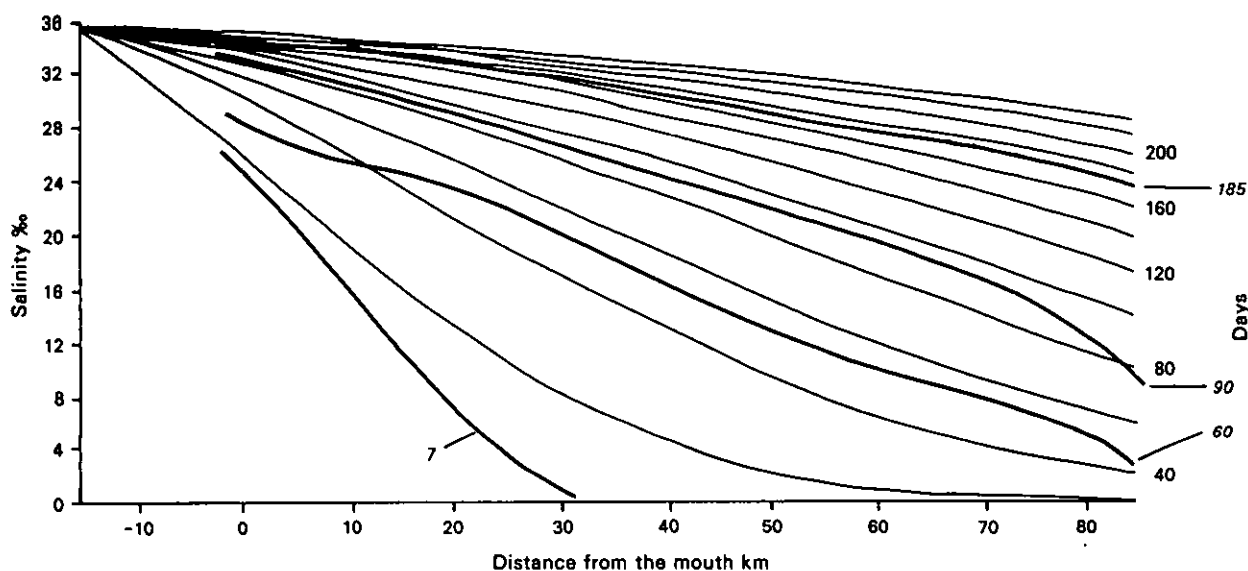


Figure 20: Salinity change in the South Alligator River through the dry season. Fine lines show prediction by turbulent diffusion model; heavy lines show observed profiles. Italic numbers show time in days after last flood peak in wet season at which observations were made; other numbers show model day-numbers. Agreement between model and observations is good.

The river was surveyed during floods of March 1984 and April 1985. Flow behaviour, sediment concentrations, and water chemistry are very different during floods from those at other times (Chappell and Ward, 1985). During and after flood peak the river was entirely freshwater upstream from about 30 km from the mouth. Water became progressively more salty seawards from this point with a salt-wedge vertical structure. Upstream from 30 km, flow reversal associated with rising tide became progressively weaker, up to the limit of tide reversal which was about 70 km upstream around flood peak. The salinity and general flow structures are shown in Figure 21, which summarises major flow and chemical data for the March 1984 floods.

Wet season water chemistry is conveniently discussed with respect to three hydrodynamic river segments:

- (i) the downstream fresh/saltwater mixing segment,
- (ii) the reversing-flow freshwater segment,
- (iii) the upstream non-reversing freshwater segment (Figure 21).

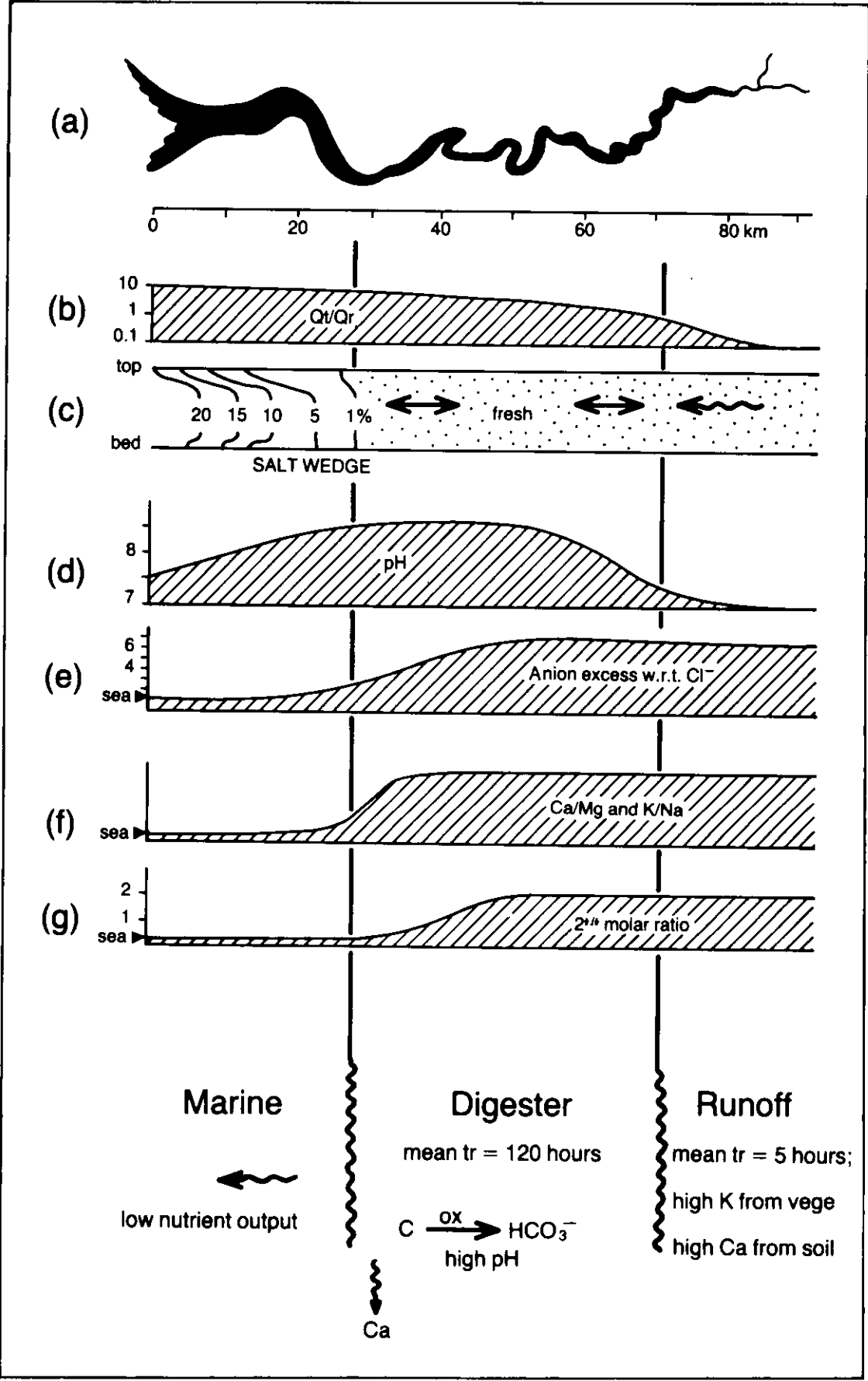


Figure 21: Inorganic water chemistry, South Alligator River: wet season, March 1984 (after Chappell and Ward, 1985)

During the two surveyed floods, freshwater flooding through the upstream segment of the river was generally of low turbidity (suspended sediment around 20-50 mg/l), carrying appreciable quantities of plant debris (leaves, stems, branches and blades of grass) as well as suspended organic particles (probably much ash from dry-season fires). Transit time is relatively short for water entering the non-reversing segment; with flow velocities around 1 m/s, water flowing in at the tide limit can move 25 km downstream in less than 7 hours. Major chemical properties were found to be fairly uniform through the non-reversing segment (Figure 21).

Passage from the limit of tide reversal down to the beginning of fresh and saltwater mixing is very much slower, as tide reversal retards the floodwater increasingly as it moves downstream. Appendix A 3 outlines how the transit time for a known freshwater input to the reversing flow segment can be estimated. Transit time through the reversing freshwater segment in the survey shown in Figure 21 is calculated to about 120 hours. The chemistry of the inflowing floodwater changes appreciably during this slow passage. The pH becomes high, approaching 8.7 (Figure 21). Increase in pH is presumed to be related to oxidation of organic debris in the floodwater. Concentrations of, and ratios between, several major ions change in this high pH segment (Figure 21).

The phosphorus nutrient source (dissolved reactive phosphorus) is relatively high through the freshwater system during floods (Figure 23) including the reversing-flow segment, suggesting low biological productivity (Sandstrom, 1985).

As the flood recedes, the salt-freshwater transition and the limit of tide reversal both move upstream. Stratification fades from the previous salt wedge and salinity starts rising progressively up river. Water chemistry starts moving towards that of dilute seawater in most inorganic aspects. Sediment concentrations become very high due to tidal turbulence, and particulate phosphorus levels are very high (Figure 23). Productivity is low, however, as light penetration is minimal (<0.3 m) in the highly turbid water. The particulate phosphorus is potentially usable seaward of the river mouth, where turbidity is lower.

Exchange of nutrients and inorganic constituents from the South Alligator River into van Diemen Gulf ceases as the dry season advances. Freshwater flow into the system effectively stops. Evaporation from the sea surface outside the mouth raises the salinity above that of normal sea water, which creates a barrier between sea and tidal river water (Figure 22). Hence, pollutants and nutrients will not leave the river throughout the later dry season. The high concentrations of nutrients such as particulate phosphorus, which develop within the river, presumably are flushed as the wet season floods set in, but we have not measured the flushing process and its effects.

It is clear that chemical output from the South Alligator River to its nearshore sea, as well as chemical exchange between water and the plains, are essentially wet season flood processes. In addition, floodwaters from the catchment change chemically as they pass, relatively slowly, through the reversing-flow freshwater zone illustrated in Figure 21. Net chemical input from the catchment and modified output both will vary with the magnitude of wet season floods. We have not enough data to establish relationships between flood magnitude and net chemical load in the South Alligator River. A limited set of data across a wide range of discharges in Daly River (Chappell and Bardsley, 1985) allow estimation of net annual output of major ions from that catchment. It is premature to estimate the proportions of major ions which reach the sea, or exchange in the floodplains of the South Alligator river system.

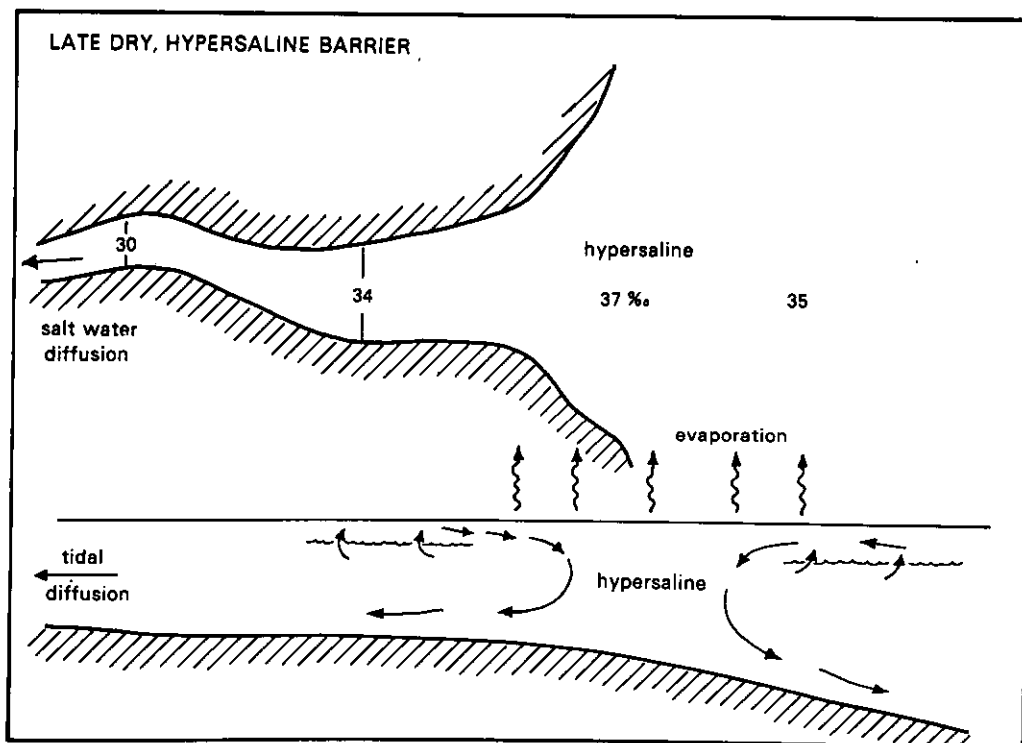
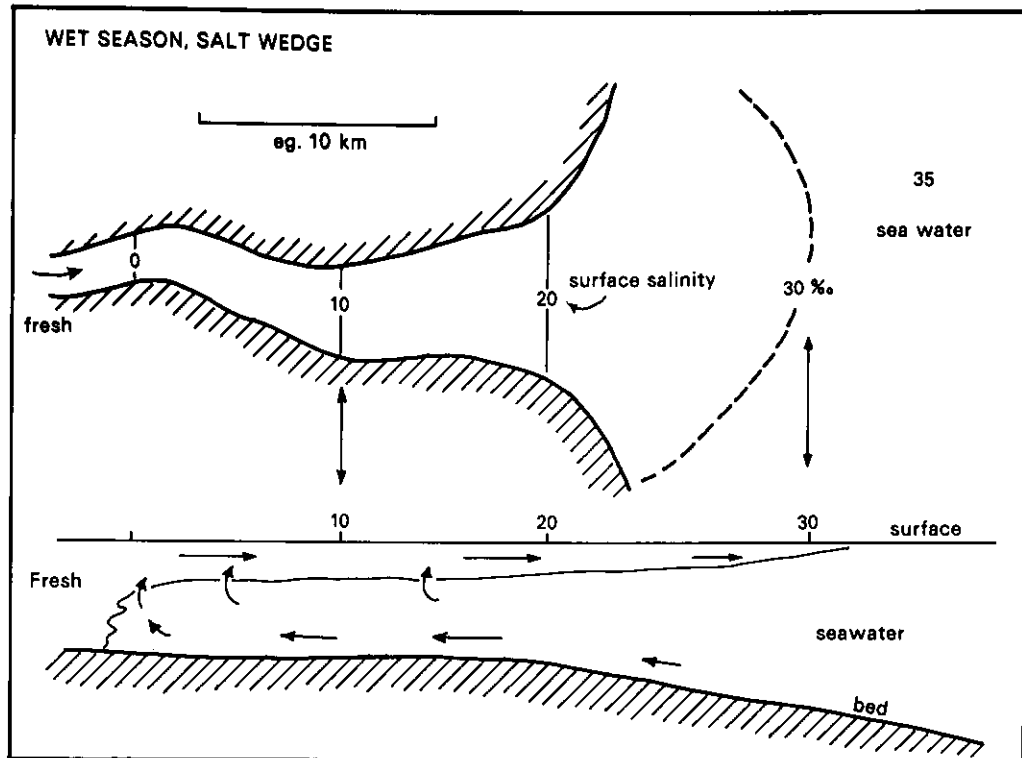


Figure 22: Wet and dry season vertical circulation and mixing in the South Alligator River

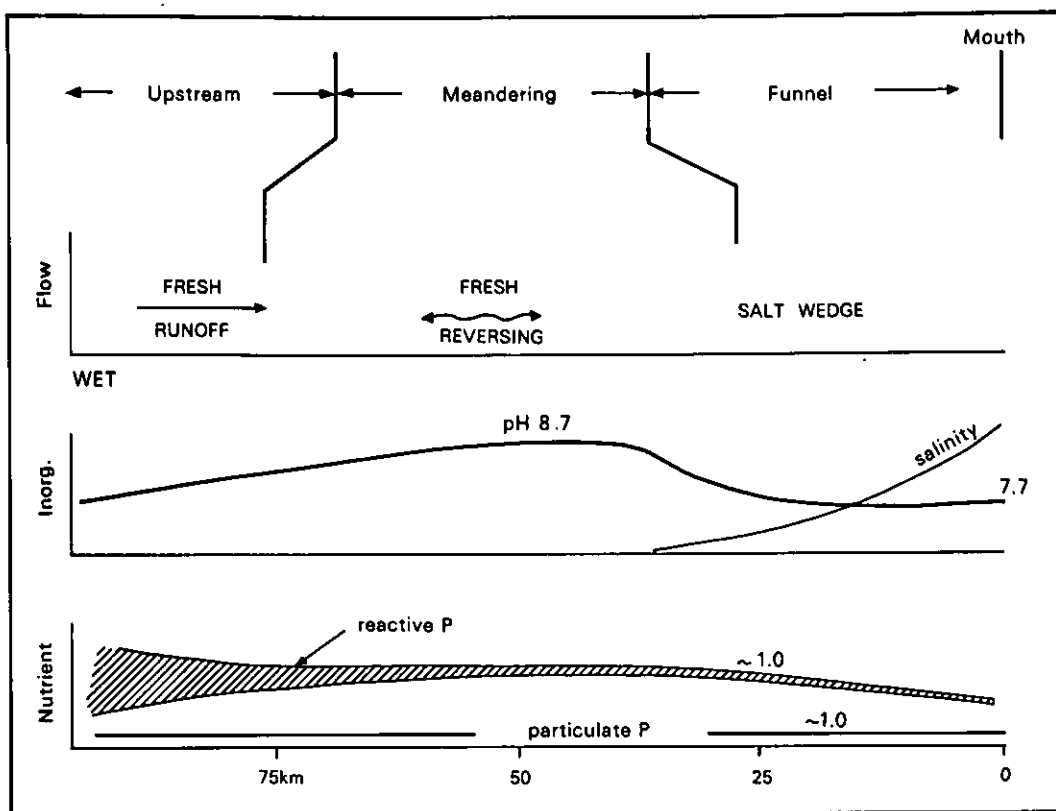


Figure 23a: Organic water chemistry, South Alligator River: wet season, March 1984

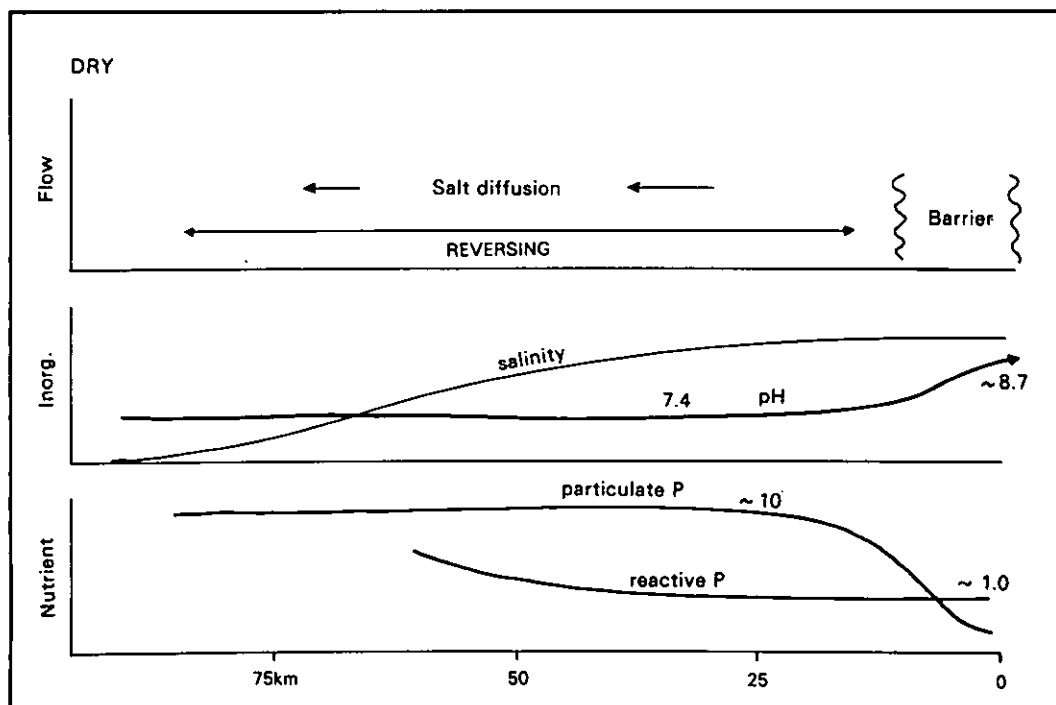


Figure 23b: Organic water chemistry, South Alligator River: dry season, 1984

2.4 Sediment Movement in the Tidal River

In common with other large macrotidal rivers in Northern Territory, concentrations of suspended sediment appear to change oddly from wet to dry season. Floodwater inflow to the upstream non-reversing segment, in the wet, carries less than 100 mg/litre in highly turbulent flow. During the dry, the water is highly turbid and sediment concentrations above 2000 mg/litre have been measured. The low concentration in floodwaters reflects a relatively low rate of sediment transport from the catchment; the high dry-season concentration represents sediment trapped within the river, moving to and fro with the highly turbulent tide. Thus, the sediment flux through the river is indicated by freshwater flood inputs, and cannot be gauged at all during the dry season. Sedimentary processes in the channel combine the wet season flood inputs with the effects of tidal reworking.

Reversing flow dominates most of the tidal river for most of the year, even during the wet season (Chapter 2.2). High velocities of tidal flow (Figures 17 and 18) combined with high sediment concentrations provide potential for changing channel form through erosion and deposition. Possible rates of such changes are discussed below. Here we review the sediment data more closely.

Figure 24 indicates particle size characteristics of river bed and overbank sediments. Fine to medium sands (and sparse gravel-sized particles) are found on the bed of the channel and are evidently moved as bed load. Fine sand is encountered in levees discontinuously flanking the banks of the upstream segment of the tidal channel, but apart from these isolated occurrences sand is not a feature of overbank deposition. Sediments filling old channel courses, predominantly clays with minor silt, are considered typical of overbank sediments.

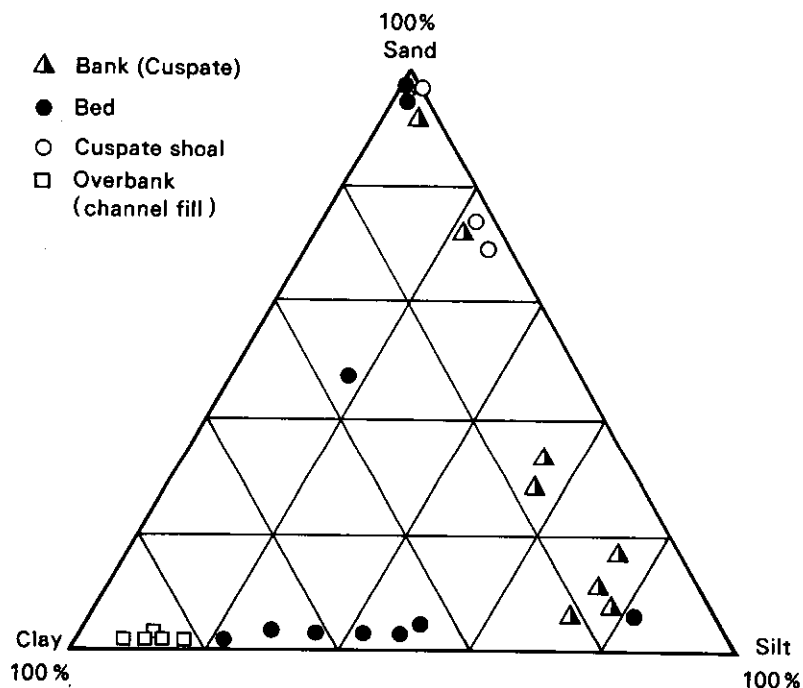


Figure 24: Particle size characteristics of river bed and bank samples and overbank sediments

In the dry season there are spatial and temporal variations in suspended sediment concentration, which vary along the length of the river or across the river cross-section, and at any one point vary through tidal cycles. Figure 25 illustrates some of this variation. There is substantial variation in inorganic suspended sediment over tidal cycles; the

range of variation at 4 sites along the river for August 1985, included in Figure 25, was from 48 to 1095 mg/l at 5 km from the mouth; 80 to 3049 mg/l at 42 km from the mouth; 105 to 3150 mg/l at 58 km from the mouth and 620 to 3360 mg/l at 75 km from the mouth. The pattern of variation over tidal cycles varies a little from one site to another, and presumably between neap and spring tides.

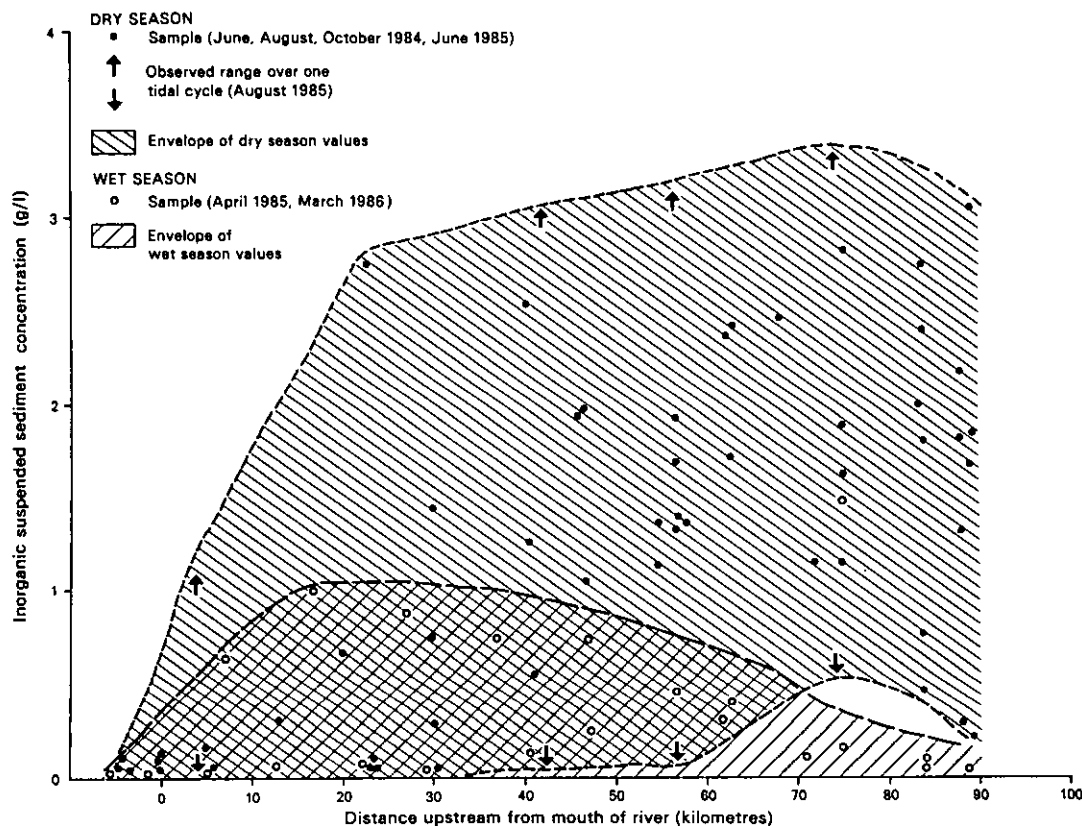


Figure 25: Observations of suspended sediment concentrations along the South Alligator River. Wet season samples below 70 km are from tidally-reversing floodwaters.

Dry season observations from August 1985 and July 1983 show a positive correlation between suspended sediment concentration and velocity of flow, with highest concentrations occurring at or close to peak velocities on ebb and flood. Despite peak flood velocities exceeding peak ebb velocities, the suspended sediment concentrations on almost all tides for which there are comparable observations were greater on the ebb. Concentrations are lowest shortly after slack water. We know little about cross-sectional variation in suspended sediment concentration, but have observed significant increases in concentration with depth in the water column. In August 1985, concentrations 75 km from the mouth at slack high varying from 985 mg/l at 0.1 m depth to 1907 mg/l at 1.5 m, 2753 mg/l at 4.0 m and 3242 mg/l at 8.0 m (R Vertessy and P Ward, pers. comm.). This more turbid water can be seen billowing up in eddies from depth.

Suspended sediment was measured during the water chemistry surveys. Despite the fact that these were taken at different stages of the tide the pattern for the dry season is one of increasing inorganic suspended sediment concentration upstream, at least to 75 km (Figure 25). This trend is consistent with the range at individual sites over tidal cycles. The contrast with wet season flood results again shows the major role of tidal turbulence in generating suspended sediment turbidity. In the wet season floods the inorganic suspended sediment concentrations are much lower, and were nowhere above 500 mg/l even in the tidally reversing region (Figure 25).

Organic suspended sediment concentrations (defined as volatiles by weight loss on ignition) are lower than inorganic suspended sediment concentrations but tend to vary in relation to the latter. The percentage of the total suspended sediment that is organic decreases upstream. Organic as a percentage of inorganic suspended sediment was 20 ± 12 per cent in April (1985), 20 ± 16 per cent in June (1984), 15 ± 5 per cent in June (1985), 20 ± 4 per cent in August (1984), 17 ± 5 per cent in August (1985) and 20 ± 10 per cent in October (1984).

High spatial and temporal variability of suspended sediment loads precludes any attempt to determine fluxes of sediment past points in the tidal river. Obviously very large quantities of sediment are moved back and forth by the reversing tide. However it is interesting to note that the South Alligator River shows an increasing asymmetry of tides with distance upstream, and hence greater tidal velocities (up to 50 per cent greater) on the contracted flood tide than on the protracted ebb tide, as observed on the Ord River (Wright *et al.*, 1973). This can be particularly significant in terms of net suspended sediment flux (see Chapter 6).

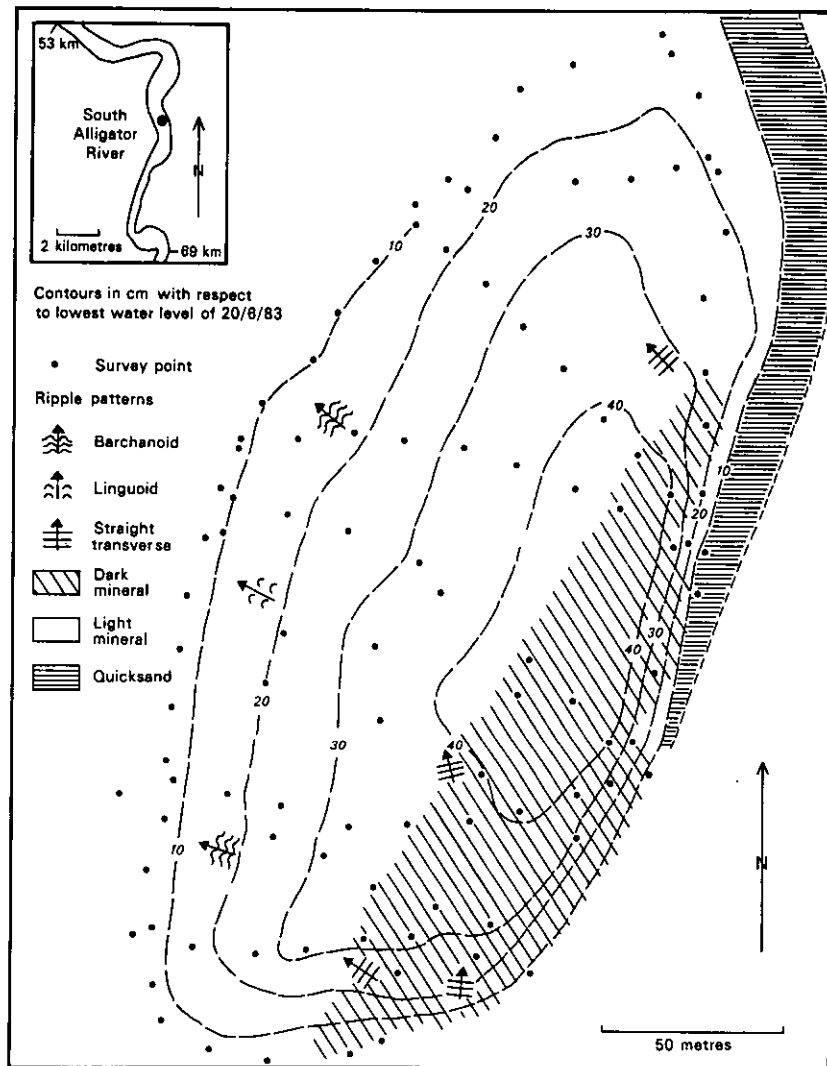


Figure 26: Detailed survey of morphology and bedforms of a mid-channel shoal in the cusped meandering section of the South Alligator River (at 60 km, June 1983)

The pattern of shoals within the river has been described briefly by Messel *et al.* (1979, 1982). At the mouth of the river there are several small sandy shoals which are shelly and contain marine infauna. The South Alligator River does not have long shoals parallel to the direction of flow towards the mouth as observed in other rivers and estuaries of great tidal range, i.e. Ord River, Western Australia and Broad Sound, Queensland, except that there is one long island on the west of the estuarine funnel. There are then no more shoals, except for a narrow bank attached to the sharp bend 15 km from the mouth, until the cusped meandering segment of the river, where there are mid-channel shoals as well as shoals attached to the point bars of the cusped meanders. These are exposed at low tide; they are composed of laminated sand and mud, and show distinct bedforms. They are similar to meander-belt deposits described from the Ord River (Coleman and Wright, 1978).

The pattern of the shoals changes seasonally, and probably from year to year. This mobility is evident from overflights along the river during the course of our project and is substantiated by the accounts of local boatmen.

A detailed investigation of one mid-channel shoal at low tide (Figure 26) revealed that it was ovate in shape with a relief of more than 50 cm. It was dominated, after the ebb tide, by flood-tide dominated bedforms, with a steep upstream face and a more gradual downstream face with barchanoid, linguoid and straight transverse ripple patterns. Fluid 'quick sand' occurs around the still submerged perimeter of the shoal. The 'quick sand' overlying rippled sand, probably represents deposition during the previous tide. These observations of sediment movement in the tidal river channel are linked to bank and overbank processes in the next section.

2.5 Bank and Creek Stability

Although the stratigraphic evidence indicates that large quantities of sediment have accumulated in the coastal and deltaic-estuarine plains of the South Alligator River during the Holocene, there are presently relatively few sites along the banks of the river where rapid recent accumulation of sediment is evident. Indeed even where the muddy banks of the river have a narrow littoral band of mangrove it is not unusual to observe active 'cliff' erosion of intertidal muds. Survey of banks at low tide has revealed that along more than half of the river erosion appears to be predominating over deposition.

Figure 27a is a map of eroding, accreting and neutral (or indeterminate) banks, determined by rapid survey from a boat at low tide. Most of the survey was conducted in the late wet 1986, and these observations supplemented earlier work in the late dry of 1984. Processes operating on river banks are likely to consist of alternate periods of cut and fill, and it is not known for how long particular stretches of bank may be in a cut phase, before reverting to fill. This rapid survey technique indicates that at present cut predominates over fill. Figure 27b summarises changes observed over the period for which aerial photographs are available. Later in the report (Chapter 6) we examine this over a longer time framework and investigate the effect that internal adjustments of channel morphodynamics will have on bank erosion or deposition.

The predominant process of bank erosion is by cliffing. Extensive recent cliffing of tidal deposits in King Sound, Western Australia has been described by Semeniuk (1981), and similar bank retreat is occurring in the South Alligator River. Mass slumping of mud on the river bank forms cliffs generally 1 to 2m high, only rarely exceeding that height. Such cliffing is most common at mid-tide levels. In the estuarine funnel there is evidence of cliffing at higher levels on banks facing the northeast, which may result from wave action. Much of this lower part of the river has a

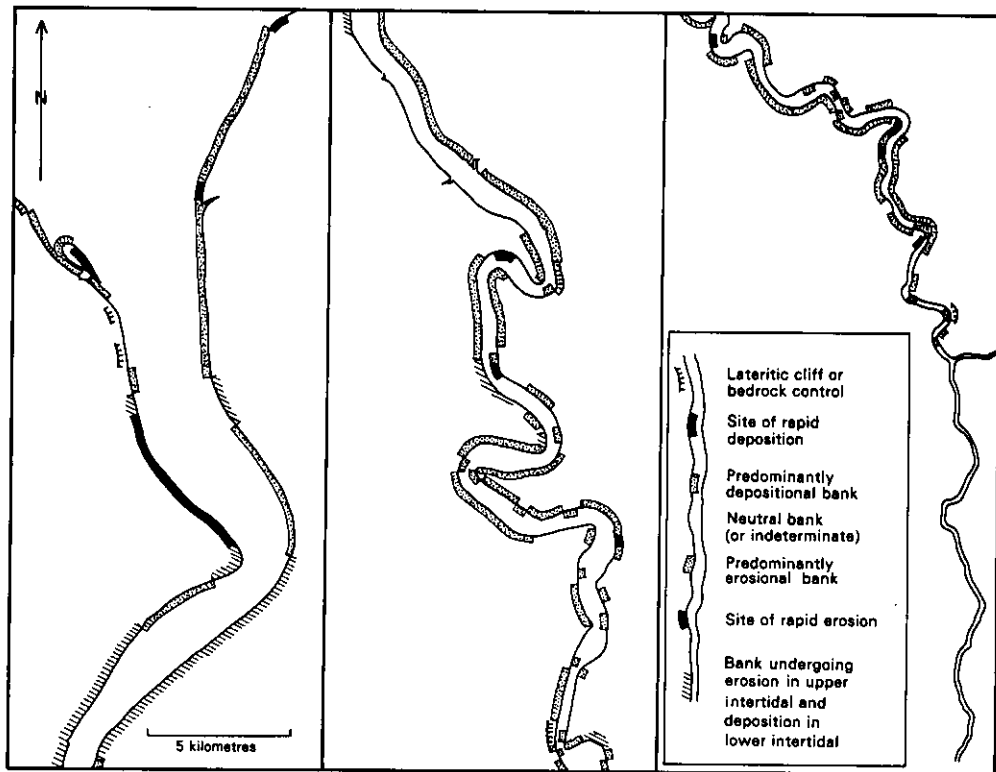


Figure 27a: Eroding, accreting and neutral (or indeterminate) banks of the South Alligator River

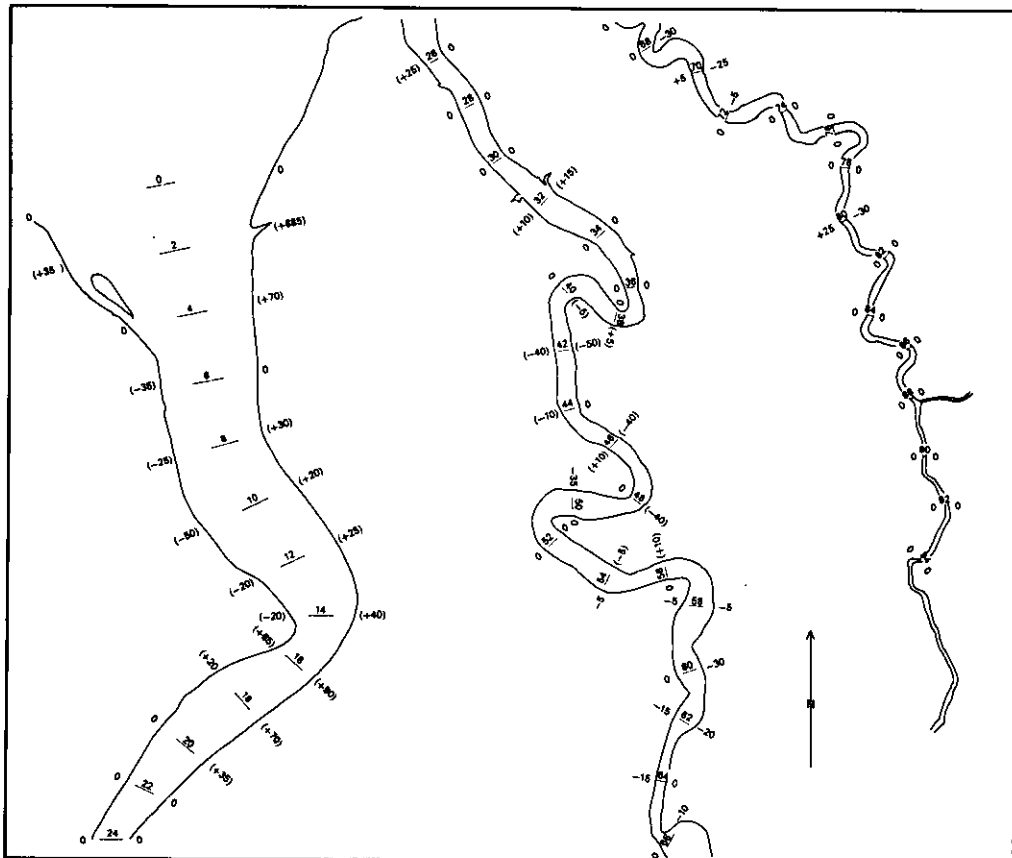


Figure 27b: Bank erosion or accretion in metres, between 1950 and 1983, determined from aerial photographs

bank profile in which cutting occurs at upper tidal levels and sediment deposition is occurring at lower tidal levels. Bank failure is probably initiated by tidal scour during the dry season, and has been observed during flood recession in the upper cusped segment in the wet. Our stratigraphic studies (Chapter 4) show that many of the sediments forming the banks are several thousand years old, and that these are being cut by present river erosion. This is particularly true in the cusped segment, where erosion is most widespread (Figure 27). These older deposits are typically bluish-gray, whereas modern muds are lighter brown and often form shallow veneers over the older sediments, equivalent to a modern veneer described from King Sound (Semeniuk, 1982).

Two other forms of bank erosion are sculpturing by ephemeral creeks and slumping. In the sinuous meandering reach of the river these ephemeral creeks draining the banks are closely spaced together and degradation of their interfluvies leads to bank retreat. Slumping becomes especially prominent in the upstream reach of the river, where the low width to depth ratio maintains steep banks and bank slumping is evidently frequent. The prominent mid-tidal mangrove Sonneratia lanceolata in this part of the river does not appear to lend much stability to the bank and can often be seen having slumped into water too deep for it to survive. The slumping of the bank leads to a prominent bench, in mid to upper tidal levels, which becomes an important mangrove habitat in its own right.

Near the mouth the infrequent accretional banks are characterised by a well-developed mangrove forest. Typically well spaced stands of Sonneratia alba on a gently sloping bank indicate gradual build out. Where erosion is prominent mangrove zonation is truncated with the more landward zones of mangrove being exposed on the shore (see also Davie, 1985, and similar accounts from elsewhere by Thom et al., 1975 and Semeniuk 1980a).

Chapter 3

Geomorphology

- 3.1 Methods
- 3.2 Morphologic Patterns
 - 3.2.1 Coastal Plain
 - 3.2.2 Deltaic-estuarine Plain
 - 3.2.3 Alluvial Plain
- 3.3 Morphologic Processes and Change

3. GEOMORPHOLOGY

3.1 Methods

Morphologic units of the South Alligator River have been mapped from aerial photographs and are shown in the accompanying 1:80,000 geomorphologic maps. In particular we used 1:25,000 colour aerial photographs of the area taken by the Australian Survey Office in 1983 with additional use of 1975 1:25,000 photographs, and 1:5,000 photographs of the southern end of the river system taken in 1981. This photography has been extensively ground truthed along numerous traverses across the plains.

Elevation data have been obtained from accurately levelled surveys undertaken for the project by the Australian Survey Office (see Woodroffe *et al.*, 1985a). All elevational data are quoted with respect to one datum, namely the Australian Height Datum, AHD. This is a datum surface derived Australia-wide in 1971 from simultaneous adjustment of the 2-way levelling network to mean sea level observed from tidal records for the period 1/1/66-31/12/68 at 30 tide gauges around Australia. Darwin was one of the stations used to control this adjustment and thus at Darwin AHD approximates true mean sea level.

Topographical data can be extended over a wider area by extrapolation of known variation along surveyed traverses to rectified photomaps of the river system. These exist for the central section of the South Alligator plains at a scale of 1:25,000, based on black and white photography taken in 1979. Photogrammetrically interpreted spot-heights on these have assigned heights with respect to AHD, to the nearest 0.5 m. Our more accurate control from the surveyed profiles indicates that these spot-heights are unreliable; nevertheless the contouring and relative height on these rectified photomaps indicate general gradients. Further rectified photomaps are available for the southern part of the plains at a scale of 1:5,000 with spot-heights of 0.1 m and contoured at 2 m intervals. The photographs were taken in 1981, and where accurately levelled topographic control is available from surveys undertaken by the Australian Survey Office both for this project, and previously for ANPWS, the photogrammetrically determined heights were found to be reliable to about 30 cm. Contouring of this part of the plains on the photomaps helps define the morphologic units described below. Vertical relationships between AHD and tidal points such as MHWS (Mean High Water Springs), MHWN (Mean High Water Neaps), and HAT (Highest Astronomical Tide) are important for understanding the geomorphology and subsurface stratigraphy of the tidal river and flood-plain system. These height relationships for Darwin and from water level records at the Arnhem Highway bridge over the South Alligator River are summarised in Figure 28.

Sediments underlying the various morphologic units were examined in shallow cores, and in the coring and augering described in the stratigraphic section (locations shown in Figure 39). Surface texture, structure, microtopography and cracking patterns were described. By combining morphologic and stratigraphic data, major units can be defined in morphostratigraphic terms. The morphologies described in this chapter are linked with stratigraphic data in the next, to define stratigraphic and morphostratigraphic units used in interpreting the history of the system.

3.2 Morphologic Patterns

The plains and wetlands of the South Alligator River can be subdivided into three morphologic provinces on the basis of landform, sediment patterns, and the dominant processes in operation. These provinces are mapped in Figure 29 and will be referred to as: (i) coastal plain; (ii) deltaic-estuarine plain; and (iii) alluvial plain. The deltaic-estuarine plain straddles the tidal river, from near the mouth of the estuarine funnel to the limit of the upstream tidal segment.

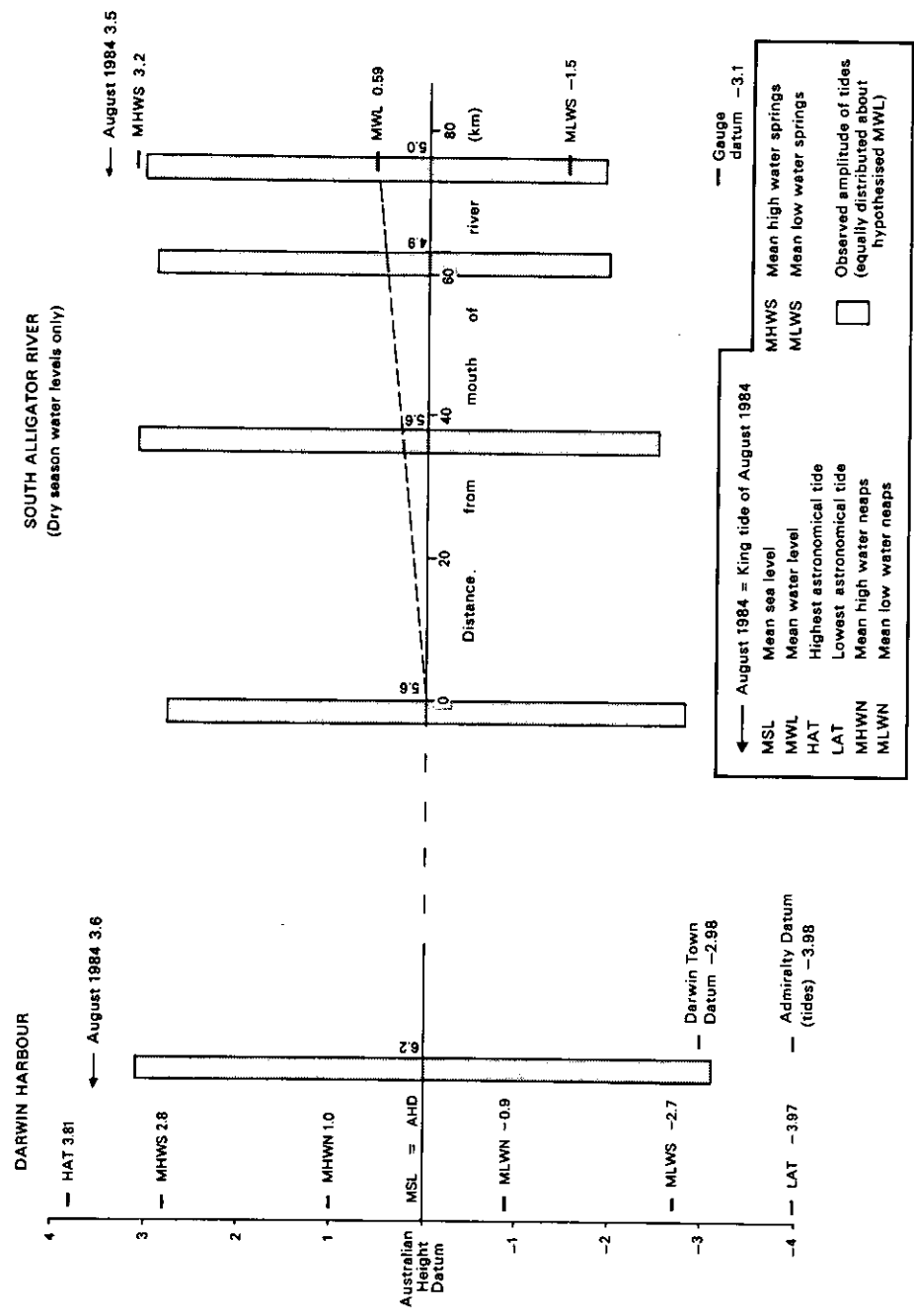


Figure 28: Definition of Australian Height Datum and its relation to surveys along the South Alligator River. MWL calculated as the mean of daily highest and lowest water levels using dry season (June-November inclusive) data for period September 1982 - August 1984 for high water and September 1983 - August 1984 for low water (1982-83 readings unreliable for low water). MHWS and MLWS defined as in National Tide Tables using two daily tides from September 1983 and June - August 1984. Tidal ranges from several months of observation (R. Vertessy, pers. comm.).

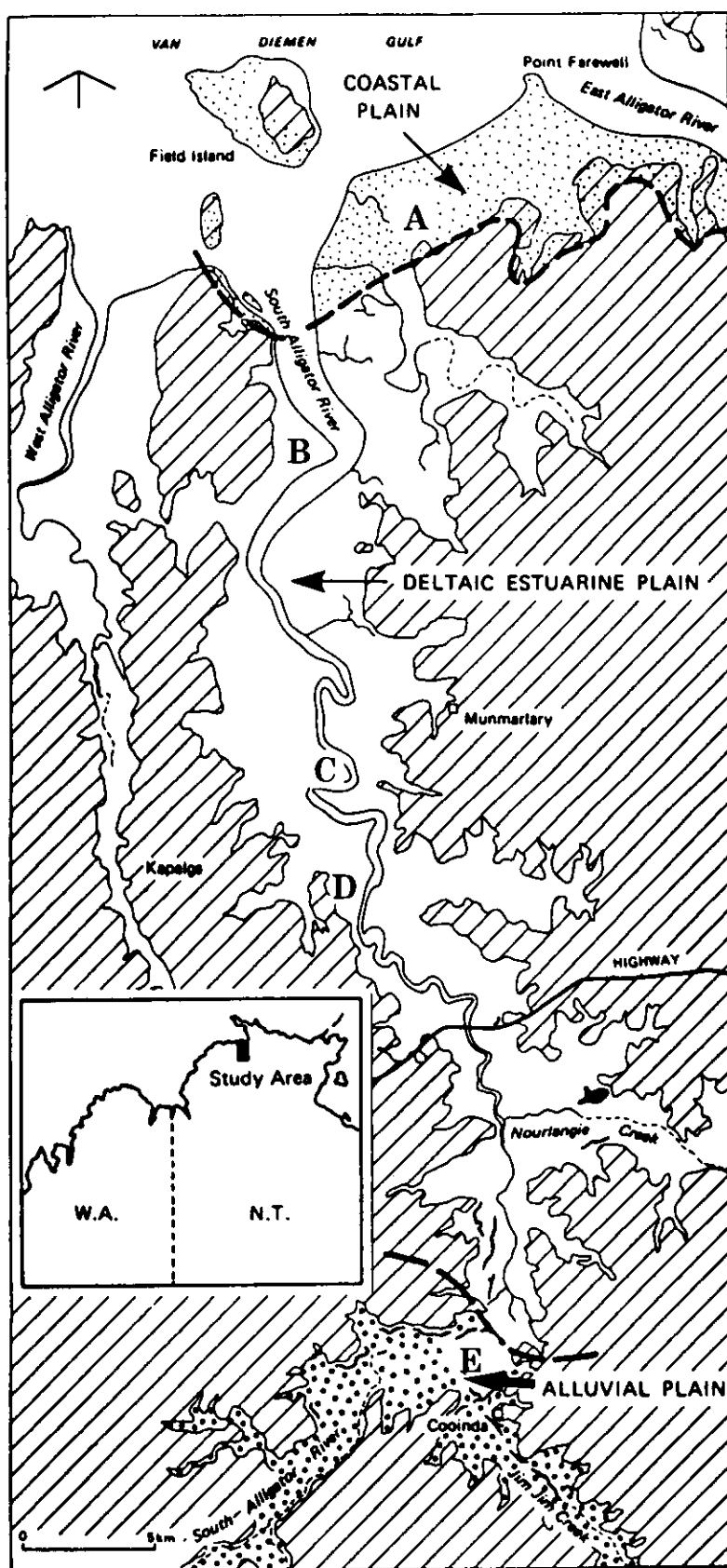


Figure 29: Morphologic provinces of the South Alligator River (after Woodroffe *et al.*, 1985a)

A number of morphologic units are recognised within each province. These are described below and are mapped in detail at a scale of 1:80,000 on the accompanying geomorphological map sheets. Most of the morphologic units have counterparts amongst CSIRO land system units, and subdivisions of the Quaternary on geological maps, of the region. Our mapping, however, is more detailed, and differs from these because of our interests in surface morphology and stratigraphy. Equivalence of our units to the CSIRO land systems in particular is shown in diagrams of selected areas of the plains, and is discussed after description of the morphologic units.

3.2.1 Coastal Plain Province

The coastal plain extends east of the mouth of the South Alligator River as a chenier plain 4 to 5 km wide. A representative segment is shown in Figure 30. Two chenier ridges of shelly sand are lodged upon fine sandy muds which form the plain. Similar chenier plains, frequently with many more ridges, extend along the south coast of van Diemen Gulf west of the Alligator Rivers (Williams, 1969b; Clarke *et al.*, 1979).

The seaward discontinuous chenier ridge lies about 200 m to the rear of the coastal mangrove belt. It stands about 1 m above the adjacent plains and is up to 25 m wide. It has a scattered tree cover, with Bombax ceiba prominent, and has several large shell middens of the bivalve Anadara granosa. A second chenier ridge up to 60 m wide lies to the rear of the plain, in places deposited directly onto the upland surface.

Within the coastal plain we identify two groups of morphologic units, a tidally-influenced group, which is not restricted to the coastal plain, as a counterpart of this unit extends up the tidal river, and a coastal plain group. These are described below:

I Tidally-influenced group.

- (a) Mangrove unit. The seaward margin of the coastal plain has a belt of zoned mangrove forest, about 250 m wide and rising from mid-tide level to about MHW level (-0.3 to 2.5 m AHD). This is referred to as the Mangrove unit, and is the only morphologic unit in the region which we define in terms of vegetation as well as elevation. The reason for using a vegetation criterion is that the mangroves are represented stratigraphically by a distinctive organic-rich mangrove mud. Furthermore where substrate occurs in the upper part of the tidal range, except where it is cliffed or clearly undergoing erosion, it is generally colonised by mangroves. The mangrove unit extends up the tidal river, although it is narrow and discontinuous beyond the lower part of the estuarine funnel except at a few points of progradation. Figure 10 indicates the extent of the unit and Figure 11 shows its species composition.

Mudflats at the coast extend seawards of the mangrove, passing below low tide level. These and their lower intertidal and subtidal counterparts within the river are not designated as a morphologic unit, although their sediments are recognised stratigraphically (Chapter 4).

- (b) Upper Intertidal and Salt Mudflat unit. To the rear of the mangrove is a saline mudflat, bare or with localised samphire. The mudflat is partly inundated by spring tides, but as we are uncertain that it is covered everywhere by highest astronomical tides we avoid defining it as intertidal or supratidal and refer to it as the Upper Intertidal and Salt Mudflat unit. This morphologic unit, like the mangrove unit, extends up the tidal river through the deltaic-estuarine plain.

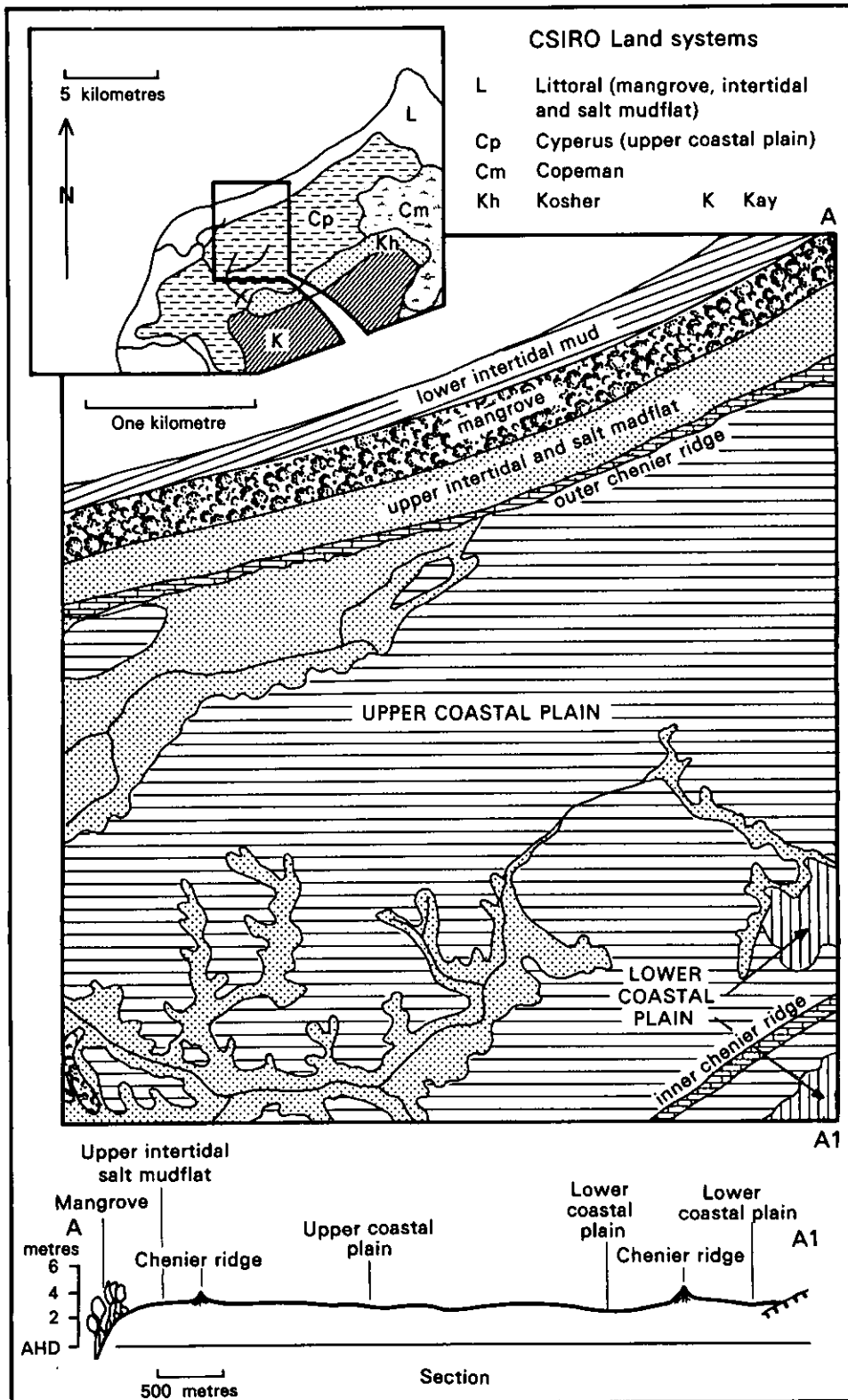


Figure 30: Coastal plain on the east side of the South Alligator River mouth. Inset map shows CSIRO land-systems mapping (from 1:250,000 map, Story et al., 1969). The larger geomorphologic map is based on 1:25,000 aerial photographs. Levelled cross-section A-A' shows surface topography.

The relationship between Mangrove and Upper Intertidal and Salt Mudflat units on the Coastal Plain is shown in Figure 30. The relationship in the estuarine funnel is shown in Figure 33, which indicates extensive Salt Mudflat on the western side of the estuarine funnel. There are also extensive anastomosing networks of Upper Intertidal and Salt Mudflat on the eastern side of the estuarine funnel (see the 1:80,000 geomorphologic map). These are not all peripheral to active tidal creeks; they divide the floodplain units into a complex mosaic.

II The Coastal Plain Group

- (a) Upper Coastal Plain. Most of the Coastal Plain of the South Alligator River falls into the Upper Coastal Plain unit. This is particularly the case landward of a discontinuous chenier ridge which lies about 200 m to the south of the mangrove unit. The Upper Coastal Plain occurs above an elevation of 2.5 m above AHD. The surface sediments are black cracking freshwater clays, typically bearing a vegetation of sedges and grasses.
- (b) Lower Coastal Plain. Lower-lying areas of coastal plain, away from tidal influence are found particularly to the rear (south) of the plain. They are not extensive in the South Alligator coastal plains but become more extensive towards the East Alligator River. The vegetation contains more herb species and the areas remain wet for a larger proportion of the year than the Upper Coastal Plain. A small area of Lower Coastal Plain is traversed by the profile shown in Figure 30 and it occurs at an elevation just below 2.5 m above AHD. Stratigraphic study shows that the coastal plain is progradational, formed upon sediments which become younger towards the sea (see Chapter 4).

3.2.2 Deltaic-Estuarine Plain Province

The deltaic-estuarine plain is the most extensive of the three morphologic provinces, extending upstream about as far as the tidal limit of the South Alligator River (Figure 29). As shown in Chapter 2, the river channel is influenced by both tidal and fluvial processes, and this has been true throughout the development of the plains. The plains are referred to as 'deltaic-estuarine' as a reflection of these two factors. The transition between this and the coastal plain occurs where wet-season flood discharges appear to have negligible overbank effect.

The geomorphology of the deltaic-estuarine plain changes between its downstream and upstream limits, partly reflecting progressive change of the river and its wet-season flood profile. Four channel types recognised in the South Alligator River were outlined in Chapter 2.2. These are reviewed again, as they are mentioned frequently from here on. Figure 31 shows schematic features of the four channel types, viz. estuarine funnel, sinuous, cusped, and upstream segments. As these occur in many of the large macrotidal rivers in northern Australia, they are described in the following general terms.

- (a) Estuarine funnel: Broad at the mouth, typically flanked by a prograding coastal plain with zoned mangrove fringe and often with chenier ridges, diminishing in width upstream negative-exponentially, and having a few large dog-leg bends. Shoals or mangrove islands may occur near the mouth. Mangrove forests fringe both banks, more or less equally.

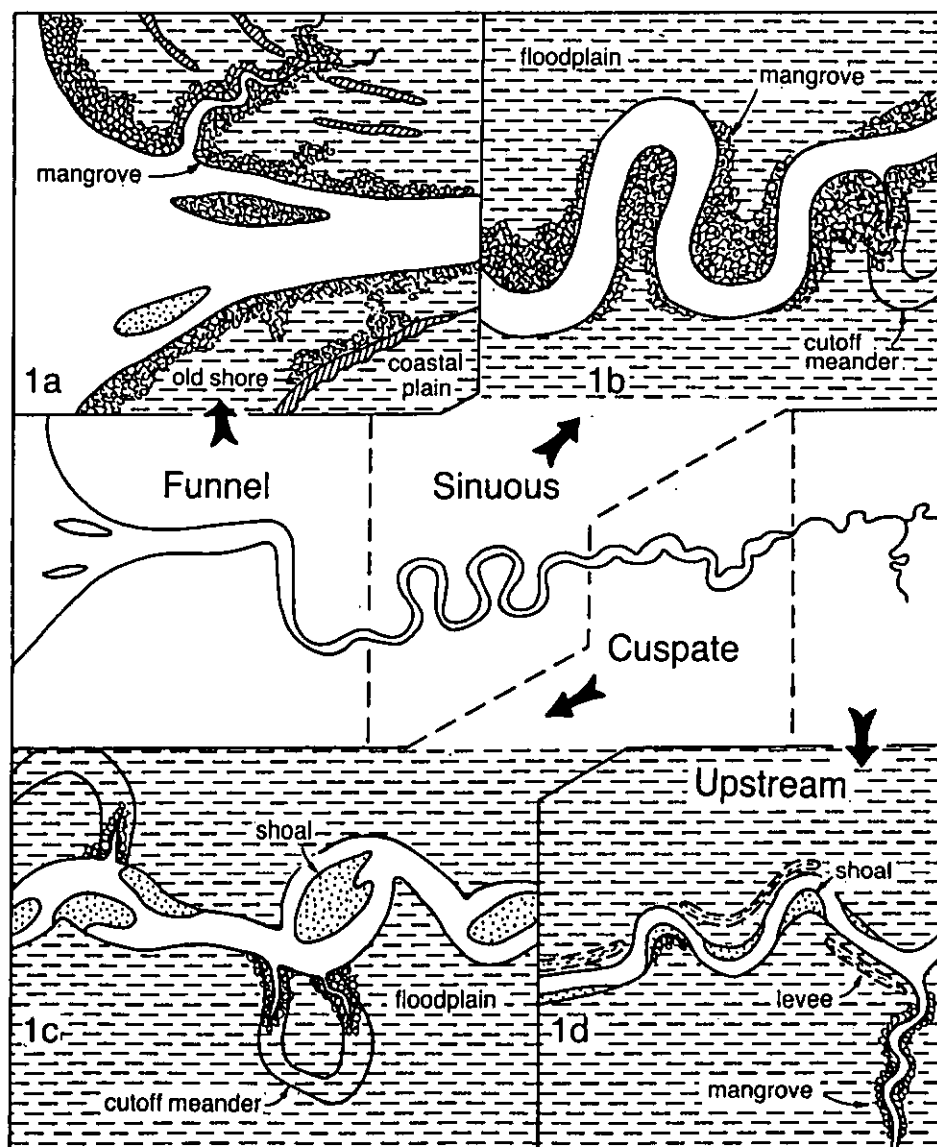


Figure 31: Schematic tidal river of the Northern Territory type showing characteristics of different river segments.

- (b) Sinuuous bends: These are one of two channel forms which can occur within the meandering channel segment identified in Figure 16 (Chapter 2.2). They resemble meanders of fluvial rivers in their sinuous form, and sediment accretion on the insides of bends is reflected by occurrence there of mangrove forests, often substantial. The outsides of bends are often cliffed and mangroves tend to be sparse or absent. Mid-channel shoals are usually absent.
- (c) Cuspate bends: This is the second channel form which can occur in the meandering segment. Insides of bends are distinctly pointed and wide reaches can occur between successive cusps. Mid-channel shoals are common, and there are also shoals attached to the banks of the cuspate meanders. Clipping may occur on both banks, and mangrove fringes tend to be sparse or absent.
- (d) Upstream tidal channel: Characterised by alternating straights and bends, often irregularly spaced, the channel may have shoals

in the typical 'point-bar' position tied to the insides of bends and extending in the down-river direction. Mangroves may occur on insides of bends, often as a narrow fringe.

Morphodynamic relationships between these channel types are discussed later (Chapter 3.3 and Chapter 6).

The greater part of the deltaic-estuarine plain consists of floodplain, commonly called the black soil plain, surfaced by black cracking freshwater clays. Most of this plain is higher than the highest spring tide levels. It is saturated or under water for 3-4 months in most wet seasons, due to water lying on the plains rather than overbank flooding. Lower-lying areas remain wet for 6 months or more.

We recognise a number of morphologic units on these floodplains which can be divided into those of higher elevation and shorter periods of flooding, the Upper Floodplain Group, and the lower-lying, longer inundated, Lower Floodplain Group. We also recognise morphologic units of the Backwater Swamp Group. Topographic relationships between these units are shown in selected cross-sections in Figure 32.

I Lower Floodplain Group.

There are substantial areas of the deltaic-estuarine plain which are low-lying and which have standing water for 6 months or more of the year. These areas often have a seasonal herbaceous vegetation, or are dominated by flood-tolerant sedges of the genus Eleocharis. The surface sediments of this group of units are typically light brown clays often with small carbonate nodules. The ground surface cracks in the dry season when the water table has dropped below the ground surface. Cracks are generally less than 2 cm across, and polygons are 10-20 cm across.

Subdivision of the Lower Floodplain group is possible on the basis of features discernible on the aerial photographs, in particular previous courses of the river channel and tidal creeks. These are referred to by us as paleochannels if they are considered to have been previous courses of the main channel, or paleocreeks if they were previously minor creek systems.

Within the Lower Floodplain group we recognise four morphologic units, (a) Paleochannel-Lower Floodplain; (b) Paleochannel-Upper Intertidal and Salt Mudflat; (c) Paleocreek-Lower Floodplain; and (d) Ill-drained Depressions. These are described below:

- (a) Paleochannel-Lower Floodplain. This unit represents areas of the floodplain that were previously part of the course of the main river, but which have been infilled and now are seasonally inundated by freshwater and have surface sediments and vegetation cover typical of the Lower Floodplain group.
- (b) Paleochannel-Upper Intertidal and Salt Mudflat. This unit is similar to that described above, except that it generally occurs closer to the present river channel and is still under tidal influence. As mentioned above, both the Mangrove unit and the Upper Intertidal and Salt Mudflat unit, described from the coastal plain, extend along the tidal river. This Paleochannel unit is also tidally-influenced and has a similar relationship to MHWS as the Upper Intertidal and Salt Mudflat unit described from the coastal province. The areas are morphologically distinct because they infill paleochannels. However they are exceptional within the Lower Floodplain group in being largely bare of vegetation and having a surface of saline, flocculated clay.

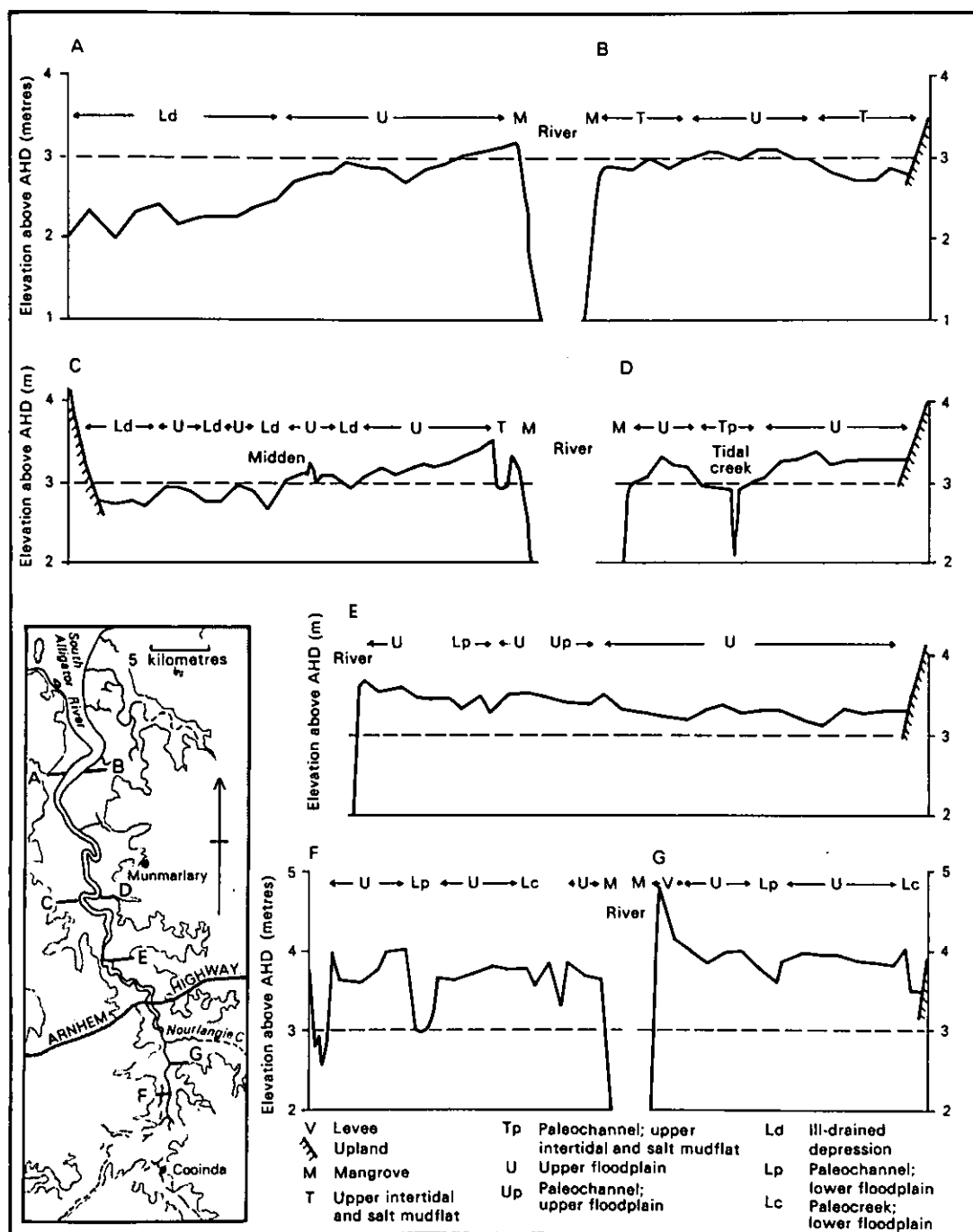


Figure 32: Cross-sectional traverses showing relationships between morphologic units and elevation at various points along the river

Table 4

Principal morphologic units of coastal, deltaic-estuarine and alluvial plains

Morphologic definition	Inundation characteristics	Surface sediment characteristics	Occurrence	Elevational range (m AHD)	Vegetation
Tidally-Influenced Group					
Mangrove	Intertidal coast and riverbank vegetated by mangroves	Tidally-flooded, regular inundation near coast; irregular inundation up river	Surface few centimetres of light brown oxidised clay grades into bluish-gray clay with abundant organic fragments	Fringing coastal plains extending up estuarine funnel, and discontinuously through sinuous and cusped channel segments; narrow fringe in upstream segment	-1.0-3.7 see figure 3.3.1b for details Mangrove spp.
Upper Intertidal and Salt Mudflat	Bare or poorly vegetated saline flats at or near highest tide level	Irregular flooding, by highest spring tides (or surges)	Light to grayish-brown vesicular flocculated saline clay	Landward of mangrove on coastal plain and fringing tidal creeks up river	Bare or samphire
Coastal Plain Group					
Lower Coastal plain	Low lying ill-drained depressions to rear of coastal plain	Wet season flooding, persists >6 months p.a.	Dark gray clay, cracked	To rear of coastal plain	<2.5 Pandanus scrub near upland, and herbaceous
Upper Coastal plain	Better drained sedge-covered coastal plain	Wet season flooding, <6 months p.a.	Black clay, massively cracked	Over much of coastal plain, especially between chenier ridges	2.5-3.0 Sedges and grasses
Lower Floodplain Group					
Paleochannel; Lower Floodplain	Former river channel course, abandoned and infilled, but seasonally inundated	Wet season flooding, persists >6 months p.a.	Light brown to black clay, with small carbonate nodules, fine cracking pattern	In cutoff former river channel courses	generally <3.0 Herbaceous vegetation or bare
Paleochannel; Salt Mudflat	Former river channel course, abandoned, infilled, and subject to tidal influence	Irregular tidal influence	Light brown flocculated saline clays	In cutoff former river channel courses, close to present river where tidal influence exerted	generally <3.0 Bare or samphire
Paleochannel; Lower Floodplain	Sinuous former creek system now beyond tidal influence	Wet season flooding persists >6 months p.a.	Light brown to black clay, fine cracking pattern	Where ephemeral streams enter floodplain or on wide expanses of floodplain beyond tidal influence	generally <3.0 Low herbaceous vegetation often Eleocharis dulcis
Ill-drained depression	Low-lying poorly drained	Wet season flooding persists >6 months p.a.	Light brown to black clay, fine cracking pattern	Low-lying areas of floodplain distant from main river	<2.5 at mouth Often Eleocharis dulcis and other flood-tolerant plants

Table 4 continued.

	Morphologic definition	Inundation characteristics	Surface sediment characteristics	Occurrence	Elevational range (m AHD)	Vegetation
Upper Floodplain Group						
Paleochannel; Upper Floodplain	Former river channel course, abandoned and filled in until no topographic expression	Wet season flooding persists <6 months p.a.	Dark gray clay, coarse cracking pattern	In cutoff meanders where infill has led to loss of topographic expression	generally >3.0	Sedges and grasses
Paleocreek; Upper Floodplain	Former creek system now infilled	Wet season flooding persists <6 months p.a.	-	Restricted to few occurrences within Upper Floodplain unit	-	Sedges and grasses
Upper Floodplain unit	Sedge-covered floodplain	Wet season flooding, persists <6 months p.a.	Black organically-rich clay, massive cracking pattern and gilgai	Covers most of deltaic-estuarine plains	>2.5 at mouth >3.5 at tidal limit	Sedges and grasses <u>Pimbristylis</u> <u>tristachya</u> near river, <u>Oryza fatua</u> away from river
Backwater Swamp Group						
Lower Backwater Swamp	Prennially wet depression in reentrant	Perennially inundated, freshwater	-	Reentrants into uplands	-	Aquatics, including <u>Hymenachne</u> and <u>Nelumbo</u>
Upper Backwater Swamp	Depression in reentrant vegetated by paperbarks	Inundated for >9 months p.a.	Gray clay and loam, cracking pattern	Fringing some reentrants and dominating others	<2.5	Paperbarks, predominantly <u>Melaleuca leucadendra</u>
Alluvial Plain Group						
Lower Alluvial plain	Low-lying areas, poorly drained on Alluvial plain	Seasonally flooded by freshwater for >6 months p.a.	Black cracking clay and gleyed mud	Towards margin of Alluvial plain, and in reentrants	c3.5	Herbaceous vegetation and paperbarks, predominantly <u>Melaleuca leucadendra</u>
Upper Alluvial plain	Better drained Alluvial plain	Seasonally flooded by freshwater for <6 months p.a.	Silty alluvium	Over much of Alluvial plain	>3.5	Grassland, Savannah

- (c) **Paleocreek-Lower Floodplain.** This unit contains narrow anastomosing irregular or sinuous depressions on the deltaic-estuarine plain surface. There are five broad settings within which paleocreeks are found. Firstly they occur where ephemeral freshwater streams flow into the deltaic-estuarine plain, as at Brooks Creek. Secondly they occur as long meandering creeks over broad areas of floodplain, near Water Recorder Point. Isolated paleocreeks in this situation often grade into presently active tidal creeks nearer to the river. Thirdly, there are paleocreeks which previously drained into paleochannels. These are interpreted as previous tidal creeks associated with the main paleochannel, but which ceased to be active when the channel changed its position. The fourth category of paleocreeks are former courses of major tidal creeks that are tributary to the main channel. The most numerous examples of these occur around Nourlangie Creek, where there are many linear depressions evident from aerial photographs which appear to indicate several previous positions of Nourlangie Creek, or smaller creeks draining from Jarrahwingkoombarngy Swamp. The final type of paleocreek is found near the tidal limit to the South Alligator River, where minor creek-like depressions running away from the river are no longer tidally-active, and have been mapped as paleocreeks.
- (d) **Ill-drained Depressions.** This is the most extensive of the units of the Lower Floodplain group on the deltaic-estuarine plain. It consists of low-lying areas having no tidal connections, generally some distance from the river channel and consequently inundated for much of the year. Their low relative elevation must be due, as must that of the backwater swamps discussed below, to a lack of sediment deposition relative to the Upper Floodplain.

II Upper Floodplain group.

The Upper Floodplain group of morphologic units are flooded for 3-4 months of the year. They are generally underlain by massive, black, organically-enriched clays. The surface may have gilgai in the dry season with cracks up to 10 cm across, and polygons 30-50 cm across. The group carries a robust grass and sedge vegetation with the sedge Fimbristylis tristachya common near the river channel, and wild rice Oryza meridionalis common over much of the rest of the area. The Upper Floodplain group can be divided into (a) Paleochannel-Upper Floodplain, (b) Paleocreek-Upper Floodplain, and (c) Upper Floodplain unit. These are described below:

- (a) **Paleochannel-Upper Floodplain.** This morphologic unit is mapped from aerial photographs and includes previous courses of the main channel in which infilling appears to have continued to the extent that the channel is no longer topographically distinct from the surrounding Upper Floodplain unit. It appears to have a similar vegetation cover and to be inundated for the same length of time during the year as other Upper Floodplain areas.
- (b) **Paleocreek-Upper Floodplain.** This is a unit of very restricted occurrence which occurs where short sinuous sections of previous creek systems have infilled to a similar elevation as the adjacent Upper Floodplain with comparable vegetation cover.
- (c) **Upper Floodplain unit.** This morphologic unit covers the largest proportion of the deltaic-estuarine plain. It shows the typical characteristics of Upper Floodplain surface sediments and vegetation, and is generally the first part of the plain to dry after wet season flooding.

Table 5
Comparison of Morphologic units with CSIRO land systems
and geological map equivalents

	CSIRO land system and land unit equivalent (after Williams et al., 1969; Galloway et al., 1976)	Geological map equivalents (Needham, 1984)
Tidally-influenced Group		
Mangrove	Littoral, unit 2 (L2)	Mud, silt, mangrove (Qcm)
Upper intertidal and salt mudflat	Littoral, unit 1 (L1)	Clay, silt, mud, coastal (Qcp)
Coastal Plain Group		
Lower coastal plain	Copeman, unit 1 (Cm1)	Clay, silt, mud, coastal mud pans (Qcp)
Upper coastal plain	Cyperus, unit 1 (Cp1)	Silt, mud, coastal alluvium (Qca)
Lower Floodplain Group		
Paleochannel; lower floodplain	Copeman, unit 1 (Cm1,Cp2) Cyperus, unit 2	Silt, clay, abandoned channel (Qas)
Paleochannel; salt mudflat	Copeman, unit 1 (Cm1,Cp2) Cyperus, unit 2	Abandoned channel, coastal mud pans (Qcp, Qas)
Paleocreek; lower floodplain	Copeman, unit 2 (Cm2)	-
Ill-drained depression	Copeman, units 1 & 2 (Cm1, Cm2)	Clay, silt, mud, coastal mud pans (Qcp)
Upper Floodplain Group		
Paleochannel; upper floodplain	Cyperus, unit 2 (Cp2)	Silt, clay, abandoned channel (Qas)
Paleocreek; upper floodplain	-	-
Upper floodplain unit	Cyperus, units 1 & 4 Some Copeman, Unit 3 (Cp1, Cp4, Cm3)	Silt, mud, coastal alluvium
Backwater Swamp Group		
Lower backwater swamp	Copeman, unit 4 (Cm4, Pw2) Pinwinkle, unit 2	Clay, silt, mud, coastal mud pans (Qcp)
Upper backwater swamp	Pinwinkle, unit 1 (Pw1)	Clay, silt, mud, coastal mud pans (Qcp)
Alluvial Plain Group		
Lower alluvial plain	Copeman, Pinwinkle,	-
Upper alluvial plain	Fabian Flatwood	-

III Backwater Swamp group.

The Backwater Swamp group of morphologic units includes low-lying depressions which fill reentrants into the uplands. The two units recognised within this group are a Lower Backwater Swamp unit, and an Upper Backwater Swamp unit. These correspond to freshwater lagoons and paperbark swamps respectively, the distributions of which are shown in Figure 10. More detailed mapping of the Backwater Swamp group is shown on the 1:80,000 geomorphological map.

- (a) Lower Backwater Swamp. The Lower Backwater Swamp unit rarely dries out during the year; it is dominated by seasonal aquatic vegetation with scattered paperbark. We have only a few samples of surface sediments in this group but they appear to be dark gray clays with some fibrous root material.
- (b) The Upper Backwater Swamp. This unit is dominated by paperbark, particularly Melaleuca leucadendra. The sediments are similar to those of the Lower Backwater Swamp unit but contain more organic material. These areas are higher, often fringing the Lower Backwater Swamp unit, and do tend to dry out for at least a few months during the year.

Principal morphologic units of the deltaic-estuarine and coastal plains are summarised in Table 4. Table 5 shows equivalents in CSIRO and geological mapping of the area. Our mapping on the accompanying 1:80,000 geomorphologic map is more detailed than either CSIRO or geological maps over the plains. Nevertheless there are equivalents in CSIRO land units. Upper Coastal Plain and Upper Floodplain correspond to unit 1 of the Cyperus land system (and occasionally to unit 4 of the Cyperus and unit 3 of the Copeman land systems). Mangrove and Upper Intertidal and Salt Mudflat fall within the Littoral land system (units 2 and 1 respectively). Lower Coastal Plain and Ill-drained Depression represent unit 1 of the Copeman land system, while Paleocreeks are perhaps closer to unit 2 of that system. Unit 2 of the Cyperus land system in particular, but also unit 1 of the Copeman, contain Paleochannels. The Backwater Swamps are equivalent to units 1 and 2 of Pinwinkle. Plant communities typical of each unit are indicated in Table 4, but more detailed plant lists can be found in Story et al. (1969, 1976). Minor morphologic features not classified in Table 4 include cheniers, levées and middens. Cheniers typically occur on the coastal plain and have already been described; however, there are also several chenier spits found in the estuarine funnel, especially on the west bank of the river. These trend from north to south and have evidently been formed on flood tides. Low levées, composed of yellow silt and fine sand, occur intermittently along the banks in the upstream segment of the tidal river. These are best developed on the convex insides of bends and are colonised by quite large trees including Bombax ceiba. In addition to these levées on the presently active upstream segment of the river there are degraded remnants of levées beside paleochannels in both the upstream and cusped segments of the river. Shell middens occur sparsely on the Upper Floodplain, often on the degraded levées near sinuous infilled paleochannels, and include mollusc species typical of mangrove communities such as Telescopium and Polymesoda. The distribution of shell middens found by us during our work on the plains is shown in a later section (Figure 74).

Representative segments of the deltaic-estuarine province are mapped in Figure 33, 34 and 35 showing different relationships between Lower and Upper Floodplain units. Topographic cross-sections, illustrating the relationships of morphologic units are shown in Figure 32. These are discussed further in section 3.4. Relationships between our morphologic units and CSIRO land systems are indicated in these figures and their captions.

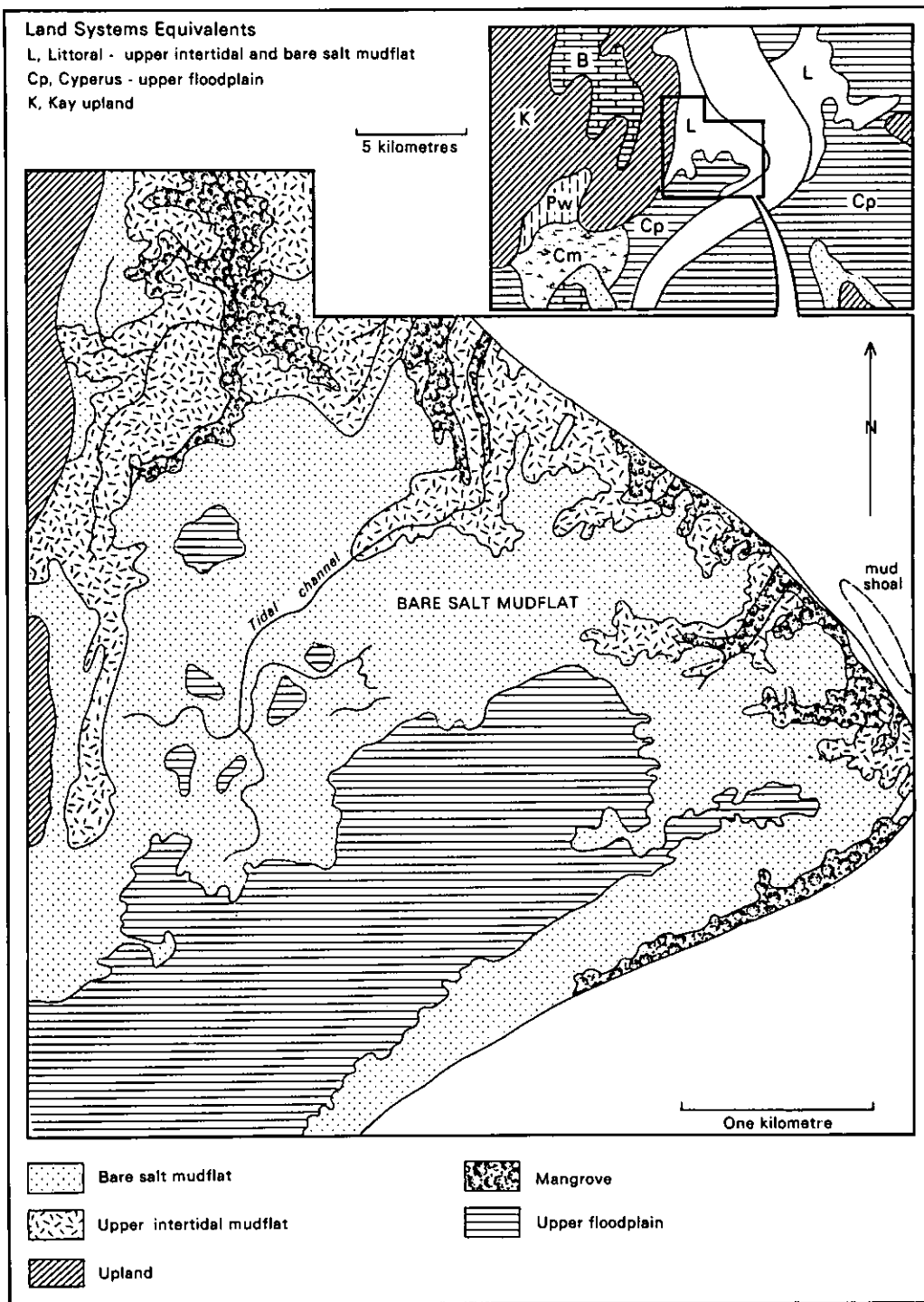


Figure 33: Detail of Lower and Upper Floodplain units on west bank of South Alligator River, about 15 km upstream from mouth. The upper intertidal mudflat has been differentiated from the bare salt mudflat on the basis of the high water mark detectable on the 1:25,000 1983 aerial photographs. Inset shows CSIRO land-systems mapping. Comparison with the larger map shows virtual equivalence of the Cyperus land system with our Upper Floodplain unit and of the Littoral with our Lower Floodplain unit.

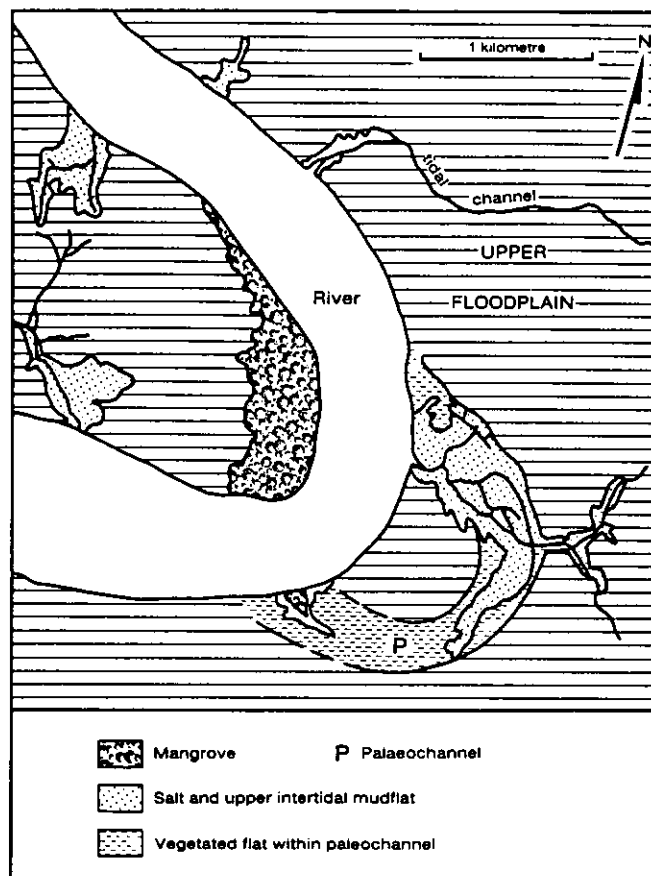


Figure 34: Detail of sinuous river bend 47 km upstream from mouth, showing infilling paleochannel to east of river and mangrove forest on prograding inside of meander to west of river.

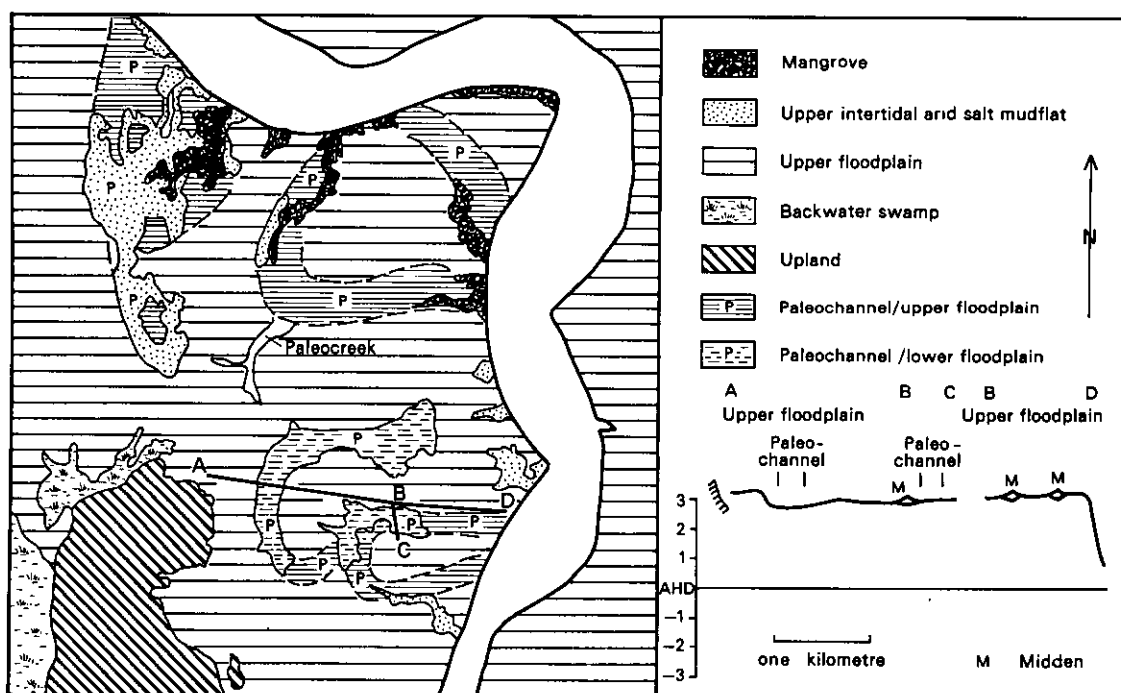


Figure 35: Detail of morphologic units at Bullocky Point about 60 km upstream of river mouth showing several infilled paleochannels on the Upper Floodplain surface.

3.2.3 Alluvial Plain Province

The alluvial plain extends southeast of the tidal limit, forming floodplains of the freshwater (fluvial) parts of the South Alligator River and Jim Jim Creek (Figure 2). The river does not extend as a distinct channel through the alluvial plain into the top of the tidal system. Instead, it is contained in multiple channels which discharge into a broad seasonal basin in which there are no discrete channels. This is an area of herbaceous aquatic vegetation in the wet season, which dries out in the dry season to form a cracked mud surface.

The alluvial plain can be divided into lower-lying areas which are inundated for much of the year, which we call the Lower Alluvial Plain unit, and better drained areas called the Upper Alluvial Plain unit.

Superficially, the Upper Alluvial Plain passes into the Upper Floodplain unit of the deltaic-estuarine province; the lower-lying Lower Alluvial Plain, with active channels or shallow gullies, passes into the Lower Floodplain unit. The main alluvial plain is more diverse than this simple classification suggests. In their land systems mapping, Story et al. (1969) distinguish several units in the alluvial plain which differ in terms of soils and elevation. Most of these units fall outside the area of this study. Figure 36 (inset) shows the land systems mapping of the alluvial plain near its transition into the upstream part of the deltaic-estuarine province, and the larger map details a small part of this area. Linear permanent lagoons such as Leichhardt Billabong shown in Figure 36, occur on the Upper Alluvial Plain, and are remnants of older channels. These often are separated by sand plugs; they have levees, and become active channels only for short periods in the wet season when even the levees are submerged. Quartz sand spreads onto the margins of the plain in floodout aprons.

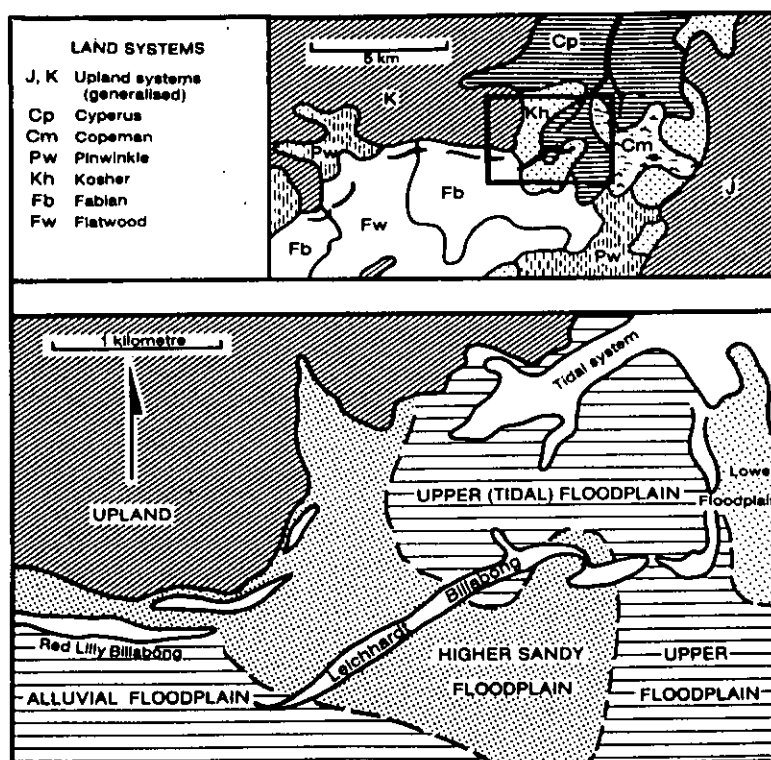


Figure 36: Transition from tidal river (deltaic-estuarine province) to alluvial plain. Inset map shows CSIRO land-system mapping (Story et al., 1969). Our mapping does not differentiate the numerous units within the alluvial plain province.

3.3 Morphologic Processes and Change

The South Alligator system, from the coastal plain to the alluvial plain, is an active sedimentary region which has developed largely since sea level stabilised about 6500 years ago. Our stratigraphic drilling and dating studies show that the visible surface, and subsurface sediments to a depth of about 5 m or so, have accumulated since this time (see section 4). Infilled paleochannels (Figures 34 and 35) show that the tidal river has changed course several times during formation of the plain in the deltaic-estuarine province. Sediments forming the plains appear to have been carried into the system by the South Alligator River and to have spread laterally from it during wet season floods. This is indicated by the occurrence of backwater swamps in most reentrant valleys at the plain margin, which are impounded by the spreading sediment sheet of the Upper Floodplain unit.

Progressive spread of floodplain sediments into distal parts of the plain seems to suggest a slowly aggrading system. This conflicts with historical observations indicating extension of tidal creeks and salt mudflats into Upper Floodplain of the deltaic-estuarine province and into lower parts of the alluvial plain province. Comparison of aerial photographs covering the last 30 years shows overbank sedimentation by highest spring tides in lowlying areas adjacent to upstream parts of the tidal river (O'Neill, 1983; D. Lindner, pers. comm.). Dieback of paperbark forests around the plains margin in the upper third of the deltaic-estuarine province reflects salt-water incursion. The location of these is shown in Figure 38. Both phenomena are popularly attributed to the effects of feral buffaloes making swim-channels (Fogarty, 1982) from tidal creeks into the plains, allowing salt water to penetrate further than it would have previously. While this may apply in some areas, there have been changes of the form and dynamics of the tidal South Alligator River in the last 2000 years, associated with shifts of the river from paleochannels to its present channel. Before assessing the consequences of these, some geomorphic details must be described. These concern elevation and micro-geomorphic relationships between Lower and Upper Floodplain units and tidal amplitudes in the deltaic-estuarine province.

Levelling surveys by the Australian Survey Office across the floodplain, both as a part of regular monitoring by ANPWS and in conjunction with our study, allow us to define the elevational range of various morphologic units relative to AHD along the length of the tidal river. Critical to process and change is the relationship between Lower and Upper Floodplain units and tidal heights.

The Lower Floodplain and Upper Floodplain were differentiated in Section 3.2.2 on the basis of elevation and the related frequency and duration of inundation. Cross-sections across the plain demonstrate that there is a general increase in elevation of the plain surface close to the river, particularly well shown in traverses A, C, and E in Figure 32. The elevation of transition from Lower Floodplain to Upper Floodplain also increases closer to the river. This is clearly shown on traverse C in Figure 32, at Rookery Point, where the general level of Upper Floodplain increases from 2.95 m AHD, near the rear of the plain, to 3.5 m near the river. Though it is not possible to determine an exact elevation for the transition from Lower to Upper Floodplain, it can be seen that this also has a similar gradient. In addition to this gentle decline in elevation away from the river channel there is also an elevational gradient along the length of the river (Figure 37). In the estuarine funnel, Lower Floodplain occurs up to an elevation of about 2.5 m AHD, with Upper Floodplain up to about 3.1 m AHD. In the sinuous meandering segment of the river the Lower Floodplain occurs at a slightly higher elevation, around 2.6-2.7 m AHD, with Upper Floodplain occurring up to 3.4-3.5 m AHD. Within the cusped segment of the river there is generally little Lower Floodplain, except in paleochannels, but where it does occur it ranges in elevation from 2.8 m

AHD to about 3.4 m AHD; the Upper Floodplain generally occurs at elevation of 3.0 to 3.8 m AHD. Within the upstream segment, Lower Floodplain occurs at elevations of about 2.8 m up to 3.4-3.6 m AHD, with Upper Floodplain generally at 3.5-4.1 m AHD. Elevations of Backwater Swamps are generally less than those of Lower Floodplain in any particular segment of the river. However, our survey data do not extend reliably into the perennially inundated Lower Backwater Swamp areas, and as these do not represent sediment surfaces linked to the river they are not shown in Figure 37a.

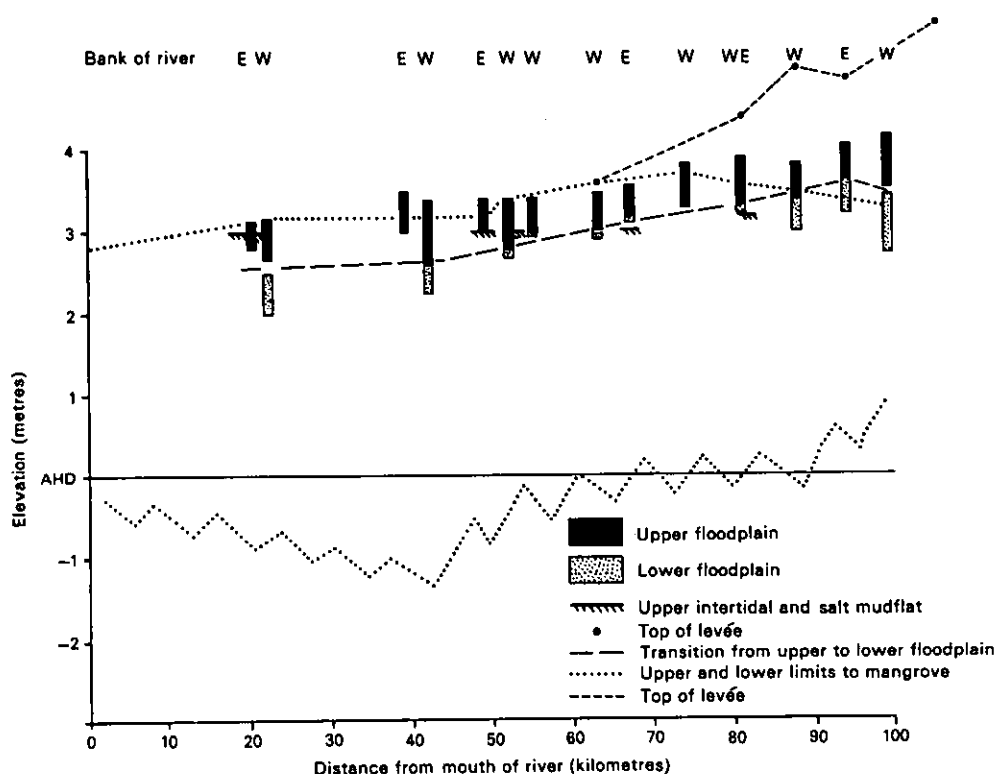


Figure 37a: The elevational range of Upper and Lower Floodplain along the South Alligator River

Figure 37a also shows leveés, where they occur. These are found at up to 3.6 m above AHD in the cusplate segment, and around 4.8 to 5.0 m in the upstream segment. Leveés around Leichhardt Billabong in the Alluvial Plain province, reach up to 5.5 m above AHD. Figure 37a shows that both Lower and Upper Floodplains descend seawards by about 1 m in 75 km. There appears to be some difference between the range of heights on the east bank of the river and those on the west bank. The east bank heights are generally higher, and there is less Lower Floodplain, which may indicate that the floodplain has filled up on the eastern side more than it has on the western side of the river. This may reflect greater sediment supply from the eastern tributaries and ephemeral streams, although the occurrence of bedrock outliers on the plain tends to locally elevate the black soil plain surface and can account for some of the higher spot heights.

Also shown in Figure 37a are elevations on the Upper Intertidal and Salt Mudflat and the upper and lower limits to mangrove growth. The Upper Intertidal and Salt Mudflat occurs at an elevation of 2.5–2.8 m AHD on the coastal plain. Within the sinuous channel segment it occurs up to 3.0 m AHD. It was also observed at this height where it is cutting back into Backwater swamps at Kapalga landing in the cusped segment, though here at more than 200 m from the river. Salt Mudflat occurs at 3.2 m AHD, again some distance from the river, at 81 km from the river mouth.

The distribution of mangrove species along the South Alligator River, described by Messel *et al.* (1979), Wells (1984) and Davie (1985), has been shown in Figure 11. Figure 37b shows the elevational range within which mangroves are found along the river. The species composition and zonation patterns differ along the river. The only components of this shown in Figure 37b, are records of *Rhizophora stylosa*, *Sonneratia lanceolata* (= *S. caseolaris*) and of the landward *Avicennia marina* and *Lumnitzera racemosa* zone. On the coastal plain the rear of the continuous mangrove belt occurs at a substrate elevation of 2.5 m AHD, however, isolated shrubby mangroves at the foot of the chenier occur up to 2.8 m AHD. The upper limit to mangrove growth occurs at 3.2 m AHD through the sinuous meandering segment, increasing at 50 km from the mouth to 3.4 m AHD, and to as much as 3.7 m AHD in the cusped meandering segment, and then decreasing again in the upstream segment. The lower limit to mangrove growth varies upstream from slightly below AHD at the coast, but is difficult to define accurately because river banks are prone to erosion often truncating the expected mangrove zonation, causing slumping of individual trees, especially of *Sonneratia lanceolata*, to levels below their usual limit (Semeniuk, 1980a; Davie, 1985). Despite significant changes in mangrove species composition along the South Alligator River, the range of mangrove elevations does not change very markedly upstream, and the present maximum mangrove range can be defined as from -1.0 m to 3.7 m AHD.

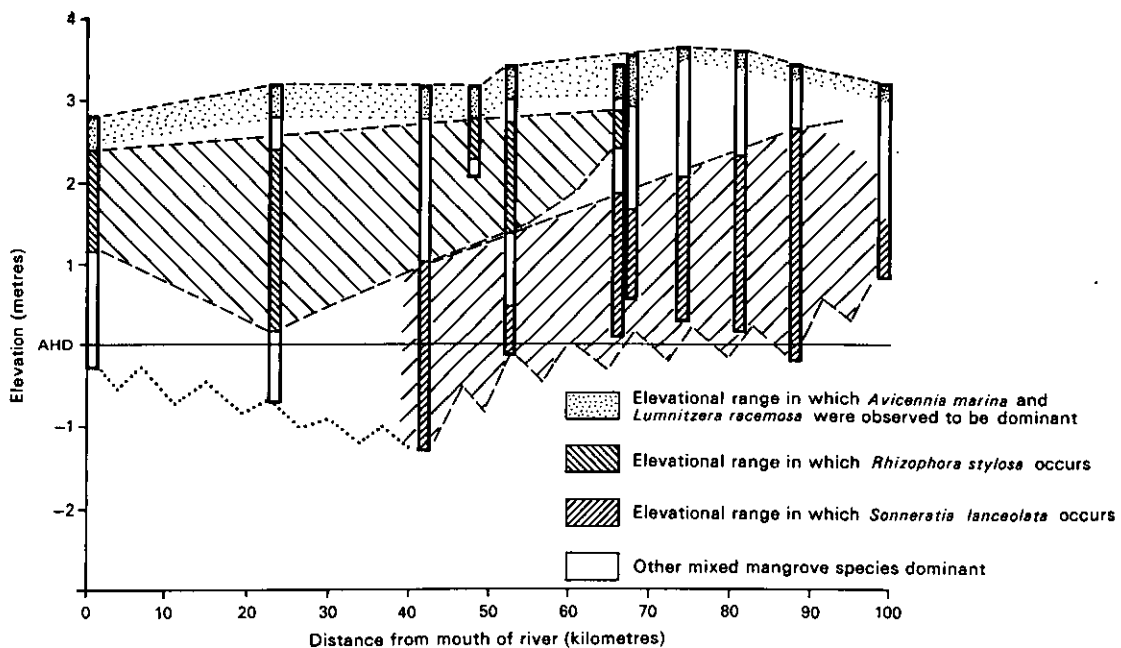


Figure 37b: The elevational range of mangroves along the South Alligator River

The seaward gradient of the Upper Intertidal and Salt Mudflat is therefore less than that of the Upper Floodplain, which is less, in turn, than that of the levées (Figure 37a). These differences reflect the relative roles of tidal and floodwater flows. The Upper Intertidal and Salt Mudflat and the upper limit of mangroves demonstrate a mild seaward gradient on the high tide water surface extending up to around 80 km from the mouth. This probably represents the effect of impedance of the longer river channel on tidal behaviour (Appendix A2). The levées and the Upper Floodplain are both built by overbank floodwater flow, which has a steeper gradient because the capacity of the tidal channel for absorbing flood discharge diminishes upstream as the channel becomes narrower. This is implicit in the flood flow rate diagram in Chapter 2 (Figure 19). Overbank depth of floodwater therefore increases upstream. The steeper gradient of the levées presumably reflects the tendency for sediment dumping from overbank flow to be greatest upstream.

It is apparent on Figure 37 that the upper limit to mangroves is often close to and occasionally even above the highest recorded Upper Floodplain. This occurs particularly where there are low levées on which individual mangroves may have established. It is also clear that much of the Upper Floodplain is at an elevation at which mangroves can grow. The decreasing gradient away from the river means that towards the rear of the plain the ground surface is lower, and would be within the tidal range if a tidal connection were made. Surveyed heights on mangroves on tributary creeks some distance from the river demonstrate a lower upper elevational limit to the occurrence of mangroves on the creek. This demonstrates dampening of tidal amplitudes up these tributaries. Nevertheless Figure 37 illustrates the point that much of the Upper Floodplain and the major part of the Lower Floodplain lie within a range of elevations which are subject to tidal influence along the river. We have observed that on high spring tides there can be delay of several tens of minutes after high water in the river channel, before high water level is recorded in the smallest of the tributary tidal creeks at any one point on the river. In the dry season, when the tidal water leaves these creeks and spreads over the salt mudflat surface there is a further deceleration in the rate of spread of the wetting front as the water soaks into the powdery sediments of the mudflat. The water surface at high tide does not therefore assume a horizontal surface, flooding all areas at or below the elevation reached in the tidal river. In the dry season successive high tides will flood progressively larger areas around a tidal creek as the wetting front moves more rapidly through the already wet muds, but decelerates again on reaching sediments not wetted by the last high tide. In the wet season, rainfall keeps the salt mudflat moist, and the less saline wet season spring tides will inundate greater areas. A similar pattern of dampening of the extent of tidal flooding over salt mudflats was observed on the mudflats associated with West African mangrove swamps (Giglioli and Thornton, 1965) with the most extensive flooding in the dry season often occurring on a tide several days after the highest spring tide in the river. This has implications for recently-observed patterns of salt water incursion which will be examined below.

A critical question is whether the tidally-influenced units are encroaching on freshwater units. The pattern of change is not altogether clear. Figure 33 shows a floodplain area in the estuarine funnel, about 16 km from the river mouth. Bare salt mudflats are extensive and surround a number of islands of Upper Floodplain. Margins of several of these islands show small steep erosional scarps 20-40 cm high. In this area the salt mudflat is invading the Upper Floodplain as can be seen by comparison of 1950, 1975 and 1983 aerial photographs. Fragmentation of the Upper Floodplain is apparent. In contrast, Figure 34 (47 km from the mouth) shows Upper Floodplain extending to both banks of the river, with a prograding mangrove forest on the inside of the meander bend. Lower Floodplain occurs only within the paleochannel on the east bank, and there is no indication of invasion of the Upper Floodplain. Figure 35, at 60 km from the mouth

depicts a series of infilling paleochannels which show negligible salinisation beyond their tidal-channel mangroves. Tidal or flood sedimentation in the paleochannels shown in Figures 34 and 35 is difficult to discern. Within the upstream segment of the tidal river, recent tidal sedimentation is well identified from aerial photos by O'Neill (1983). This sediment is colonised by Sporobolus virginicus and Paspalum sp.. Mangroves have extended their coverage along expanding tidal creeks in this segment, but in places are being overwhelmed by local sedimentation (Figure 38).

Figure 38 maps the location of tidal creeks which have extended markedly since aerial photography was taken in 1950 (compared with aerial photography taken in 1983). It indicates notable changes, including extension of mangrove and upper intertidal and salt mudflat, death of paperbark, recent tidal sediment deposition, and salt water incursion into freshwater billabongs. While changes in the cusplate and upstream segments of the river are highlighted, and have been the subject of most concern, the figure inset also indicates that there has been significant extension of creeks in the rest of the cusplate and in the sinuous segments of the river, and local extension of creeks in the estuarine funnel into the salt mudflat surface shown in Figure 33.

In the cusplate segment of the river two creeks have extended westward from the river to the rear of the plain and caused salt water penetration into backwater swamp areas. The shorter creek, 600 m long, extends landwards from Kapalga Landing. Salt water has caused the death of most of a small stand of paperbark at the rear of the plain. Mangroves have established along the creek and on the bare salt mudflat surface between the paperbarks, at an elevation 3.0 m AHD. At this point on the river mangroves are found at up to 3.6 m AHD.

The second creek, with a well-developed dendritic pattern, occurs at about 71 km from the river mouth, and meanders for nearly 3 km across the plains to a backwater swamp. This has allowed extensive salt water penetration onto the plains, with a broad salt mudflat surface around the creek itself, and has led to mortality of paperbarks over a 1.5 km front to the reentrant. Paperbarks have died within the reentrant and small clumps of dead paperbark are visible in the Lower Backwater Swamp area of this reentrant. This creek, unlike most tidal creeks adjacent to the river, does not show very rapid decrease in channel width with distance from the river. This may indicate that rather than tidal processes initiating the channel, that it was drainage out of the backwater swamp which formed or further widened the channel. Mortality of paperbarks has been observed along other river floodplains in the region. Localised mortality due to salt water incursion is recorded in the Magela Creek system (Williams, 1979), and more extensive mortality is recorded on the Mary River (Stocker, 1970). The latter has been ascribed to buffalo damage by Stocker, though this is questioned by Tulloch (1982).

In the upstream segment of the river there are several tidal creeks which have lengthened and extended headwards towards freshwater wetlands. These are shown on Figure 38, after Fogarty (1982), O'Neill (1983), and our own observations. Mangroves have extended along some of these creeks as they have become more tidally active. Salt water incursion along several of the creeks has led to salinisation of previously freshwater billabongs. This is particularly highlighted by the establishment of mangrove stands, particularly of Sonneratia lanceolata, but also of Avicennia marina, away from the main river especially at KF305798 and KF303840. The latter stand of mangroves, at the rear of the plain and about 98 km from the mouth of the river are growing at 2.8 m AHD, while we note that at a similar point on the river itself mangroves grow up to 3.3 m AHD. At this site some mortality of Sonneratia lanceolata has occurred, apparently resulting from continued sedimentation within the tidal creek.

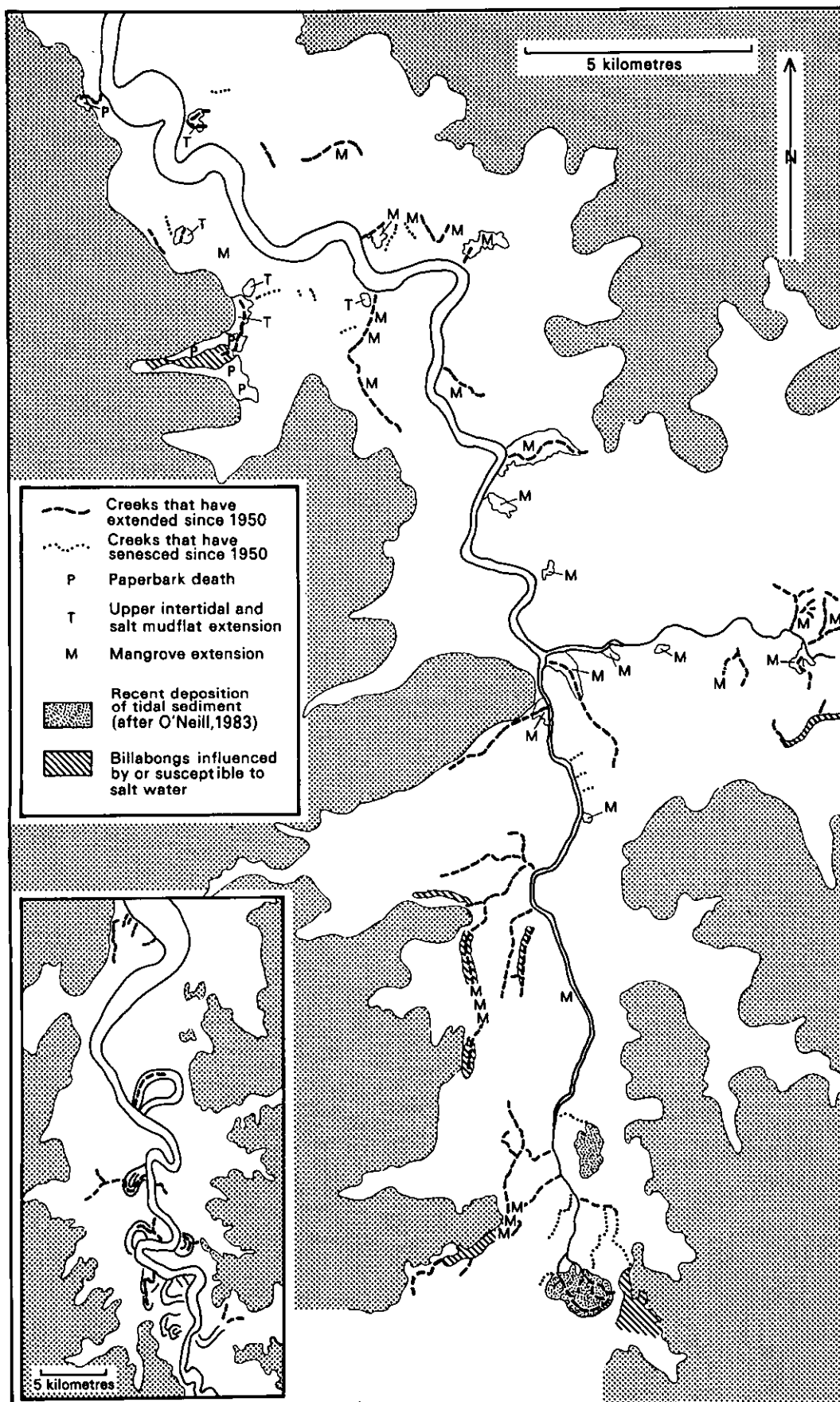


Figure 38: Map of recent channel changes and tidal creek extension derived from a comparison of 1950 and 1983 aerial photography

Water level records from the recorder at the bridge allow some definition of the upper height that tidal flows achieve 80 km up the river. Wet season flood flows are elevated above dry season maximum levels. Figure 28 show that MHWS, defined on two dry seasons flows reaches 3.2 m AHD, and the highest tidal water level observed during dry seasons of our study reached 3.5 m AHD (a level of 3.6 m AHD was recorded at that time, late August 1984 in Darwin). This corresponds closely to observations of mangroves up to 3.6 m AHD at this point on the river. In the absence of water level records at other points on the river, we suggest that the upper level of mangrove growth is an indicator of the level to which highest tidal levels might be expected.

The increase of the upper mangrove level up the river has been commented on above. It can be seen in Figure 37 that upstream of about 75 km from the river mouth elevation of the upper mangrove level decreases. Whereas much of the Upper and all of the Lower Floodplain could be susceptible to flooding by the highest tides up to a point 75 km from the mouth, beyond there only parts of the Lower Floodplain lie in the elevational range attained by these highest tidal levels. This is confirmed when the patterns of creek extension shown in Figure 38 are compared with the morphologic units mapped on the geomorphologic map. It can be seen that the creeks have extended back along the linear paleochannels of the Lower Floodplain.

The association of creek networks with paleochannels can be seen still more clearly in the inset in Figure 38 where creeks now several kilometres long have extended since the 1950 aerial photography was taken, through the paleochannels that exist on the deltaic-estuarine plain. The figure shows only the creeks which have expanded markedly since 1950. Other creek systems occupying paleochannels were already in existence in 1950 and have shown negligible change. It can be seen from Figure 37 that these paleochannels, in the Lower Floodplain group of morphologic units, are at a lower elevation than most of the deltaic-estuarine plain and are therefore particularly susceptible to inundation. At their landward end many of these creeks grade into Lower Floodplain paleocreeks and these must be susceptible to further extension of the tidal creeks across the plain.

The pronounced pattern of creek extension into channels that were previously part of the river system is discussed further in Chapter 6, after we have examined the stratigraphy of the plains, and patterns of their long-term development. Nevertheless we can state at this point that there is morphologic evidence that previous episodes of creek expansion and creek infill have occurred. The paleochannels and the paleocreeks associated with them have been infilled. Present tidal creeks draining into the river where the river is paralleled by paleochannels, must have extended into the Upper Floodplain surface after the channel had abandoned its old course and adopted its new course.

There are places where extension of tidal creeks appears to result from salt water incursion into buffalo swim channels, and erosion of levees and banks of freshwater billabongs can be observed along buffalo pads (Fogarty, 1982; O'Neill, 1983). In these instances salt water incursion into billabongs may have been exacerbated by buffalo activity. Nevertheless our observations reinforce the suggestion made by Fogarty (1982) that creek extension and senescence are natural processes. The morphologic evidence indicates that such processes have operated in the past. Moreover the tendency for extension to take place along the paleochannels, which are the areas which are lowest-lying, suggests that it should be possible to identify those areas which are more susceptible to future salt water incursion. This is discussed in Chapter 6.

Chapter 4

Stratigraphy

- 4.1 Methodology
 - 4.1.1 Field Methods
 - 4.1.2 Laboratory Methods
- 4.2 Stratigraphic and Morphostratigraphic Concepts
- 4.3 Stratigraphic and Morphostratigraphic Units
 - 4.3.1 Morphostratigraphic Group
 - 4.3.2 Stratigraphic Group
- 4.4 Stratigraphic Patterns
 - 4.4.1 General Pattern
 - 4.4.2 Stratigraphy of the Coastal Plain
 - 4.4.3 Stratigraphy of the Estuarine Funnel
 - 4.4.4 Stratigraphy of the Sinuous Meandering Segment
 - 4.4.5 Stratigraphy of the Cuspate Meandering Segment
 - 4.4.6 Stratigraphy of the Upstream Segment
 - 4.4.7 Summary

4. STRATIGRAPHY

4.1 Methodology

4.1.1 Field Methods

Surface sediments have been examined in short cores, as a part of the study of morphostratigraphic units. In addition 131 drill holes have been sunk into the floodplains, and cores and probes of subsurface sediments recovered. Initially probing was undertaken using a Jacro 100 portable drill. Subsequently the University of New South Wales (Duntroon) Mole Pioneer drill, mounted on a Scania truck was used. This permitted sampling and coring of unconsolidated sediments to 27 m depth. The location of holes is shown in Figure 39. Exposures of sediments in the river bank were examined at low spring tide. Surveys of ground surface topography were undertaken along the drill transects by the Australian Survey Office (Darwin) with further survey of sites of particular interest by ourselves. All drill samples and cores were described in the field in the first instance and redescribed in the laboratory at a later date (a compilation of all core logs has been separately bound and deposited with ANPWS).

4.1.2 Laboratory Methods

Examination of cores and probe samples in the laboratory enabled us to select materials for the following specific analyses:

- (a) Radiocarbon dating. A measure of absolute age of material containing organic carbon can be obtained by determining the amount of radioactive C^{14} isotope remaining. The dating method is based on the assimilation of C^{14} into the molecular structure of living organisms in the ratio to the two stable carbon isotopes (C^{13} and C^{12}) in which it occurs in the atmosphere (about 1 in 10^{12}). After the death of the organism exchange of carbon ceases and C^{14} is not replenished so long as the remains behave as a closed system. From this time on the radioactive C^{14} begins to decay with a half-life of about 5,700 years. The ratio of C^{14} remaining to C^{12} provides a measure of the age of remains.

Samples were submitted to the ANU Radiocarbon Dating Laboratory for determination of C^{14} and laboratory methods are outlined by Gupta and Polach (1985). Each age is given with a standard error which is a measure of counting reliability and background levels. Ages are quoted in radiocarbon years, B.P. (before present; actually before 1950 for standardisation). C^{14} years are not quite the same as solar years. The relationships known from combined tree ring and dating analysis are often used to place C^{14} dates on a calendar basis (Clark, 1975). However, in keeping with common practice in Quaternary research, we use the C^{14} time scale directly.

Radiocarbon dating can be applied over an age range of up to about 50,000 years B.P.. It can be carried out on both wood material and shell material. However ages from wood and shell are not directly comparable until shell sample ages are 'environmentally-corrected' for the apparent age of modern shells (1950 shells). These have an apparent age of several hundred years because they assimilate carbon from the ocean which because of the residence time of carbon is depleted in C^{14} with respect to the atmosphere. For most marine shell species from around much of Australia's coastline, the environmental-correction is 450 ± 20

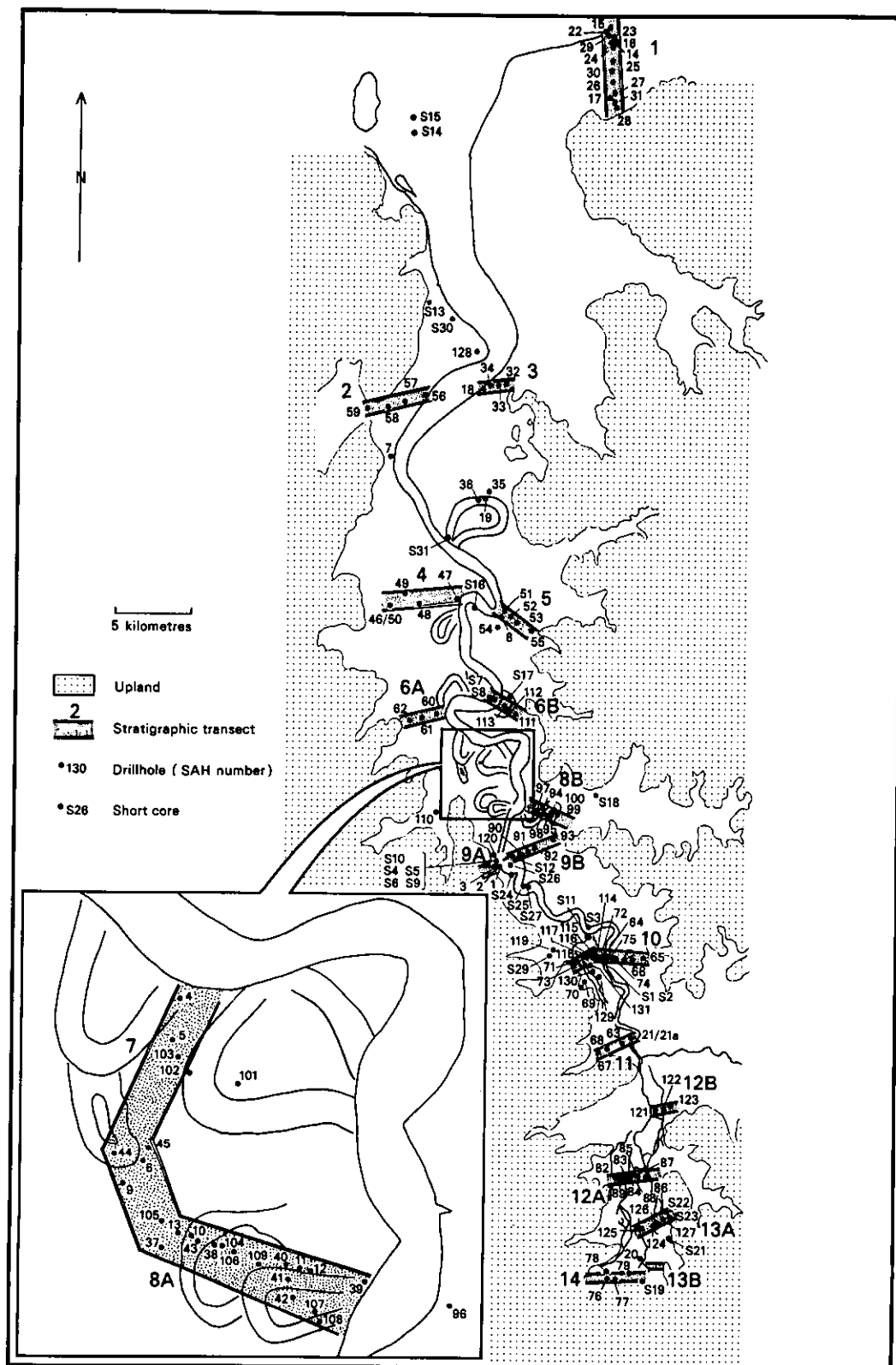


Figure 39: The location of drillholes SAH 1 to SAH 131, the numbering of transects, and the location of short cores, South Alligator River

years (Gillespie and Polach, 1979). The shells in our samples come from estuarine environments where gaseous exchange with the atmosphere occurs; we note some ages less than 450 years B.P. and several not much older. The environmental-correction for this environment is not known, and it would be premature to assume a value of 450 years. Our shell dates are not environmentally-corrected and are not therefore directly comparable with wood dates.

Selection of material for dating was based primarily on visual assessment of sufficient carbon in a sample. Shell material from in situ shell beds and aboriginal middens and pulverized shell hash from chenier ridges, fossilized wood, shells and lobsters and fine organic fragments were all dated.

Wood samples were washed in distilled water, oven-dried and weighed prior to submission to the ANU Radiocarbon Dating Laboratory. Samples of finer organic fragments were mechanically disaggregated, wet-sieved through a 30 (125 μ) sieve, separated, dried and weighed. Shell material was washed, scrubbed clean from surface contamination using diluted hydrochloric acid, vibrated ultrasonically, rinsed in distilled water, dried and weighed.

In some instances very low concentrations of organic material led to the use of a technique to chemically convert small fractions of organic carbon into a datable medium in the form of strontium carbonate (SrCO_3). This process involved oxidizing the organic matter to carbon dioxide using chromic acid, then introducing nitrogen gas to act as an agent to carry the carbon dioxide through an ammonia solution, resulting in the CO_2 being trapped as ammonium carbonate. The 'pregnant' ammonium carbonate was then boiled and strontium chloride added. This resulted in a precipitate which was subsequently scrubbed clean by suction filtration and the filtrate oven-dried, yielding datable strontium carbonate.

A total of 184 South Alligator samples have been submitted for dating. These include 110 samples of fine mangrove fragments, 27 mangrove wood, 11 SrCO_3 , 5 in situ shell, 19 midden samples and 12 fossil wood; shell or lobster samples (see Appendix A8).

- (b) Sediment size analysis. All samples selected for sediment particle size analysis needed to be initially cleansed of salt which was achieved by adding distilled water to the sample, then centrifuging the resultant slurry and decanting the water. The process was repeated three times to yield a salt-free sediment sample.

The hydrometer method was used to determine fractions in the range 4 to 90 while coarser fractions were obtained by dry sieving, using methods described in Folk (1980). Sediment size results for South Alligator samples analysed so far are presented in Appendix A4.

- (c) Soluble salt concentrations. The concentration of chloride in samples was measured in order to investigate the salinities which might have been experienced at the time of deposition of sediments. Post depositional movement of salt, leaching, and evaporative concentration will have masked some of the initial concentrations but results are possibly some guide towards differentiation of freshwater and estuarine clays.

Initial soil water salinities cannot be reproduced as cores had lost moisture before being sampled. Samples were therefore

suspended in a 1:5 sediment:water mixture, and results are reported in total parts per thousand of the sediment dry weight.

Six grams of sediment, oven-dried at 105°C for 24 hours, was dispersed in 30 grams of distilled water and allowed to stand over night. The sample was then agitated for one minute and its electroconductivity was measured using a Crison 523 Conductimeter. The conductivity of standard solutions of potassium chloride are also measured and a calibration curve obtained to convert conductivity to equivalent KCl salinity. Results are presented in Appendix A5.

- (d) Organic content. Estimates of the organic content of particular sediments are useful for interpreting the sedimentary environment sampled as well as providing a quantitative guide to obtain, sufficient organic material to provide a radiocarbon age. Samples were weighed, oven-dried at 105°C for 24 hours, reweighed and combusted at 500°C in a muffle furnace for 6 hours.

This weight loss on ignition is converted to a percentage. It should be noted that not all loss of weight occurred as a result of combustion of organic matter, some additional water may be lost from clays; this percentage therefore gives an upper limit value of organic content.

- (e) Calcium carbonate content. Calcium carbonate values were determined to provide information on the nature of the environment being studied. Marine environments tend to have greater concentrations of CaCO_3 because of inclusion of shell or shell hash. A Volumetric calcimeter was used to measure the gaseous product resulting from the addition of hydrochloric acid (50 per cent) to a preweighed, finely-ground sediment sample. Results of the initial batch of samples are shown in Appendix A7.
- (f) Microfossil analysis. Pollen analytical techniques are described in Appendix A6.

4.2 Stratigraphic and Morphostratigraphic Concepts

Stratigraphic drilling provides us with quite comprehensive information about the sediments which infilled the prior South Alligator valley during sea-level rise and the subsequent stable sea-level interval of the last 6000 years or so. Several different sedimentary facies are recognised. Some are widespread, and their depths and characteristics indicate deposition during valley flooding and infilling when sea level was rising. These widespread subsurface deposits are sedimentary formations in the normal stratigraphic sense. Nearer the coast, their geometry is such that widely used interpretative terms, e.g. 'transgressive' and 'regressive', can be applied to particular units. These deposits have sedimentary counterparts today, in the river channel, estuary and nearshore areas, but their subsurface form or distribution at any locality can rarely be interpreted in environmental terms. Hence, the relatively widespread subsurface deposits are described and interpreted in terms of stratigraphic units. Their depositional history and associated changes of the evolving estuary are interpreted from the broad-scale distributions of these units, and from their internal age structure revealed by radiocarbon dates.

The morphologic units described in Chapter 3 are built of sediments. Generally, the surface morphology is the expression of a discrete subsurface body of sediment. Infilled paleochannels are an example. Deposits which can be defined in terms of their surface and subsurface geometry as well as their sedimentary characteristics can be defined as morphostrati-

graphic units, a concept introduced by Frye and Willman (1960) for use in mapping Pleistocene glacial deposits. Morphostratigraphic units have an advantage over stratigraphic ones in that separate units or depositional episodes can be distinguished in terms of form, within otherwise rather monotonous deposits. Morphostratigraphic principles have been applied in coastal geomorphology by Thom (1967), and to coastal studies in Australia by Rhodes (1982), and others as a formal means of linking surface morphology and subsurface deposits.

Some of the subsurface deposits of the South Alligator plains are identified with morphostratigraphic units. These include paleochannel deposits, deposits of the Upper Floodplain unit, and levees. Other subsurface deposits are identified only as stratigraphic units. These include basal transgressive sediments, various estuarine and tidal river deposits, and organic-rich muds identified as being of mangrove origin. Subsurface margins of morphostratigraphic units, and boundaries between stratigraphic units, are interpreted from field logs of drillholes and cores, supported by diagnostic laboratory tests in some cases.

Stratigraphic units are defined in sedimentologic terms and each is uniform or covers a limited range of textures and other sedimentary characteristics. It is not always possible for each morphostratigraphic unit to have uniform sedimentary characteristics as more than one sedimentary mode may exist within a unit. Paleochannels provide an example. After a meander loop is abandoned by the main channel it may persist as a backwater into which the tide flows and within which suspended sediment from the river accumulates. As it infills, a stage is reached when only floodwater enters, either because its ends become plugged by a levee of the main channel or because its surface builds above high spring tide. After this, sedimentation is of freshwater deposits, essentially clays, similar to the floodplain in general. Pedogenesis, including oxidation below the topsoil, ensues. Hence, a paleochannel may contain channel sediments, 'backwater' saline muds, a topping of freshwater clay, and a pedogenic overprinting near the surface. Nevertheless, where the subsurface margin or base of the paleochannel is identified by drilling, it is more valuable to describe it and its various deposits as a morphostratigraphic unit rather than classifying the deposits as a variant of one of the stratigraphic units.

The following section defines stratigraphic and morphostratigraphic units used for interpreting the history of the South Alligator plains.

4.3 Stratigraphic and Morphostratigraphic Units

Six stratigraphic and five morphostratigraphic units are defined below. Subsequent interpretation of our 131 stratigraphic drillholes is based on these, to provide a model of the evolution of the tidal river and plains system. Morphostratigraphic units are defined in relation to surface features of known process origins, and therefore have genetic connotations. The stratigraphic units have lateral connections (seen in some cases, inferred in others) with present sedimentary environments, and most of these have genetic connotations also. Such units obviously are useful for interpreting past environments from drill logs. However, some sediment textures occur in different environments and, where diagnostic tests are lacking or untried, cannot be linked back to environment when found in drillholes. We refer to these as undifferentiated.

Table 6 summarises the units which are defined below. Frequent reference is made to diagnostic sedimentary textures and in the figures which show cross-valley transects we illustrate both sedimentary textures and our stratigraphic and morphostratigraphic interpretation.

Table 6
Main characteristics of stratigraphic and morphostratigraphic units

	Texture	Other features	Surface form
Morphostratigraphic unit			
Floodplain clay unit	Clay	Organically-enriched	Extensive floodplain
Paleochannel unit	Mud/clay	Featureless, sparse organic flecks	Meandering channel or anabranch
Levée unit	Fine sand/silt	Sometimes laminated	Elongate levée beside river channel
Chenier unit	Sand/shell hash	Shelly	Elongate low ridge on coastal plain
Midden unit	Shelly	Bone and stone	Low mound
Stratigraphic unit			
Marine sand and mud	Sand and mud	Shelly	Nearshore
Estuarine sand and mud	Sand and mud	Sometimes shelly	Subtidal/intertidal
Undifferentiated sediments	Sand and mud	Featureless, occasional organic flecks	Estuarine/tidal river
Mangrove mud	Mud	Organic	Mangrove/intertidal
Laminated channel sediments	Mud/fine sand	Laminated	Channel margin and shoal
Basal sediments	Sand/mud/gravel	Pallid sand/oxidised/ lateritic	Prior valley margin and valley floor

4.3.1 Morphostratigraphic Group

- (a) Floodplain clay unit. The Upper Floodplain and Lower Floodplain groups defined in Chapter 3.2 are formed of dark cracking clays ('black soil'), except for the saline and the perennially swampy units of the Lower Floodplain group. There are differences in surface appearance between the soils of different units, i.e., in colour, cracking patterns, and soil nodules (Chapter 3.2). However, all appear to be composed of clays, median size 1 micron, and dominantly of kaolin and illite clay minerals. The unit overlies saline muds and sandy muds of various stratigraphic units defined below. It is between 0.5 and 1.5 m thick but the exact transition to underlying units is difficult to recognise in field samples due to pedogenic overprinting. Overprinting takes the form of organic enrichment and soil cracking to 0.3 to 0.4 m. Furthermore oxidation producing pale brown or weakly mottled light grayish-brown to orange or yellow colours occurs to 1 to 2 m. Soil nodules, carbonate or ferruginous, may occur within the pedogenic zone. Small (<3 mm) gypsum crystals have been found near the base of the oxidised zone. Analyses of salt and pollen spectra (Chapters 5 and 6) show that the transition from floodplain clays to underlying units usually occurs within the oxidised zone.
- (b) Paleochannel Unit. Paleochannels are mapped in the geomorphologic map and Figure 34 and 35. They are relict meander loops in the middle reaches of the plains while they appear as abandoned anabranches further upstream. Due to varying elevations of their surface they occur in both Lower and Upper Floodplain groups defined in Chapter 3.2. The base of paleochannel infill is usually a distinctive sedimentary break in drillholes; in many cases it is the basal sediments that formed the prior valley. The bulk of the infill is fine mud, dominantly clay, median particle size 1 to 2 microns (Figure 40), structureless, with sparse and dispersed fine, dark organic flecks. Thin (0.5 to 2 cm) lenses of layered platy organic particles occur occasionally. Near the base of paleochannels the sediments are sometimes silty or fine sandy muds. Where their surface occurs in sedge/grassland of the Lower or Upper Floodplain units, the top 0.5 to 1 m of sediment is the dark or oxidised freshwater clay described above under the Floodplain clay unit. In exposures of this unit in river bank sections the clay is often blocky, and there are irregular, nodular carbonate concretions, perhaps formed as burrow-fill.
- (c) Levée Unit. Levées found in the upstream segment of the river (Chapter 3.2) are low river-bordering bodies of light brown to yellow silt and fine sand, up to 60 m wide. Root channels mark the sediments, which have been drilled in only a couple of holes, but have been observed in bank exposures to be up to 1.5 m thick. The degraded levées associated with paleochannels consist of similar sediments but are not more than 30-40 cm thick.
- (d) Chenier Unit. Cheniers on the coastal plain (Chapter 3.2) are bodies of sparse to rich shelly sand, elongate, parallel to the coast, up to 60 m wide and up to 1 m above plains surface. Drilling shows that chenier sediments usually rest on floodplain clays or mangrove muds, usually about 0.5 m below the coastal plain surface.
- (e) Midden unit. Middens, composed largely of shell material are described in detail in Chapter 5 and Table 8.

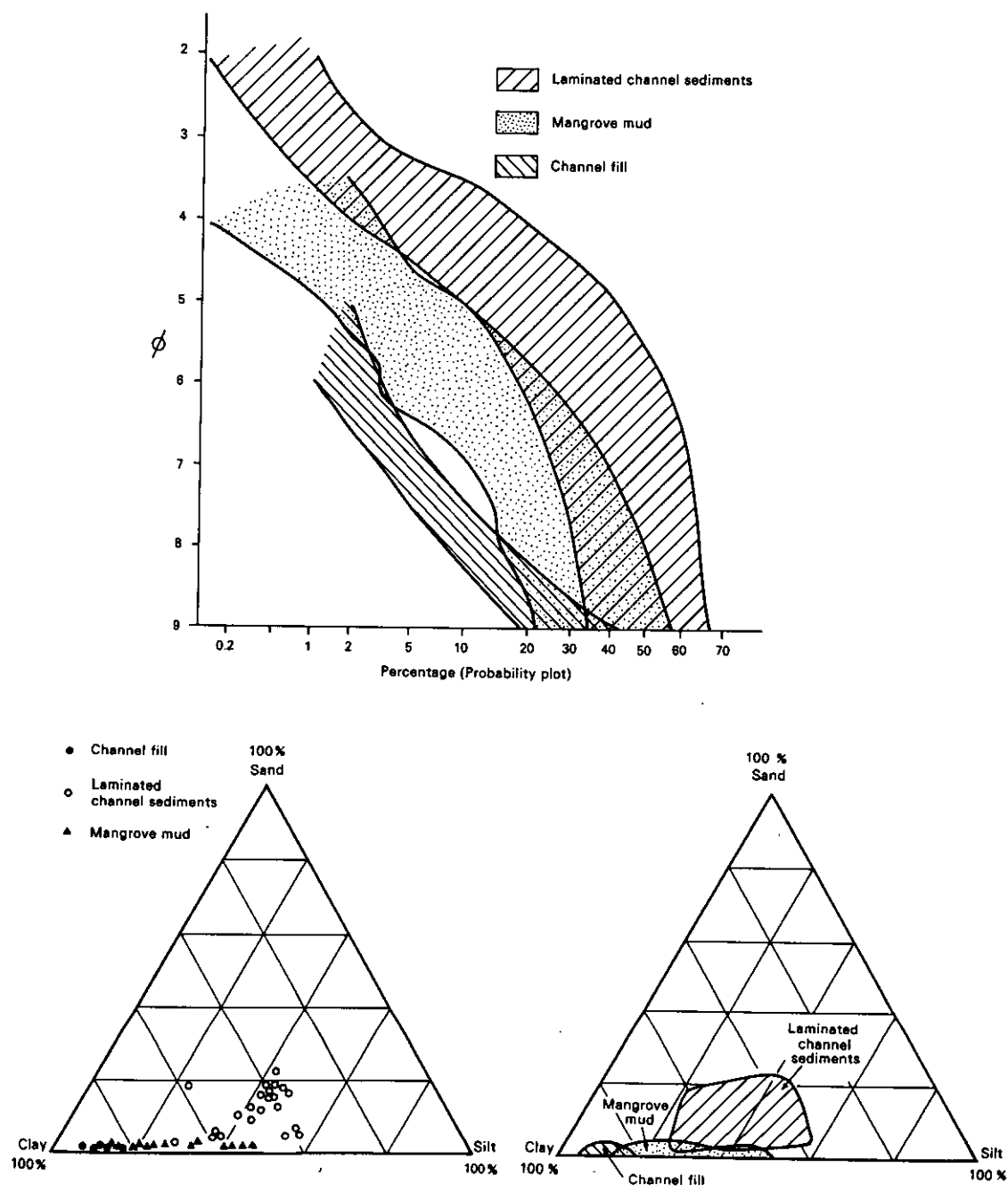


Figure 40: Particle size characteristics of laminated channel sediments, channel fill and mangrove mud

4.3.2 Stratigraphic Group

- (a) Marine sand and mud. Gray to bluish-gray muddy medium sands and sandy muds containing whole and broken small shells occur in dredge samples from the lower intertidal zone down to about 8 m depth off the coastal plain and South Alligator mouth. Median particle size is 30 to 60 microns and shell carbonate ranges up to 27 per cent. Drillholes find similar sediments at intermediate depths below the coastal plain, and show that they are generally structureless or faintly laminated.
- (b) Estuarine sand and mud. These comprise light gray to bluish-gray muddy sand to sandy mud, often prominently laminated with fine organic particles and sand-size shell hash. Shell carbonate ranges from 0 to about 10 per cent. Sparse fragments of calcified or silicified wood are found, probably derived from outcrops in the estuarine funnel which contain these materials. Similar sediments are dredged from the wide channel and shoals in the lower estuary.
- (c) Undifferentiated sediments. A variety of sediment types, recovered in drillholes, cannot be linked to specific depositional environments. These include bluish-gray mud with sparse organic flecks and with negligible carbonate, and occasional clean sands. Such sediments occur sporadically in drillholes throughout the plains, at various depths. As they may represent several different environments they are referred to as 'undifferentiated'. A common position of occurrence is between the mangrove mud, described below, and deposits of the Floodplain unit. In this position it may be mangrove mud from which the organics have been oxidised.
- (d) Mangrove mud. Bluish-gray soft muds, generally sulphurous, moderately to highly organic often with fibrous and wood fragments, and median grain size around 4 microns (Figure 40). This unit is exposed at many points along the river bank, with numerous in situ preserved mangrove stumps and a sub-fossil fauna of calcified lobsters (Thalassina squamifera) and molluscs (Polymesoda, Telescopium, and Terebralia). These fauna are encased in mud ball concretions which were found by X-ray diffraction to be formed by calcite with magnesium contents of 0.8 to 3.0 per cent. They vary in shape; those around Thalassina are ovate, up to 20 cm in length, and usually occur with claws uppermost and tail lowermost; those around molluscs are more spherical. Similar concretions have been reported from Fitzroy and Daly rivers, Port Darwin and Gunn Point (Etheridge and McCulloch, 1916; Cambell and Woods, 1967; Semeniuk, 1982). Some of these have been composed of dolomite (i.e. King Sound, Anson Bay, Etheridge and McCulloch, 1916; Semeniuk, 1980b), and this may indicate that the nodules could eventually be replaced by dolomite, like nodules described from Broad Sound (Cook, 1973). Association of this fauna with mangrove stumps is widespread (Wright et al., 1972; Semeniuk 1982). Further detail of sites along the South Alligator is given below (see Table 7). Often the preserved wood is calcified and burrows of borers are also calcified. Bioturbation is common in drill cores of this unit. This is the most distinctive and ubiquitous stratigraphic unit within the sediments beneath the plains. Its mangrove origin is confirmed not only by macrofossils, but also by the fact that similar deposits are found accumulating within present mangroves.

- (e) Laminated channel sediments. Bluish-gray silt and clay with laminae of fine sand, prominently laminated, are common in drill-holes near the axis of the valley. Laminae are generally less than 4 mm thick, though thicker ones have been observed. They range from horizontal up to 25° dip. The close proximity of these sediments to the present channels and paleochannels along the axis of the floodplain, together with contemporary deposition of similar laminated sediments on mid-channel shoals, on point bars and on channel sides, leads us to identify these as sediments characteristic of margins and shoals of active channels. In some cores similar laminated sediments with laminae dipping at up to 15° show truncation by slumping or by bioturbation. These are believed to have been deposited, or modified, in channel bank situations.
- (f) Basal sediments. At most sites drilling ceased when a distinct discontinuity was found. Underlying sediments are firmer, often laterised gravels, or heavily oxidised quartz sands and are interpreted as relict pre-Holocene or early Holocene deposits. Clean white sand deposits were found at the base of many cores, these may be alluvial or colluvial in origin and may be early Holocene in age. Elsewhere clays with a high content of quartz sand and gravel or of lateritised gravel are found. At the base of other drillholes sand is recorded in the basal bluish-gray muds, and some reworking of the basal sediments is believed to have led to incorporation of this material into the muds.

4.4 Stratigraphic Patterns

4.4.1 General Pattern

The interpretation of sedimentary history in this section is based on stratigraphic and morphostratigraphic units determined primarily from field descriptions of cores and probes. The interpretation is amplified by the use of selected cores in which pollen analysis has been undertaken.

The general Holocene history is one of sedimentary infilling of the South Alligator valley during sea-level rise, with changing patterns of tidal river activity and morphometry, and rates of floodplain formation during and after the rise. The prior valley or unconsolidated surface, comprising the basal sediments, is often overlain by mangrove mud. In this context mangrove mud can be termed transgressive as it records marine drowning of the pre-Holocene valley. Where mangrove mud is recorded at the base of a drillhole it is often peaty and compacted with compressed organic remains. It was deposited beneath mangrove forests which formed as sea level rose across subaerial surfaces during the final stages of the Post-glacial Marine Transgression (P.M.T.). Several radiocarbon dates have been obtained on the basal transgressive mangrove mud and fall into the 8000-6500 years B.P. range.

In places the transgressive mangrove mud continues unbroken upwards to within a metre or so of the surface of the plains. Continuity of mangrove muds was particularly observed in drillholes close to the valley margin, and implies that mangrove forests existed near the valley margins throughout sea-level rise. Elsewhere the lower transgressive mangrove mud and the upper mangrove mud are separated by laminated channel sediments or undifferentiated estuarine deposits. The upper mangrove mud is regressive in some locations in which it is found (i.e. on the coastal plain). Not everywhere do we know that it formed while the sea was regressing, and the shoreline was building seawards, and in these situations it would be incorrect to term it regressive. The mangrove swamp phase represented by

the upper mangrove mud began as sea level had stabilised and continued during the early phase of sea-level stillstand. This is known to have occurred at around 6500-6000 years B.P. around much of the coastline of Australia (Thom and Chappell, 1975; Thom and Roy, 1983, 1985), and dates from the South Alligator River on this regressive mangrove mud are also of this period (see Chapter 5). After the rate of sea-level rise decelerated and stabilised mangrove swamps and later freshwater floodplains developed extensively throughout the valley of the South Alligator River. Since that time the tidal channel has been particularly mobile, as illustrated by a series of paleochannels visible on the present floodplains of the river. We discuss the stratigraphy of the plains in this chapter and then re-examine the course of development of the river as a whole in Chapter 5.

The stratigraphy of each of the segments of the tidal river is described below in more detail using a series of cross-valley transects. Transects are drawn in a format which shows the surface topography and the sedimentary characteristics of the probes or cores in the upper diagram. These sedimentary descriptions are generalised from drillhole descriptions. The lower diagram gives our interpretation of these sedimentary characteristics in terms of stratigraphic and morphostratigraphic units. Radiocarbon ages are shown on the upper diagram, (s indicates dates on shell) and in a few instances isochrons of progradation or sediment aggradation are shown in the lower.

4.4.2 Stratigraphy of the Coastal Plain

The subsurface sediments of the coastal plain were examined along transect I (Figure 39), consisting of 11 probes and 3 cores running at right angles to the shore, roughly midway between Midnight Point and Point Farewell. Figure 41 illustrates the stratigraphy along the transect. The pre-Holocene surface occurs as a near-horizontal platform 7-9 m below the plain surface descending from less than 4m below AHD in the south to more than 7 m below AHD in the north. Overlying the pre-Holocene basement is a thin basal sand unit composed of poorly sorted sand and gravel, of mixed mineralogy, but with angular quartz fragments. This in turn is overlain by mangrove mud parallel to the pre-Holocene surface.

The mangrove mud has been radiocarbon-dated to 6330 ± 150 and 6350 ± 260 years B.P. at a depth of 8.15 m in core SAH 29 and 6560 ± 270 years B.P. at similar depth in adjacent SAH 22 (dates appear to be slightly anomalously young when compared with other dates at this depth.) It has been dated at 6700 ± 150 and 6580 ± 280 years B.P. at 6.7 m in probe SAH 25, 6720 ± 350 years B.P. at 7.3 m in probe SAH 26, 6550 ± 200 years B.P. at 6.7 m in probe SAH 27, and 6640 ± 110 years B.P. at 5.5 m (-1.49 m AHD) in probe SAH 17 through the landward chenier ridge. Mangroves evidently colonised this gently sloping platform rapidly as sea level rose over it.

Except at the rear (south) of the coastal plain, the transgressive mangrove mud is overlain by marine sand and mud, indicating that the sea-level rise drowned most of the mangrove forest that had established over the pre-existing platform. At the southern margin of the coastal plain, behind the landward chenier ridge, the transgressive mangrove mud grades up into a regressive mangrove mud on which we have radiocarbon dates of 6320 ± 170 and 6240 ± 130 years B.P. at 2.45 m and 3.95 m respectively in SAH 28. Regressive mangrove mud is evident beneath the seaward chenier and seaward of that chenier to the present mangrove fringe. However it is absent from much of the central portion of the plain. A radiocarbon-modern age has been obtained from this regressive mangrove mud just landward of the present mangrove fringe at a depth of 3.7 m in SAH 15, while an age of 2200 ± 60 years B.P. was recorded on mangrove fragments at a depth of 1.5 m in core SAH 29.

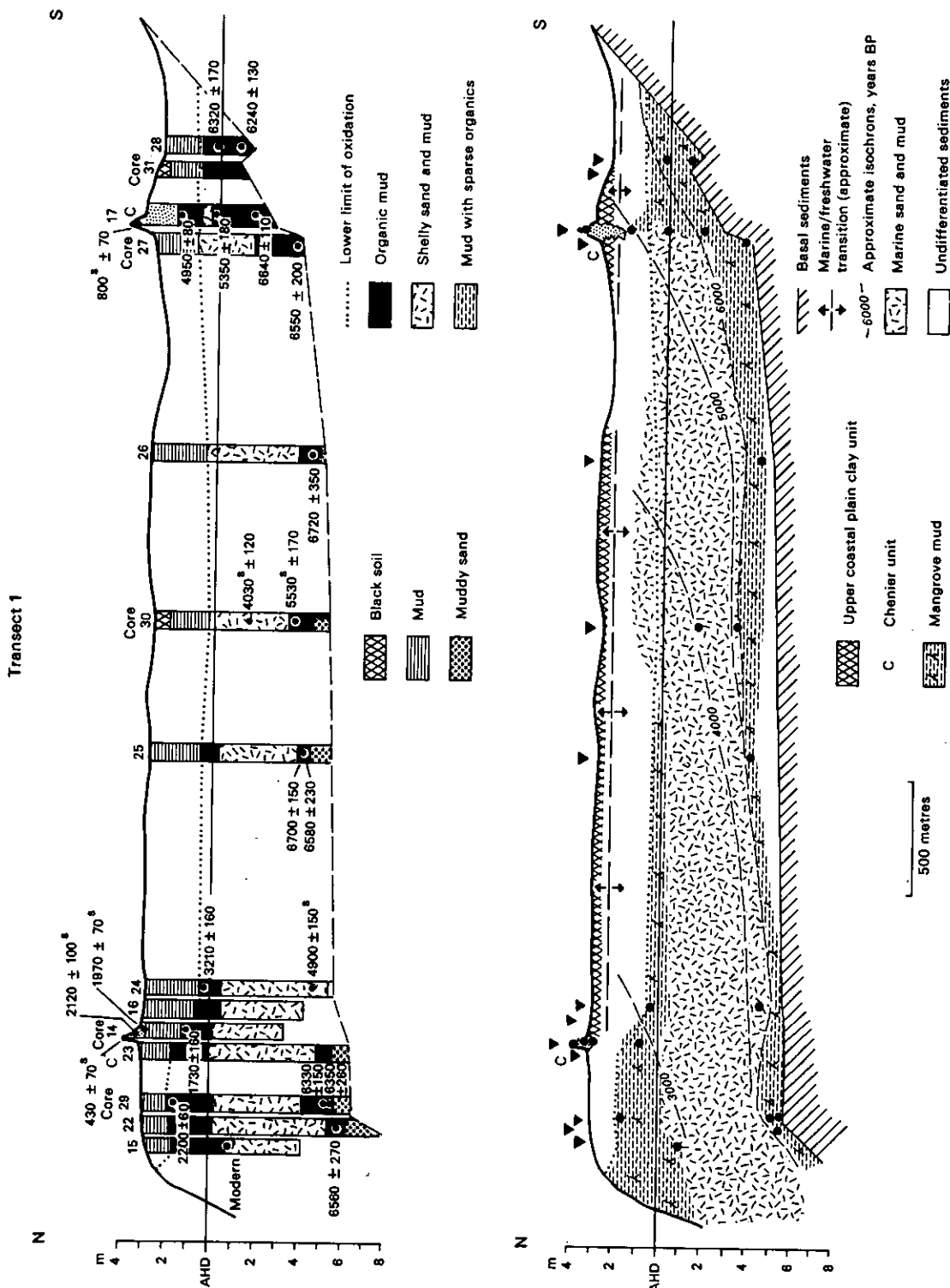


Figure 41: Stratigraphy of Transect 1, Coastal plain and tentative isochrons of coastal progradation. Upper diagram shows sedimentary characteristics of drillholes (identified by SAH number), and radiocarbon dates in years B.P. (s indicates date on shell). Lower diagram shows interpretation in terms of stratigraphic and morphostratigraphic units; location of cores shown by triangles and of radiocarbon dates by dots.

The marine sand and mud is interpreted as deposited in a shallow water nearshore environment, seaward of the mangrove fringe. This unit is sandier and has more abundant whole shells and shell fragments in holes towards the northern end of the transect. Radiocarbon ages on shells in the unit are 4900 ± 150 years B.P. at 7.6 m in SAH 24, and 5530 ± 170 and 4030 ± 120 years B.P. at 6.05 and 4.18 m respectively in core SAH 30 in the centre of the plain. In Figure 41 environmental-corrections have not been applied to these shell ages consistent with our uncertainty about the value by which shells, particularly intertidal shells, should be corrected (see Section 4.1.2). Subtracting 450 years from the measured age is presently the best estimate of the apparent age of modern pre-1950 shells; without correction shell ages and mangrove ages are not directly comparable (Gillespie and Polach, 1979). Figure 41 also shows isochrons reconstructing the probable shoreline position at 6000, 5000, 4000 and 3000 years B.P. The absence of a regressive mangrove mud beneath the centre of the plain and consequently the paucity of dateable material leaves the shoreline position uncertain at 4000 and 3000 years B.P. However, the dates from shells in the marine sand and mud indicate that the shore was likely to have been south (landward) of core SAH 30 in the centre of the plain at least 3500 years ago.

The isochrons in Figure 41 indicate that the rate of progradation has not been uniform over the last 6000 years. Initially it appears that the rate of progradation was slow. The shore was close to the landward chenier 5000 years ago and the chenier was probably formed at about that time. Between 5000 to 3000 years ago there appears to have been rapid progradation with the 3000 year-old shoreline around the location of the seaward chenier, but remains of mangroves are not preserved to confirm this. There has been comparatively little progradation since 2000 years ago; the seaward chenier was probably deposited about 1700-1500 years ago.

The present mangrove forest on the coastal plain is a narrow band about 200 m wide. This belt is prominently zoned. The landward zone of Avicennia and the central zone of Rhizophora exhibit extensive tree mortality at their landward sides, where the zones are evidently contracting. However, the seaward zone of Sonneratia and Camptostemon does not seem to be prograding seaward, as the most seaward fringe is composed of large mature trees and not a regenerating zone of pioneer individuals. Thus it appears that the present mangrove is contracting rather than prograding, and the radiocarbon evidence suggests that the shoreline has changed little since about 2000 years ago. There may have been periods of cut and fill, perhaps associated with chenier formation 1700-1500 years ago, but little or no net progradation.

4.4.3 Stratigraphy of the Estuarine Funnel

The estuarine funnel is an area where access is particularly difficult. On the western side it is bounded by the uplands of Mount Hooper. Occasionally these are undercut by the river and form cliffs as at KG 160440; elsewhere they form the locus from which sandy chenier-spits have developed with distal ends to the south apparently formed by flood tides. A short core (S14, see Figure 39) through one of these chenier spits confirmed that the sands overlies saline mud at shallow depth, and that the spits are developed over salt mudflat surfaces. This western side has extensive intertidal areas covered with mangrove. On the eastern side the floodplains are dissected by numerous tidal creeks, and the large sinuous loop of Brooks Creek makes access difficult. The pattern of dissection is particularly pronounced, though comparison of 1950 and 1983 aerial photography suggests that little change has occurred over that period.

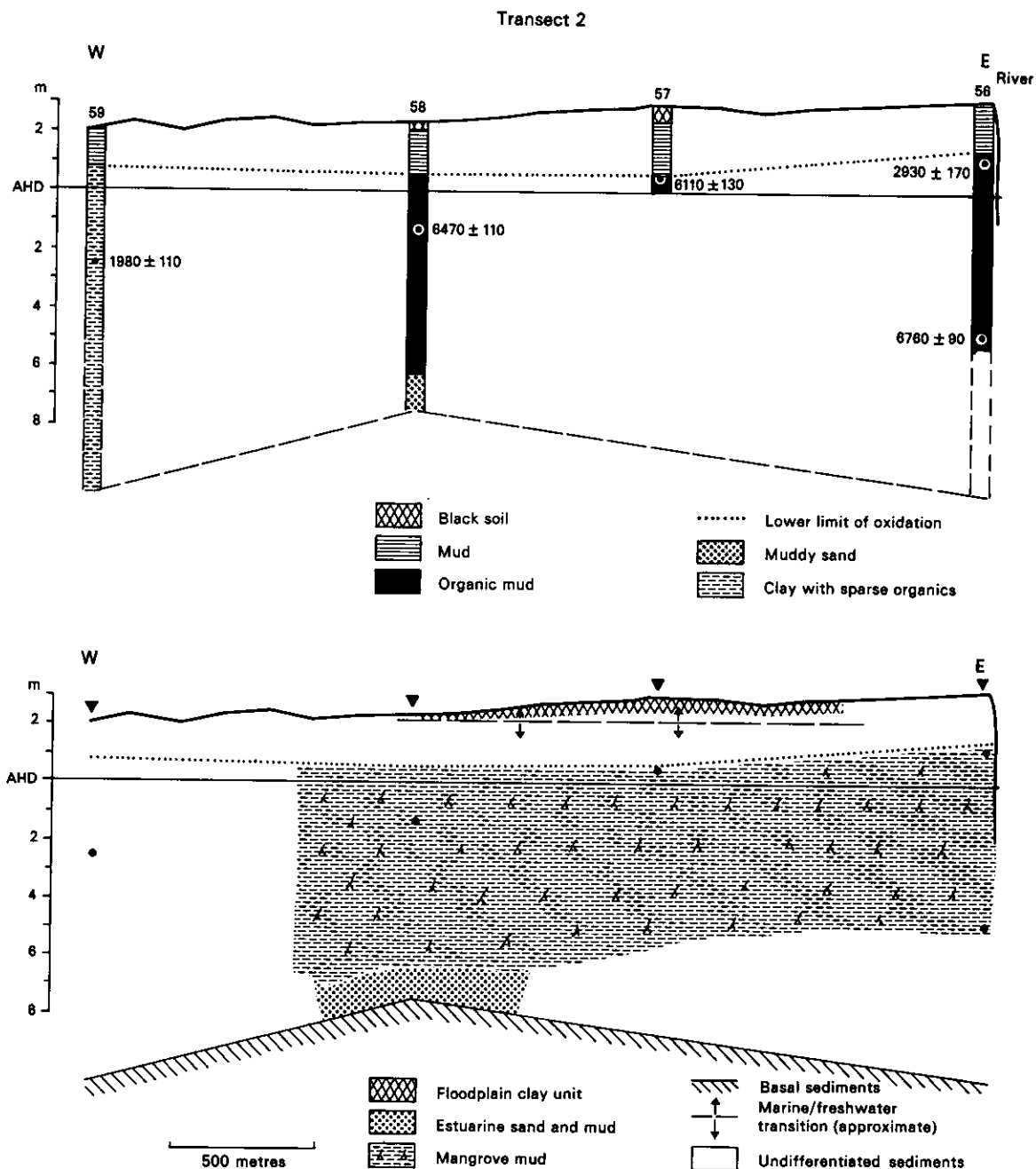


Figure 42: Stratigraphy of Transect 2, estuarine funnel

Stratigraphy has been examined in several probes and cores in the North Point area. Transect 2 (Figure 42) runs across North Point causeway on the western side of the funnel and transect 3 (Figure 43) traverses Culaly Plain on the eastern side. Core SAH 128 is in the elbow of the sharp bend at 16 km from the river mouth (see Figures 39 and 81).

The stratigraphy of transect 2 is relatively straightforward, as shown in Figure 42. The upper 1 to 2 m of sediment is heavily oxidised; mangrove mud is apparent below the oxidised zone in holes SAH 56, 57 and 58. Hole SAH 59 showed bluish-gray muds or clays to depths of about 6 m, with mud, possibly but not unequivocally mangrove in origin, below that. Radiocarbon ages on mangrove material of 6760 + 90 years B.P. at 8.1 m in SAH 56, 6470 ± 110 years B.P. at 3.7 m in SAH 58 and 6110 ± 130 years B.P.

at 2.3 m in SAH 57 indicate that mangroves became well-established at the western side of the estuarine funnel before sea level stabilised, about 6500 to 6000 years ago. The radiocarbon age of 2930 ± 170 years B.P. at 2.0 m in SAH 56, above the older age recording initial sea-level stabilisation, indicates either gradual migration of the mangrove margin by slow species succession, or more likely continued mangrove growth at this site which is only 10 m from the present mangrove fringe. As this probe is at the river's edge, changes since about 2900 years B.P. are unknown. The bluish-gray mud, with fine organic flecks, at the rear of the plain in SAH 59 could be interpreted as paleochannel or ill-drained depression deposits. A date of 1980 ± 110 years B.P. at 4.6 m in SAH59 indicates this to have been infilling about 2000 years ago.

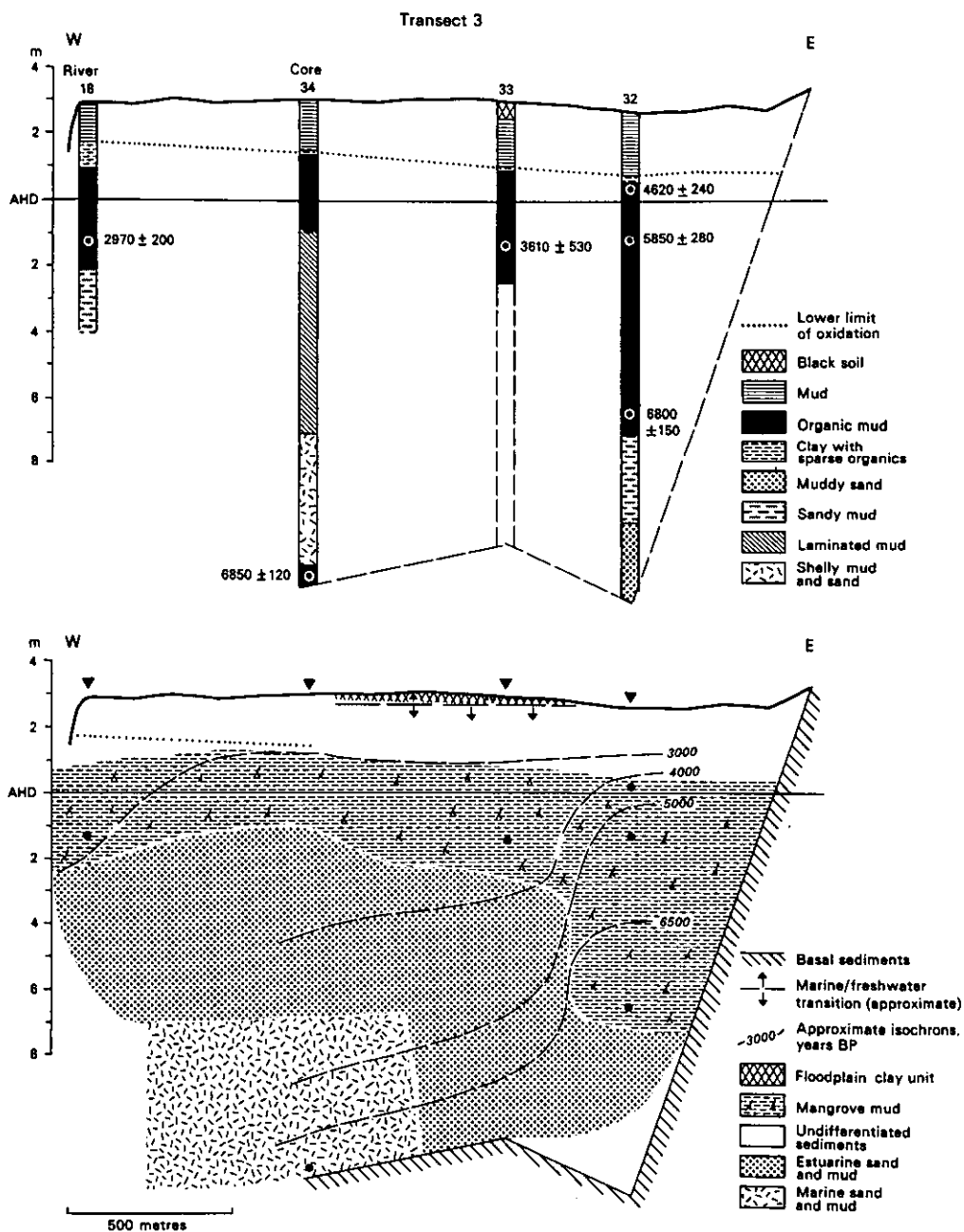


Figure 43: Stratigraphy of Transect 3, estuarine funnel and tentative isochrons of coastal progradation

The stratigraphy of transect 3 (Figure 43) on the eastern side of the river shows some similarities with transect 2 (Figure 42). Basal sands overlie the pre-Holocene surface in SAH 32 at the eastern edge of the floodplain, and these are overlain by laminated estuarine sand and mud. Core SAH 34 has sandy sediments with abundant shell hash at the base. This is interpreted as marine sand and mud, the abundant shell being typical of nearshore environments. Above these shelly deposits there is laminated mud which is considered estuarine. There is mangrove mud in the upper part of all the holes on the transect, below the heavily oxidised surface sediments. A number of radiocarbon dates have been obtained on the mangrove material and are younger than most results from further south. The deeper date from 9.15 m in SAH 32, 6800 ± 150 , records the late transgressive period prior to sea-level stabilisation, and the upper dates at 3.95 m and 2.45 m of 5850 ± 280 and 4620 ± 240 years B.P. respectively, indicate mangrove persistence at this site after sea-level stabilisation. Mangrove then migrated slowly towards the present river, reaching the present river bank at about 3000 years ago, as indicated by an age of 2970 ± 200 years B.P. at 4.2 m in SAH 18 (Figure 43). The age of 3610 ± 530 at 4.25 m in SAH 33 records the migration of the mangrove margin. We would predict that an age of around 3000 years B.P. would be obtained on the regressive mangrove mud in core SAH 34, where the mangroves can be seen to have prograded over laminated estuarine sediments.

It appears that after about 4000 years B.P. the estuarine funnel prograded at this point on the eastern side of the South Alligator River. Figure 43 also shows a reconstruction of isochrons recording this progradation. The site of probe SAH 32 probably remained close to the shore and accreted vertically until after 4000 years B.P., with estuarine sedimentation to the west of it with a more pronounced marine influence. The change in the marginal mangrove sedimentation rate, indicated by the alteration from predominantly vertical accretion in the mangroves to lateral progradation at around 4000 years B.P., may also coincide with the change from shelly marine sand and mud to the less shelly estuarine sand and mud recorded towards the base of SAH 34. Similarly a shelly layer was found at the base of SAH 128 on the western side of the river, with a radiocarbon date of 3930 ± 120 years B.P. on shells at 11.3 m (age not environmentally-corrected). This is overlain by laminated less-shelly estuarine sediments in SAH 128, very similar to SAH 34.

The rapid progradation of the east bank of the estuarine funnel coincided with rapid progradation of the coastal chenier plain. Comparison of the spacing of isochrons in Figures 41 and 43 reinforces this point.

4.4.4 Stratigraphy of the Sinuous Meandering Segment

In the sinuous meander segment of the river we have examined transects 4 (Figure 44), 5 (Figure 45), 6a (Figure 46) and 6b (Figure 47), and additionally have drilled the large paleochannel north of Munmalary (holes SAH 19, 35 and 36). Figure 44 shows a schematic section of the salient stratigraphic points on transect 4. This consists of a probe, SAH 47, adjacent to the river bank in a mid-plains location, and holes within and on either side of a paleocreek feature on the floodplains in the vicinity of Water Recorder Point. Mangrove mud occurs on either side of the paleocreek, radiocarbon-dated to 7070 ± 90 , 5800 ± 120 and 5630 ± 120 years B.P. on the western side. Mangrove mud occurs to 11.8 m below the surface in probe SAH 47 adjacent to the river, dated 6540 ± 240 years B.P. at 11.7 m, and 5600 ± 210 years B.P. at 6.3 m. These dates are rather young for their depth and the significance of this will be discussed below. Mangrove mud overlies more silty and less organic sediments considered estuarine in origin.

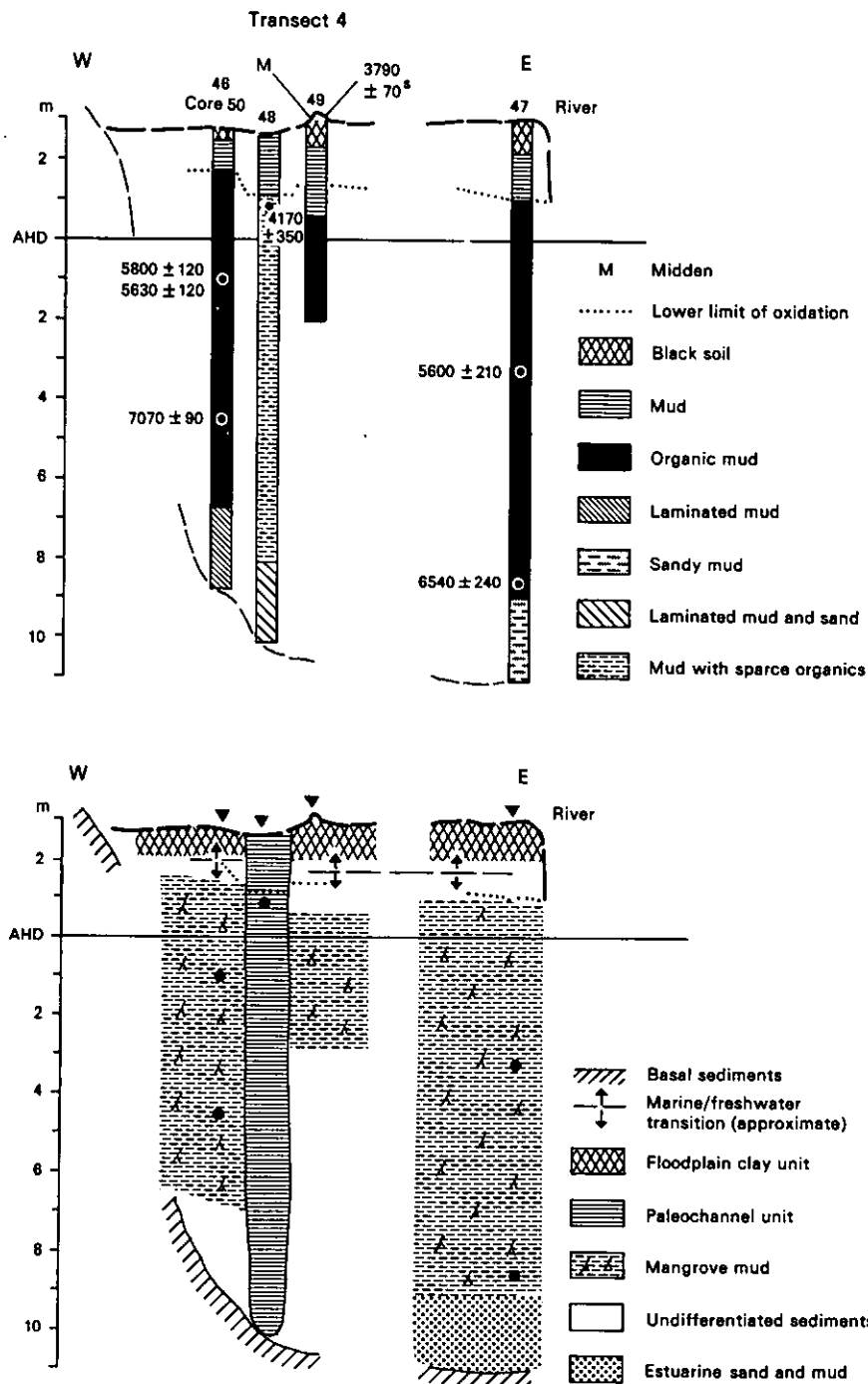


Figure 44: Schematic stratigraphy of Transect 4, sinuous meandering segment

We do not have a date on mangrove mud in probe 49, however a date on midden shells on the surface of 3790 ± 70 years B.P., serves as a minimum age. It seems likely that this mangrove mud also dates from the period of stabilisation of sea level. The paleocreek is filled with fine mud, with a radiocarbon date of 4170 ± 350 years B.P. from close to the sediment surface. The feature has evidently not been active for more than 4000 years.

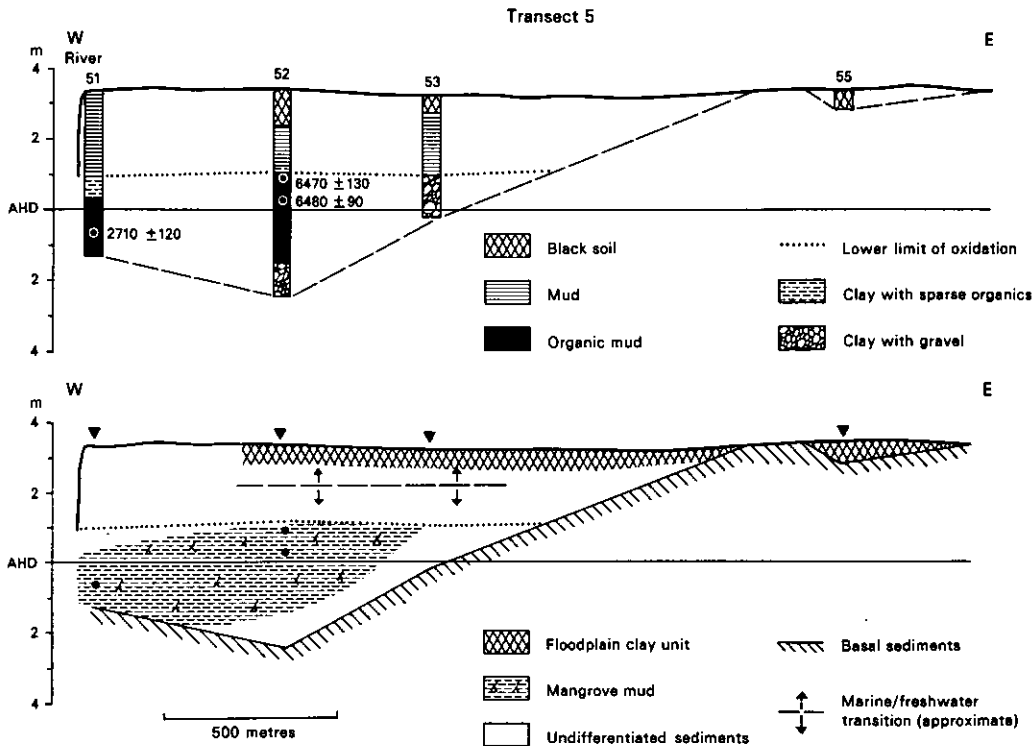


Figure 45: Stratigraphy of Transect 5, sinuous meandering segment

Figure 45 shows the stratigraphy of transect 5 from Munmaly Landing along the track back to the Munmaly homestead. The basal sediment is never more than 5.8 m below the surface, it forms a small island in the floodplain at the eastern end of the transect and outcrops on the river bank at low tide. It is overlain along much of the transect by basal sands and gravels, over which occurs mangrove mud. Radiocarbon dates of 6470 ± 130 and 6480 ± 90 years B.P. from 2.4 m and 3.7 m respectively in SAH 52 are on organic fragments in mangrove mud. A date of 2710 ± 120 years B.P. from 4 m in SAH 51 and dates of 2100 ± 370 and 1880 ± 290 years B.P. from 6.4 and 2.3 m respectively in SAH 8, just south of the transect, adjacent to a creek draining into the South Alligator River indicate younger mangrove close to the river. These are both locations adjacent to the present littoral mangrove fringe. The ages indicate that the river bank was in much its present position, if not further riverward, by 2000 years ago. It is noteworthy that, by contrast to the pre-Holocene beneath transect 5, the river is uncommonly deep on this bend and it is likely that it occupies a prior channel. The pre-Holocene exposed in the river bank may mark the top of a prior cliff or river gorge 20-25 m high.

Figure 46 shows the stratigraphy of transect 6a at Rookery Point. The basal sediment surface slopes away towards the river at a gentle gradient. Overlying basal sediments from SAH 60 are bluish-gray clays with sparse organic fragments which may be mangrove mud or have been deposited in some other undifferentiated estuarine environment (as discussed in more detail in 5.1). Holes SAH 60 and 61 contain mangrove mud on which radiocarbon ages have been determined indicating establishment of mangrove by the time of sea-level stabilisation. An age of 5940 ± 90 years B.P. was determined at 2.4 m in SAH 61, and 6660 ± 100 and 5850 ± 100 years B.P. at 7.0 and 4.6 m respectively in SAH 60. In addition sub-fossil mangrove stumps are exposed on the river bank at the eastern end of the transect. Ages of 5690 ± 90 , 5460 ± 90 and 5560 ± 80 years B.P. have been determined on stumps from this site, and 5950 ± 100 on a specimen of *Polymesoda* associated with the stumps. The river has evidently not been west of its present course at this point since the deposition of this mangrove mud. Probe SAH 62 did not encounter mangrove mud; the sediments are faintly laminated bluish-gray clays with sparse disseminated organic fragments, indicating deposition in a shallow water body, perhaps a channel or ill-drained depression.

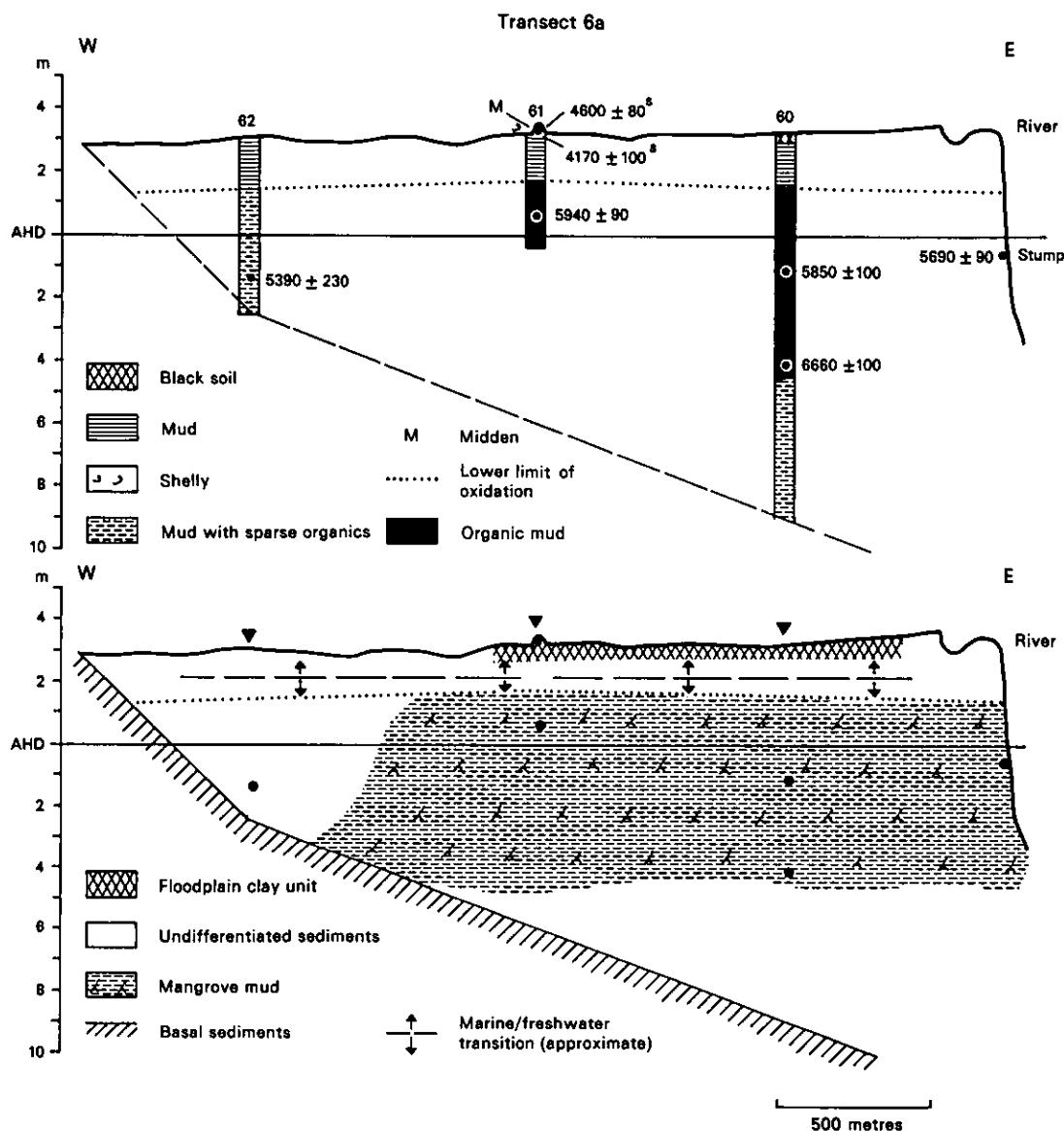


Figure 46: Stratigraphy of Transect 6a, sinuous meandering segment

Figure 47 shows Transect 6b, to the east of Apple Tree Bend on the South Alligator River. It is the area mapped in Figure 34 in which a distinct paleochannel occurs, occupied by mangrove and salt mudflat. Probe SAH 111 lies outside the paleochannel and mangrove mud is encountered throughout, though with an increase in shell below 6 m below ground level. Core SAH 112 penetrates channel fill deposits in the paleochannel. Probe SAH 113 records a series of laminated bluish-gray silty clays with fine disseminated organic fragments, typical of active channel and similar to sediments clearly exposed in truncated and eroded banks on the convex bank of the Apple Tree Bend. Thus laminated channel sediments are found within the paleomeander and mangrove mud is found outside.

Figure 48 summarises the relationships in the Rookery Point and Apple Tree Bend part of the river in a schematic block diagram. It indicates that on either side of the valley there are mangrove muds, dated to around the time of sea-level stabilisation on the western side, and almost certainly of similar age on the eastern side also. There are two main paleochannels, the eastern one filled with channel fill sediments (core SAH 112), and the western one recognisable in bank exposures by blocky clays veneered by recent laminated muds, in contrast to the strongly laminated channel sediments underlying the present river point bar and extending back along the river bank.

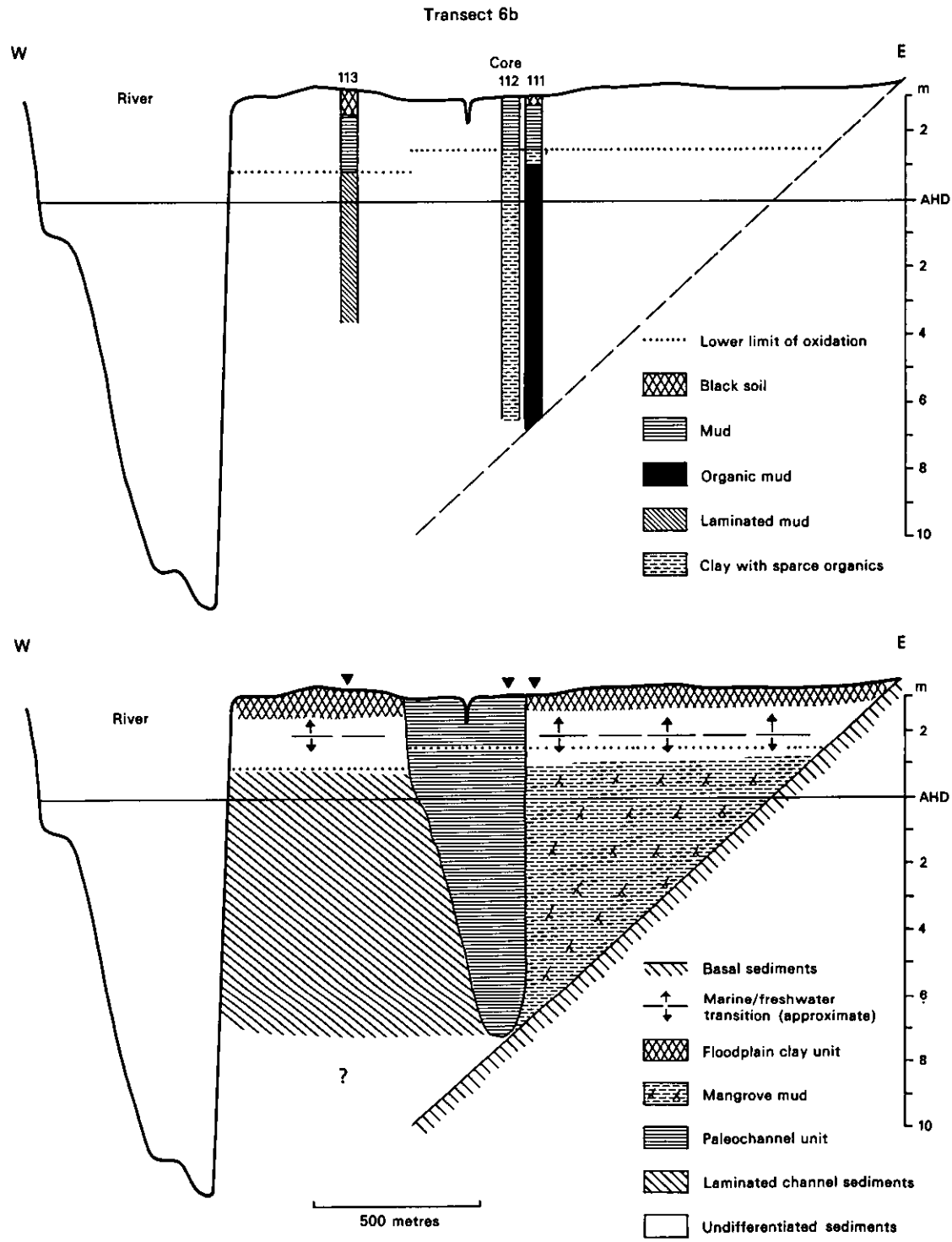


Figure 47: Stratigraphy of Transect 6b, sinuous meandering segment

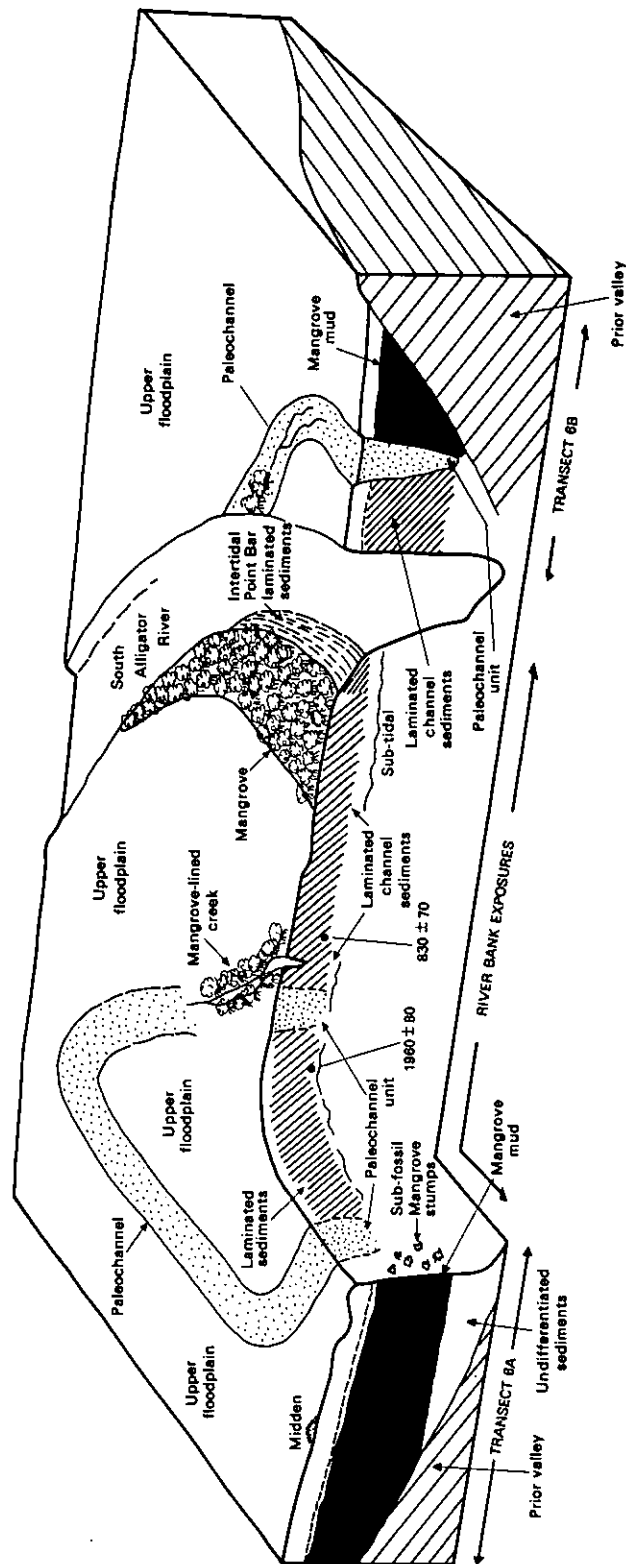


Figure 48: Block diagram showing stratigraphic relationships in the Apple Tree Bend and Rookery Bend region of the sinuous meandering segment. Viewed from the south-southeast.

4.4.5 Stratigraphy of the Cuspate Meandering Segment

South of Rookery Point the South Alligator River enters its cuspate meander phase. We have examined this segment of the river in considerable detail. In particular, the Bullocky Point area has been a focus of attention because of the large number of paleochannels which can be seen on the aerial photographs in this area (Figure 35). Figure 49 reproduces the map of morphologic units in this area, showing the location of 26 drill holes. Details of stratigraphy are shown in transect 7 (Figure 50) and transect 8a (Figure 51). A schematic block diagram which attempts to reconstruct the development of this area is shown in Figure 52.

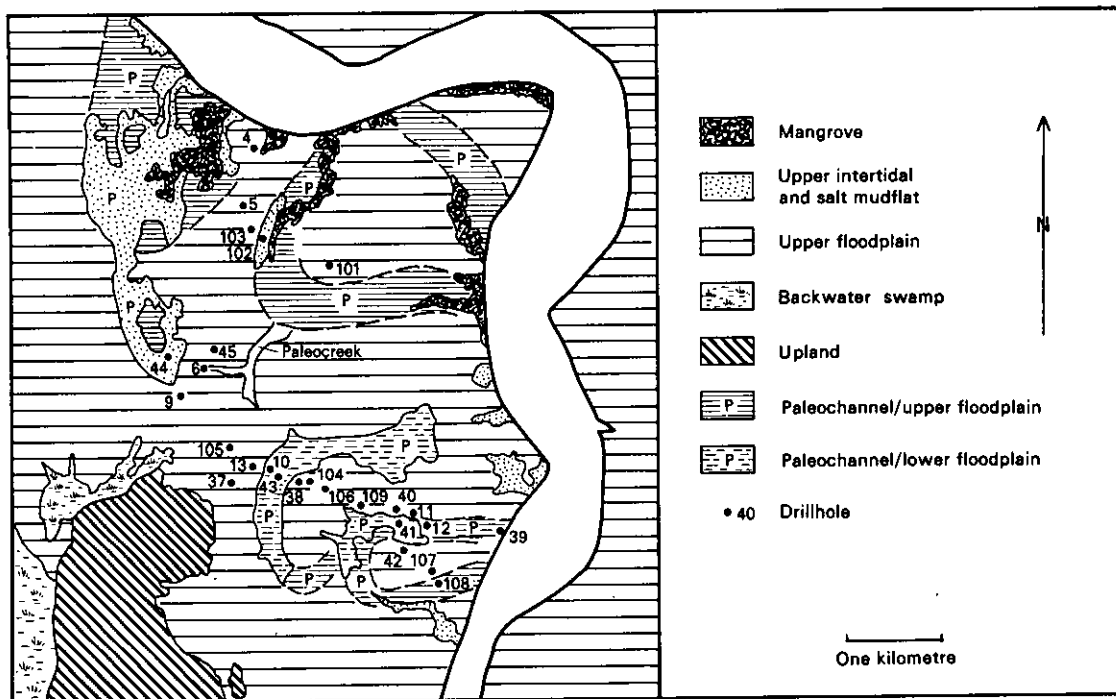


Figure 49: Detailed map of morphostratigraphic units and drillholes in the Bullocky Point area

In addition, within the cuspate segment of the river the following transects were examined: transect 8b across a series of less distinct paleochannels opposite the Bullocky Point area on the eastern side of the river (Figure 53), transect 9a to the west of Round the World (Figure 54), transect 9b to the east of Round the World (Figure 55), and transect 10 (Figure 56) which is adjacent to the Arnhem Highway. This last transect is at the limit of the cuspate section; it shows a series of paleochannels and many similarities to the Bullocky Point transect 8a, but as is discussed below the paleochannels take on the characteristics of upstream channels.

In the Bullocky Point area the pre-Holocene surface falls relatively steeply from the upland margin to a depth of about 16 m below the surface of transect 8a and to more than 18 m on transect 7. Basal sediments were encountered at below 26 m in SAH 44. The sediments on transect 7 are laminated silt and clay and bluish-gray clay with sparse disseminated organic fragments (Figure 50). Their deposition has been associated with movements of a channel of which there is now no clear evidence. We record much of this transect as undifferentiated as it would require sophisticated microfossil analysis to interpret it more fully.

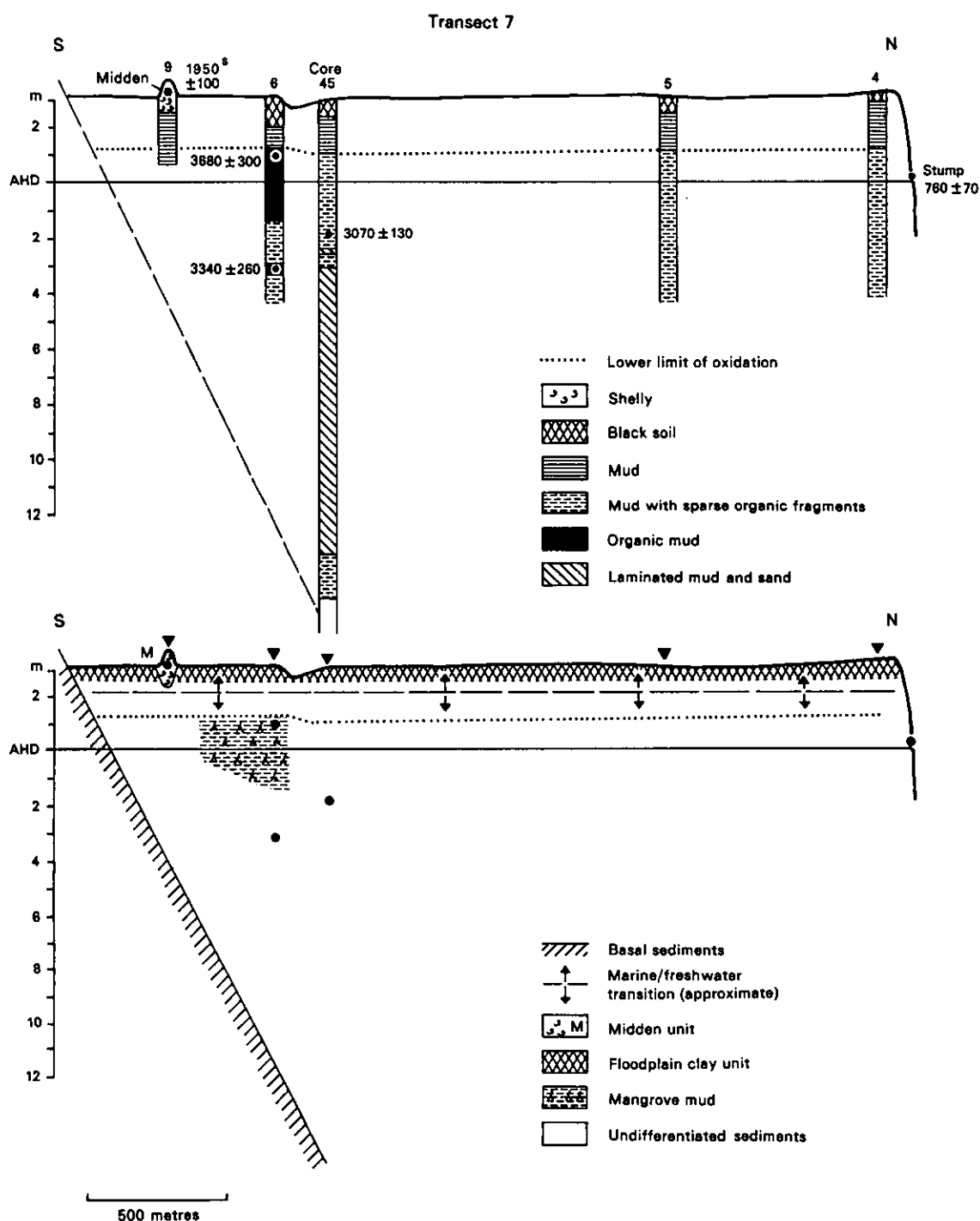


Figure 50: Stratigraphy of Transect 7, Bullocky Point, cusped meandering segment

Transect 8a (Figure 51), supplemented by several additional adjacent probes, traverses the two nested, sinuous paleochannels. Overlying the pre-Holocene basement there are deposits of other basal sediments. Transgressive mangrove mud is encountered in probe SAH 37 from which mangrove remains at 12.6 m, overlying basal sediments, have been dated at 7470 ± 120 years B.P. Wood, identified as mangrove wood at similar depths in other holes on the transect, underlying laminated channel sediments dated anomalously young. The radiocarbon age on a large piece of wood at 14.3 m in SAH 40 6730 ± 90 years B.P., and those of 5310 ± 200 and 5490 ± 100 years B.P. at 14.0 m and 11.0 m in SAH 41 and SAH 38 respectively, date from the time when sea level was stabilising or had stabilised, and when there is abundant evidence of well-established widespread mangrove forest elsewhere in the river system. These remains must therefore have been deposited in active channels as the channel migrated across transect 8a (see below). Mangrove mud is recorded throughout drillhole SAH 105 and is presumed throughout SAH 37 which was not sampled continuously. These holes indicate the existence of mangrove forests from a time before sea level stabilised up to and beyond the time of sea-level stabilisation which accords with observations elsewhere along the margin of the floodplains.

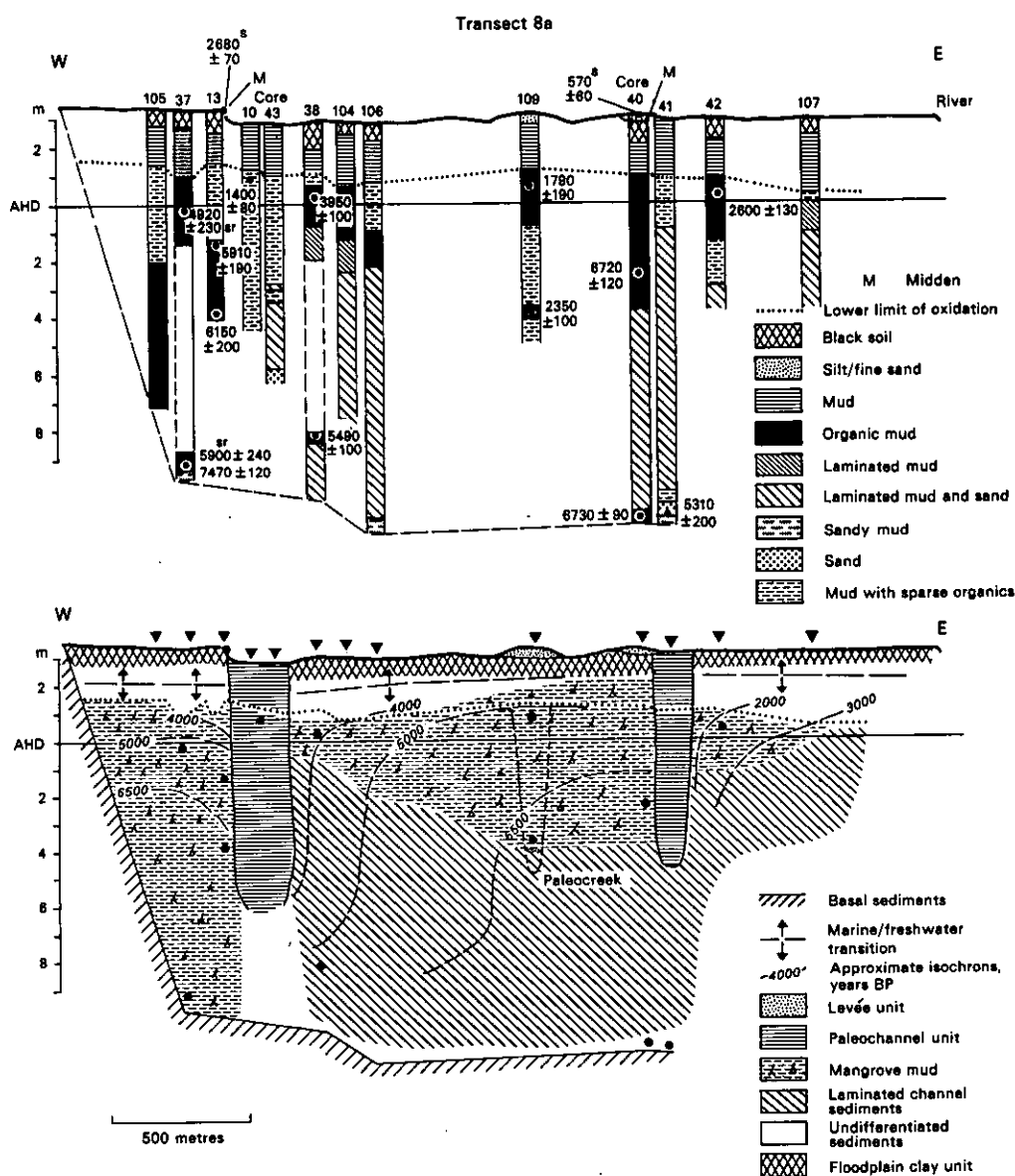


Figure 51: Stratigraphy of Transect 8a, Bullocky Point, cusped meandering segment, and tentative isochrons of channel migration

Radiocarbon dates of 6150 ± 200 and 5910 ± 190 years B.P. at 7.2 m and 4.7 m respectively in SAH 13 confirm the contemporaneity of mangrove forests at this site with those on transects further north on the deltaic-estuarine plain. The paleochannel unit contains channel fill clays in their upper part and laminated units similar to the adjacent laminated channel sediments in their lower parts (Figure 51). Much of the centre of transect 8a is composed of laminated channel sediments. These lie within the bend of the meander and are considered to have been deposited as a channel migrated across the plain.

The significance of sinuous paleochannels in the presently cusped meandering segment of the river will be discussed in Chapter 5, and in relation to other rivers in Chapter 6. A feature of sinuous bends on other rivers (particularly the Adelaide River) is the extensive mangrove forests that develop on the convex banks of the meander. The stratigraphy shown in Figure 51 illustrates that mangrove mud is found in drillholes located on the convex banks of paleochannels. Radiocarbon ages can be used to indicate the time at which these mangrove forests flourished, which in turn indicates when the paleochannel was tidally active, and pre-dates abandonment of the channel. A radiocarbon age of 3950 ± 130 years B.P. was obtained on mangrove mud at 2.7 m in SAH 38, and an age of 2600 ± 130 years B.P. was obtained on mangrove mud at 2.7 m in SAH 42, indicating that the inner paleochannel was active at least 2500 years ago. Other radiocarbon dates suggest that the channel was active from 2600-1800 years B.P., particularly dates of 1790 ± 190 and 2350 ± 100 from a paleocreek cored in SAH 109 (Figures 49 and 51). Although the outer bend was abandoned some time after 4000 years ago, and must have been inactive by 2500 years ago, when a younger channel was truncating the abandoned course of this older paleochannel, infill of the cutoff was not immediate. It would seem that infill must have been gradual and that a relatively open lagoon must have persisted in the cutoff paleochannel until at least 1400 years ago, as a date of 1400 ± 80 years B.P. has been obtained on wood fragments in the paleochannel unit at 1.9 m in SAH 10.

Thus, in the cusped segment, two episodes of active channel migration are envisaged as shown by isochrons on Figure 51 and in block diagrams in Figure 52. The first is indicated by the log at the base of SAH 40 dating at 6730 ± 90 years B.P., anomalously young for its depth. The laminated sediments overlying this must have been deposited rapidly in association with active channel migration to the west, because these sediments are overlain by mangrove mud which dates at a depth of 5.6 m to 6720 ± 120 years B.P., that is not significantly different from the basal date. This indicates the rapidity with which a vertical depth of 8-9 m of active laminated channel sediments can accumulate. The upper date records establishment of mangrove here, as through much of the deltaic-estuarine plain at the time that sea level stabilised. Two further dates on basal mangrove material beneath laminated channel sediments give some ideas of the rate of migration of the channel (see Chapter 5). In probes SAH 38 and SAH 41 the basal dates of 5490 ± 100 and 5310 ± 200 years B.P. described above have been obtained. We interpret that the channel was actively migrating in this area, both outwards (from SAH 40 to 38) and upstream (from SAH 40 to 41), from 6700 to 5300 years ago. It was then fairly stable in the course indicated by the outer paleochannel until at least 4000 years ago.

The inner, younger paleochannel may have been shallower than the outer, older paleochannel. Its base is defined by a prominent colour change at 7.5 m depth in probe SAH 41. Though this may be unrepresentative of the channel depth as a whole, the laminated channel sediments drilled between the two channels indicate that the channel depth, even after sea level stabilised around 6000 years ago, was 10-14 m prior to 4000 years ago, and appears at least 8.5 m in the outer paleochannel.

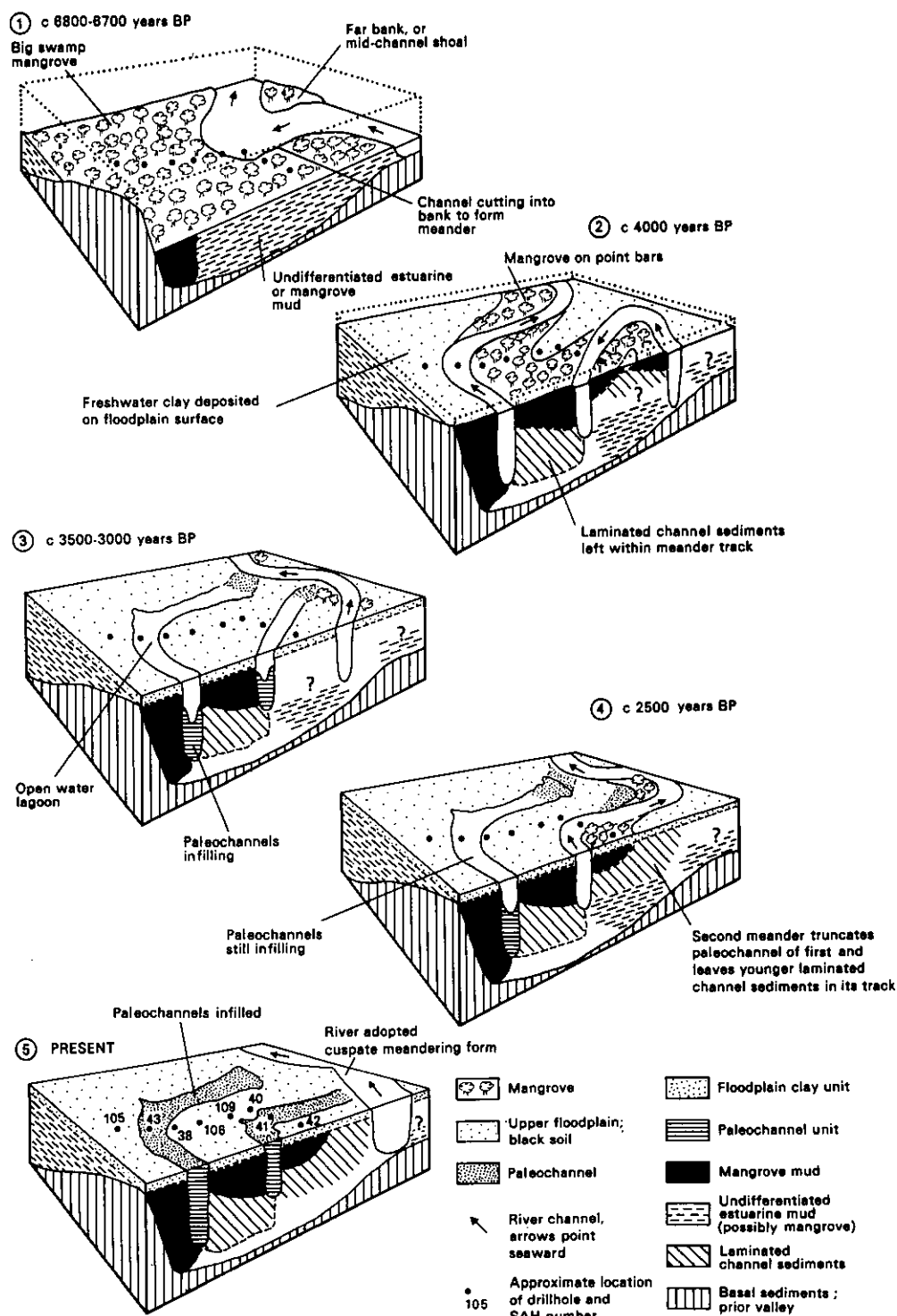


Figure 52: Block diagram showing schematic interpretation of channel migration in the Bullocky Point area

Figure 53 shows transect 8b across a series of paleochannels on the eastern side of the river. There are laminated channel sediments between the bends, and the paleochannels contain channel fill sediments of the paleochannel unit. The history of channel migration is probably similar to that in the Bullocky Point area. However, the continuity of paleochannels is less apparent in this area. Furthermore, whether paleochannels rejoined the main river or were carrying large volumes of freshwater from Boggy Plains is unresolved. The only radiocarbon date, 5580 ± 200 years B.P. from 2.9 m in SAH 100 indicates that this part of the plain was mangrove around the time that sea level stabilised.

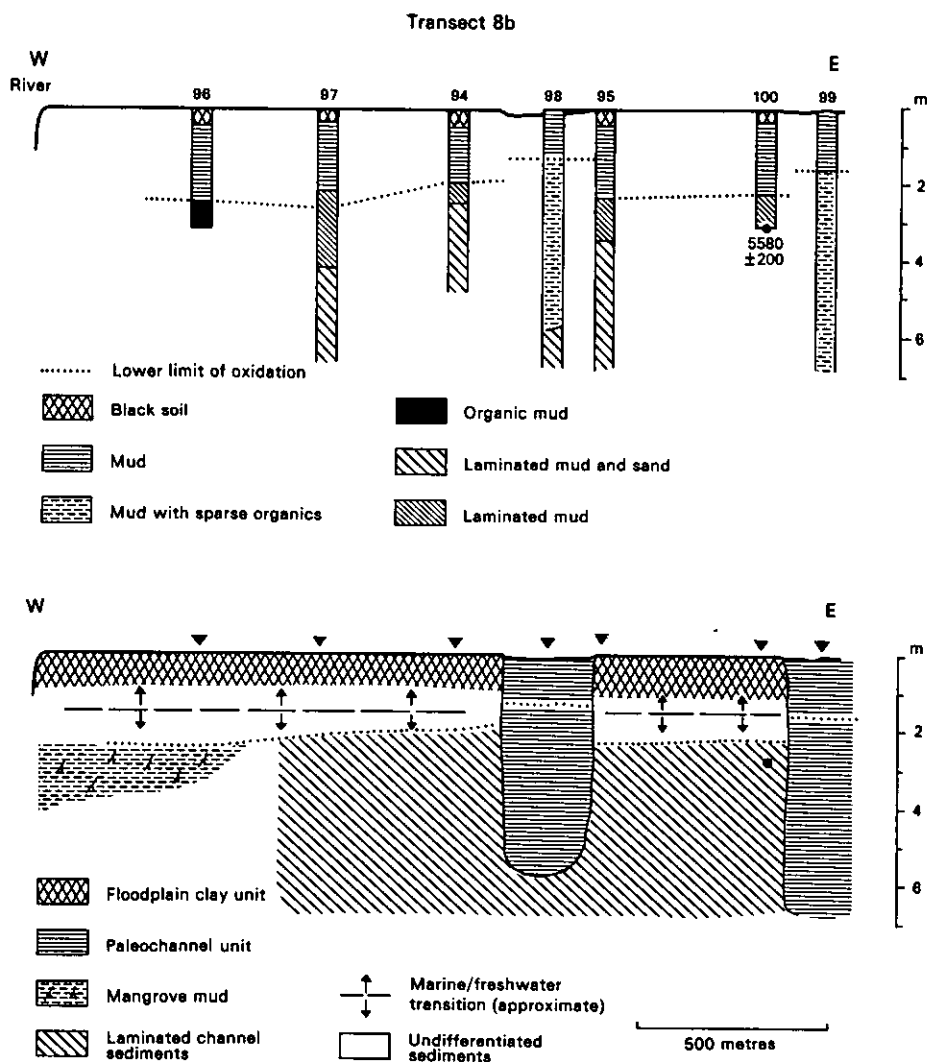


Figure 53: Stratigraphy of transect 8b, Boggy Plains, opposite Bullocky Point, cusped meandering segment. Note this transect is not reduced to AHD.

Transect 9a (Figure 54) to the west of Round the World is a short transect on which mangrove mud is encountered. Radiocarbon ages on organic fragments in the mud are 6530 ± 690 and 6390 ± 130 years B.P. at 4.8 m and 4.7 m respectively in SAH 1. Recent sedimentation on the river bank at Kapalga Landing on this transect means that this mangrove mud is not exposed on the bank, but a short distance to the north mangrove stumps are exposed on the banks adjacent to core SAH 120 (see below). The exposure of mangrove stumps is discussed in more detail in Chapters 5 and 6, but both stumps and mangrove mud appear to date from the time that sea level stabilised.

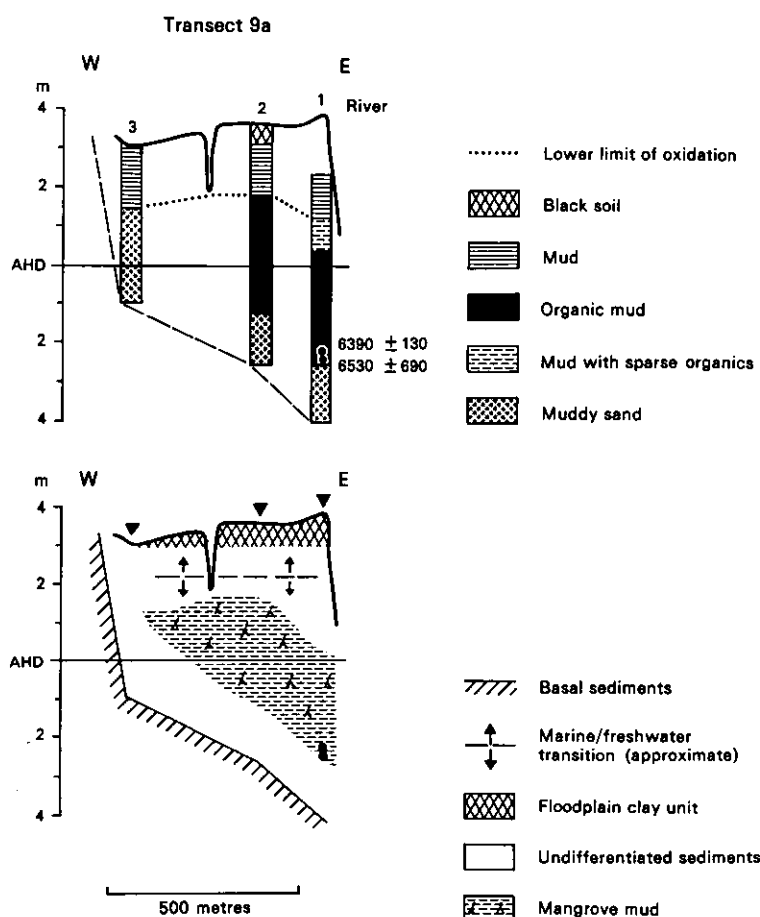


Figure 54: Stratigraphy of Transect 9a, cusped meandering segment

Transect 9b (Figure 55) to the east of Round the World traverses several paleochannel features seen on aerial photographs. Holes were drilled on banks of these features. Core 92 is located just east of the outer paleochannel. It can be seen in Figure 55 that mangrove mud occurs in core SAH 92 and SAH 93 towards the eastern end of the transect. The western half of the transect is underlain by laminated channel sediments which were laid down as the channel migrated through this area. The two features identified on the aerial photographs and just discernible on the ground by small changes of gradient on the surveyed traverse are expected to be of different ages indicating different periods of river activity to the east of Round the World.

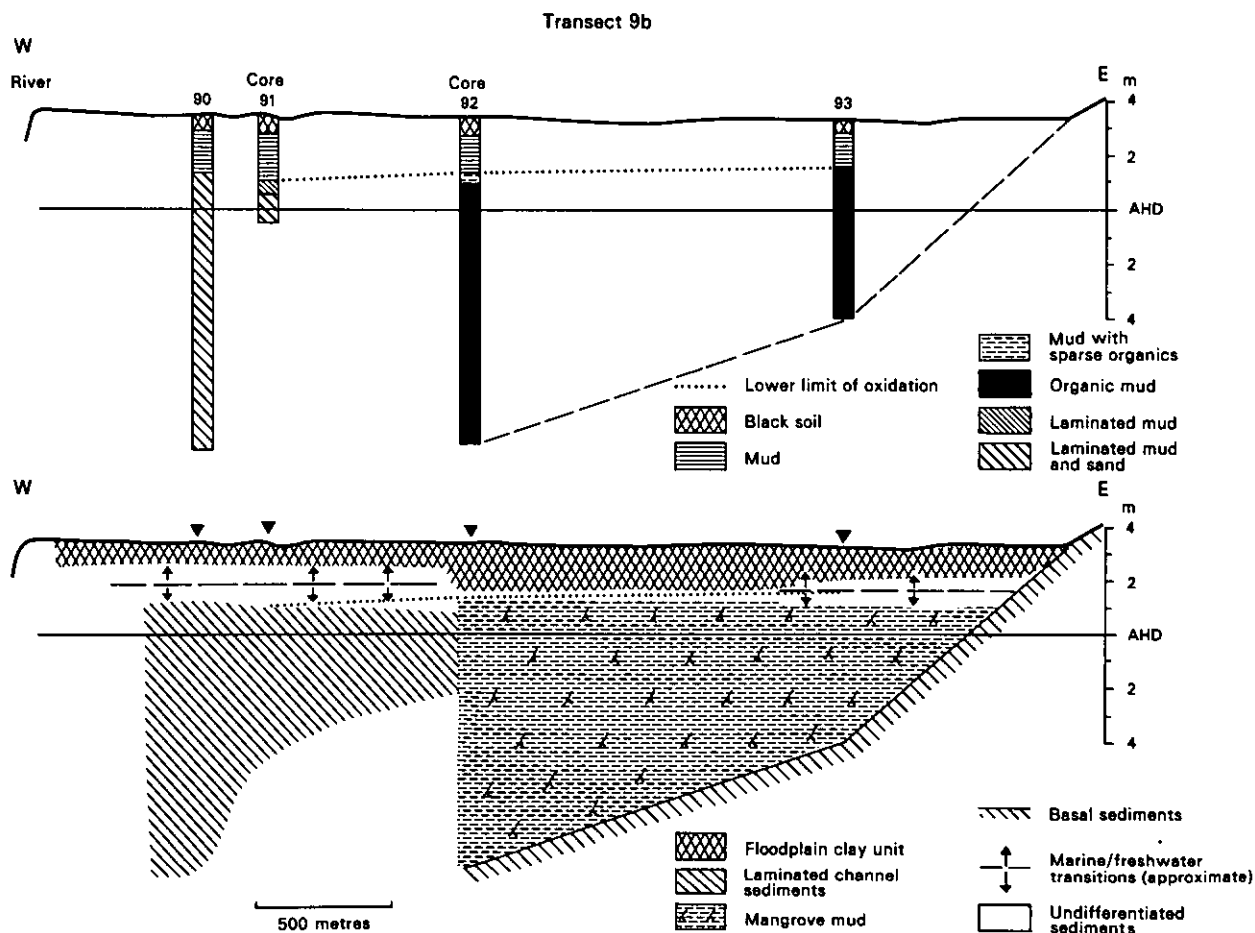


Figure 55: Stratigraphy of Transect 9b, cusped meandering segment

Figure 56 shows transect 10 which runs adjacent to the Arnhem Highway on both sides of the river. The pre-Holocene basement is exposed at a couple of locations to the east of the river, one of those exposures including the rocks of Water Monitor Dreaming. To the east of the transect a second basin has been infilled largely with mangrove mud, in which organic fragments have been radiocarbon dated to 6710 ± 140 and 6260 ± 100 years B.P. at 7.9 m and 5.5 m in SAH 66, and to 5990 ± 130 years B.P. at 2.45 m in SAH 65. West of the river the aerial photographs reveal that there are several paleochannels and these have been examined in a number of drillholes close to the highway. Outside the course of the paleochannels, in SAH 73, organic fragments in this have been dated to 6550 ± 140 and 5850 ± 90 years B.P. at 3.1 m and 1.5 m respectively, again indicating extensive mangrove forests at the time when sea level stabilised. The most obvious paleochannel is a large one cored by SAH 71. This is filled with channel fill clay of the paleochannel unit with a radiocarbon date of 1290 ± 140 years B.P. at 11.75 m. Between the paleochannel and the river there is a second paleochannel, again filled with muds with sparse organics; the base of the paleochannel unit is dated 2880 ± 100 years B.P. at 9.6 m in SAH 114. Holes between these channels contain laminated channel sediments and there is a date of 5110 ± 120 years B.P. on these at 9.5 m in SAH 117 (Figure 56). Similar laminated sediments were encountered in SAH 131 within the paleomeander. Outside the course of the meander, to the south in SAH 129, and to the west in core SAH 73 mangrove mud has been encountered (see Figure 63).

Transect 10 occurs at the transition between cusped and upstream segments of the river. This transition is important in interpreting what has happened here and so transect 10 will be reconsidered below when the upstream segment has been examined.

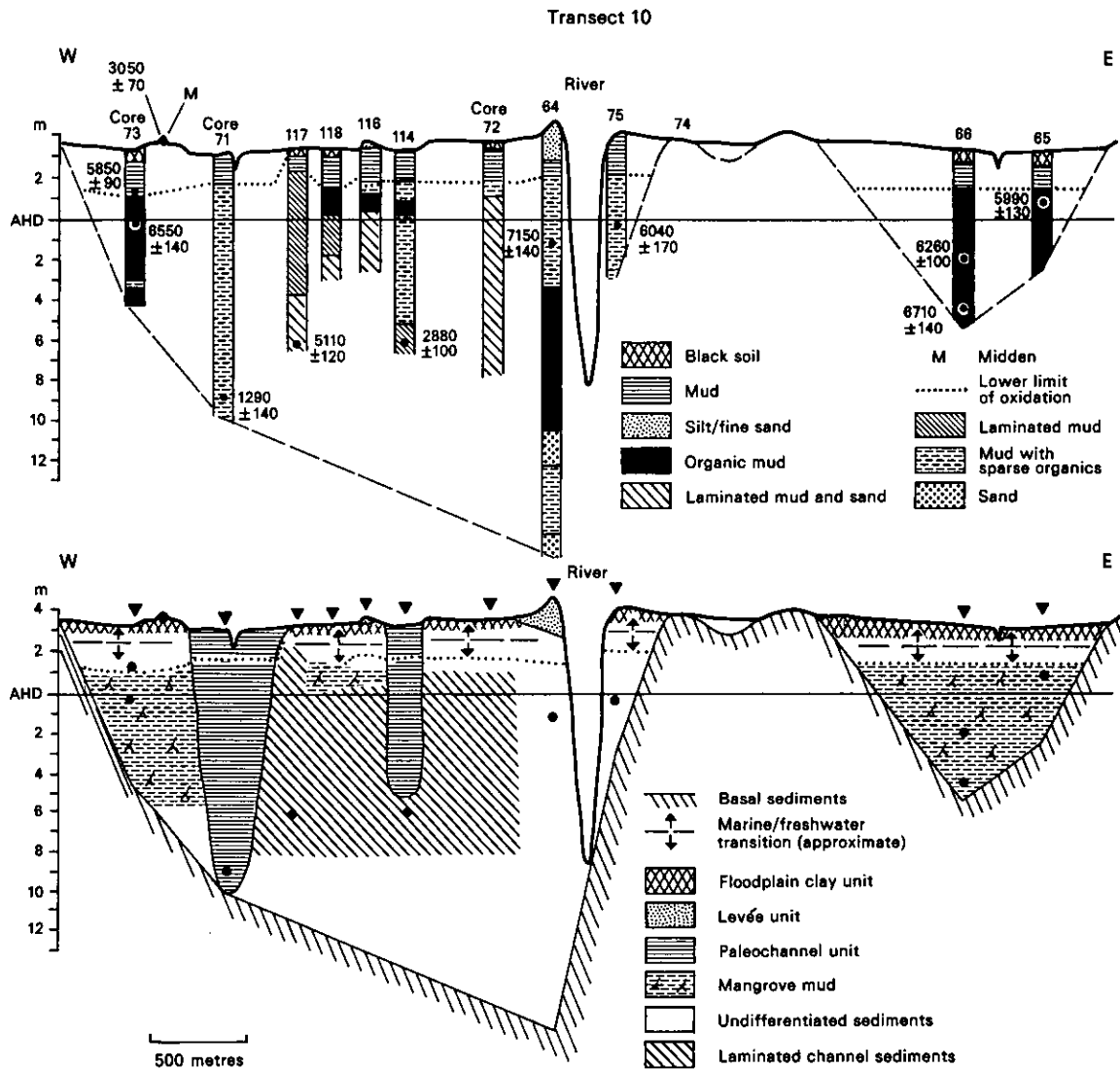


Figure 56: Stratigraphy of Transect 10, cusped meandering segment

4.4.6 Stratigraphy of the Upstream Segment.

The stratigraphy of the upstream segment of the South Alligator River, the segment which is characterised by a series of irregularly spaced bends interspersed with straight stretches, has been examined in a series of traverses: transect 11 (Figure 57), transect 12a (Figure 58) and transect 12b (Figure 59). In addition, a transect was examined west of Horseshoe Billabong, transect 13a (Figure 60) and data on environmental change are available from a series of pits near Kiina, described by Hope *et al.* (1985), labelled transect 13b by us, and redrawn in Figure 61.

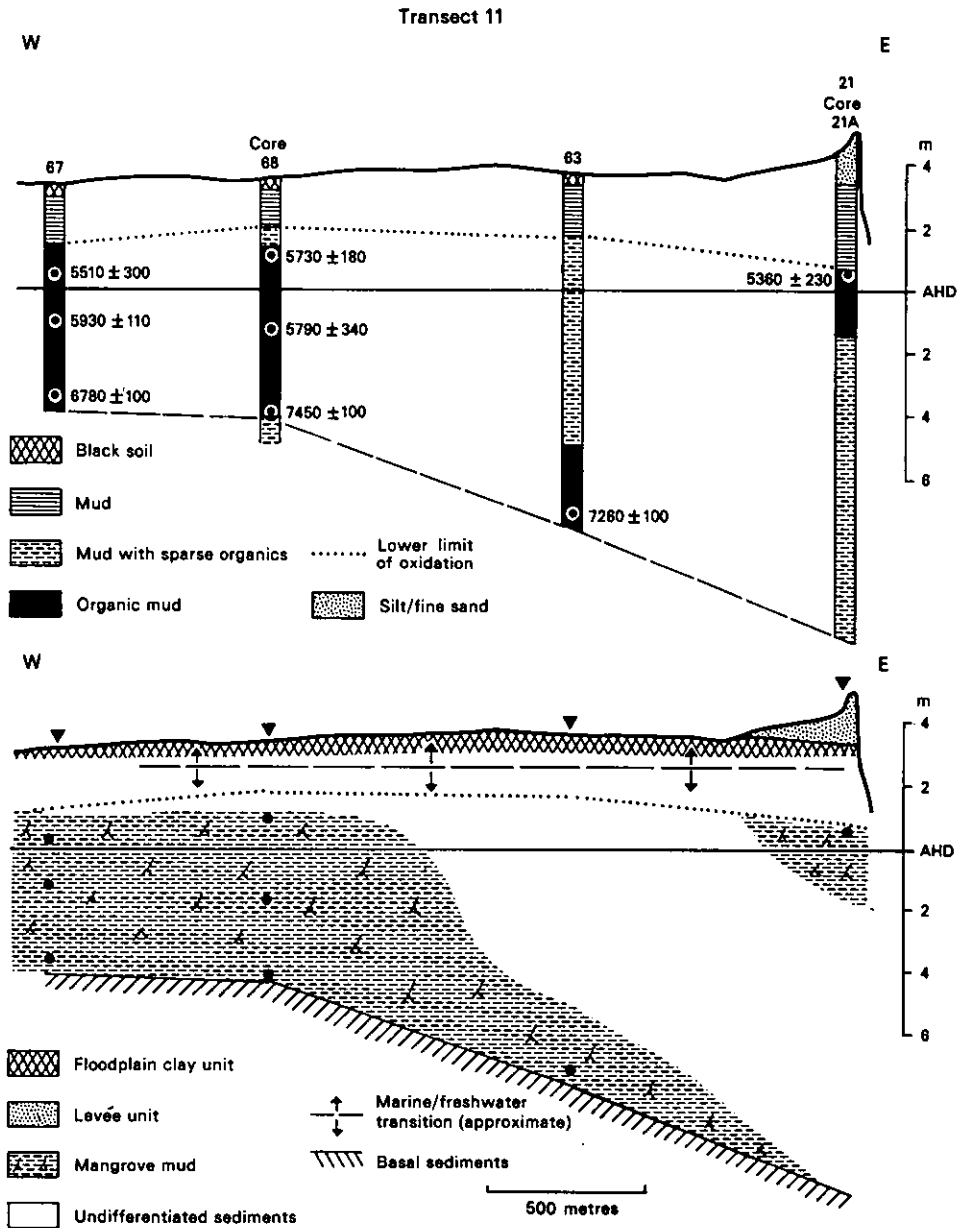


Figure 57: Stratigraphy of Transect 11, upstream segment

At present mangroves extend to the tidal limit of the river, 105 km from the mouth. However, the only species of mangrove represented here are *Avicennia marina* and *Sonneratia lanceolata*. One of the most important observations of our studies in this segment is that in the mid-Holocene there was more extensive mangrove this far upstream. Hope *et al.* (1985) and Russell-Smith (1985b) record a sedimentary unit of gray clay with wood fragments, which they have shown to contain abundant mangrove pollen, particularly of *Rhizophora*, and which they have radiocarbon-dated 5840 ± 100 years B.P. (recorded as 6200 years B.P. on Figure 10.5 of Hope *et al.*, 1985, and 5990 ± 100 years B.P. on Figure 2 of Russell-Smith, 1985b). We similarly record mangrove mud still further upstream in our probe SAH 20, and in this probe we have a radiocarbon date of 6170 ± 260 years B.P., on mangrove mud at 2.1 m.

In the upstream segment of the river there is no evidence of sinuous paleochannels as found in the deltaic-estuarine plain to the north. Instead paleochannels are long anabranches, almost straight with irregularly spaced bends. They are similar in morphology to the presently active upstream segment of the river which they parallel. There are up to two of these paleochannels on both sides of the main South Alligator River. In places the silty or fine sandy levée deposits similar to those of the main channel can be seen, although degraded, adjacent to the paleochannels.

Transect 11 (Figure 57) illustrates the stratigraphy of the deltaic-estuarine plain opposite Nourlangie Creek. Much of the cross-section contains mangrove mud. This was deposited at the base of drillholes SAH 63 and SAH 68 while sea level was still rising as shown by radiocarbon dates of 7260 ± 100 years B.P. at 10.7 m in SAH 63 and 7450 ± 100 years B.P. at 7.4 m in SAH 68. Mangrove was well established in the area when sea level stabilised as indicated by radiocarbon dates of 6780 ± 100 years B.P. at 6.7 m in hole SAH 67, 5930 ± 110 and 5360 ± 230 at 4.3 m and 4.0 m in SAH 67 and SAH 21A, respectively and 5790 ± 340 and 5730 ± 180 years B.P. at 4.7 m and 2.3 m in core SAH 68. There is no evidence preserved of younger mangrove on this part of the plain. On transect 11 the South Alligator River is bordered by a silty or fine sandy levée. Probe SAH 63 may be in a paleochannel though this has hardly any surface expression; we prefer to record it is undifferentiated.

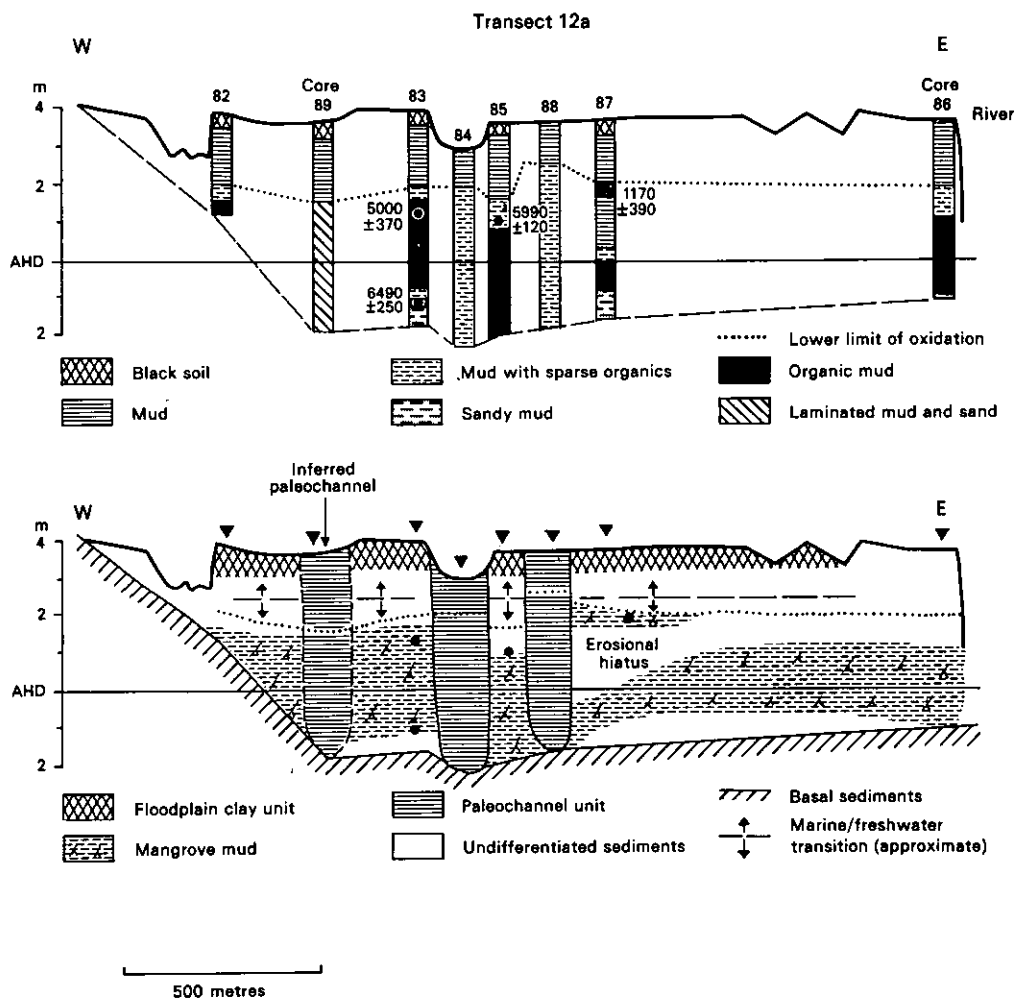


Figure 58: Stratigraphy of Transect 12a, upstream segment

Transect 12a (Figure 58) traverses several paleochannels. The most obvious are the two in the centre; however the depression to the west of the transect which is filled with mangroves may represent another paleochannel. The paleochannel morphostratigraphic unit consists of channel fill clay with fine disseminated organic flecks. We found no indication that these were laminated as suggested from a similar channel by Hope *et al.* (1985), except that we do record laminated mud and sand in core SAH 89, where we infer a paleochannel which no longer has surface expression. Figure 58 indicates that mangrove mud occurs on both sides of the paleochannels and is dated 6490 ± 250 and 5000 ± 370 years B.P. on the western side and 5990 ± 120 years B.P. on the eastern side of one paleochannel. In SAH 87 an erosional period is indicated by oxidation in the middle of the core and later mangrove establishment is dated 1170 ± 390 years B.P.. The stratigraphic expression of the paleochannel morphologic unit recognised from aerial photographs indicates that these are not merely seasonally-occupied channels but are indeed a morphostratigraphic paleochannel unit comparable with those found in the meandering segment of the river. Although the Paleochannel-Lower Floodplain morphologic unit now serves as a seasonal conduit by which wet season floodwaters are channelled to the river, and are also the locus of tidal creek extension and salt water incursion (see Chapter 3.3), their morphostratigraphic expression, confirms that they are channels that were previously active and that have now filled in.

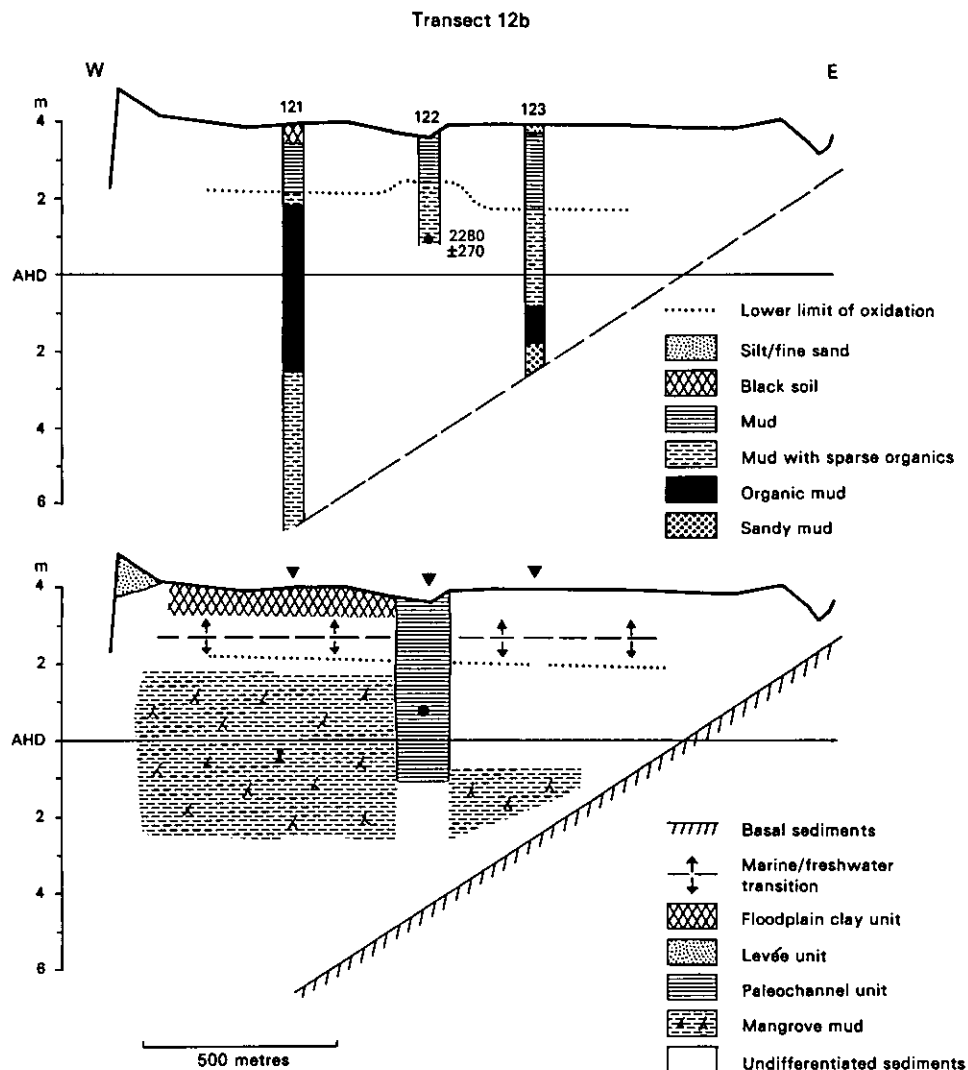


Figure 59: Stratigraphy of Transect 12b, upstream segment

The fact that mangrove mud is found on either side of the river and of paleochannels in the upstream segment, and that there are no laminated channel sediments as in the track of the meandering segments of the river, implies operation of different processes of channel initiation and abandonment from those operating downstream. The manner in which paleochannels have changed location in this part of the river is examined in Chapter 5. Several channels may have been active concurrently in the upstream segment of the river, and the least active channels may have infilled to form the paleochannels observed and mapped.

Transect 12b (Figure 59) is a traverse across another upstream paleo-channel. There is mangrove mud on either side of the paleo-channel on which we have a date of 2280 ± 270 years B.P. It seems highly probable that the mangrove mud will be of the same age on either side and hence indicate that the channel has been occupied and abandoned without reworking of sediments between the channels as on transect 12a (Figure 58). There is a silty or fine sandy levée on transect 12b, while there is not one on transect 12a.

Transect 13a, just west of Horseshoe Billabong (Figure 60) also traverses a paleo-channel, in which the paleo-channel unit consists primarily of clay with finely disseminated organic flecks. Mangrove mud is recorded on both sides of the paleo-channel, in drillholes SAH 125 and SAH 126. A levée deposit is found on the plain more than 100 m east of the river on this transect.

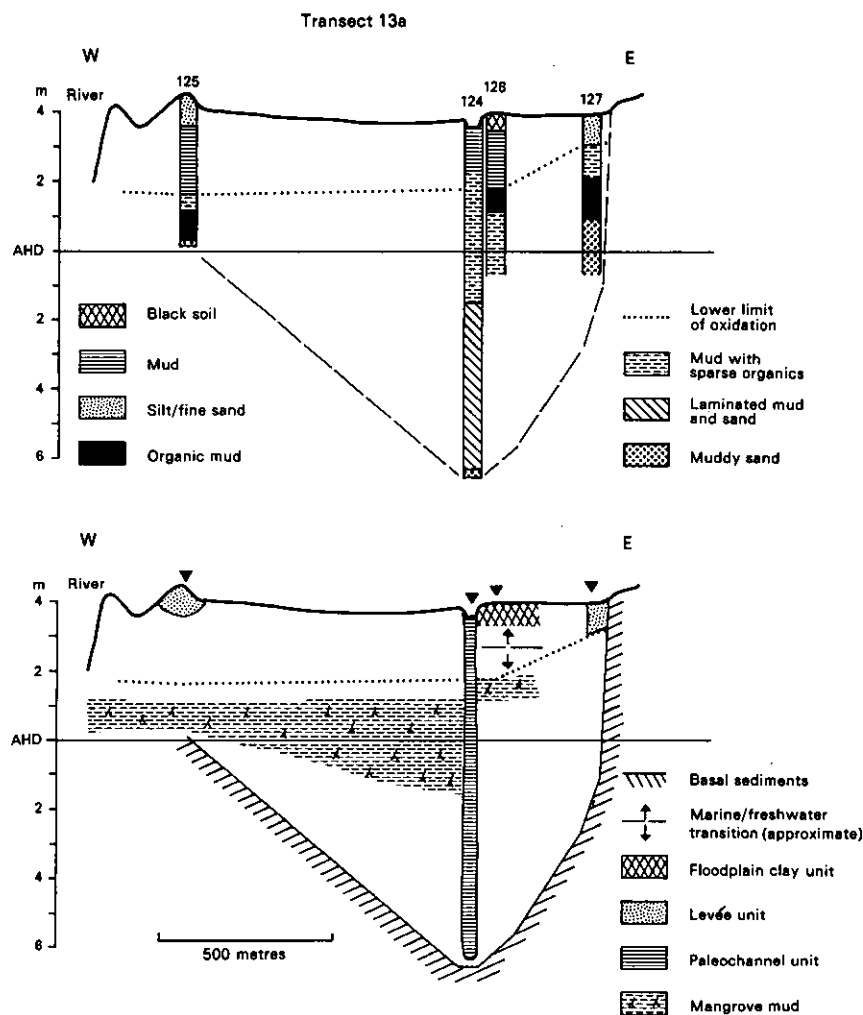


Figure 60: Stratigraphy of Transect 13a, upstream segment. AHD determined from spot heights on photomosaics.

Transect 13b, that described by Hope *et al.* (1985), is redrawn in Figure 61. These authors report dates of 6040 ± 100 and 5840 ± 100 years B.P. from mangrove mud between a paleochannel, their pit 2, and the South Alligator River. These ages accord with our observations of mangrove mud deposition at the time of sea-level stabilisation elsewhere in the deltaic-estuarine plain, and the age of 6170 ± 260 years B.P. from SAH 20, which is at a similar distance upstream and on the west bank of the river. While Hope *et al.* (1985) do not have a radiocarbon age from a comparable depth between the paleochannel and the valley margin (that is outside of what we would call the track of the river further downstream), they do record an age of 4320 ± 80 years B.P. on material from 1.5 m in pit 5, sediments that cannot easily be differentiated but which are over-printed by oxidation (interpreting their descriptive terms in accordance with our own terminology). This presumably comes from the upper level of the mangrove mud stratigraphic unit, and can be correlated from their diagram to coincide with the upper level of the mangrove-dominated section of the pollen diagram from their pit 3. It would represent a period around the transition from *Rhizophora* to *Avicennia* dominated forest if sedimentation occurred simultaneously at both sites. The sediments below this level, in their pit 5 and hence of comparable elevation to those dated around 6000 years B.P. in their pit 3, must be older than 4300 years B.P.. We suggest these mangrove muds are approximately 6000 years old.

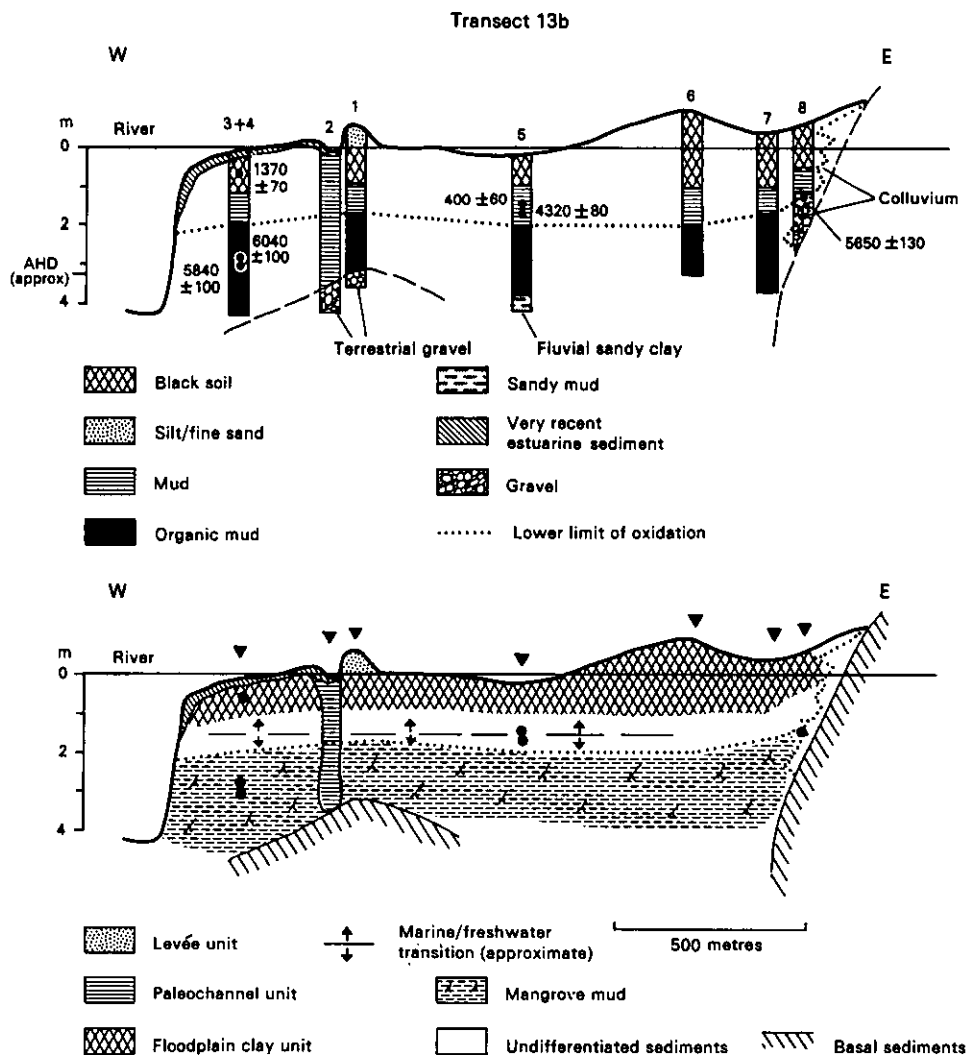


Figure 61: Stratigraphy of Transect 13b, upstream segment (after Hope *et al.* 1985).

The upstream segment merges into the alluvial plain and transect 14, Figure 62, is a west-east cross-section from Leichhardt Billabong to the South Alligator River's most upstream tidal creeks in the area called the Forks. Isolated *Sonneratia lanceolata* on the bank of the river attest to the saline nature of the dry season river at this point. The transect shows the development of levées adjacent to Leichhardt Billabong, and the shallow, oxidised, undifferentiated clays that overlie, heavily oxidised basal sediments in this area. We found no evidence of organic material that might be of mangrove origin in these clays. Therefore the area west of SAH 79 has not been under the influence of tidal waters as the deltaic-estuarine plain has developed. The fact that all of this area is above AHD may indicate that it would have been beyond the reach of tidal waters until sea level stabilised and that even then it may have been too distant and too elevated from the areas subject to regular tidal influence.

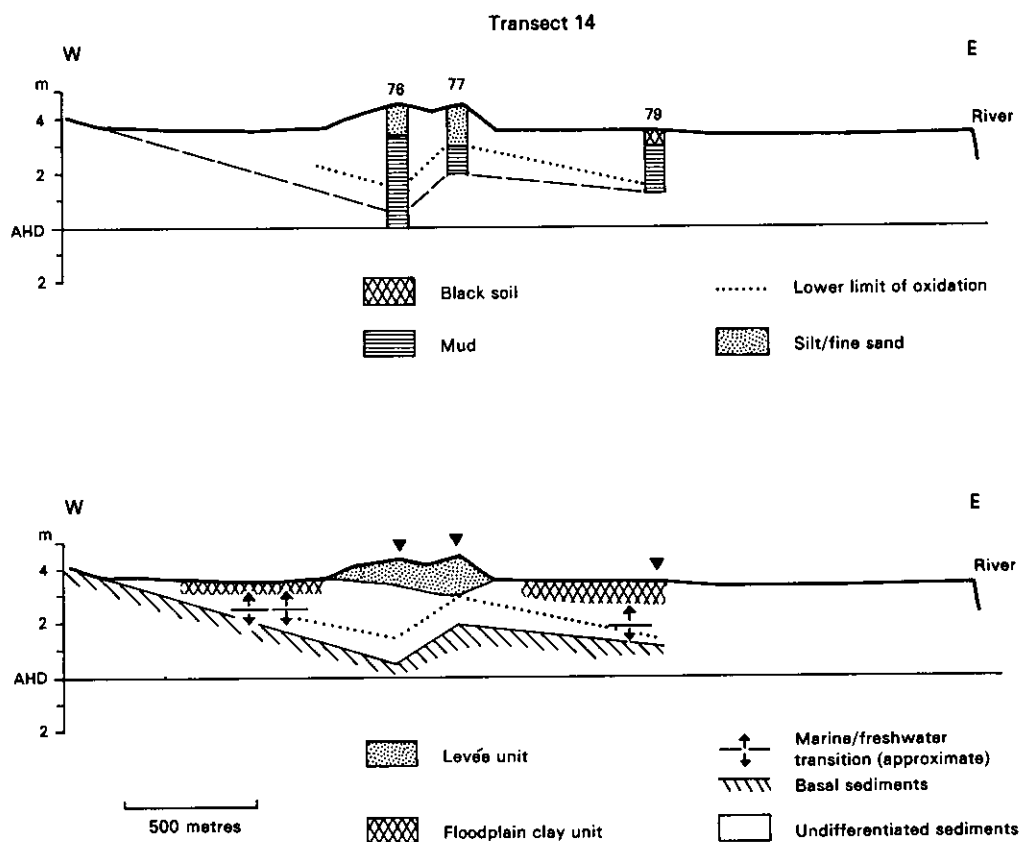


Figure 62: Stratigraphy of Transect 14, Leichhardt Billabong, Alluvial plain

It is now instructive to re-examine transect 10, at the Arnhem Highway (Figure 56), where the upstream and cusped meandering segments of the river meet. The major paleochannel cored by SAH 71 can be seen from the aerial photographs to continue south as a long straight and angular paleochannel adopting the form of present channels and paleochannels in the upstream segment of the river and paralleling the main river channel. A secondary channel feature between the paleochannel and the main channel which is, however, difficult to follow on the ground, has similar features to a sinuously meandering river. Sinuous meanders have been shown to have preceded cusped meanders in the cusped meandering segment of the river. Figure 63 is a block diagram which shows the location of probes taken to examine the nature of sediments between the paleochannels and the main river. Two patterns are observed along the river, and these are examined

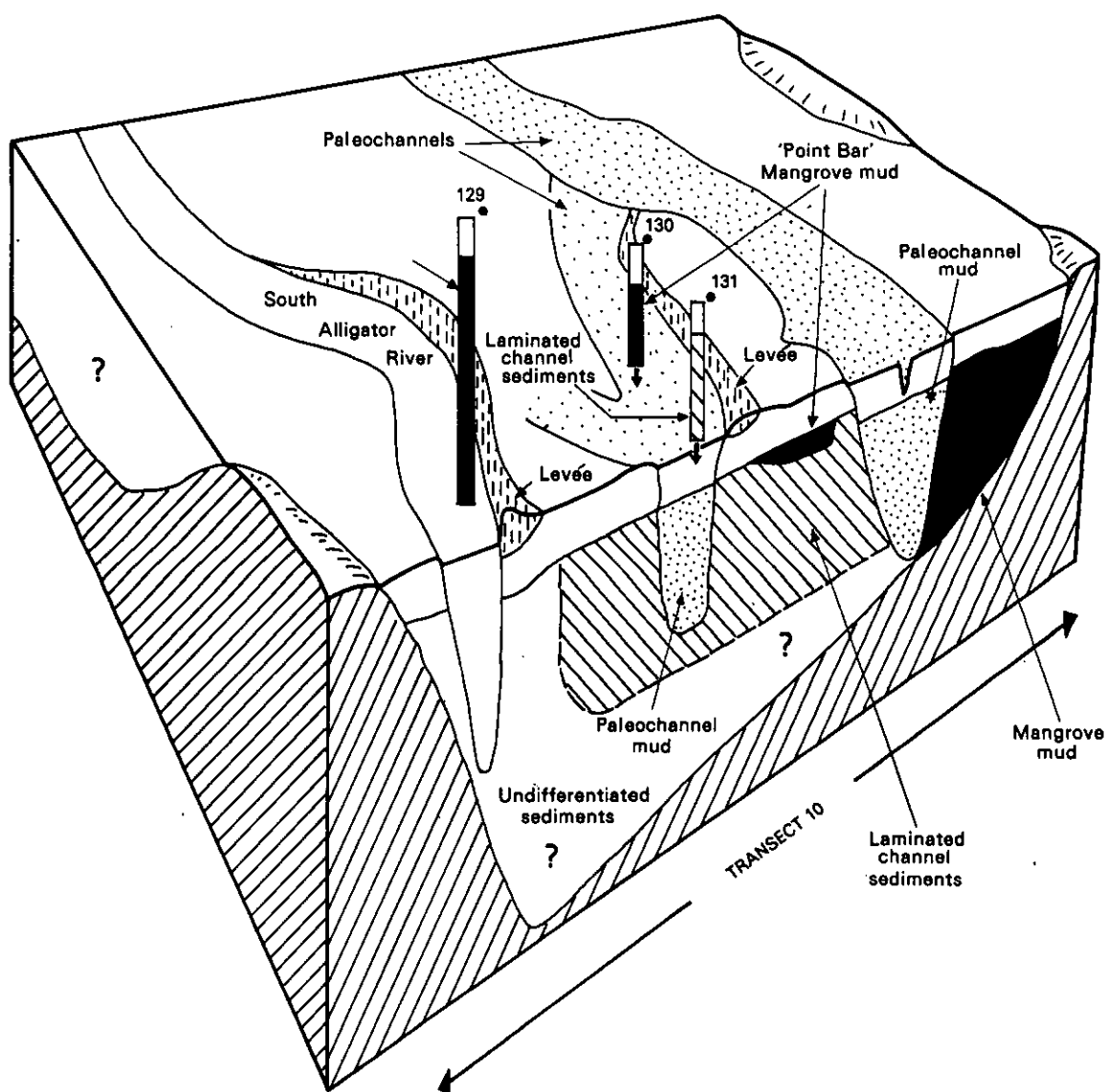


Figure 63: Block diagram showing interpretation of stratigraphic relationships in the vicinity of Transect 10. Viewed from the north northeast.

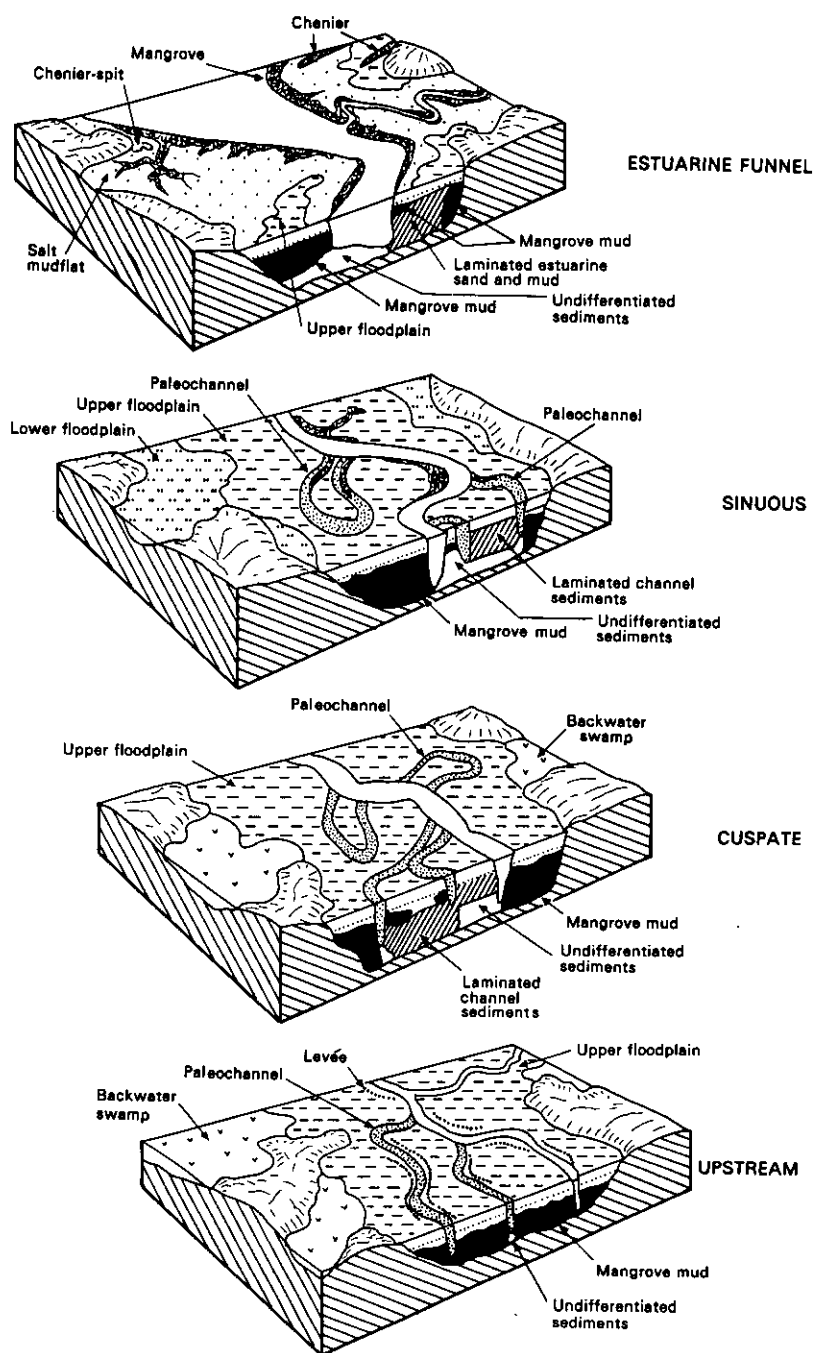


Figure 64: Block diagrams summarising morphologic and stratigraphic relationships in the estuarine funnel, sinuous meandering, cuspate meandering and upstream segments of the river

in terms of a model of channel change in Chapter 5. The first pattern is that paleochannels are separated from the main river by laminated channel sediments in the sinuous and cusped meandering segments of the river. The second pattern is that the paleochannels, or anabranches, of the upstream segment are separated by mangrove mud which was deposited about 6000 years ago.

Probe SAH 129 demonstrates that mangrove mud occurs between the paleochannel and the main river south of the secondary channel, suggesting that south of that point it behaves as part of the upstream segment. However, within the secondary channel there are laminated channel sediments (SAH 131, 117, 118, 116 and 115) and here the channel appears to have behaved as a sinuous meander. These are dated to 5110 ± 120 years B.P. in SAH 117 and indicate the early stage at which this part of the river was actively migrating. This represents the southernmost sinuous paleochannel and the northernmost section of upstream channel that we have recognised. The sinuous channel seems to have been active at least 2880 years ago, but must have adopted the upstream pattern by 1300 years ago.

4.4.7 Summary

The most salient features of the morphology and stratigraphy of each of the estuarine funnel, sinuous meandering, cusped meandering, and upstream segment of the deltaic-estuarine plains of the South Alligator River are summarised in block diagram form in Figure 64.

In the estuarine funnel there are extensive areas of the upper intertidal and salt mudflat unit, adjacent to, and in some cases eroding by sheet erosion into Upper Floodplain deposits. Drilling reveals widespread mangrove mud, in some cases developed over estuarine sediments. Progradation of at least the eastern margin and a smaller area of the western margin of the funnel is indicated by estuarine sand and mud overlain by younger mangrove mud.

Within the sinuous meandering segment of the river, mangrove mud was deposited both while sea level was rising and after sea level had stabilised. This mud is well preserved towards the floodplain margins. There are distinct paleochannels apparent on both sides of the main channel. These contain the paleochannel morphostratigraphic unit, but are separated from the main river channel by laminated channel sediments, which are encountered within the 'track' of the river, along the valley axis.

Within the cusped meandering segment of the river there are often several nested sequences of sinuous paleochannels. Although floodplain margins may contain continuous sequences of mangrove mud from base to upper levels of a core, these are often obscured or reworked nearer the axis of the valley, and laminated channel sediments and paleochannel sediments have been deposited in the 'track' of the river.

The upstream segment of the river contains paleochannels (anabranches) that are generally straight with angular bends mirroring the form of the upstream channel itself. These paleochannels are infilled with clay with sparse organic flecks, but are separated from each other and from the main channel by mangrove mud.

The overall evolution of the coastal and deltaic-estuarine plains is examined in detail in the next chapter.

Chapter 5

Depositional History and Evolutionary Model

- 5.1 Models of Tidal River and Plains Evolution
 - 5.1.1. Alternative Models for Holocene Development of Deltaic-estuarine Plains
 - 5.1.2 Alternative Models for Channel Change
- 5.2 Transgressive Phase, 8000-7000 years B.P.
 - 5.2.1 Sea-level rise relative to South Alligator area
- 5.3 Big Swamp Phase, 6800-5300 years B.P.
 - 5.3.1 Mangrove Succession in Big Swamp Times
- 5.4 The Sinuous River Phase, 4000-2500 years B.P.
- 5.5 The Cuspate River Phase

5. DEPOSITIONAL HISTORY AND EVOLUTIONARY MODEL

5.1 Models of Tidal River and Plains Evolution

In this chapter we outline and test alternative models of evolution of the deltaic-estuarine plains and of the mobile channel developed within those plains.

5.1.1 Alternative Models for Holocene Development of Deltaic-estuarine Plains

In Figure 65 three models are presented which might explain the development of Holocene deltaic-estuarine plains such as those of the South Alligator River. Each of the three is drawn assuming that the prior valley of the South Alligator River was inundated during the later stages of the Postglacial Marine Transgression at which time the basal mangrove mud was deposited. The mangrove mud encountered at the base of drillholes is termed transgressive because it formed as the sea has transgressed landward. The models differ in interpretation of subsequent phases of development during which sea level has been relatively stable. The three models are the progradational, the big (mangrove) swamp and the tidal delta/mud basin models, and they are described as follows:

- (a) The progradational model implies landward migration of the mangrove fringe as sea level rose, with the marine transgression represented by a basal mangrove mud. Shallow water estuarine sediments were deposited over much of this transgressive mangrove mud. Mangroves were confined to the landward-migrating fringes of the drowned valley system. As the estuarine sediments continued to build up in the drowned valley after sea level stabilised, the mangrove fringe migrated seawards as the estuary and adjacent coast prograded. Sedimentation landward of the mangroves initiated floodplain formation. According to this model, mangrove and other intertidal sediments found immediately beneath the floodplain clays should become progressively younger towards the sea (Figure 65a). Such shoreline progradation indicates regression of the sea, and the deposits can be termed regressive. The coastal plain is an example of this model. As shown in Chapter 4.4.2 the coastal plain consists of basal transgressive mangrove mud overlain by marine sand and mud and then by a regressive mangrove mud. The progradational model shown in Figure 65a is an extension of the transgressive/regressive model of coastal plain to the entire South Alligator Valley.
- (b) The 'big (mangrove) swamp' model differs from the progradational model during both the rising and the stable sea level phases. Mangrove established during drowning of the valley continued growing over its vertically-accreting substrate in many areas throughout the valley. Much of the valley was mangrove swamp at the time when sea level stabilised, and remaining estuarine backwaters infilled and became mangrove. This big mangrove swamp then transformed to floodplain by overbank sedimentation from the tidal river, under stable sea level. The model implies that mangrove sediments immediately beneath the floodplain clays should be about the same age throughout the system (Figure 65b). While the basal stratigraphy is transgressive, the upper stratigraphy is not regressive in a strict sense of the term, because the shoreline remains relatively stable at the seaward extreme of the valley system.

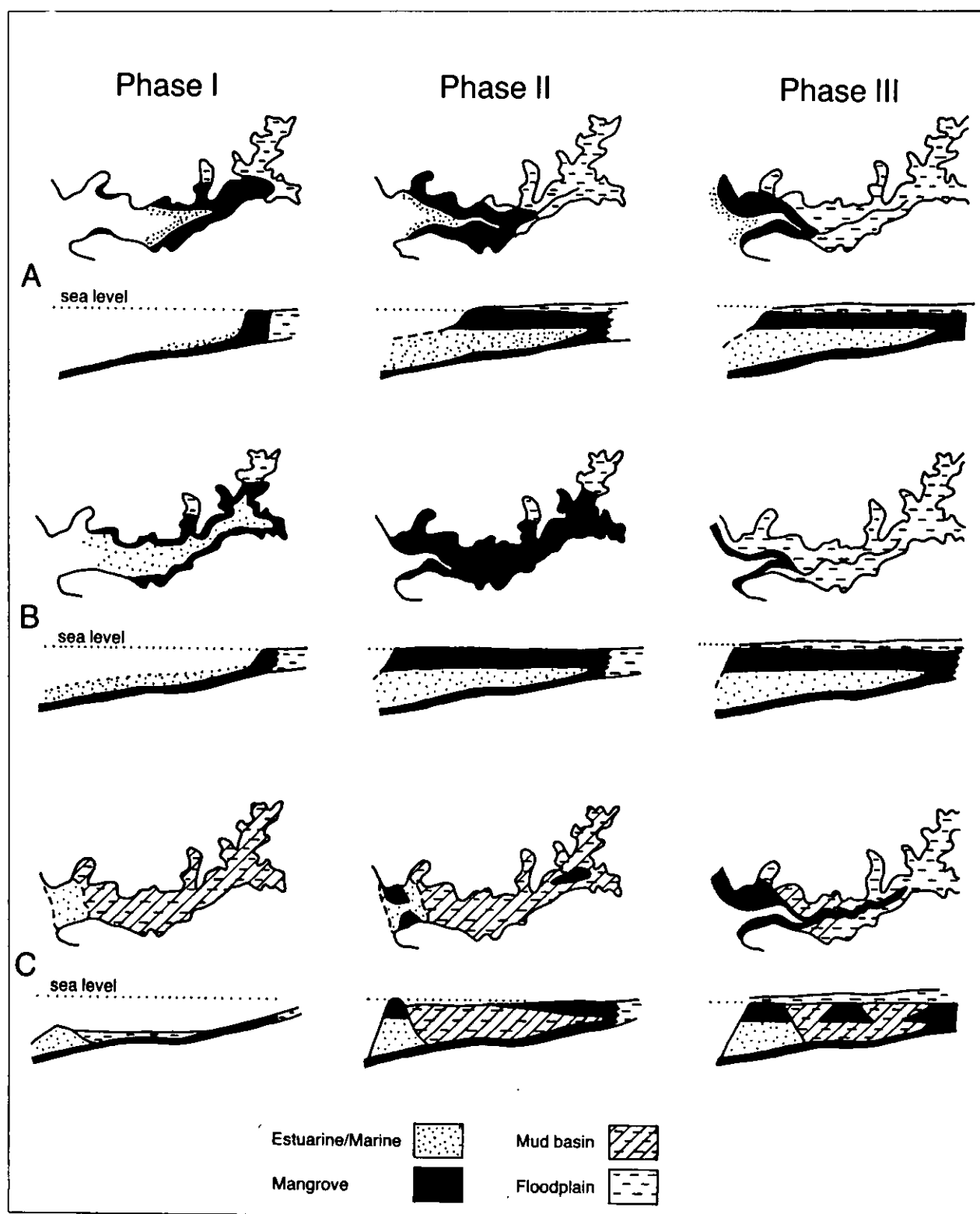


Figure 65: Three models of Holocene estuarine sedimentation, involving mangrove mud deposition during transgression and regression, set out in three successive phases I, II, III. Model A shows progressive progradation within estuary, Model B shows rapid development of extensive mangrove swamp followed by floodplain burial of swamp, Model C shows formation of tidal delta at estuary mouth and subsequent mud basin infill.

- (c) The tidal delta/mud basin model is based on the evolutionary sequence of change determined for the drowned river valleys of New South Wales by Roy *et al.* (1980). A tidal delta dominated by flood tide sedimentation builds up at the mouth of the valley during the final stages of sea-level rise. The barrier formed creates a quiet basin behind it, and within this basin there is gradual infill with sediment until the surface reaches a level that can be colonised by mangroves. Mangroves are again replaced by floodplains as the surface accretes, to rise above high spring tide level (as occurred in the Shoalhaven delta in NSW, Thom and Roy, 1985). This model predicts that mangrove sediments capping the tidal delta will date around 6000 years B.P., when sea level stabilised, and that younger mangrove deposits will lie beneath the floodplain inland of this (Figure 65c). Like the previous model the initial stages are transgressive, but the upper stratigraphy is not regressive in that there has not been progradation of the coast since the establishment of the tidal delta.

The differences between these 3 models, manifest by different stratigraphic geometries (Figure 65), lead to different spatial patterns of radiocarbon ages. We have shown (Chapter 4) that mangrove mud underlies the freshwater floodplain clay unit at depths of 2 to 3 metres, throughout most of the tidal river system. Except for localities which lie within the track of the river as recognised from present and paleomeanders (Chapter 4.4) almost all dated occurrences of this upper mangrove mud, often richer in organic fragments than mud below it, are between 6800 and 5300 years B.P.. This is shown in Figure 66. Many of the results in Figure 66 represent paired samples, where one member of the pair is from near the top of the mangrove mud (usually within 3 m of the ground surface), and the other is from continuation of the same material metres lower (usually 5 to 7 m below ground surface). In some cases there is no statistical age difference between upper and lower samples but more often the lower date is in the age range 6800-6500 years B.P., while the upper date is in the range 6500-5300 years B.P. The results show that an extensive mangrove forest was established throughout the South Alligator plains region around 6800-6500 years ago at which time sea level was still rising, and persisted until around 5500 years ago. There are no apparent spatial trends in the age data. It appears that mangrove flourished throughout this large area, more than 80,000 ha, during this time interval. As argued by Woodroffe *et al.* (1985c), these results support the big (mangrove) swamp model of Figure 65b. The swamp developed during the time when sea level stabilised, around 6000 years ago (Chapter 1.5). Subsequent floodplain sedimentation through vertical accretion has eliminated the mangrove throughout most of the system, away from the margins of sinuous meandering parts of the river.

Interpretation of stratigraphy in the Bullocky Point area (Figures 51, and 52) indicates that the river existed as a distinct channel during the big swamp phase. The present river has evolved since then, occupying the various paleochannel locations such as are shown in Figure 35. Alternative models for this are developed below.

5.1.2 Alternative models for channel change

Several shifts of position of the meandering river followed the 'big swamp' phase. In Figure 67 two alternative models by which paleomeanders are initiated and subsequently abandoned are shown. These are the point bar migration and channel cut-off model, and the channel avulsion model. These are described as follows:

- (a) The point bar migration and channel cut-off model (Figure 67a) involves channel migration by erosion of the bank on the outside of a river bend and deposition on the inside of the river bend.

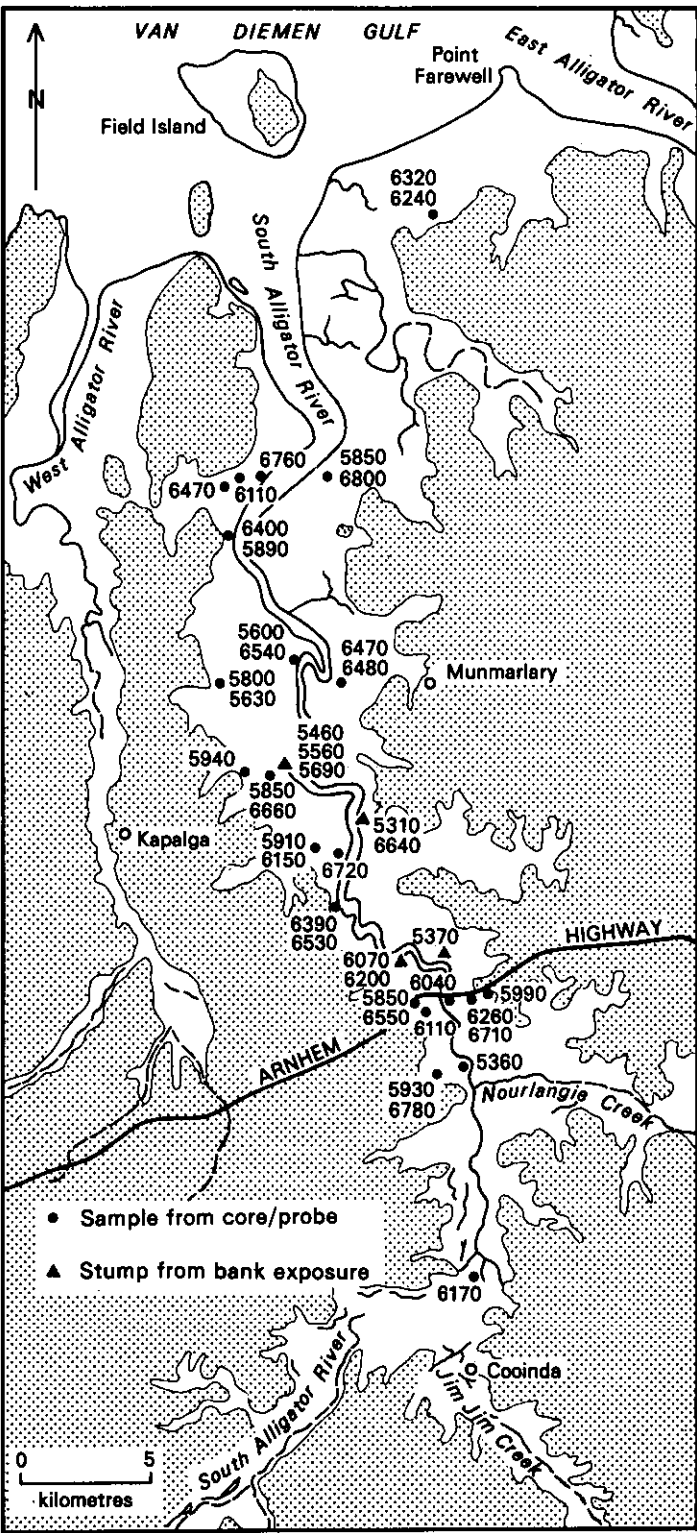


Figure 66: Location of samples and radiocarbon dates on buried mid-Holocene mangrove mud recorded in drillholes and river bank exposures. Paired dates show results from upper and lower levels in mangrove mud.

It is the common model of meandering in fluvial systems. The river meander cuts into older sediments ('big swamp' sediments in the case of the South Alligator River) on the outside of the bend, and deposits younger, or reworked sediments on the inside of the bend. The meander becomes increasingly lobate, leading to convergence of the upstream and downstream reaches of the river at the neck of the meander. After cut-off of the river at this point the paleochannel remains as an ox-bow, which gradually infills and is visible on the floodplain (Figure 67a, Stage III). Subsequent channel movement by further point bar migration and cut-off may lead to other abandoned paleochannels (Figure 67a, Stage IV). The stratigraphic signature of this pattern of channel movement is that older sediments occur around the outside of the 'track' of the river and younger active channel sediments occur within the 'track' of the river.

- (b) The channel avulsion model is shown in Figure 67b. In this model the river channel switches from one course to another without migrating between channel locations. Avulsion, or jumping, from one channel to another is likely to occur during a flood event of uncommonly high magnitude, leaving the old river course as an abandoned paleochannel. The stratigraphic geometry of this type of channel movement would differ from that of point bar migration in that sediments of the same age would occur on both sides of a channel.

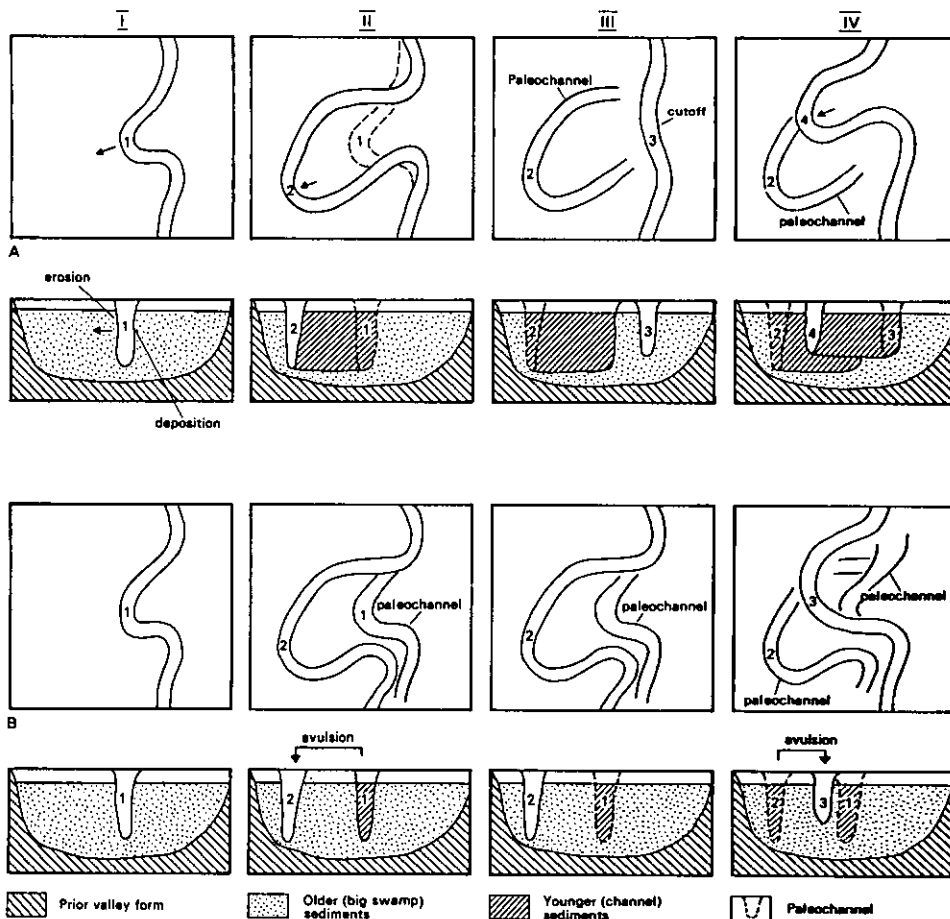


Figure 67: Two models of channel migration on the deltaic estuarine plains. Model A, point bar migration and cut-off; Model B, channel avulsion.

The stratigraphic evidence presented in Chapter 4 allows selection between these alternative models. Interpretation of the Bullocky Point area (Figure 51 and 52) supports the model of point bar migration and channel cut-off. Figure 68 shows more general evidence, indicating the distribution of drillholes and bank exposures within which laminated channel sediments have been found. These sediments almost exclusively occur between the present river and the paleochannels on the deltaic-estuarine plain surface. The radiocarbon ages on channel fill or active channel deposits are also shown, including basal dates beneath sequences of laminated channel sediments. These clearly show that the channel has migrated between present and paleochannel locations. The deposits together with position of fossil stump sites of 'big swamp' age (also shown in Figure 68) allow us to identify the 'track' within which the river has migrated since 'big swamp' times. We note that the paleochannel drilled on transect 4 (Figure 44) has mangrove muds of similar age on both sides of it. This transect is relatively close to the river mouth, where multiple channels may have occurred in 'big swamp' times.

It was indicated in Chapter 4 that stratigraphic relationships in the upstream segment of the river differ from those of the meandering segments of the river. In the upstream segment extensive mangrove mud has been identified in drillholes between the present river channel and the paleochannels. 'Big swamp' ages for these muds are recorded on transect 12a (Figure 58) and by Hope *et al.* (1985, Figure 61). It appears that avulsion may have occurred, with the upstream channel having jumped from one paleochannel to another or to the present river. However, we are not certain that the upstream segment always consisted of a single channel, and it is possible that more than one channel was active at the same time. Not all paleochannels can have been active at the same time, as some paleochannel courses cross or truncate each other (i.e. at KF 330868), but several parallel channels may have co-existed.

The 'big swamp' model outlined in Figure 65b and the point bar migration and channel cut-off model in Figure 67a provide the context in which details of the history of the tidal river and plains system are discussed in the following sections. We believe that the 'big swamp' model applies in broad terms in many other northern macrotidal river systems (Woodroffe *et al.* 1985c), and note that stratigraphic drilling and dating analysis demonstrates a similar history for the lower Daly River (Chappell, in prep). The pace of geomorphologic change, following the 'big swamp' phase, varies from one river to another according to hydrologic and other factors related to their catchments. We outline this in Chapter 6, after detailing in this chapter the following evolutionary stages: transgression, 'big swamp', sinuous river, cusped river.

5.2 Transgressive phase, 8000-7000 years B.P.

Marine invasion of the South Alligator River valley occurred when rising seas reached a level 10 to 12 m below AHD, which is the average position of the old valley floor (Figure 12). According to sea-level data from eastern Australia (Figure 13), this was 8500 to 8000 years ago. Tidal flooding of the South Alligator valley is shown by organic mangrove mud, substantiated in some instances by pollen analysis (Appendix A6), which is found overlying the prior valley surface or basal sediments in several drillholes and which has radiocarbon ages around 8000-7800 years B.P. Existence of the river at the time is indicated at a few localities where drilling indicated the prior surface at depths up to 10m below the average prior valley-bottom surface (Figure 12). It is very likely that the initial tidal river occupied this prior channel. As sea level continued to rise mangrove flourished on vertically-accumulating sediment in many localities. It is likely that the organic muds found in lower and middle parts of many cores represent lower intertidal flats or subtidal banks in other parts of the developing estuary. There may have been more than one tidal channel near the estuary mouth at this time.

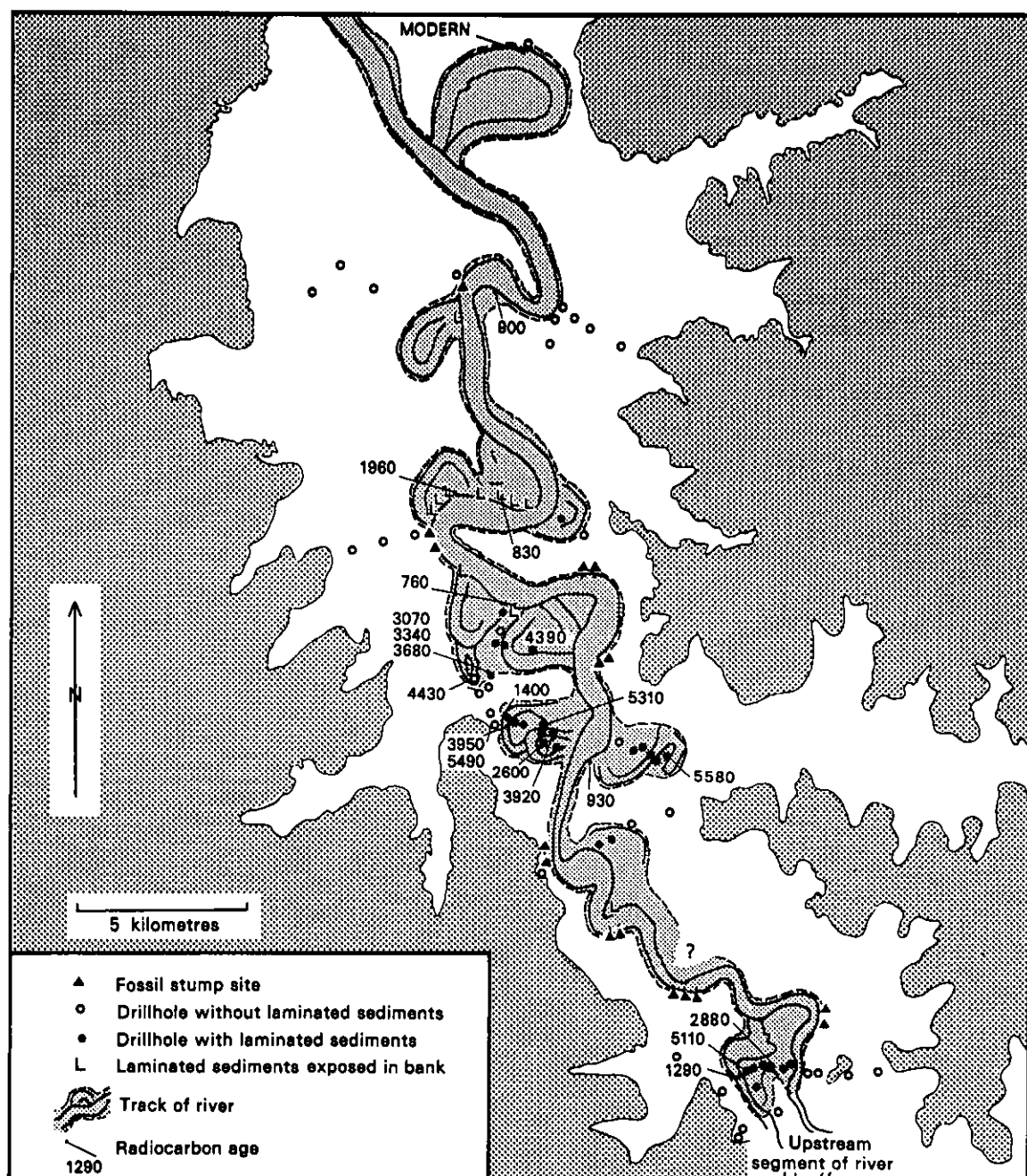


Figure 68: Distribution and radiocarbon dates of channel fill and laminated channel sediments in the deltaic-estuarine plains showing the 'track' of the South Alligator River

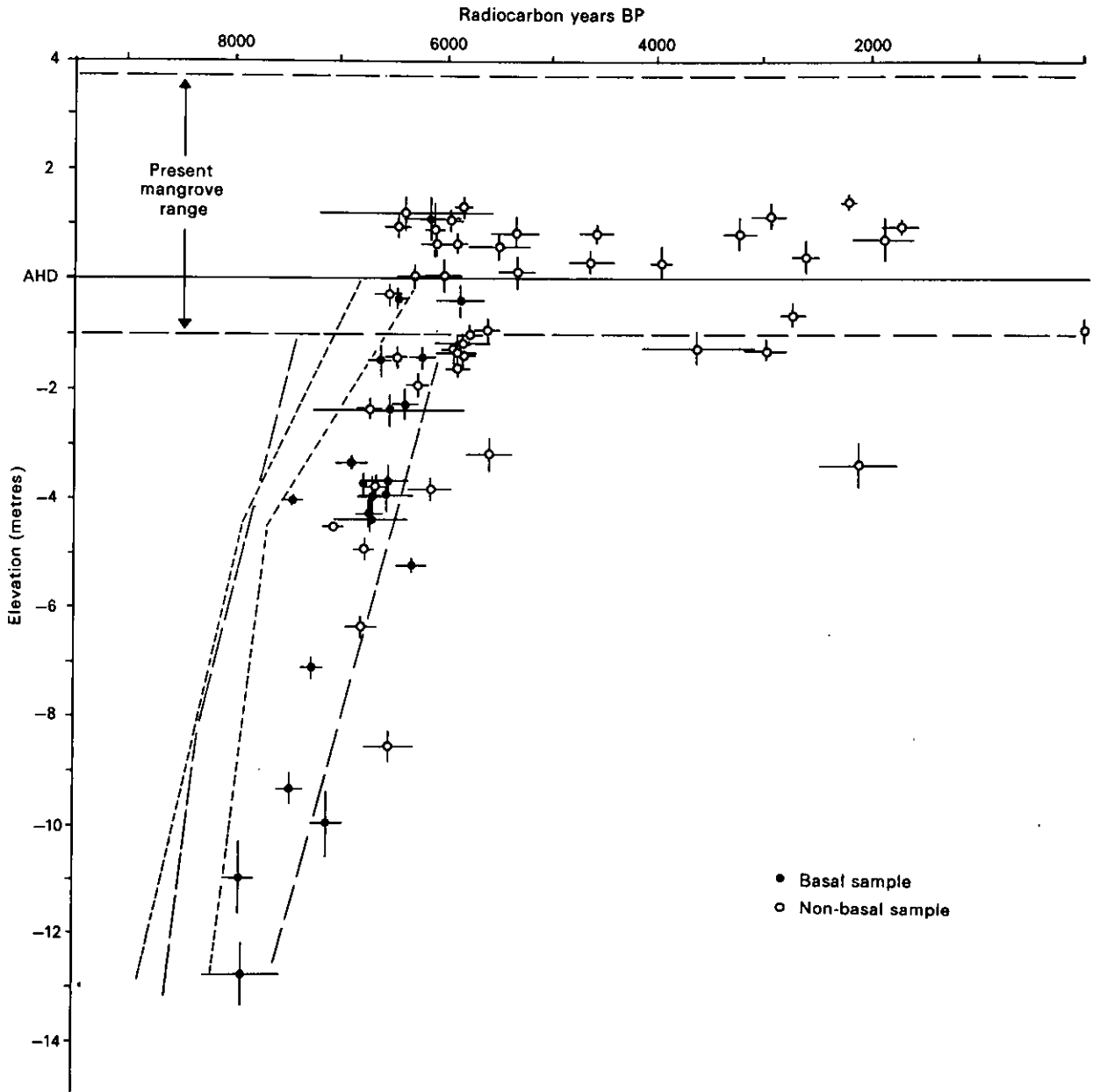


Figure 69: Age-depth plot of radiocarbon dates on mangrove material, indicating relative sea-level change, South Alligator River. Light dashed line : SE Australian curve, from Figure 13 (after Thom and Roy, 1985). Longer dashed line envelope from Queensland curve, also from Figure 13 (after Grindrod and Rhodes, 1984). See Appendix A9 for data.

5.2.1 Sea-level rise relative to South Alligator area

Up until now we have made reference to sea-level data from eastern Australia as a reference for sea-level change in the area of study (Chapter 1, Figure 13). These results may not apply exactly in the South Alligator area. There are variations in the pattern of late Holocene relative sea level for different parts of Australia, which appear partly to be due to hydro-isostatic adjustments around the coastline (Chappell *et al.*, 1982; Hopley and Thom, 1983). Our data from the transgressive and big swamp phases indicate some differences from the east Australian curve shown in Figure 13.

Mangrove remains are a reasonably good indicator of sea level because they are almost exclusively found growing intertidally. Figure 37 indicates the upper and lower limit of mangroves along the length of the river, and demonstrates that they are found at elevations of up to 3.7 m above AHD. The lower limit of mangroves is below AHD. As mangrove material recovered in drillholes is most likely to have been deposited on the sediment surface, or to be root material shallowly buried at time of growth, and as we have a radiocarbon-modern date on mangrove material at about 1 m below AHD, we take -1 m AHD as the lower limit at which mangrove material is presently forming.

Figure 69 shows an age-depth plot of mangrove dates from the South Alligator River. Radiocarbon ages are shown plus and minus one standard deviation, and sample depth with respect to AHD is shown with error bars indicating the accuracy of depths. Details of location of samples used in Figure 69 and of the basis of error estimation is given in Appendix A9. The age-depth data portrayed in Figure 69 cannot exactly be related to past sea levels due to several factors. One source of error which is known to affect mangrove sediments is compaction of muds and consequent downward displacement of material (Chappell and Grindrod, 1984). This does not appear to have had any major effect, as there is good agreement in terms of age and depth between basal samples, which cannot have been compacted, and those from above large unconsolidated sediment columns (Figure 69).

Figure 69 shows a relatively narrow envelope within which age-depth data fall. The course of sea-level rise is clearly apparent from the figure, and mangrove remains first occur within the same range as present mangroves between 6600 and 5800 years B.P.. The sea-level rise data barely overlap with the results from eastern Australia introduced in Figure 13 (Chapter 1). Figure 13 shows that sea level was 10-12 m below present 8500-8000 years B.P. relative to the eastern Australian coast, while the earliest dates recording transgression into the South Alligator prior valley at this depth are 8000-7500 years B.P. Similarly, whereas in eastern Australia the sea level was about 5 m below present around 7500 years ago, it appears to have reached this level around 6800 years ago in the South Alligator River system. The South Alligator River has a much larger tidal range (c 6 m) than Hinchinbrook Island (c 3 m) where comparable mangrove results shown in Figure 13 were reported by Grindrod and Rhodes (1984); one would expect earlier incursion of the prior valley by tidal water where there is greater tidal amplitude. In fact the opposite appears to be true, and reinforces the slightly different sea-level history of the South Alligator River area.

Figure 70, based on drillhole data, shows an environmental interpretation of the South Alligator River around 7000 years B.P., when sea level was about 5 m below the present.

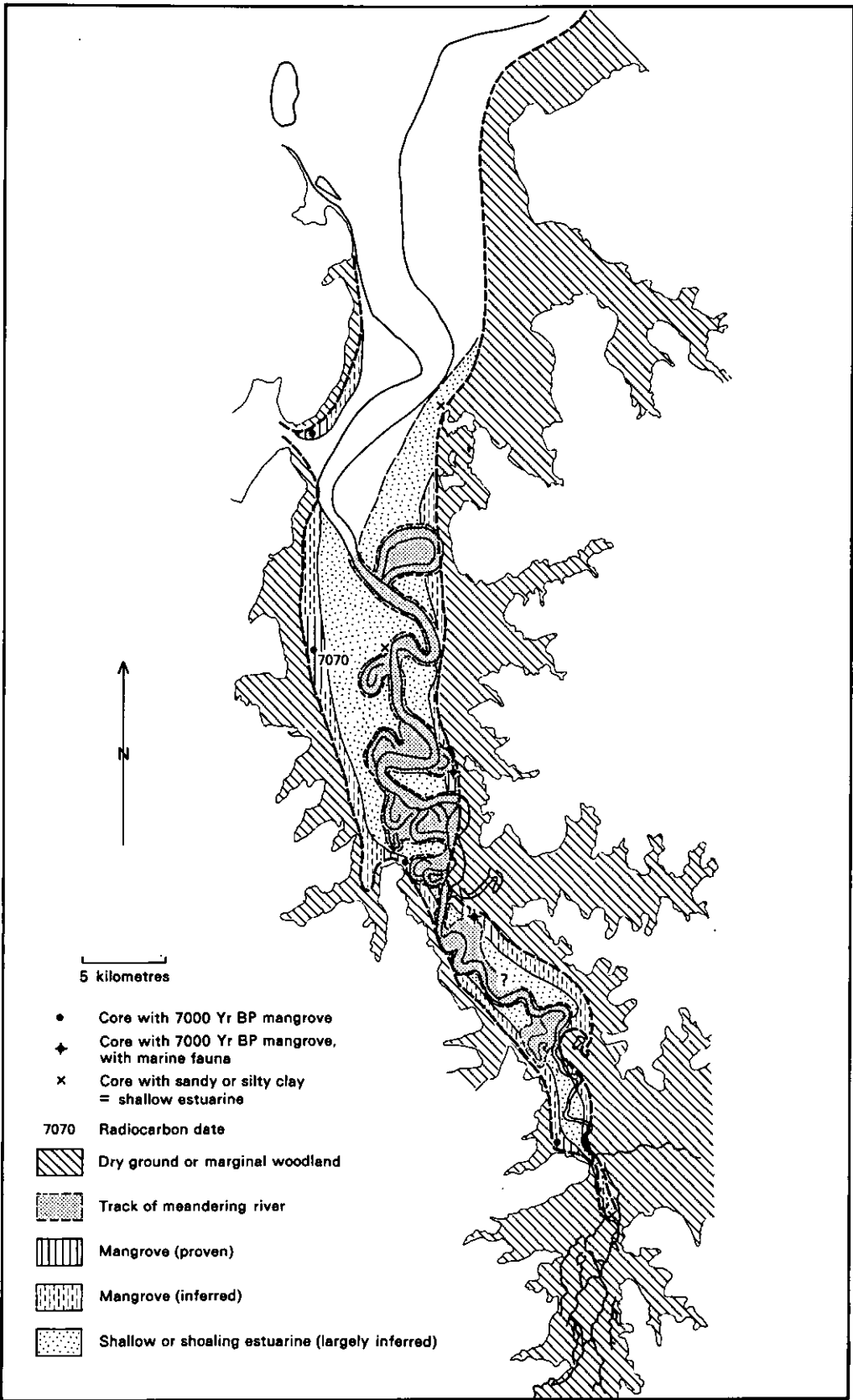


Figure 70: Map of the distribution of environments recorded (and inferred) 7000 years B.P., during the big swamp phase, when sea level was about 5 m below the present. Note: track of meandering river is derived from Figure 68 and denotes areas where sediments have been reworked by post-7000 river channel migration.

5.3 Big Swamp phase, 6800-5300 years B.P.

Sea level stopped rising around 6500 to 6000 B.P. (Figures 13 and 69). The intertidal and subtidal volume which existed while sea level was rising could now be filled with sediment. The entire estuarine system appears to have shoaled, leading to establishment of the widespread 'big mangrove swamp'. Mangroves became well established at the coast northeast of the estuary. The form of the tidal river at this time is not known but the occurrence of thick sequences of laminated channel sediments, dating around 6500-6000 B.P. (Figure 51) suggests active meander migration in the middle and upper reaches of the system. More than one main channel may have existed in the lower part of the estuary, indicated by the paleochannel near Water Recorder Point (Grid Ref KG161215) which has 'big swamp' mangrove on both sides (Figure 44). Fossil mangrove stump sites exposed on the river banks date from this big swamp time; their location is shown in Figure 71 and specific occurrences are outlined in Table 7. Figure 71 shows the facies distribution and inferred form of the estuary around 6500-6000 B.P.

5.3.1 Mangrove Succession in Big Swamp Times

The most accurate picture of development and decline of the big mangrove swamp may be gained from pollen analysis (Chappell and Grindrod, 1985; Grindrod, 1985). As the method is time consuming (Appendix A6), it is not practicable to analyse more than a few cores from each phase of the system's development. Two cores passing through representative big swamp deposits have been analysed, one from the middle reaches (SAH 40) and the other from near the floodplain margin in the upstream segment of the system (SAH 67). Pollen diagrams and interpretations are shown in Figures 72 and 73. These diagrams are interpreted by referring to pollen spectra from surface sediment samples collected on transects through and outside existing mangrove forests, as explained in Appendix 6. The proportions of different pollen taxa preserved in sediments rarely conform to proportions of different plants in the surrounding vegetation. Nevertheless, by using the keys provided by the modern surface samples, the vegetation history at the core sites can be determined with reasonable confidence.

Core SAH 40 (Figure 72) shows that mangrove forest established at this site when the sedimentary surface was 8m below the present plains, over laminated channel sediments (muddy fine sands) of a prior channel (Chappell and Grindrod, 1985; Woodroffe et al., 1985c). Mangrove persisted through 7 metres of vertical accretion, and gave way to sedge and grassland deposition in the floodplain clay unit at about 1 m below core top. As the maximum vertical range of the mangrove habitat in the area is about 3 m to 3.5 m (Figure 37b) from somewhat below MWL up to above MHWS, that part of the core between 8 and 4 m must represent persistent mangrove growth with sea level rising. An age of 6720 ± 120 B.P. at 6 m is consistent with lower sea level, according to Figures 13 and 67. The forest was Rhizophoraceous with Rhizophora slowly gaining ascendancy over Bruguiera/Ceriops. Sonneratia became locally important around 3 m core depth, which is thought to correspond with sea-level stabilisation. Continued sedimentation was accompanied by successional change from Sonneratia through Rhizophoraceous forest to final stands of Avicennia, before freshwater floodplains overtook the mangrove. This succession conforms with the zonation found downstream through existing coastal and near-coastal mangrove forests in the region. Although the analysis is not sensitive at the species level making exact definition impossible, these results indicate that mangrove forest composition and succession were very similar, in big swamp times, to those found in the lower estuaries and coasts of northern Australia today. Forests of this sort do not now exist upstream of about 7 km from the present South Alligator mouth.

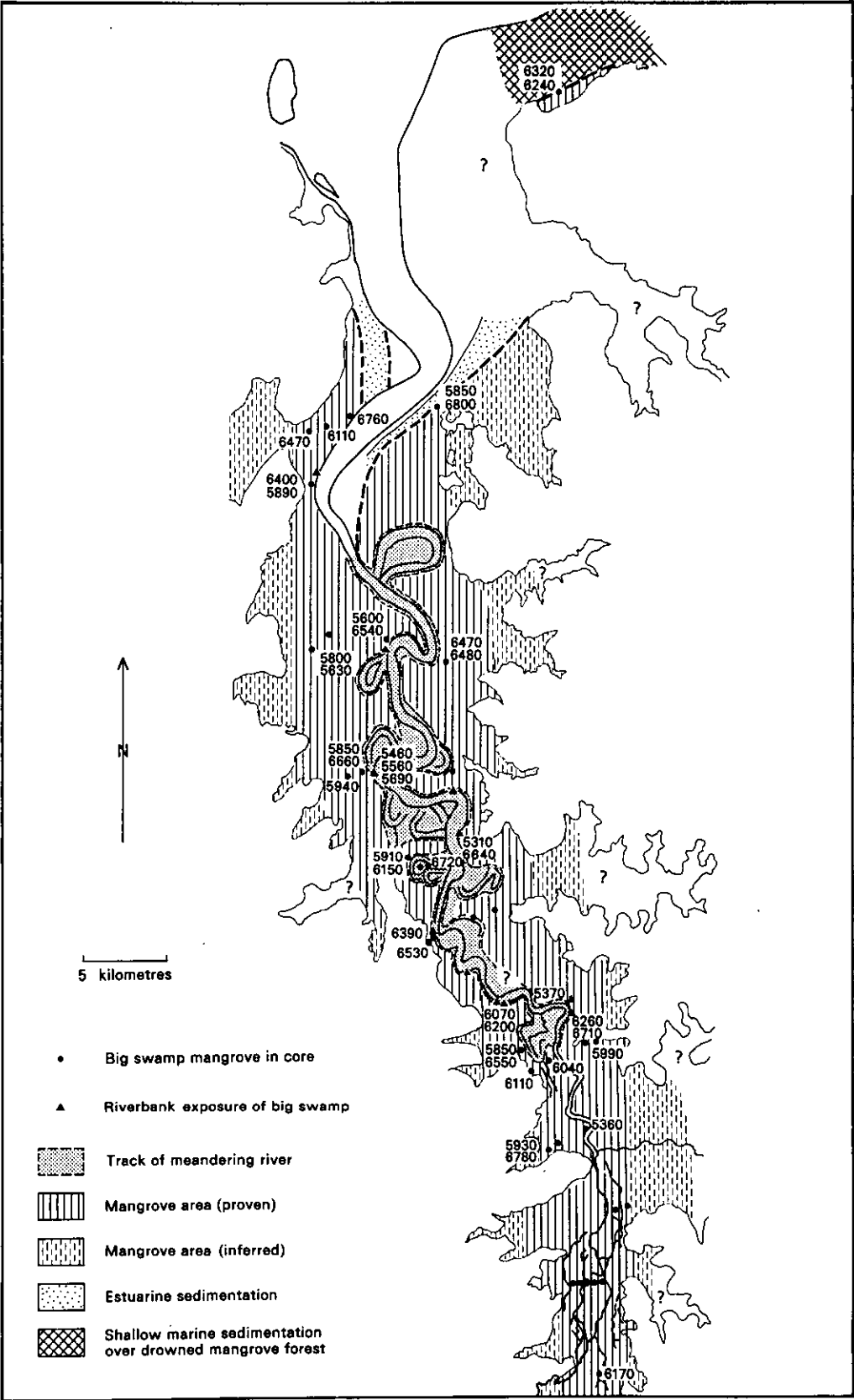


Figure 71: Map of the distribution of environments recorded (and inferred) 6500-6000 years B.P., during the big swamp phase, when sea level had stabilised at or close to its present level

Table 7
Big swamp fossil stump sites; species recorded and their age

Approximate distance from mouth (km)	Bank (W/E)	Mangrove stumps (species identifications where confirmed)	Concretions (species predominantly forming nucleus)	Mollusc species	Other comments	Radiocarbon age (years B.P.) (s on shell L on lobster)
25	W	Numerous	<u>Thalassina squamifera</u>	<u>?Polymesoda coaxans</u>		6010±90s 6550±100L
40	W	Numerous, Rhizophora <u>Avicennia</u> Cerlops <u>?Bruguiera</u>	<u>Thalassina squamifera</u>	<u>?Austriella sordida</u>	Lower fibrous layer, possibly Rhizophora root mat	
50	W	Numerous, Avicennia <u>Cerlops</u>	<u>Thalassina squamifera</u>	<u>?Austriella sordida</u> <u>?Polymesoda coaxans</u> <u>Terebralia palustris</u> <u>?Voilegalea wardiana</u>	Calcified borers Lower fibrous layer, possibly Rhizophora root mat	5690±90 5460±90 5560±80 5950±100s
55	E	Numerous	<u>Thalassina squamifera</u>	-	Several boulders up to 35cm long	
57	E	Numerous	<u>Thalassina squamifera</u>	<u>?Polymesoda coaxans</u>	Fossil stump >1m tall Fibrous lower <u>?Rhizophora layer</u>	upper 5310±110 lower 6640±100
62	W	Numerous, Cerlops <u>Avicennia</u>	<u>Thalassina squamifera</u> and molluscs	<u>Telescopium telescopium</u> <u>Polymesoda coaxans</u> <u>Cerithidea sp.</u>	Gravel from basal sediments, buried midden, fibrous lower <u>?Rhizophora layer</u>	
66	W	Numerous	-	-	-	
69	W	Numerous, Avicennia	<u>Thalassina squamifera</u>	<u>Polymesoda coaxans</u> <u>Cerithidea sp.</u>		6070±90 6200±80

Core SAH 67 (Figure 73), from quite close to the tidal limit and near the plains margin, shows a similar pattern. Mangrove forest dominated by Rhizophora established before sea level reached its present position, and continued until sedimentation approached about 2.5 m below the present surface. Radiocarbon dates show that the forest existed from about 6800 to about 5500 years B.P. (Figures 66 and 73). Rhizophoraceous forest was succeeded by an Avicennia/Lumnitzera community in the upper part of the sequence, after sea level stabilised. The latter conforms with present communities in the middle parts of the West Alligator river. The lower part of the diagram, 6.7 to 4.0 m, shows that Rhizophoraceous forest extended to areas close to the present tidal limit in 'big swamp' times. Further evidence of similar successional change is recorded in a pollen diagram reported by Russell-Smith (1985b) from pit 3 of transect 13b, Kiina (location, Figure 61). Initially this site was dominated by Rhizophora, with Bruguiera/Ceriops also important. About 1 m below the surface there is a transition from Rhizophoraceous forest to stands of Avicennia followed by replacement of mangroves by Poaceae and Cyperaceae typical of the freshwater floodplains. It is likely that the big swamp phase is also recorded in the rock art of the area. 'X-ray descriptive' paintings of barramundi, mullet, salt water crocodile and estuarine catfish probably correlate with big swamp times, while 'X-ray decorative' paintings of magpie geese may date from the time of disappearance of the big swamp (Chaloupka, 1983, 1985).

In summary, these results confirm the 'big swamp' model for the South Alligator tidal region at the time when sea level stabilised, 6500-6000 years B.P. Rhizophoraceous forest was widespread, compared with the scanty mangroves which fringe the present river. Rhizophora appears to have dominated 'big swamp' forests as far inland as transect 13b, presently 100 km river distance from the mouth. Salt-tolerant Rhizophoraceous forest does not imply higher salinities than today, because present-day salinities approach sea water values near the tide limit in the dry season (Figure 20).

The wide occurrence of Rhizophora-dominated forests around 6000 years ago indicates that tidal inundation was general throughout the plains area. The upper limit of Rhizophora-dominated zones in the pollen diagram for SAH 40 (Figure 72) occurs at about 1.5 m AHD and mangrove pollen persists to 2.2 m AHD. These levels are about 1.6 m and 2.0 m AHD respectively in pit 3 of Russell-Smith (1985b; using aerial photomosaics and A.S.O. survey data to reduce this to AHD). The significance of this is discussed in Chapter 6 (see Figure 80).

5.4 The Sinuous River phase, 4000 to 2500 years B.P.

The demise of the mangrove and transition to freshwater floodplain, dominated by grasses and sedges is recorded at 1 m below the surface in core SAH 40 and at about 2 m below the surface in core SAH 67. This is higher than the change from mangrove mud to oxidised muds or to undifferentiated bluish-gray clays with sparse organics. As the upper levels of the mangrove mud therefore lie in the zone overprinted by oxidation, we are unable to establish the precise transition from mangrove to freshwater environments by field examination of drillhole samples. The important transition from saline intertidal sediments to freshwater floodplain clays is best established by pollen analysis. The transition is not particularly clearly shown by salinity. For example, salinity measurements from core 40 (Appendix A5) can be compared with pollen results (Figure 72). Salt migration from the intertidal into the freshwater floodplain clays is obvious in the case of core 40. This shows high salinity towards 80 cm, within the sedge/grass-dominated floodplain clays. Salinity values fluctuate below this but are generally high. Further work is needed to analyse this salt diffusion process, but these results confirm the value of pollen analysis in these sediments.

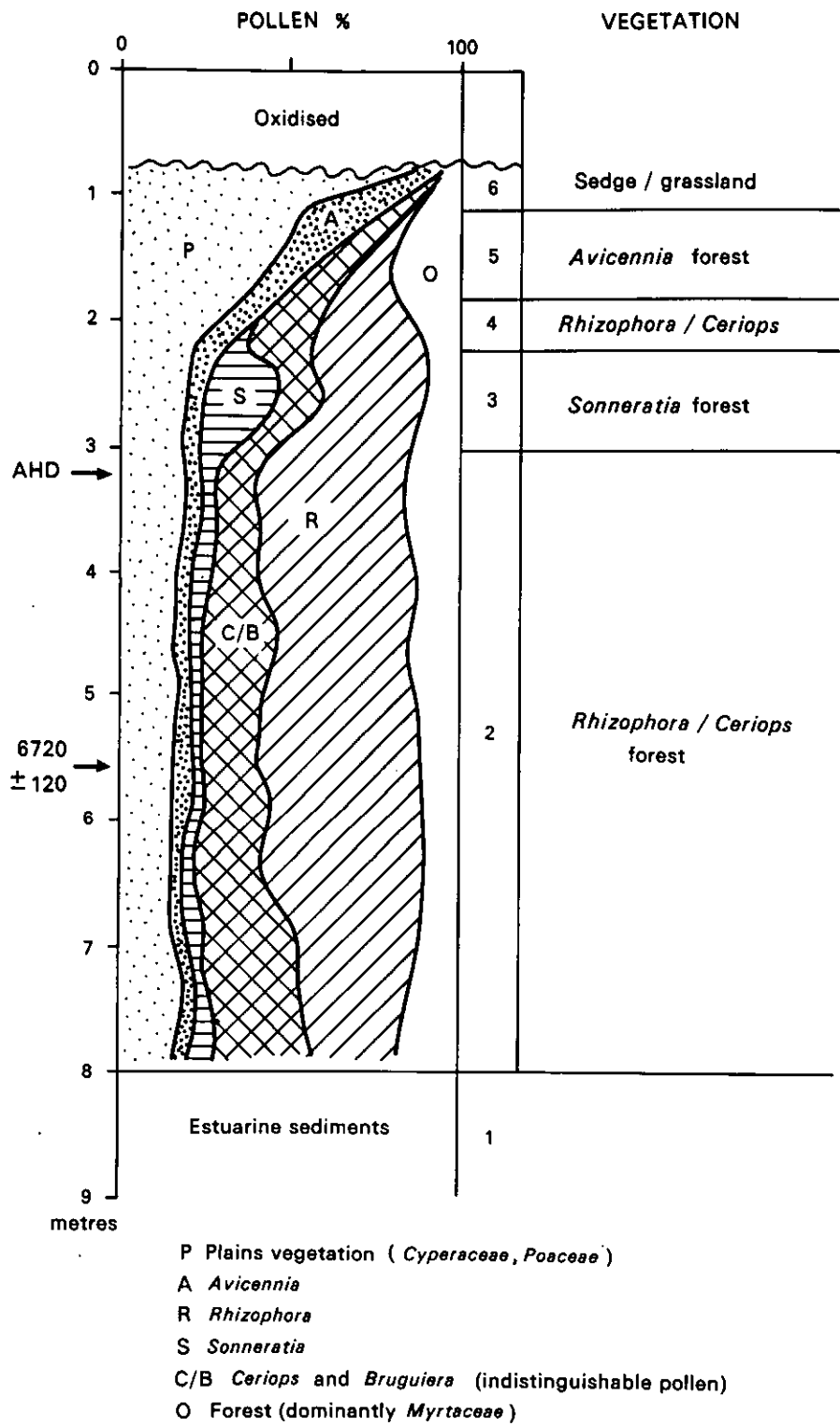


Figure 72: Pollen diagram of core SAH 40

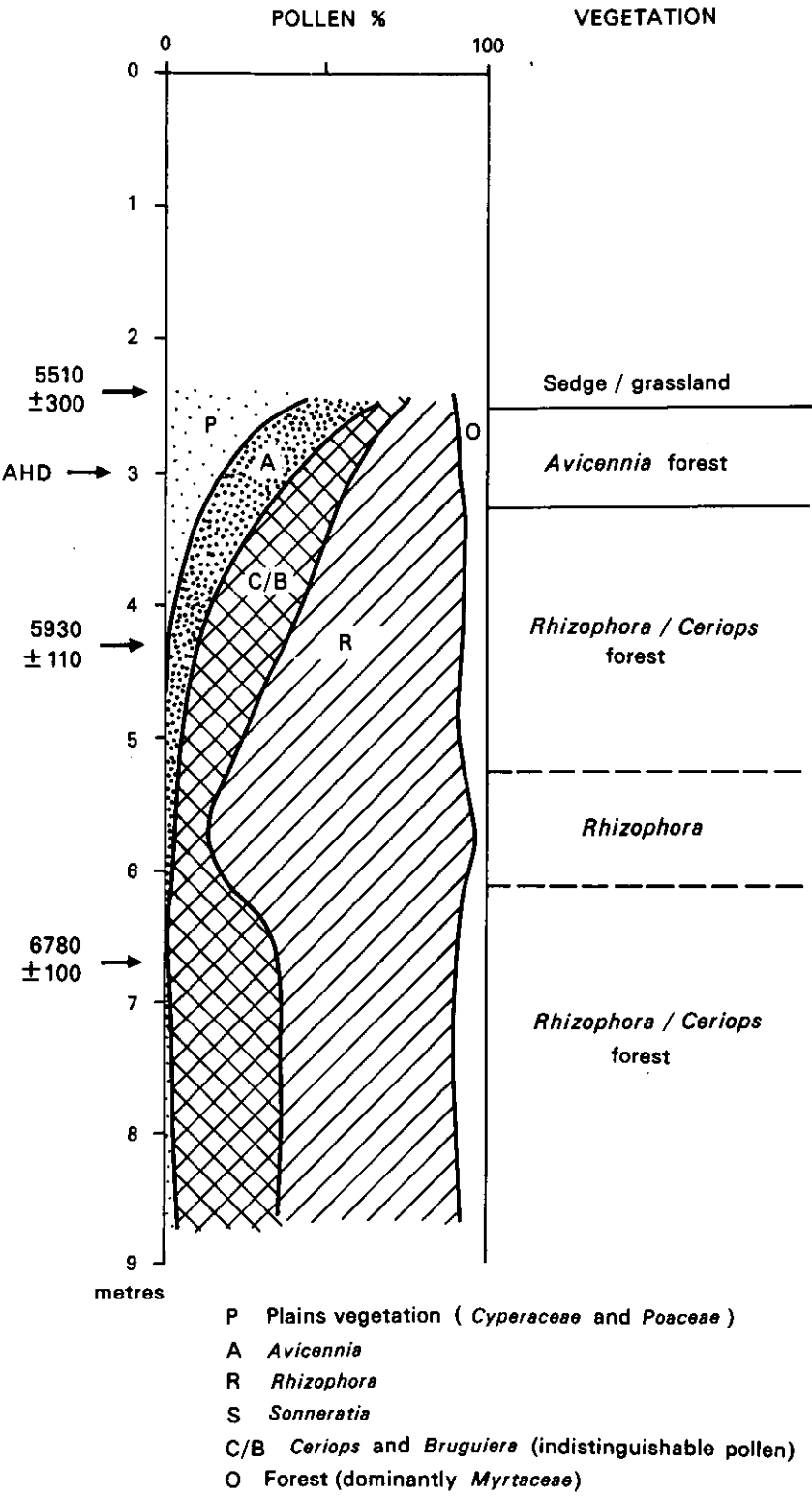


Figure 73: Pollen diagram of drillhole SAH 67

We believe that most of the 'big swamp' had disappeared by 4000 years B.P.. By this time sedges and grasses covered much of the plains away from the active channel. Dating of shell middens overlying black soil plain sediments, shown in Figure 74 and Table 8, supports this. Ages of 4600 ± 80 and 4170 ± 100 years B.P. on the midden at Rookery Point (Transect 6a, Figure 46) are the oldest we have recorded (with the exception of the buried midden within a 'big swamp' stump site at Kapalga Landing). As stated earlier (Chapter 4.2) we have not applied a radiocarbon environmental correction to shell dates, but they will not be more than 450 years younger than these reported ages. Midden dates of 3000 years B.P. or younger become common throughout the plains. These middens are often associated with the banks of paleochannels, sometimes sited on degraded silty levees. The shell fauna (Table 8) is largely intertidal and generally associated with mangroves experiencing regular tidal inundation, but the fact that the middens overlies freshwater silts and clays, and are not buried, or are only shallowly buried (20-40 cm) implies that the sites were in use at a time when freshwater floodplains had built up to a level close to their present elevation. Schrire (1982) records middens composed of marine shells in rock shelters of the East Alligator river which date from near to big swamp times. Compositional changes in those middens, and the onset of other midden deposits 3500-3000 years B.P. (Kamminga and Allen, 1973) appear to fall into the period in which we record floodplain middens, and all may be linked to the disappearance of big swamp mangrove. Middens containing marine shells have not been found south of site N (Figure 74), but occupation sites on the plains margin appear to become more common in this southern part of the plains (Meehan *et al.*, 1985).

Existence of a sinuous meandering tidal river, through the South Alligator plains, prior to development of the present river with its long cusped reach, is indicated by the paleochannels visible throughout the plains (Figures 34 and 35). These older sinuous courses lie within the axial belt of paleochannel and laminated channel sediments (Figure 68), and appear younger than the big swamp phase. The best known set are near Bullocky Point shown in Figures 35 and 49, and radiocarbon dates show that the outer paleomeander at Bullocky Point was active until at least 4000 years ago. The inner paleomeander was active more recently than 2600 years ago, and perhaps as recently as 1800 years ago as shown in Figure 75 which reproduces the data. Although the time of transition from 'big swamp' to sinuous meandering river amidst blacksoil plains is not known precisely, it was before 4000 B.P. in the Bullocky Point area. The alternative estuarine channel, further downstream near Water Recorder Point (Figure 44), was infilling by 4000 B.P., and a single sinuous channel was established at least by this time, upstream from this point. Dates from paleochannel fills, shown in Figure 76, indicate that some of these prior meanders were active less than 1400 years ago.

Paleochannels of the sinuous phase invite comparison with the present Adelaide River, as noted in Chapter 3.4. Although the overall sinuosity in the South Alligator was somewhat less, the relationship between channel width and distance from the coast was similar. Width-distance relationships of the present and sinuous river are shown in Figure 77. Furthermore the insides of meander bends include well-developed mangrove mud (as at Bullocky Point, Figures 51 and 52), indicating similarity to the thickly forested insides of meanders on the present Adelaide and lower West Alligator Rivers. Past tidal discharges in the sinuous river were less than today, calculated by methods in Appendix A2, as shown in Figure 77.

Rates of meander migration can be calculated from transect 8a at Bullocky Point (Figures 51 and 52). Basal dates of 6720 and 5480 years B.P. in SAH 40 and SAH 38 respectively, record the initial channel deposition prior to rapid vertical accumulation of laminated channel sediments. These are 1.15 km apart and indicate an average migration rate of 0.93 m/yr. Basal dates from SAH 40 and SAH 41, in a similar way, indicate slow migration of the channel upstream as this bend extended

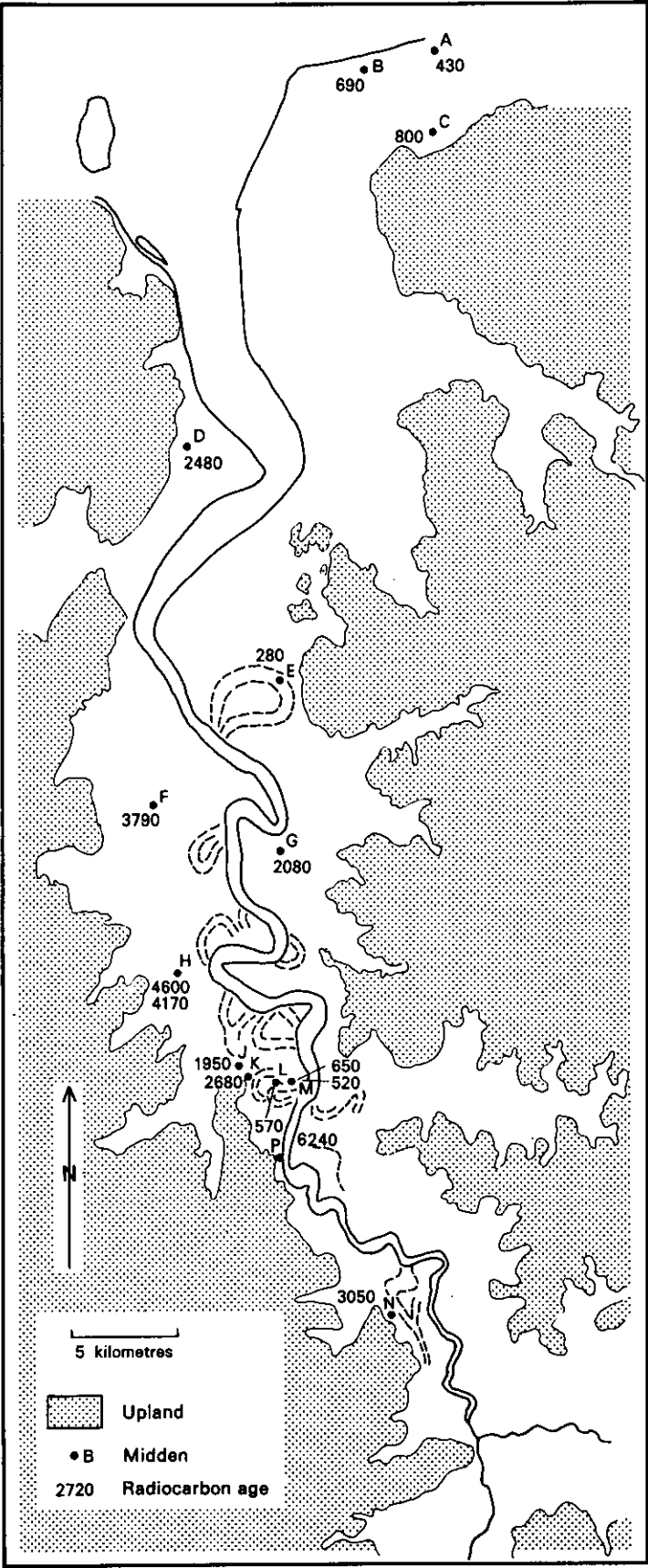


Figure 74 Distribution and age of middens on the South Alligator plains

Table 8
Composition and age of middens on South Alligator Plains

Midden (Figure 74)	Drill hole	Grid Reference	Surface expression	Substrate	Principal mollusc species	Additional remains	Radiocarbon age (years B.P.) all on shell
A	SAH14	KG 283570	Shell mound	Sandy/shell hash chenier ridge	<u>Anadara granosa</u> <u>Telescopium telescopium</u> <u>Terebralia palustris</u> <u>Turritella terebra</u> <u>Nerita lineata</u> <u>Naquetia capucina</u> <u>Polymesoda coaxans</u> <u>Mactra alta</u> <u>Elliptium aurisjudae</u>	-	430±70
B	-	KG 245558	Shell mound			-	690±70
C	SAH17	KG 287526	Scattered shell	Sandy chenier ridge	<u>Telescopium telescopium</u> <u>Terebralia palustris</u> <u>Anadara granosa</u>	Rock fragments	800±70
D	-	KG 160387	Scattered shell	Salt mudflat surface	<u>Terebralia palustris</u> <u>Telescopium telescopium</u>	-	2480±70
E	-	KG 213273	Scattered shell	Paleochannel surface	<u>Telescopium telescopium</u> <u>Cerithidea</u> sp.	-	280±60
F	SAH49	KG 149218	Scattered shell	Black soil	not collected	-	3790±70
G	SAH54	KG 211197	Degraded surface mound	Black soil	not collected	Stone and bone	2080±70
H	SAH61	KG 165138	Surface mound	Black soil	not collected	Worked stone, grindstone	4600±80 4170±100
J	SAH9	KG 193095	Surface mound	Black soil	<u>Meretrix meretrix</u> <u>Nerita lineata</u> <u>Cerithidea</u> sp.	Ochre, worked stone	1950±100
K	SAH13	KG 199090	Scattered shell	Bank of paleochannel	<u>Polymesoda coaxans</u> <u>Cerithidea</u> sp.	-	2680±70
L	SAH40	KG 215085	Surface mound	Degraded silty levée	<u>Cerithidea</u> sp.	Dolerite and quartzite stones (standing)	570±60
M	SAH11 SAH12	KG 217083	Surface mound	Degraded silty levée	<u>Meretrix meretrix</u> <u>Cerithidea</u> sp. <u>Telescopium telescopium</u> <u>Terebralia palustris</u> <u>Volgalea wardiana</u>	Rock fragments, worked stone	650±70 520±60
N	-	KF 280983	Degraded surface mound	Black soil	<u>Meretrix meretrix</u> <u>Cerithidea</u> sp.	-	3050±70
P	-	KG 214055	Buried	At 'big swamp' mangrove stump site	<u>Telescopium telescopium</u>	Rock fragments	6240±100

westwards, and this occurred at an average rate of 0.06 m/yr (see Figure 52). If the inner paleochannel at Bullocky Point migrated at a similar rate from a point approximately where the present channel is, to end up at the position of SAH 42 2600 years B.P., it must have cutoff from the outer bend about 3600-3300 years B.P.. This is entirely consistent with the age of 3950 years B.P. on mangrove mud on the inside of the outer bend.

If these rates can be extrapolated to other bends, then the large paleochannel 32 km from the mouth would have taken 3500-2300 years to have migrated to its present position, and that 41 km from the mouth would have taken 1800-1200 years to have assumed its present position. We cannot say whether migration occurred as a continuous process or whether it may have been episodic.

Coastal progradation accelerated during the sinuous river phase (Figure 41). Meandering appears to have advanced downstream in sympathy with this. The largest paleomeander, about 30 km from the coast, has 3830 B.P. deposits on its outer bank and cuts into estuarine deposits of 'big swamp' age at 6m (Figure 76). This channel appears to have been active until recently, as shown by a radiocarbon-modern age at 2.45 m. In comparison, dates on fill in paleochannels further upstream are older than this with the oldest paleochannel sediments being recorded 2280 \pm 270 years B.P. in transect 12b (Figure 59) and 2880 \pm 100 years B.P. on transect 10 (Figures 56 and 76).

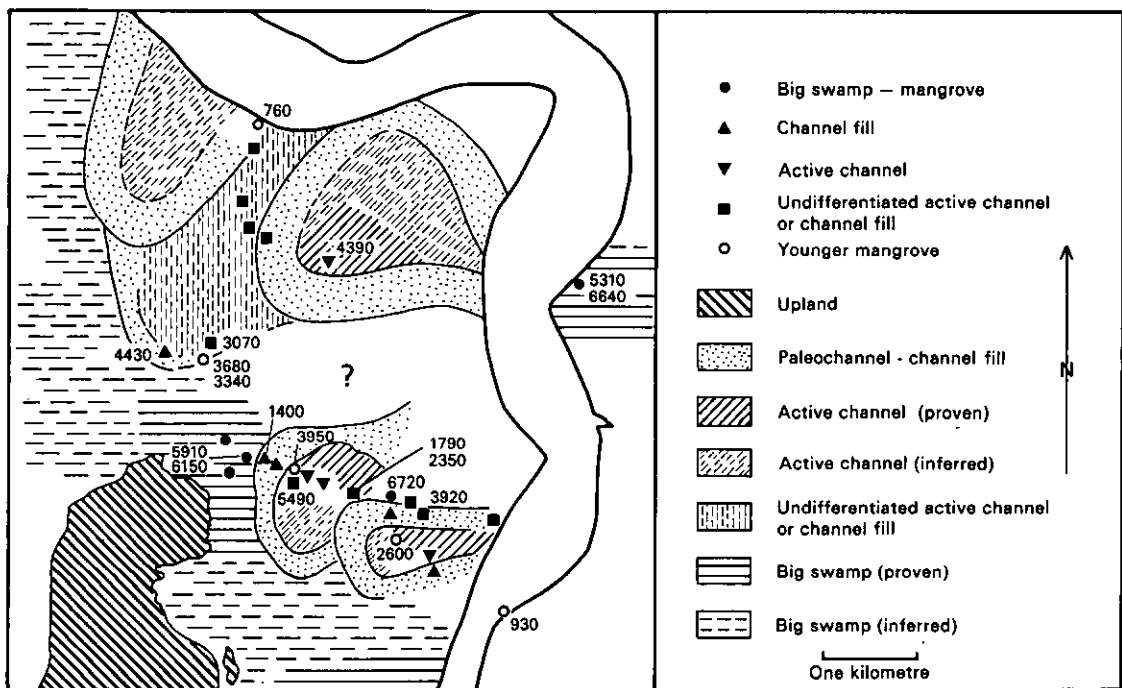


Figure 75: Bullocky Point, distribution of shallow subsurface sediments and radiocarbon dates

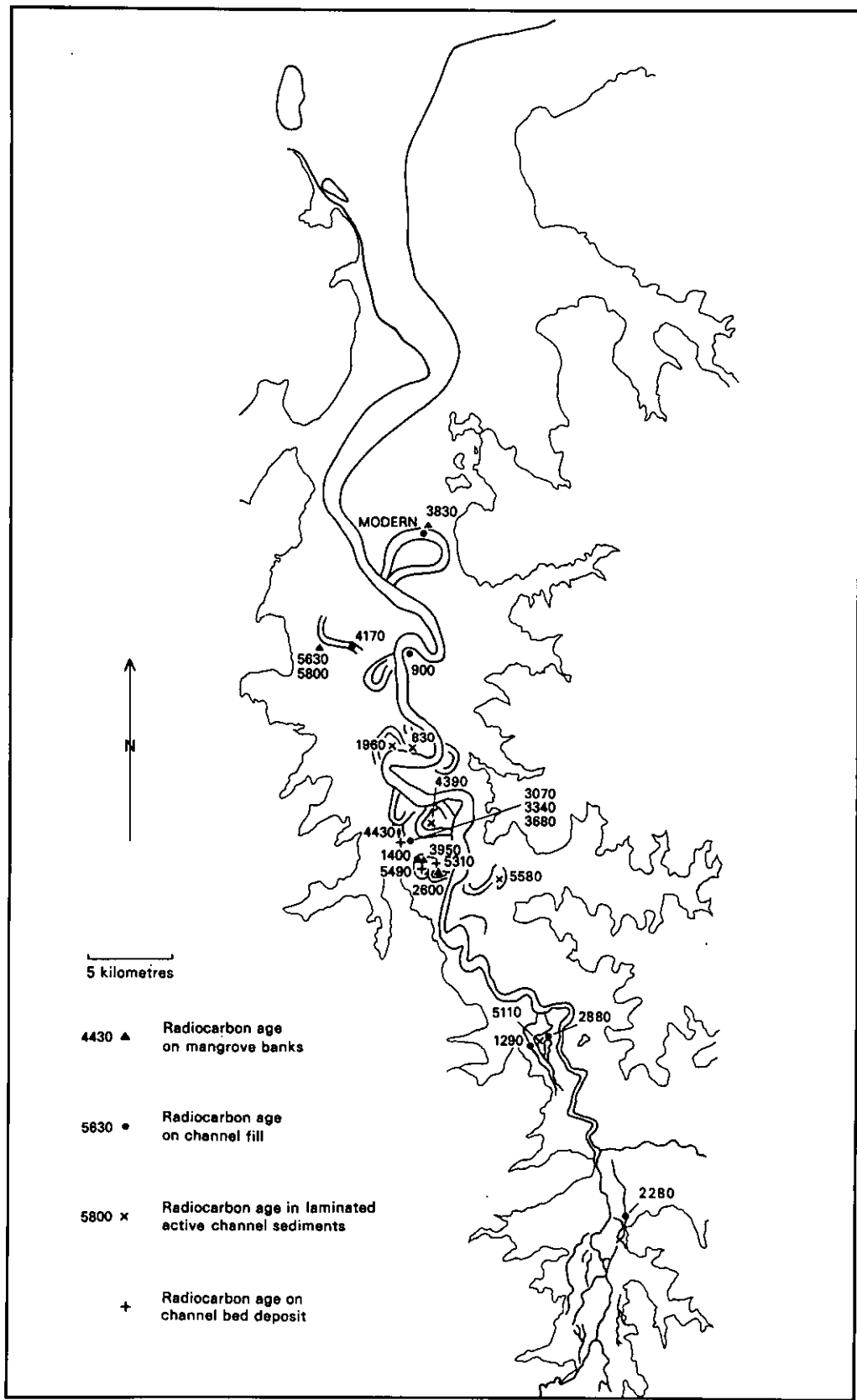


Figure 76: Paleochannels and radiocarbon ages of their margin and fill deposits

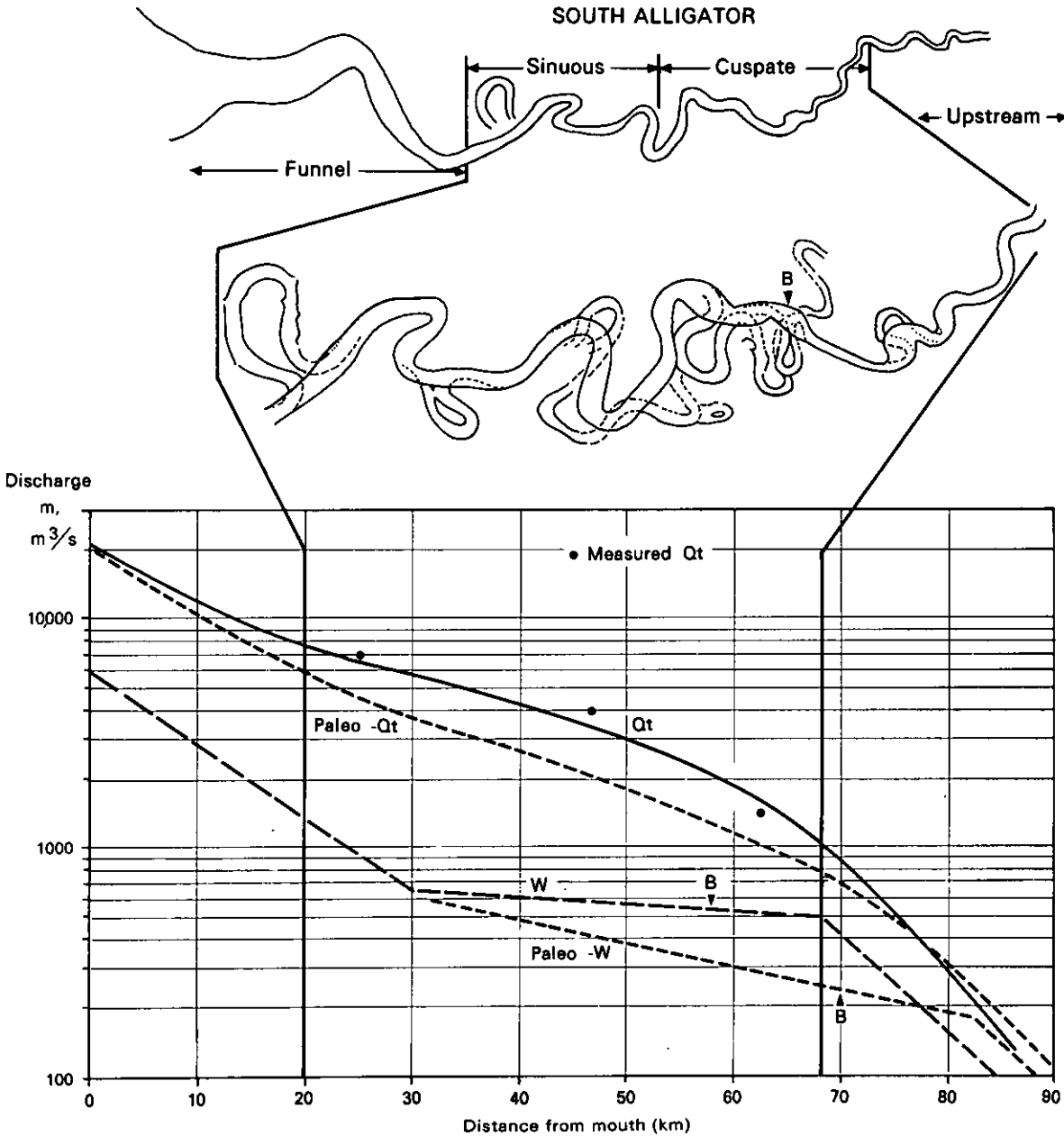


Figure 77: Paleochannels in the deltaic-estuarine plains of the South Alligator River, and their width and discharge relationships to distance from the mouth, compared with present day. Qt = mean tidal flow (m /sec), W = width (m).

5.5 The Cusate River phase

The cusate bends of the South Alligator River contrast strikingly with the sinuous meandering bends of the former river, and with those of other modern rivers such as the Adelaide (see Figure 79). Similar cusate bends occur on the East Alligator River. The cusate segment of the river is characterised by a generally shallower channel, with sandy mid-channel and point bar shoal development. The paleochannels which can be seen on the accompanying 1:80,000 geomorphological map, and the discussion in the previous section, show that the cusate bends developed at the expense of sinuous meandering bends. Anomalously greater width of the cusate segment, and evidence of erosion into 6000 year old big swamp deposits, demonstrate lateral expansion of the present river. As we will show in Chapter 6, this is an important change leading to increase of tidal flow and high tide levels in the upstream parts of the river. Channel widening must reflect bank failure of the previous sinuous river and, whatever the causes, the consequences are significant for the adjacent plains. The time when this process began, and its rate of progression, are obviously of interest for predicting the future. It is an unfortunate fact that erosional processes cannot be measured by the stratigraphic dating methods used above. The maximum age of the present channel can only be gauged, by dating the deposits which underlie the river banks, and from the ages of deposits infilling prior channels.

Figure 78 summarises shallow stratigraphy revealed in river bank exposures and radiocarbon ages of deposits cut or immediately adjacent to banks of the present river, as well as dates on channel fill in paleochannels. Results show that the processes adjacent to the channel in the deltaic-estuarine and in the coastal plains, have changed in the last 3000 years, particularly in the last 1000 years. Progradation of the coastal plain has been negligible since about 2000 years ago (Figure 41). The estuarine funnel seems to have changed little since nearly 3000 years ago, and it appears that the inner Bullocky Point paleochannel may have been abandoned soon after 2500 years ago.

Infill of paleochannels however does not appear to have been completed immediately after abandonment. The outer paleochannel at Bullocky Point was active 4000 years ago (probably contemporaneously with the paleochannel to the north probed by SAH 44, with a basal date of 4430 ± 150 years B.P. and SAH 101 into laminated channel sediments dating 4390 ± 130 years B.P.). It must have been abandoned before 2600 years ago by which time the inner paleochannel was well established, but mudfill in the outer paleochannel has been dated 1400 years B.P. The paleochannel on transect 10, cored by SAH 71, has a date near the base of channel fill of 1290 ± 140 years B.P.. An upstream paleochannel is dated 2280 ± 270 years B.P. in SAH 122. These dates indicate at least some paleochannels existed as open perennial water bodies until 1400-1300 years ago.

We are unable to identify the time of abandonment of other paleochannels, or initiation of flow in the present channel. In the Apple Tree Bend area a radiocarbon age of 1960 ± 80 years B.P. (Figure 78) on a log in laminated channel sediments exposed in the bank indicates channel migration into the position of the paleochannel to the north of the sample point (see Figure 48). This must have been cutoff prior to initiation of the sequence of laminated channel sediments which prograded eastwards to the present location of Apple Tree Bend. Within these younger channel sediments, close to the initial channel margin we have a radiocarbon date on a log of 830 ± 70 years B.P. The 1.2 km long exposure of laminated sediments underlying the present point bar must have accumulated since then, indicating a rate of progradation of at least 1.45 m/yr. This must be regarded as a minimum rate because the present point bar is being eroded by cliffing and slumping, and may have been in this erosional phase for some time, and because the log died before it was redeposited. The cutoff must have occurred between 1900 and 800 years ago, perhaps a little over 800 years

ago. The paleochannel was sinuous whereas the river at this point is now at the transition between cusped and sinuous meandering forms.

There are several sites along the river where erosion of banks has exposed mangrove stumps or logs on which radiocarbon ages in the range 1000-750 years B.P. have been obtained. The most pronounced erosional area is on the western bank in the estuarine funnel where bank retreat can be detected by comparison of aerial photographs (Figure 27b), and ages of 1000-900 years B.P. have been obtained. Other sites in which mangrove stumps have been exposed along the river with ages of 900-700 years B.P. also appear to indicate incision of the banks, particularly in the cusped segment in the last 1000 years (Figure 78). A similar recent erosional phase is reported from the Fitzroy River and King Sound (Jennings, 1975; Semeniuk, 1981). It should be noted that there has been very little observed change in the position and shape of the banks on the South Alligator River in historic time (Figure 27b). This contrasts with historic changes on the Daly River, and trends observed by Jennings (1975) on the Fitzroy River. On the latter, comparison of aerial photographs showed shifts of the point of contact of tidal creeks with the main channel, shift of meanders down the estuary, and a sharpening of meander spurs, perhaps as a more cusped form is developing.

We conclude that transition to the cusped phase may have begun as early as 2000 years ago, but change including channel widening accelerated within the last 1000 years.

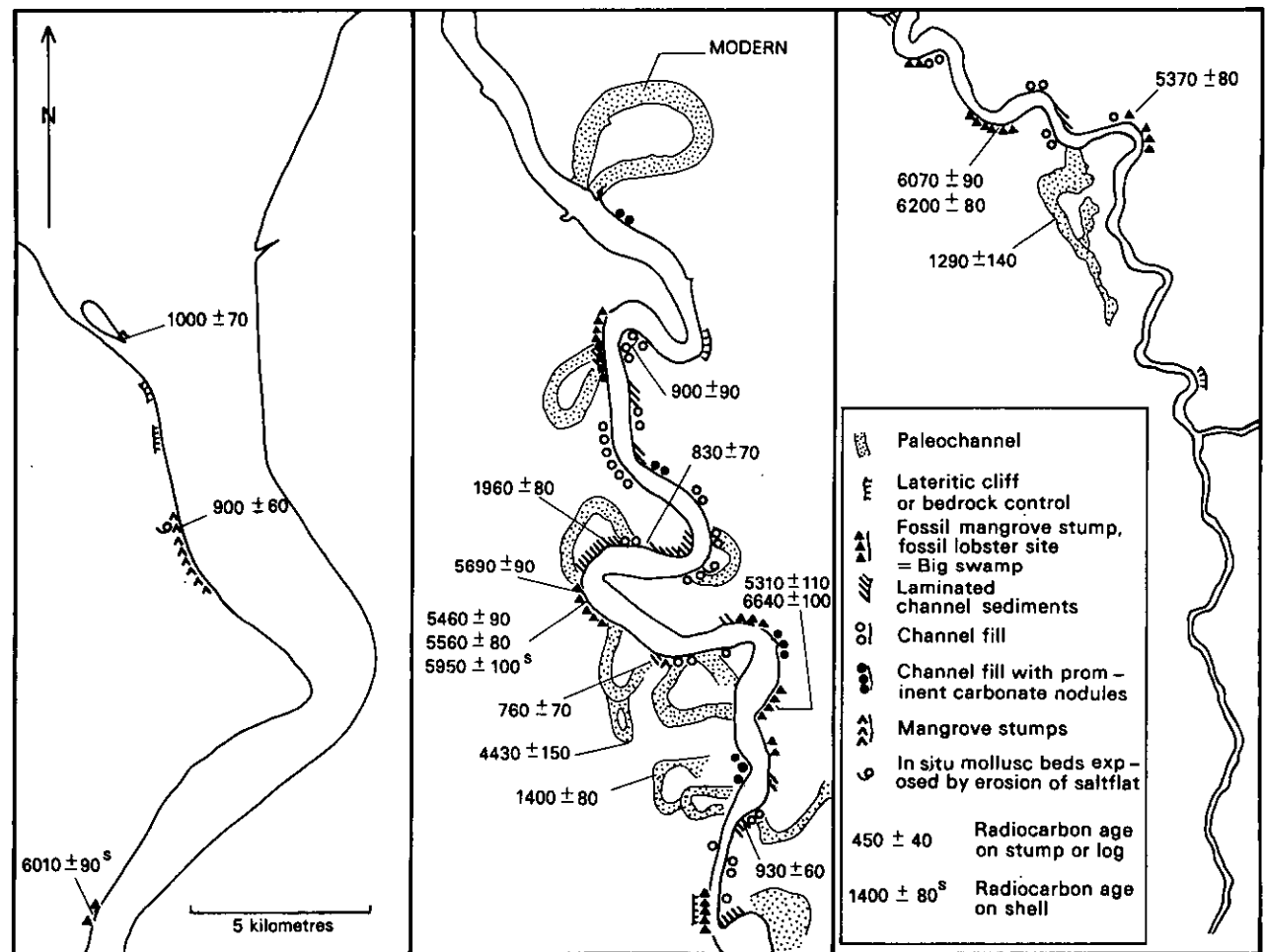


Figure 78: Shallow stratigraphy revealed in bank exposures, and radiocarbon ages of deposits cut or adjacent to banks of present river

Chapter 6

Morphodynamics over the last 6000 years

- 6.1 Comparison of the South Alligator and other rivers
- 6.2 Tidal changes during evolution of the South Alligator
- 6.3 Changing patterns of sedimentation

6. MORPHODYNAMICS OVER THE LAST 6000 YEARS

6.1 Comparison of the South Alligator and other rivers

No tidal river in the top end of the Northern Territory should be seen as unique, as most have the same boundary conditions of being affected by the monsoonal climate, of drawing from catchments of roughly similar geology, and of being affected by similar macrotidal conditions with relatively low-energy wave climates at their mouths. Yet, it is notable that tidal river channel form differs substantially between cases. The South Alligator and its neighbour, the East Alligator, have wide cusped channels while the Adelaide River has a long procession of exquisitely sinuous meanders. The Daly River contrasts by having a highly active meander plain where meander cutoffs, and both cusped and sinuous forms have formed within historical times. It is a reasonable assumption, increasingly supported by data, that each of these valleys have experienced the same history of Holocene sea-level changes. These examples have a floodplain contained within a prior valley which is much longer than it is wide. The major difference between the systems is in the size of its catchment.

There is evidence that a 'big swamp' phase was experienced in several rivers and it can be inferred in others. Jennings (1975) reported 8 radiocarbon ages in the range 7450-5840 years B.P. on mangrove wood from the Fitzroy River, and Thom *et al.* (1975) recorded radiocarbon ages of 6810-6200 years B.P. on organic clay beneath tidal flats of the King River in the Cambridge Gulf-Ord River area of north Western Australia.

Similar deposits have been dated to 'big swamp' times in the Daly River (Chappell, in prep.). Undated mangrove stumps, almost certainly of similar age, are reported from King Sound, upstream on the Ord River, and the East Alligator River (Semeniuk, 1980b; Wright *et al.*, 1972; T. East, pers. comm.). The 'big swamp' phase appears to have been widespread throughout many of the long, narrow drowned river valley systems of north Australia (Woodroffe *et al.*, 1985c). It extended almost contemporaneously in these river systems because of the decelerating rise and stabilisation of sea level; we do not subscribe to the view advanced by Jennings (1975) that large mangrove trees formerly developed in the Fitzroy River and in Darwin Harbour indicate a wetter climate in mid-Holocene times.

Onset of the 'big swamp' phase was broadly simultaneous in these rivers as widespread shallowing occurred when sea level was stabilising. We believe contraction and disappearance of the mangrove forests occurred as a result of continued sedimentation throughout the estuary and tidal river, eliminating most of the mangrove habitat. This need not have taken place concurrently along the north coast. On the South Alligator plains most of the mangrove had disappeared by 5500 years B.P., and a few radiocarbon dates indicate local mangrove 4600-4300 years B.P. The extensive mangrove forests which exist today around the meanders of the Adelaide River may therefore have been vanishing from the South Alligator as early as 4000 years ago.

Floodplain and channel development in macrotidal rivers is affected by the contest between tidal and fluvial flows. The negative-exponential decline of width in the upstream direction in the estuarine funnel indicates tidal dominance (Chapter 2.2, Appendix A2). Width does not decline significantly with discharge through the sinuous and cusped segments, which is the region of most active meander development and channel change. The relative roles of tidal and floodwater flows here is an important issue. We examine this by contrasting fluvial and tidal factors in the South Alligator with those in the Adelaide River, which has a smaller catchment, and those in the Daly River which has a much larger catchment.

Figure 79 shows the channels of the tidal Adelaide, South Alligator and Daly rivers. The relative lengths of specific channel segments - estuarine funnel, meandering (sinuous plus cusped), and upstream - differ between these rivers, with the Adelaide having the longest meandering segment and the Daly the shortest. The meandering segment is bounded on the downstream side by the estuarine funnel, i.e. by tidal morphodynamics. Floodwater/tide interaction becomes significant upstream of this boundary, and must be manifest in some way in the morphology of the meandering segment (Chappell and Woodroffe, 1985). With this in mind it is notable that the meandering channel of the Daly River is the most mobile while that of the Adelaide is the least mobile. The evidence for this is found, in the Daly, in historical migration of meander loops which are seen from successive aerial photos to shift by up to 30 m/year. Aerial photos of the South Alligator show channel migration of only about 1 m/year (Figure 27b) similar to the rate inferred from stratigraphic studies (Chapter 5). Different rates of mobility of different rivers are also shown by the relative abundance of cutoff paleochannels on the floodplains. The Daly has nests of up to 5 successive paleochannels adjacent to its sinuous segment, the South Alligator has well preserved paleochannels but rarely more than one cutoff in any area, and the Adelaide River has very few paleochannels adjacent to its sinuous segment.

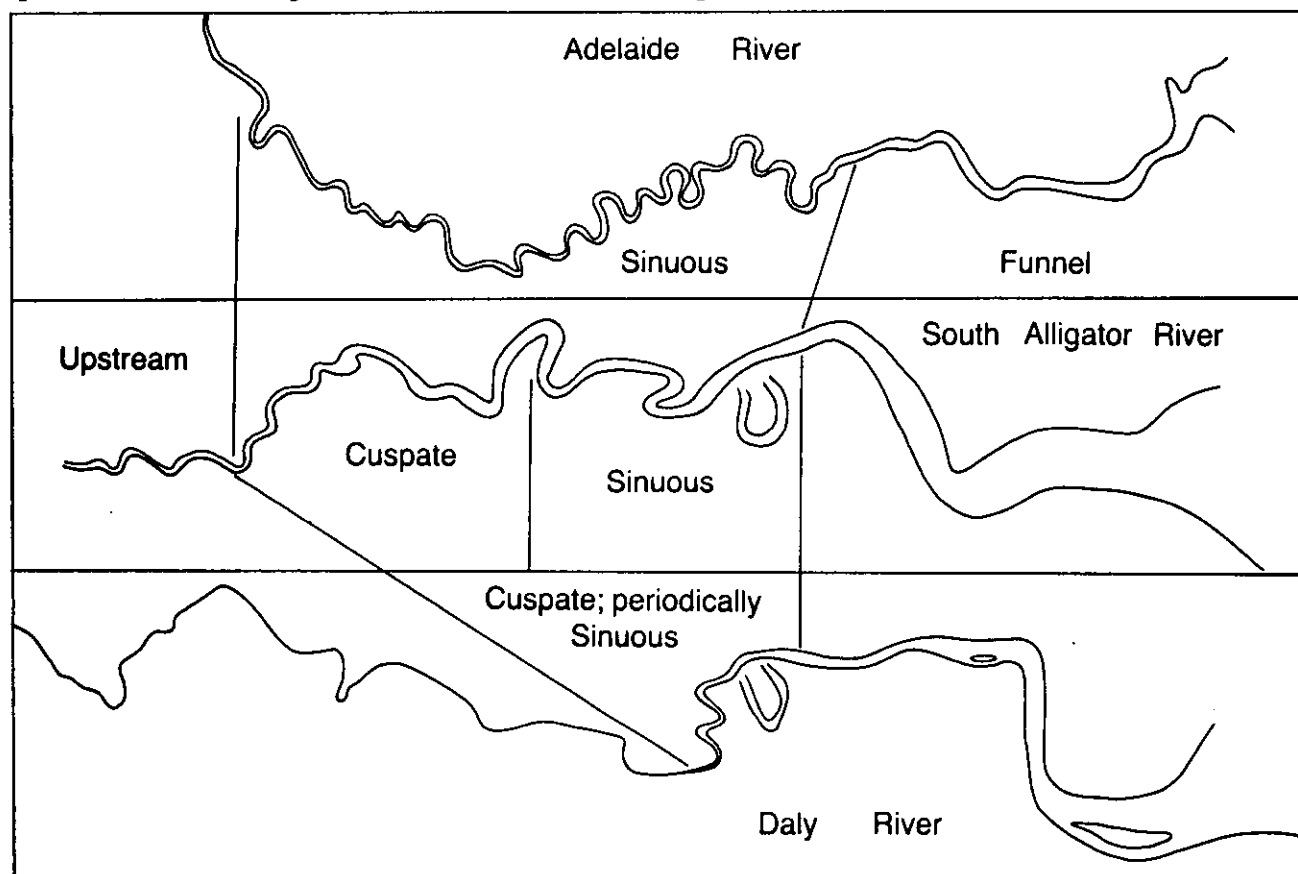


Figure 79: Channel segments of Adelaide, South Alligator and Daly Rivers

Evolution of the South Alligator River from the 'big swamp' phase through a sinuous river to the present mixed cusped/ sinuous condition was described in Chapter 5. It was noted that the sinuous phase resembled the present Adelaide River. The fact that channel mobility differs between the Adelaide, South Alligator and Daly (in increasing order) suggests that the rate of channel and floodplain evolution increases similarly. Chappell and Woodroffe (1985) suggested that this may be directly linked to relative catchment size, on the grounds that sediment discharge is expected to be proportional to catchment size when rainfall, geology, and topography are

similar. A second factor is the size of the Holocene sedimentary basin, which in the case of tidal rivers similar to the South Alligator is effectively the floodplain area. Provided that the mean thickness of sediment deposited since sea level stabilised is the same for different cases, and that the sediment deposited offshore is negligible relative to that trapped in the floodplain system, the volume of the sedimentary basin is roughly proportional to the floodplain/ coastal plain area. Hence, the ratio of catchment to floodplain area should be a rough indicator of the rate of sediment input to the tidal/river and floodplain system. The rate of channel and plains evolution should be proportional to this factor.

Table 9 lists estimates of mean rates of channel migration, and of catchment/floodplain area ratios, for the Adelaide, South Alligator, and Daly rivers. Both parameters are smallest for the Adelaide and largest for the Daly, but the relationship is not linear. Channel migration rate appears to increase very much more rapidly than simply proportional to catchment/floodplain ratio. Other factors likely to be implicated are sediment texture and the relationship between flood and tidal discharges. In general, excluding braided channels, the greater the sand/mud ratio the wider a channel tends to be (Schumm, 1969) and the more active is the meandering process. Table 9 shows that sediment is least sandy in the Adelaide River and most sandy in the Daly. The table also shows that the ratio of flood discharge to tidal flow around the middle part of the meandering segment is greatest in the Daly, least in the South Alligator and Adelaide. Supposing that the channels are adjusted to their dry season tidal flows, this means that wet season floods have a greater capacity for work on the channel in the Daly and the least capacity in the Adelaide. All factors together in Table 9 act similarly to cause the observed differences of channel activity.

Table 9
Comparisons between South Alligator,
Adelaide and Daly rivers

	Adelaide R.	South Alligator R.	Daly R.
Channel migration rate (m/yr)	0.1	1*	25
Catchment/ Floodplain area ratio	4	9	29
Sediment texture	mud	sandy mud	muddy sand
$\frac{Q_2^{**}}{Q_t}$	0.25	0.17 (0.25)p	0.7
Notes	<p>* Determined from Figure 27b, and minimum average rates of meander migration at Bullocky Point (Chapter 5.4), Apple Tree Bend (Chapter 5.5) and West Alligator River</p> <p>** Q_2 = 2-year flood discharge, Q_t = mean tidal flow around middle of meandering segment</p> <p>p = figure for paleo (sinuous) South Alligator</p>		

It is interesting to ask whether the South Alligator, having passed through an Adelaide River-like sinuous phase, will eventually enter a Daly River-like phase where meander loops form, cut off, and reform with cusped meanders occurring intermittently. We think that this is unlikely, on the grounds that the dynamics of the Daly meanders are different from the long cusped segment of the South Alligator. Cusped bends form in the Daly immediately after meander cutoff (most recently in 1977), but sinuous bends immediately begin to propagate from the new cusp (Chappell, in prep.). We have no evidence for this in the South Alligator. In any case, the observed rates of channel migration in the South Alligator are so much slower than the Daly (Table 9).

6.2 Tidal changes during evolution of the South Alligator

Changes of tidal creeks and salt invasion of paperbark and other freshwater wetland areas are issues of importance, both scientifically and for future park management (Chapter 3.3). Recent bank erosion particularly in the cusped segment, described in Chapter 2.5, may be linked with this. Both seem to imply a rise of maximum tidal levels in relatively recent time, either through sea-level rise or through increase of tidal range throughout the river, particularly in the cusped and upstream segments.

An historical rise of global sea level has been invoked to explain widespread coastal erosion in many parts of the world (Bird, 1985). Sea-level rise of several centimetres in the last 100 years or so is known from tide gauges in several countries, mostly northern hemisphere, although local factors including isostatic movements account for many such observations. Data appear to be scanty in Australia, although Thom (1974) and Thom and Roy (1985) have concluded that the standard gauge at Fort Denison, Sydney, shows no significant net change in the last 100 years. Sydney is remote from the South Alligator, but we know of no reason to expect that trends here will be different. Sea-level data discussed in Chapter 5.2 and 5.3 indicate that levels relative to the South Alligator 6000 years ago may have been a metre lower than for coastal eastern Australia. Even if this were a trend continuing to the present, this amounts to about 2 centimetres apparent subsidence of land relative to Sydney over the last 100 years, which we feel is insignificant if it happened at all. Hence, we exclude an historical sea-level rise. Longer-term rise is excluded also, as the general trend has been sea-level fall, relative to Australia, over the last 6000 years (Chapters 1.5 and 5.3).

Changes of tidal amplitude throughout the river, during its evolution since the big swamp phase, are more likely. Chapter 5.4 showed that the sinuous river phase, 4000 to 2500 years B.P., resembled the present Adelaide River in channel form and width-distance relationships. Because the Adelaide River has a substantially smaller tide range at the Arnhem Highway than the South Alligator (3.2 m versus 5.6 m, at roughly equal distances from the mouth), a more detailed discussion is warranted. If, for sake of argument, the South Alligator in its sinuous phase had similar tides upstream to the Adelaide then high spring water level could rise by about 1 m as the river changed to its present form. This would have significant consequences. The question can be addressed both theoretically and empirically.

The South Alligator has become wider and perhaps shallower, through the cusped segment, since its prior sinuous river phase. According to Green's law, in a tidal river

$$a w^{0.5} h^{0.25} = \text{constant} \quad (6.1)$$

Where a is tidal amplitude, w is channel width and h is depth. Green's law applies only if friction is zero, however. When friction is included, the simplest model for an exponentially tapering channel is

$$\eta = a_0 e^{mx/2} e^{-\mu x} \cos(\sigma t - kx) \quad (6.2)$$

Where η is tide height (above MWL) at x at moment t , a_0 is amplitude at the river mouth, m is the exponential tapering coefficient (taken as a positive number), and μ and k are friction-related parameters modifying and tidal phase respectively (Appendix A2). When friction is zero, eq. (6.2) is equivalent to (6.1) with depth h constant. Simple tests for significance of friction are (i) to examine departures from Green's law (6.1) and (ii) to examine the difference between observed tidal celerity ($C = \sigma/k$) and theoretical frictionless celerity. Table 10 shows these comparisons for the present South Alligator and for the Adelaide River. Friction is significant in both cases, but is substantially greater in the sinuous Adelaide River. However, if the coefficients μ and k for the Adelaide River are used for the paleo South Alligator, the tidal range at the position of the Arnhem Highway is predicted to have been only about 0.2 m less than present (Table 10), which is small. This result, based on eq. (6.2), neglects the possible effect of shallowing during formation of the cusped segment.

The mean depth relative to high tide level in the cusped segment is 9.0 m, while that in the present sinuous segment is about 13 m, similar to mean depth relative to HWL in the Adelaide River. If the former sinuous South Alligator were similar to either of these then depth may have reduced by a factor of 0.7 during formation of the cusped segment. Although Green's law is not strictly applicable due to friction, eq. (6.1) suggests that tide range may have been 0.4 m less at the Arnhem Highway location during the sinuous river phase. This will be an overestimate, but combined with the results in Table 10 it does indicate increase of tidal range since the end of the sinuous phase, perhaps by about 0.4 to 0.5 m. These rough estimates take no account of non-linear effects, which can affect the slope of the mean tidal surface.

Table 10

Comparisons of present and paleo South Alligator Rivers
and Adelaide River, tidal parameters

	x	m	t	$2\eta_1$	$2\eta_2$	k	μ	f
South Alligator, sinuous + cusped	51	0.64	105	5.5	5.1	1.72	0.17	0.0014
Adelaide River, sinuous	52	1.35	140	3.5	3.0	2.03	0.75	0.007
Paleo South Alligator, sinuous	55	1.9	-	5.5	4.9	-	0.75	-

Notes (see eq. (6.2)) :

x = length of meandering segment to position of Arnhem Highway (km)

m = channel tapering coefficient ($\times 10^{-5}$)

t = tidal lag/length x (min)

$2\eta_1, 2\eta_2$ = tidal ranges (m) at lower limit and Arnhem Highway points of meandering channel

k and μ defined in eq. (6.2) ($\times 10^{-5}$)

f = Darcy friction coefficient

Field data suggest that the mean tidal surface may have a slope which is different from that of the past. Once again, we compare rivers. The upper limit of mangrove growth is linked to high spring tide level, and in the South Alligator indicates that high spring level is about 0.7 m higher at the Arnhem Highway than at the coast. The salt mudflats of the Lower Floodplain Unit similarly increase in elevation upstream. The data, from Figure 37 are reproduced in Figure 80. Mean water level also increases upstream, being 0.6 m higher at the highway than at the coast (Figure 28). At the Adelaide River on the other hand, mean water level at the Arnhem Highway appears to be <0.1 m AHD, i.e. at about the same level as at the coast, and the top of the mangroves increases in elevation by only 0.1 m from the Narrows to the Highway. Figure 80 summarises the data. The difference of 0.5 m in mean water level between the Adelaide and the South Alligator, at their respective Arnhem Highway bridges, is presumed to be due to different tidal properties of the two rivers. On the South Alligator the rise upstream of high spring tide level, indicated by the mangroves (Figure 80) is greater than the rise of mean water level. The highest mangroves near the highway are 0.7 m above those at the coast, yet the tidal range is greater at the coast by 0.6 m (Table 3, Chapter 2). Hence, the effective super-elevation of the mangroves at the highway is about 1.0 m relative to the coast.

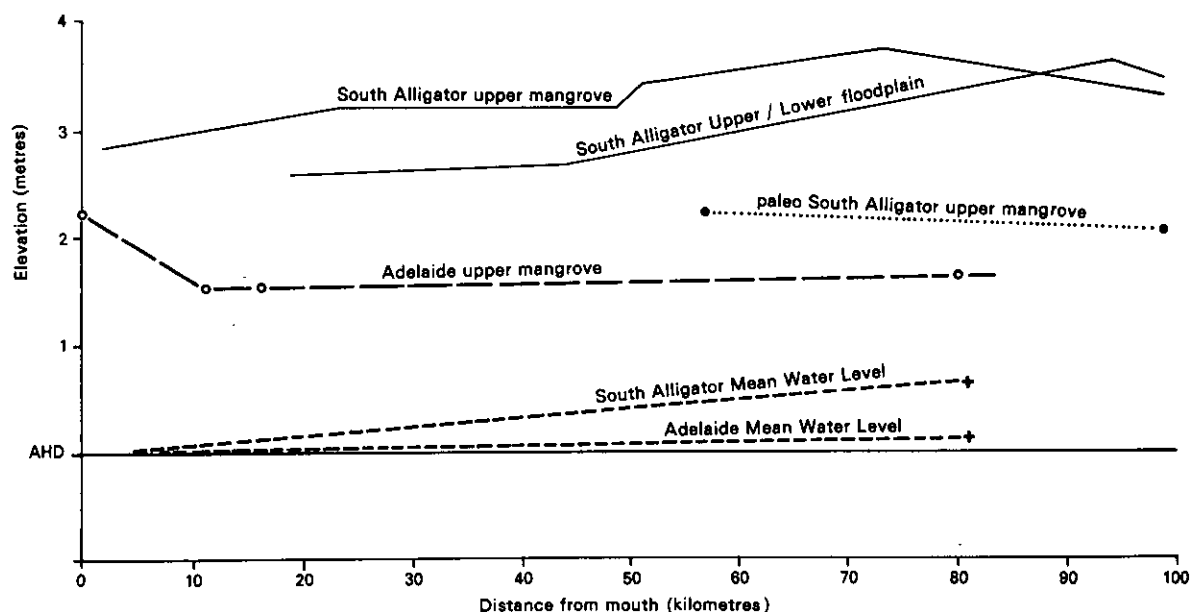


Figure 80: High spring tide and mean water levels along the South Alligator, Adelaide and paleo South Alligator rivers. Mean water level defined as in Figure 28 (using data from dry season 1981-1984 for Adelaide River). Elevational data from our surveys and from N.T. Department of lands.

All the above factors add to the same result, that the sinuous paleo South Alligator had lower tidal levels than the present river. The full set of effects at the highway location is this:

- (i) Change of friction parameters, 0.2 m.
- (ii) Effect of shallowing (Green's law), <0.4 m.
- (iii) Change of mean water level, 0.5 m.

Adding (i) and (ii) and (iii) gives something over 1 m, which is the observed total difference in highest mangrove levels between the coast and the highway. The Adelaide River, which provides the comparative baseline, shows only 0.1 m difference in highest mangrove levels, between the mouth inside the Narrows and the Highway. The figures appear to be consistent, and we conclude that highest spring tide levels have risen by perhaps 1 m around the Arnhem Highway area of the South Alligator, since the sinuous river phase.

There is some field evidence supporting this. Pollen analysis of cores, reviewed in Chapter 5.3, allows us to pinpoint the transition from mangrove to plains vegetation, which is the high spring tide level (Figures 72). These data and those of Russell-Smith (1985b), discussed in Chapter 5.3.1, are plotted on Figure 80, showing that high tide levels from the 60 km point to the tide limit were at least 1 m lower than present around 5500 years ago. This supports the above conclusion. We believe, therefore, that high tide levels began rising since initiation of the cusped river phase, which began no more than 2500 years ago. A conservative estimate of the rate of high tide rise is 4 cm per century, if the process has been uniform over the last 2500 years. As some of the meander cutoffs in the sinuous segment are more recent, the rate of rise may well be greater than this in more recent times.

There is evidence of changes of tidal range along other macrotidal estuarine systems in late Holocene times. Emergent mangrove deposits, which we would infer to be of big swamp age (c6500-6000 years B.P.), have been described above present tidal levels in the upstream segment of the Ord River (Wright et al., 1972), and in this case tidal range appears to have decreased upstream since their establishment. In Broad Sound, Queensland, Cook and Mayo (1977) recorded an increase of 1 m in elevation of mangrove deposits from 6000 years B.P. to present, which they attributed to a change of tidal range.

6.3 Changing patterns of sedimentation

Sediment deposition in the South Alligator tidal river and plains has changed in pattern and perhaps in rate over the last 6000 years. Passage from the big swamp to the sinuous river and floodplain system, between about 5500 and 4000 years B.P., must have been due to widespread deposition of fine sediment throughout the previous big mangrove swamp. Coastal progradation, on the other hand, was minor until 4000 years B.P. by which time the sinuous river and floodplain was well established. Figure 81 shows that progradation of the coastal plain, and probably the eastern side of the lower funnel, was rapid, averaging 1.7 m/yr, between 4000 and 3000 years B.P. and has been negligible since.

We interpret chenier ridges themselves as being formed by storm concentration of coarse material which is winnowed from lower intertidal and subtidal sediments during periods of decreased mud deposition. By 3000 years B.P. the coastal plain and probably also the estuarine funnel, had almost reached its present position (Figure 81). There appears to be a hiatus in sediment deposition until the chenier was deposited 1700-1500 years ago. Cheniers are more numerous further west in van Diemen Gulf, at

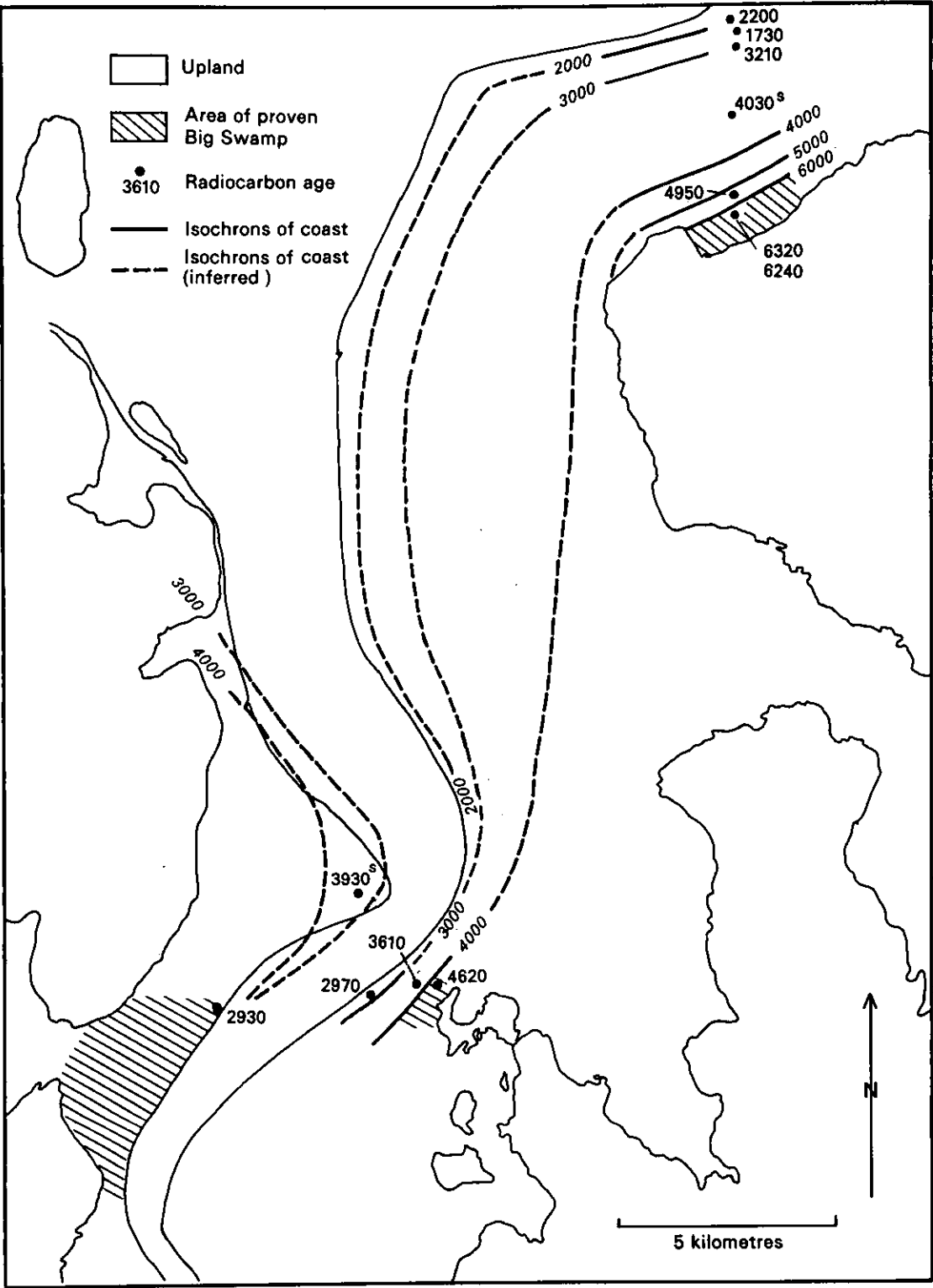


Figure 81: Reconstruction of isochrons of coastal progradation in the estuarine funnel of the South Alligator River

Point Stuart, and here progradation appears to have been continuous at a more rapid, fairly uniform rate (Clarke *et al.*, 1979), though this interpretation is based on few dated ridges. A depositional hiatus between about 3000 and 1700 years B.P. may be indicated there also if both radio-carbon ages of 3195 ± 85 and 1725 ± 80 years B.P. quoted from the same central chenier at Point Stuart are valid (Clarke *et al.*, 1979). We note however that chenier ridges were deposited at other sites in North Australia during this period (Rhodes, 1980; Hickey, 1981; Lees, 1985).

The period of slow progradation, on the coastal plain and estuarine funnel, after 3000 years B.P. coincides with development of the cusped river. These results suggest that sediment delivery to the coast changes according to the geomorphic condition of the tidal river. In particular they suggest that the sinuous river is a sediment conduit while the cusped river is a sediment trap, particularly for the sand-sized fraction provided that sediment input has been constant throughout.

Sediment budget figures show that the story is not so simple. Sediment input can be calculated either from floodwater sediment concentrations multiplied by flood discharges through the wet season (Chapter 2.4), or by estimating the total sediment deposited in the floodplain system over a given period of time such as the last 6000 years and converting this to average annual sedimentation rate (Chappell, 1984). It appears that there is a substantial discrepancy between results of these two methods, direct gauging giving much the lower estimate. It was shown in Chapter 2.4 that the average annual input appears to be 2×10^4 to 4×10^4 tonnes/year. Williams' (1976) figures from the Adelaide River are consistent with about 3×10^4 tonnes/year, after allowing for differences in catchment sizes (Chapter 2.4). We now make estimates based on sediment volume accumulated in the floodplain system over the last 6000 years.

The area of the deltaic/estuarine plain plus the coastal plain is about 1×10^9 square metres. The thickness of sediment deposited in the last 6000 years amounts to the average thickness of blacksoil clay of the Upper Floodplain plus the sediment which eliminated the big mangrove swamp. It is not known whether the big swamp 6000 years ago was dominantly *Rhizophora* or dominantly *Avicennia/Ceriops*, hence the thickness of sediment needed to eliminate the mangrove cannot be known with certainty. However, the following figures give a rough guide to the total:

- (a) close to the upstream river, about 4 m of sediment probably bury the 6000 B.P. surface,
- (b) near the coastal plain perhaps 2 m maximum have accumulated over the 6000 B.P. surface,
- (c) the coastal plain has prograded, involving about 6 m over the prior surface including the eastern part of the lower estuarine funnel, and
- (d) accumulation at the distal backwater swamps has been negligible.

Excluding (c), the mean thickness overall is about 2 m. Adding all together over the total area gives 5×10^5 tonnes/year, allowing for bulk density. This is over an order of magnitude greater than the input calculated from stream discharge and sediment concentrations.

The large discrepancy between observed sedimentation and calculated input is hard to explain. The long-term estimate cannot be reduced; in fact it is probably too low, being based on a mean thickness of 2 m accumulation over 6000 years. Our drilling and dating studies indicate more than 4 m accumulation of big swamp and floodplain sediments over the last 7000 years. Not all of this is clastic sediment, of course. In the coastal plain area, marine shell makes an average 12 per cent of the

sediment. The upper big swamp deposits range to about 10 per cent organic carbon, although the overlying oxidised muds and floodplain clays contain only 0 to 5 per cent. The backwater swamps at the plains' margin are reported by Hope *et al.* (1985) to contain up to 60 per cent fine sediment of organic origin, including phytoliths and diatoms. Hence, although the estimate of 5×10^5 tonnes per year could be reduced by allowing for these factors, it appears to be almost 50 per cent too low compared with an estimate based on 7000 years of deposition. Therefore we adopt 5×10^5 tonnes/year as a fair long-term estimate. The difference between this and the discharge-based estimate implies either a) that the discharge-based estimate is much too low, b) that there is another sediment source or c) that this long-term average rate no longer applies.

- (a) The discharge-based estimate may well be too low. Suspended sediment concentration varies widely through flood events, usually being much higher during rise than recession (e.g. Derbyshire *et al.*, 1979; Schumm, 1977). Our own measurements have been taken during flood recessions. Very large floods have not been sampled and may provide disproportionately more sediment. The duration of high sediment concentrations is short, however. In summary, the discrepancy may solely be due to errors in the discharge-based estimates but we cannot establish this.
- (b) An additional sediment source appears unlikely in the contemporary river. Studies elsewhere, such as the Severn estuary (Murray and Hawkins, 1976) suggest that marine mud contributes to estuarine wetland accretion, but whether this is the case in the South Alligator is debatable. While the tidal South Alligator River contains about 5 to 10×10^5 tonnes of suspended sediment (calculated from dry season concentrations), it is hard to see how much of this will reach the floodplains of the meandering and upstream segments, particularly for mud moving in from the sea. Even when overbank flooding occurs with highest tides augmented by flood or storm-surge effects, most of the suspended mud remains in the river. Mud of marine origin will diffuse upstream in the dry, but more slowly than the salts. Hence, any marine contribution should accrete in the funnel region. Figure 81 shows that accretion in this area has been negligible over the last 2000 years, and we therefore discount a marine source in the present day context. The possibility of mud accretion from a seaward direction at an early stage is discussed below.

While input of sediment from the sea appears unlikely, redistribution of sediment within the channel of the macrotidal river is possible. The asymmetry of tidal flows increases with distance from the mouth (Figure 17). Accentuated peak velocities on flood tides and the more gradual attenuation of flood tide velocities with depth at stations (Figure 18) imply an increasing competence to carry material upstream. This asymmetry will become more pronounced if sediment accumulates on the channel bed causing shoaling. Further sediment movement upstream is impeded by high wet season flood flows which carry sediment downstream until their transport efficiency is in turn decreased by impedance from increasing tidal discharge. The potential for sediment accumulation in the upstream parts of the deltaic-estuarine system is known from other systems, such as the Ord River (Wright *et al.*, 1973, 1975). If this internal redistribution of sediment, particularly of sand-sized material, takes place it may lead to shoaling in the cusped segment.

The final possibility is that sediment supply from the catchment is diminishing and that the long-term rate does not apply in recent times. Sediment accumulation rates for each of the big swamp, sinuous, and cusped river phases can be estimated on the same basis as the mean post-6000 B.P. rate. Results set out in Table 11 suggest that sedimentation has declined. The estimate of 2×10^5 m/year for the last 2000 years is almost certainly

too high, as it assumes that sedimentation over the plains has kept pace with rising tidal levels. The evidence of shell middens dating back to 4000 B.P., which show no sign of burial, is against this (Figure 74). Hence, the diminution of sedimentation rate by at least a factor of 3 since mid-Holocene times, suggested by Table 11, can account for some of the discrepancy between mean long term and short term rates. Independent support for this comes from the apparent accumulation of sand in the braided channel systems of the surrounding lowlands, where efficiency of transport appears to have declined (Duggan, 1985).

The contrast between high mud sedimentation rates in big swamp times and apparently low rates today is interesting. The big swamp period of high sedimentation coincides with culmination of sea-level rise, and also with the mid-Holocene interval when rainfall in north Queensland seems to have been higher (Figure 14a). Higher rainfall may have caused higher denudation and sediment input, although the direct-gauging data suggest that this figure would be too small even if rainfall was doubled. The other possibility is that muds were moved shorewards during the later stages of rising sea level, analogous to the process invoked by Thom and Roy (1985) to account for mid to upper Holocene sand accretion on the high energy coast of New South Wales. Rapid sedimentation during big swamp times would then be seen as the final result of this shoreward movement, with strong tidal currents distributing the mud throughout the estuary as sea level stabilised. This hypothesis can be investigated by sediment coring in van Diemen Gulf, which would have been the source area.

Table 11

Sedimentation during different phases of
South Alligator system

Phase	Interval	Area (m ²)	Thickness (m)	Volume (m ³)	Tonnes/year
Big Swamp to Plains	7000-4000 BP	9x10 ⁸	3*	2.7x10 ⁹	1.3x10 ⁶
Coastal Plain (sinuous phase)	4000-2000 BP	1.1x10 ⁸	6**	6.6x10 ⁸	5x10 ⁵
Cusplate phase floodplain	2000 BP- present	9x10 ⁸	0.3***	2.7x10 ⁸	2x10 ⁵
Notes	* Conservative estimate supported by widespread drilling. ** Minimum thickness required by progradation of coast and lower estuary. *** Estimated average for plains, given 1 m tide rise near Highway, no rise at mouth, negligible new sedimentation at rear of plains.				

Summarising this section, the discrepancy between discharge-based and long term estimates appears partly to be due to a long-term decline of mud sedimentation. However, the matter cannot be laid to rest until comprehensive sediment gauging data are obtained from the catchment. The most important change in the last few thousand years has been the shift from sinuous to the cusped river channel. Shoaling associated with channel widening has caused high tide levels to rise upstream, inducing upward growth of the plains at the expense of coastal progradation. The balance between plains aggradation and incursions of highest tidal waters is ecologically significant. If tide levels rise without concomitant sedimentation, tidal creeks will extend headwards. Long-term diminution of sediment supply will aggravate this while the tides continue to amplify. The figures in Table 11, together with the low discharge-based sediment estimates, strongly suggest that sediment input has diminished in relatively recent times. It clearly is important to establish the facts more exactly.

Chapter 7

Summary and Conclusions

- 7.1 Concluding review
- 7.2 Recommendations

7. CONCLUSIONS AND RECOMMENDATIONS

7.1 Concluding Review

The South Alligator River is one of many in northern Australia which are influenced by large tidal ranges and a strongly monsoonal climate. A smaller group, essentially in the 'top end' region where rainfall exceeds 1000 mm, resemble the South Alligator in having floodplains of sedge and grassland extending virtually from the river mouth to beyond the tidal limit, a distance exceeding 100 km in some cases. The Daly, Adelaide, Wildman, and West and East Alligator rivers are examples. Their elongate floodplains usually are flanked by low ridges of hills, and the floodplain sediments fill former valleys which graded to a lower sea level than that of today. All respond strongly to the monsoonal seasons, tending to run freshwater during floods which occur near the end of the wet season and then becoming progressively more saline as the dry season advances.

Despite these general similarities there are pronounced differences between rivers, reflecting their different catchment sizes, or, more precisely, the different sizes of their catchments relative to their tidal river and floodplain systems. The South Alligator is intermediate in these terms, with a catchment/floodplain area ratio of 9, compared with values around 4 to 5 for the Adelaide and West Alligator and about 29 for the Daly River. These differences correlate with various other features such as wet season flood discharge which is lowest in rivers with small catchments and highest in large-catchment rivers such as the Daly. Other correlations include the area of mangrove forest relative to floodplain, which is greatest in rivers with small catchment/floodplain ratios. The rivers also differ geomorphically, in that rivers with the lowest rates of channel migration have small catchment/floodplain area ratios, while the Daly with the highest channel activity has the highest ratio (Chapter 6, Table 9). There are related differences of channel form, shown by the contrast between the long sinuous segment of the Adelaide River and the cusped segment of the South Alligator (Chapter 6, Figure 79).

Formation of all these river and floodplain systems began around 8000 years ago when rising sea level invaded their prior valleys. Evolution of the plains and visible river systems began essentially when sea level stabilised around 6000 years ago. As there are differences of process rate and channel form, related to the catchment/floodplain area ratio, it is likely that some aspects of the present rivers represent different stages in an evolutionary sequence. Determination of this in the case of the South Alligator is a central part of our study, as it is through knowledge of processes and longer-term trends that present and future management is best informed.

Geomorphic mapping, stratigraphic drilling, and radiocarbon dating studies show that the system has evolved from an infilling estuary during the last stages of sea-level rise 7000 years B.P. (Figure 70), through the big swamp phase around 6000 years B.P. (Figure 71) into the sinuous river phase (Figure 77), and finally to the present cusped condition. Shoaling sediments prepared the basis for big mangrove swamp development as sea level was stabilising, and probably reflect the effectiveness of strong tidal flows in redistributing fine sediment at a relatively uniform level throughout the estuary. The rate of mud sedimentation appears to have been higher at this time than it has been since (Table 11), and it is unknown whether all of the sediment was derived from the catchment. Chapter 6.3 suggested that mud may have been reworked shorewards as the sea flooded the shallow basin of van Diemen Gulf, but further research is needed to investigate this.

The exact time at which the sinuous river began to adopt the form shown in Figure 77 is not known, but the course was probably sinuous at least in part when the big swamp was declining, 5500 years ago. The lower river may have had more than one entrance at this time, suggested by the paleochannel near Water Recorder Point (Figure 44). There appears to have been more than one channel in the upstream tidal segment (Figures 58, 60 and 64). Although multiple courses may have persisted until rather recently in the upstream area, the essential form of the sinuous river and the floodplain was established around 4000 years ago. Progradation of the coastal plain and eastern side of the estuarine funnel accelerated during the lifetime of the sinuous river phase, to about 2000 years ago (Figure 81).

Initiation of cusped channel development at the expense of the sinuous river has had significant effects on the modern system. The process involves channel widening and elimination of former sinuous curves, with the more sandy fraction of the eroded sediment lodging in mid-channel shoals. It is unclear whether this widening is initiated by shallowing of the sinuous river, which might occur through progressive accumulation of fluvial sediment, through upstream movement of estuarine sediment by the increasingly asymmetrical tidal flows, or through a combination of both processes, or whether it is caused by bank failure for some other reason. Whatever the cause, the consequence is that tidal levels rise in the upstream direction. Using tidal comparisons with the Adelaide River as well as stratigraphic data, we conclude that high spring levels have risen by one metre in the Arnhem Highway area since the sinuous river phase (Figure 80).

Progressive rise of high tide levels over the last 2000 years or so places the floodplains at risk of saltwater invasion, unless sedimentation keeps pace. The evidence of shell middens, ranging back to 4000 B.P. and showing little sign of burial, indicates that sedimentation has been negligible over much of the plains for several thousand years. It is reasonable to conclude that much of the observed tidal creek extensions (Figure 38), and dieback of paperbarks through salt invasion, is partly a consequence of this longer term rise of high tidal levels. Areas at risk are the Lower Floodplain paleocreek and paleochannel environments, which are identified on our 1:80,000 geomorphologic map sheets.

Evolution through the sinuous and cusped river phases has had other consequences. Mangrove forests on the insides of sinuous meander bends, similar to those of the present Adelaide River, existed during the sinuous phase (Figure 52). These have been eliminated in the cusped segment, leaving only sporadic stands of forest (Figures 10 and 11). Water chemistry also has changed. The present river reaches salinities close to sea water throughout its tidal length by the end of the dry season (Figure 20). During its sinuous phase it is expected to have experienced the lower tidal currents and greater lags more typical of the present Adelaide River. Under these conditions, upstream salinities are expected to have been substantially lower than those of today, at the end of the dry season.

7.2 Recommendations

- (1) The similarity of the course of development of tidal rivers with similar boundary conditions along the north Australian coast has been emphasised above. We see further comparative work on other rivers as an important strategy for establishing an evolutionary sequence through which such rivers develop. Such study is analogous to looking at one river system at a number of different points in time and more detailed study of other river systems should allow more accurate appraisal of threshold conditions and causes of change. Comparisons, using the same dynamic and morphostratigraphic techniques as used

here, should be made with other rivers. The East Alligator, which is morphostratigraphically most similar to the South Alligator, should be the first candidate. This will allow better prediction and explanation of changes in river morphodynamics and allow more effective management of ecosystems associated with those tidal rivers. Recognition of naturally-induced changes is an important element of such management.

- (2) Better understanding of changes in tidal range and patterns of sedimentation in the South Alligator tidal river and plains is necessary to refine our model of evolution and to increase its predictive value. In order to understand whether sediment supply has declined through time it will be necessary to monitor discharge and sediment flux at gauging stations in the lower catchment, particularly where river systems are discharging into the deltaic-estuarine plain. Further analysis of water level data already collected by Water Division (N.T. Department of Transport and Works) is warranted. We consider it desirable that discharge rating of the station at the road crossing over Nourlangie Creek (GS 820112) be attempted and suspended sediment and bedload be monitored at that site. Installation of a gauging station on the South Alligator River itself, as close to the deltaic-estuarine plain as possible, perhaps at the old Jim Jim to Darwin road crossing, should be considered. Installation and maintenance of such stations can be costly and the possibility of applying results of detailed discharge and sediment studies on the East Alligator River to the South Alligator should be examined as an alternative.
- (3) It is important to examine water levels within the tidal river, in more detail, particularly if salt water incursion continues as a problem. This is especially desirable in the cusplate and upstream segments of the river where internal morphological changes within the river system may have repercussions in terms of changes in tidal range or changes in mean tidal (water) surface slope. These two adjustments combine to determine the highest level tidal waters reach and consequently tidal penetration up creeks. It is highly desirable that a permanent tide gauge is installed at the mouth of the South Alligator River. This will not only be useful in calibrating our tidal model but will be important for recording and predicting tides for the whole of the eastern end of van Diemen Gulf. Temporary tide gauges within the river should be established in the cusplate segment and in the upstream segment to be read in conjunction with the gauge at the bridge and analysed along with records from other existing and discontinued Water Division gauges. Locations which might be logistically easiest are in order of priority in which they should be established a) at the junction of Nourlangie Creek and the river and b) at Kapalga Landing. A recorder still further upstream or on individual tidal creeks would be warranted if further salt water incursion is found to occur in that part of the plains. Portable water level recorders installed for several months at any one site should be used in the first instance.
- (4) The need for accurate knowledge of height of areas of the plain should be apparent from our work. All plains and tidal river recording stations should be levelled in to AHD. Further surveys of elevation of the plains and maintenance of regular re-surveys as advocated in the report of O'Neill (1983), and a denser network of control points and temporary benchmarks are justified. We believe that areas of greatest susceptibility to tidal creek extension and salt water incursion are in the paleochannels of the Lower Floodplain, and in the upstream segment locally in the paleocreek morphologic unit. These

areas can be identified from our 1:80,000 geomorphological map sheets, which can be used to rank wetland sites in terms of their susceptibility to inundation in view of the proximity of such channels. Concentration of levelling survey effort in and along such paleo-channels should further indicate areas prone to such inundation.

- (5) The question of the source area of mud, and to a lesser extent sand-sized material is unresolved. This is a question of broad regional significance and an avenue of scientific research which may ultimately explain changes in rates of sedimentation. The suggestion that mud might have been worked landward with mid-Holocene rise in sea level can be tested by a vibrocore programme in van Diemen Gulf, aimed to reveal truncation of the sedimentary sequence if such landward transport of mud has taken place.
- (6) It is desirable to monitor sediment accumulation within the tidal channel, particularly in the cusped segment and on the floodplain as well. Similar detailed analysis of the clastic versus organic constituents (e.g. phytoliths, diatoms) of the floodplain and back-water swamp sediments is a necessary adjunct to monitoring sedimentation away from the river. Our study indicates that shoaling in the channel, associated with bank failure and widening initiates changes of tidal levels and ranges and will have implications for other rivers. In view of the logistical difficulties of working in such areas, most sediment labelling techniques are impracticable. Further work, on microfossils which might act as natural markers of particular size fractions, such as foraminifera, diatoms or ostracods, should be undertaken. The surface, river bed and stratigraphic material collected during our work provides one avenue to begin this work. Our pilot work with foraminifera allows some differentiation of species assemblages but indicates widespread dispersal through the system (P. Wang, pers. comm.).
- (7) Aerial photographic coverage of shoals within the cusped segment of the river, taken vertically at low tide with good ground control, during both wet and dry seasons is desirable. This will be necessary over several years before any generalisations about the patterns of shoal development and migration can be made. It seems desirable to do this firstly as an aid to navigation within that part of the river, and secondly to predict patterns of sediment movement and redeposition. When this has been achieved it may prove fruitful to monitor cross-sectional depth variation at several cross-sections. This however will not be warranted if planimetric generalisations about shoals cannot be made. Because this work does not guarantee results, it may be assigned a lower priority than the foregoing areas.

In conclusion we reemphasise that the South Alligator River is one of many tidal rivers along the north coast of Australia that have experienced similar broad controls on river morphology and plains development during the Holocene. We feel that our detailed study of the evolution of the South Alligator River has implications for other river systems, particularly the East Alligator River. We also believe that further study of those other river systems will augment our understanding of the development of the South Alligator River system. Our study has highlighted the need for detailed morphologic and stratigraphic work in order to determine patterns of erosion and sedimentation over time in the Holocene, and has shown that present and future trends can be established from such research.

References

- Aharon, P. (1983). The δO^{18} and δC^{13} isotope enrichment in the Postglacial reef complex I from Papua New Guinea and its interpretation. In Proceedings of 1st CLIMANZ conference, Feb. 1981, Dept. Bio & Geo., RSPacS, ANU (Canberra), 85.
- Aldrick, J.M. (1976). Soils of the Alligator Rivers area. pp71-88 in Story, R. et al. Lands of the Alligator Rivers area, Northern Territory. CSIRO Land Research Series 38.
- Anon. (1961). Climatology survey. Region 1: Darwin-Katherine, Northern Territory. (Bur. Meteorol. Aust.: Melbourne.)
- Ash, J. (1983). Rainfall patterns in northeastern Queensland 7+2KA. In Proceedings of 1st CLIMANZ conference, Feb. 1981, Dept. Bio & Geo., RSPacS, ANU (Canberra), 90.
- Bird, E.C.F. (1985). Coastline changes: a global review. Chichester: Wiley.
- Burgman, M.A., and Thompson, E.J., (1982). Cluster analysis, ordination and dominance-structural classification applied to diverse tropical vegetation at Jabiluka, Northern Territory. Aust. J. Ecol. 7:375-387.
- Campbell, B.M. and Woods, J.T. (1967). Quaternary crustaceans from Northern Australia in the collections of the Bureau of Mineral Resources, Canberra. B.M.R. Bull. Paleontological Papers 108:41-42.
- Chaloupka, G. (1983). Kakadu Rock Art: its cultural, historic and pre-historic significance. pp.1-33 in Gillespie, D.(ed.) The Rock Art Sites of Kakadu National Park - some preliminary research findings for their conservation and management. ANPWS Spec. Pub. 10.
- Chaloupka, G. (1985). Chronological sequence of Arnhem Land Plateau rock art pp.269-280 in Jones, R. (ed.) Archaeological Research in Kakadu National Park. ANPWS Spec. Pub. 13.
- Chappell, J. (1982). Evidence for smoothly falling sea-levels relative to north Queensland, Australia, during the past 6000 years. Nature 302:406-408.
- Chappell, J. (1984). Denudation and Sedimentation in some Northern Territory river basins. Proc. 1st Australian Erosion Conf., Newcastle University 1984, v2.
- Chappell, J. (in prep.). Geomorphology of the Daly River.
- Chappell, J., Rhodes, E.G., Thom, B.G. and Wallensky, E. (1982). Hydro-isostasy and the sea level isobase of 5500 B.P. in North Queensland, Australia. Mar. Geol. 49:81-90.
- Chappell, J., Chivas, A., Wallensky, E., Polach, H.A. and Aharon, P. (1983). Holocene palaeo-environmental changes, central to north Great Barrier Reef inner zone. BMR J. Aust. Geol. Geophys. 8:223-235.
- Chappell, J. and Grindrod, J. (1984). Chenier plain formation in Northern Australia. pp197-231 in Thom, B.G. (ed.) Coastal Geomorphology in Australia, Academic Press.
- Chappell, J. and Grindrod, J. (1985). Pollen analysis: key to past mangrove communities and successional changes in North Australian coastal environments pp225-236 in Bardsley, K., Davie, J.D.S. and Woodroffe, C.D. (eds) Coasts and Tidal Wetlands of the Australian Monsoon Region. NARU Monograph.

- Chappell, J. and Bardsley, K. (1985). Hydrology of the Lower Daly River, Northern Territory. NARU Monograph.
- Chappell, J. and Ward, P. (1985). Seasonal tidal and freshwater chemistry of the South Alligator and Daly Rivers. pp.97-108 in Bardsley, K.N., Davie, J.D.S. and Woodroffe, C.D. (eds) Coasts and Tidal Wetlands of the Australian Monsoon Region, NARU Monograph.
- Chappell, J. and Woodroffe, C.D. (1985). Morphodynamics of Northern Territory Tidal Rivers and Floodplains pp.85-96 in Bardsley, K., Davie, J.D.S. and Woodroffe, C.D. (eds) Coasts and Tidal Wetlands of the Australian Monsoon Region. NARU Monograph.
- Christian, C.S. and Aldrick, J.M. (1977). Alligator Rivers Study: a review report of the Alligator Rivers Region environmental fact-finding study. Aust. Govt. Publ. Serv., Canberra 174pp.
- Christian, C.S. and Stewart, G.A. (1953). General report on survey of Katherine-Darwin region 1946. CSIRO Land Research Series 1.
- Clark, R.M. (1975). A calibration curve for radiocarbon dates. Antiquity 69:251-266.
- Clarke, M.F., Wasson, R.J. and Williams, M.A.J. (1979). Point Stuart chenier and Holocene sea levels in Northern Australia. Search 10:90-93.
- Climanz (1983). Proceedings of 1st CLIMANZ conference, Feb. 1981. Dept. Bio and Geo., RSPacS, ANU (Canberra).
- Coleman, J.M. and Wright, L.D. (1978). Sedimentation in an arid macrotidal alluvial river system: Ord River, Western Australia. J. Geol. 86:621-642.
- Cook, P.J. (1973). Supratidal environment and geochemistry of some recent dolomite concretions, Broad Sound, Queensland, Australia. J. Sedim. Petrol. 43:998-1011.
- Cook, P.J. and Mayo, W. (1977). Sedimentology and Holocene history of a tropical estuary (Broad Sound, Queensland). BMR Bull. 170. 206pp.
- Davie, J.D.S. (1985). The mangrove vegetation of the South Alligator River, Northern Territory pp.133-152 in Bardsley, K., Davie, J.D.S. and Woodroffe, C.D. (eds) Coasts and Tidal Wetlands of the Australian Monsoon Region. NARU Monograph.
- Derbyshire, E., Gregory, K.J. and Hails, J.R. (1979). Geomorphological Processes. Studies in Physical Geography, London. Butterworths 312pp.
- Duggan, K. (1985). Erosion and sediment transport in the lowlands of the Alligator Rivers region, Northern Territory, pp.53-61 in Bardsley, K., Davie, J.D.S. and Woodroffe, C.D. (eds) Coasts and Tidal Wetlands of the Australian Monsoon Region. NARU Monograph.
- Dunn, P.R. (1962). Alligator River, Northern Territory. 1:250000 Geological series. Explan. Notes. Bur. Miner. Resour. Geol. Geophys. Aust.
- Etheridge, R. and McCulloch, A.R. (1916). Sub-fossil crustaceans from the coasts of Australia. Rec. Aust. Mus. 11:1-14.
- Fitzpatrick, E.A. (1963). Estimates of pan evaporation from mean maximum temperature and vapor pressure. J. Appl. Meteorol. 2:780-792.

- Fogarty, P.J. (1982). A preliminary survey of environmental damage associated with activity of feral buffalo. Darwin: Feral Animals Committee, Conservation Commission of the Northern Territory, Technical Report, 88pp.
- Folk, R.L. (1980). Petrology of Sedimentary Rocks. Austin: Hemphill, 182pp.
- Frye, J.C. and Willman, H.B. (1960). Classification of the Wisconsin stage in the Lake Michigan glacial lobe. Illinois State Geol. Surv., circular 285:16pp.
- Galloway, R.W. (1976). Geomorphology of the Alligator Rivers area. pp52-70 in Story, R. et al. Lands of the Alligator Rivers area. CSIRO Land Research Series 38.
- Galloway, R.W., Aldrick, J.M., Williams, M.A.J. and Story, R. (1976). Land systems of the Alligator Rivers area. ppl5-34 in Story, R. et al. Lands of the Alligator Rivers area. CSIRO Land Research Series 38.
- Giglioli, M.E.C. and Thornton, I. (1965). The mangrove swamps of Keneba, Lower Gambia River Basin I Descriptive notes on the climate, the mangrove swamps and the physical composition of their soils. J. appl. Ecol. 2:81-103.
- Gillespie, R. and Polach, H.A. (1979). The suitability of marine shells for radiocarbon dating of Australian prehistory, pages 404-421 in Berger, R. and Suess, H. (eds.). Proceedings Ninth international conference on Radiocarbon. University of California Press.
- Grindrod, J. (1985). The palynology of mangroves on a prograded shore, Princess Charlotte Bay, North Queensland, Australia. J. Biogeogr. 12:323-348.
- Grindrod, J. and Rhodes, E.G. (1984). Holocene sea level history of a tropical estuary: Missionary Bay, North Queensland. ppl51-178 in Thom, B.G. (ed.) Coastal Geomorphology in Australia, Academic Press.
- Gupta, S.K. and Polach, H.A. (1985). Radiocarbon dating practices at ANU. Radiocarbon Dating Laboratory, Research School of Pacific Studies, ANU.
- Hickey, S.H. (1981). Preliminary investigation of stranded beach ridges, Shoal Bay, Northern Territory: a small chenier plain? N.T. Geol. Surv. Tech. Rept. GS 81/1.
- Hooper, A.D.L. (1969). Soils of the Adelaide-Alligator area. pp95-113 in Story, R. et al., Lands of the Adelaide-Alligator area, Northern Territory. CSIRO Land Research Series 25.
- Hope, G. (1983). Montane Papua New Guinea 9000-5000 B.P. In Proceedings of 1st CLIMANZ conference, Feb., 1981, Dept. Bio & Geo, RSPacS, ANU (Canberra), 97.
- Hope, G., Hughes, P.J. and Russell-Smith, J. (1985). Geomorphological fieldwork and the evolution of the landscape of Kakadu National Park pp229-240 in Jones, R. (ed.) Archaeological Research in Kakadu National Park. ANPWS Spec. Publ. 13.
- Hopley, D. and Harvey, N. (1979). Regional variations in storm surge characteristics around the Australian coast: a preliminary investigation. In Heathcote, R.L. and Thom, B.G. (eds) Natural Hazards in Australia, Aust. Acad. Sci., Canberra: 164-185.

- Hopley, D. and Thom, B.G. (1983). Australian sea levels in the last 15,000 years: an introductory review. pp3-26 in Hopley, D. (ed.) Australian sea levels in the last 15,000 years. Geog. Dept. James Cook Univ. Occas. Pap. 3.
- Ippen, A.T. (1966). Estuary and Coastline Hydrodynamics, McGraw-Hill.
- Ippen, A.T. and Harleman, D.R.F. (1966). Tidal dynamics in estuaries pp493-545 in Ippen, A.T. (ed.) Estuary and Coastline Hydrodynamics, McGraw-Hill.
- Jennings, J.N. (1975). Desert dunes and estuarine fill in the Fitzroy estuary, north-western Australia. Catena 2:215-262.
- Jongsma, D. (1970). Eustatic sea level changes in the Arafura Sea. Nature 228:150-151.
- Kamminga, J. and Allen, H. (1973). Report of the archaeology survey. Alligator Rivers Environmental Fact-finding study, Canberra.
- Kershaw, A.P. (1983). The vegetation record of northeastern Australia, 7+2KA. In Proceedings of 1st CLIMANZ conference, Feb., 1981, Dept. Bio & Geo, RSPacS, ANU (Canberra), 100.
- Komar, P.D. (1976). Beach processes and sedimentation. New Jersey, Prentice-Hall. 429pp.
- Komar, P.D. and Gaughan, M.K. (1973). Airy wave theory and breaker height prediction. Proc. 13th Conf. Coast Eng., 405-418.
- Lees, B.G. (1985). Geomorphology and development of the Victoria Delta in Bardsley, K., Davie, J.D.S. and Woodroffe, C.D. (eds) Coasts and Tidal Wetlands of the Australian Monsoon Region. NARU Monograph, pp31-42.
- McAlpine, J.R. (1969). Climate of the Adelaide-Alligator area pp.49-55 in Story et al. Lands of the Adelaide-Alligator area, Northern Territory. CSIRO Land Research Series 25.
- McAlpine, J.R. (1976). Climate and Water balance pp35-49 in Story et al. Lands of the Alligator Rivers area, Northern Territory, CSIRO Land Research Series 38.
- Meehan, B., Brockwell, S., Allen, J. and Jones, R. (1985). The Wetland sites. pp.103-153 in Jones, R. (ed.) Archaeological Research in Kakadu National Park. ANPWS Spec. Pub. 13.
- Messel, H., Wells, A.G. and Green, W.J. (1979). The Alligator region river systems. Monograph 4. Surveys of tidal river systems in the Northern Territory of Australia and their crocodile populations. Pergamon Press.
- Messel, H., Green, W.J., Vorlicek, G.C. and Wells, A.G. (1982). Work maps of tidal waterways in Northern Australia. Monograph 15. Surveys of tidal waterways in Northern Australia. Pergamon Press.
- Murray, J.W. and Hawkins, A.B. (1976). Sediment transport in the Severn Estuary during the past 8000-9000 years. Jl. Geol. Soc. Land. 132:385-398.
- Needham, R.S. (1984). Alligator River, Northern Territory (second edition) 1:250,000 Geological Series - Explanatory notes, Canberra: AGPS, 41pp.
- Needham, R.S., Wilkes, P.G., Smart, P.G. and Watchman, A.L. (1973). Alligator Rivers region environmental fact-finding study geological

- and geophysical reports. Rec. Bur. Miner. Resour. Geol. Geophys. Aust. 1973/208.
- Ogata, A. and Banks, R.B. (1961). A solution of the differential equation of longitudinal dispersion in porous media. U.S. Geol. Surv. Prof. Pap. 411-A: A1-A7.
- O'Neill, G.C. (1983). An investigation of recent geomorphological change on sections of the South Alligator River floodplain, Kakadu National Park. Unpub. report to ANPWS.
- Power, N.A., Pidsley, D.G. and Reinhard, R.J. (1983). Lower Daly River Basin investigation of flood protection and flood forecasting. Unpubl. rept. Investigations Branch, Water Division, N.T. Dept. Transport and Works.
- Rhodes, E.G. (1980). Modes of coastal progradation, Gulf of Carpentaria. PhD thesis, Canberra: ANU, 357pp.
- Rhodes, E.G. (1982). Depositional model for a chenier plain, Gulf of Carpentaria, Australia. Sedimentology 29:201-221.
- Rice, B., and Westoby, M. (1985). Structure of local floristic variation and how well it correlates with existing classification schemes: vegetation at Koongarra, N.T. Australia. Proc. Ecol. Soc. Aust. 13:129-137.
- Roy, P.S., Thom, B.G. and Wright, L.D. (1980). Holocene sequences on an embayed high-energy coast: an evolutionary model Sedim. Geol. 26:1-19.
- Russell-Smith, J. (1985a). Studies in the jungle: people, fire and monsoon forest pp241-267 in Jones, R. (ed.) Archaeological Research in Kakadu National Park. ANPWS Spec. Publ. 13.
- Russell-Smith, J. (1985b). A record of change: studies of Holocene vegetation history in the South Alligator River region, Northern Territory. Proc. Ecol. Soc. Aust. 13:191-202.
- Sandstrom, M. (1985). Phosphorous geochemistry in the South Alligator River System ppl09-117 in Bardsley, K., Davie, J.D.S. and Woodroffe, C.D. (eds) Coasts and Tidal Wetlands of the Australian Monsoon Region. NARU Monograph.
- Schrire, C. (1982). The Alligator Rivers - prehistory and ecology in western Arnhem Land. ANU, Department of Prehistory.
- Schumm, S.A. (1969). River metamorphosis. J. Hyd. Div. Am. Soc. Civil Eng. 95:255-273.
- Schumm, S.A. (1977). The Fluvial system. New York: Wiley.
- Semeniuk, V. (1980a). Mangrove zonation along an eroding coastline in King Sound, Northwestern Australia. J. Ecol. 68:789-812.
- Semeniuk, V. (1980b). Quaternary stratigraphy of the tidal flats, King Sound, Western Australia. J. R. Soc. West. Aust. 63:65-78.
- Semeniuk, V. (1981). Long-term erosion of the tidal flats, King Sound, northwestern Australia. Mar. Geol. 43:21-48.
- Semeniuk, V. (1982). Geomorphology and Holocene history of the tidal flats, King Sound, north-western Australia. J. R. Soc. West. Aust. 65:47-68.

- Southern, R.L. (1966). A review of weather disturbances controlling the distribution of rainfall in the Darwin-Katherine region, N.T. Bur. Meteorol. Aust. Work. Pap. 65/3203.
- Stocker, G.C. (1970). The effects of water buffalo on paperbark forests in the Northern Territory. Aust. For. Res. 5:29-34.
- Story, R. (1969). Vegetation of the Adelaide-Alligator Area. pp.114-130 in Story, R. et al. Lands of the Adelaide-Alligator area, Northern Territory. CSIRO Land Research Series 25.
- Story, R. (1976). Vegetation of the Alligator Rivers area. pp.89-111 in Story, R. et al. Lands of the Alligator Rivers area, Northern Territory. CSIRO Land Research Series 38.
- Story, R., Williams, M.A.J., Hooper, A.D.L., O'Ferrall, R.E. and McAlpine, J.R. (1969). Lands of the Adelaide-Alligator area, Northern Territory. CSIRO Land Research Series 25.
- Story, R., Galloway, R.W., McAlpine, J.R., Aldrick, J.M. and Williams, M.A.J. (1976). Lands of the Alligator Rivers area, Northern Territory. CSIRO Land Research Series, 38.
- Taylor, J.A., and Dunlop, C.R. (1985). Plant communities of the wet-dry tropics of Australia: the Alligator Rivers region, Northern Territory. Proc. Ecol. Soc. Aust 13:83-127.
- Taylor, J.A. and Tulloch, D., (1985). Rainfall in the wet-dry tropics: extreme events at Darwin and similarities between years during the period 1870 - 1983 inclusive. Aust. J. Ecol. 10:281-295.
- Thom, B.G. (1967). Mangrove ecology and deltaic geomorphology, Tabasco, Mexico. J. Ecol. 55:301-343.
- Thom, B.G. (1974). Coastal erosion in eastern Australia. Search 5:198-209.
- Thom, B.G. and Chappell, J. (1975). Holocene sea levels relative to Australia. Search 6:90-93.
- Thom, B.G., Wright, L.D. and Coleman, J.M. (1975). Mangrove ecology and deltaic-estuarine geomorphology, Cambridge Gulf-Ord River, Western Australia. J. Ecol. 63:203-222.
- Thom, B.G. and Roy, P.S. (1983). Sea-level change in New South Wales over the past 15,000 years, pp64-84 in Hopley, D. (ed.) Australian sea levels in the last 15,000 years, a review: Dept Geography, James Cook University, Monograph Series, Occasional Paper 3.
- Thom, B.G. and Roy, P.S. (1985). Relative sea levels and coastal sedimentation in southeast Australia in the Holocene. J. Sedim. Petrol. 55:257-264.
- Tulloch, D.G. (1982). Buffalo in the northern swamp lands. N.T. Dept. Primary Production, Division of Agriculture and Stock. Technical Bulletin no. 62:60-66.
- van Andel, T.H., Heath, G.R., Moore, T.C. and McGeary, D.F.R. (1967). Late Quaternary history, climate and oceanography of the Timor Sea, Northwestern Australia. Am. J. Sci. 265:737-758.
- Webster, P.J. and Stretten, N.A. (1978). Late Quaternary Ice Age climates of tropical Australasia: interpretations and reconstructions. Quat. Res. 10:279-309.

- Wells, A.G. (1984). Mangrove vegetation in Northern Australia. Unpub. PhD thesis, University of Sydney, 236pp.
- Whittingham, H.E. (1964). Extreme wind gusts in Australia. Commonwealth Bureau of Meteorology, Bull 46.
- Williams, A.R., (1979). Vegetation and stream pattern as indicators of water movement on the Magela floodplain, Northern Territory. Aust J. Ecol. 4:239-247.
- Williams, M.A.J. (1969a). Geology of the Adelaide-Alligator area. pp56-70 in Story, R. et al. Lands of the Adelaide-Alligator area, Northern Territory. CSIRO Land Research Series 25.
- Williams, M.A.J. (1969b). Geomorphology of the Adelaide-Alligator area. pp71-94 in Story, R. et al. Lands of the Adelaide-Alligator area, Northern Territory. CSIRO Land Research Series 25.
- Williams, M.A.J. (1976). Erosion in the Alligator Rivers area. pp.112-125 in Story, R. et. al. Lands of the Alligator Rivers area, Northern Territory. CSIRO Land Research Series 38.
- Williams, M.A.J., Hooper, A.D.L. and Story, R. (1969). Land systems of the Adelaide-Alligator area. pp24-48 in Story, R., et al. Lands of the Adelaide-Alligator area, Northern Territory, CSIRO Land Research Series 25.
- Woodroffe, C.D., Chappell, J.M.A., Thom, B.G. and Wallensky, E. (1985a). Geomorphology of the South Alligator Tidal River and Plains, Northern Territory pp3-16 in Bardsley, K., Davie, J.D.S. and Woodroffe, C.D. (eds) Coasts and Tidal Wetlands of the Australian Monsoon Region. NARU Monograph.
- Woodroffe, C.D., Chappell, J.M.A., Thom, B.G. and Wallensky, E. (1985b). Stratigraphy of the South Alligator Tidal River and Plains, Northern Territory pp17-30 in Bardsley, K., Davie, J.D.S. and Woodroffe, C.D. (eds) Coasts and Tidal Wetlands of the Australian Monsoon Region. NARU Monograph.
- Woodroffe, C.D., Thom, B.G. and Chappell J. (1985c). Development of wide-spread mangrove swamps in mid-Holocene times in northern Australia. Nature 317:711-713.
- Wright, L.D., Coleman, J.M. and Thom, B.G. (1972). Emerged tidal flats in the Ord River estuary, Western Australia. Search 3:339-341.
- Wright, L.D., Coleman, J.M. and Thom, B.G. (1973). Processes of channel development in a high-tide range environment: Cambridge Gulf-Ord River Delta, Western Australia. J. Geol. 81:15-41.
- Wright, L.D., Coleman, J.M. and Thom, B.G. (1975). Sediment transport and deposition in a macrotidal river channel: Ord River, Western Australia, in Cronin, L.E. (ed.) Estuarine Research, vol. 11. Geology and engineering. London: Academic Press, pp309-321.
- Wright, L.D. and Thom, B.G. (1977). Coastal depositional landforms: a Morphodynamic approach. Prog. Phys. Geog. 1:412-459.
- Wright, L.D., Chappell, J., Thom, B.G., Bradshaw, M.P. and Cowell, P (1979). Morphodynamics of reflective and dissipative beach and inshore systems: Southeastern Australia. Mar. Geol. 32:105-140.
- Wu, J. (1975). Wind induced currents J. Fluid Mechanics 68:49-70.

Appendices

- A1 Estimation of South Alligator floodwater discharges
- A2 Tide modelling
- A3 Seasonal salinity modelling
- A4 Particle size analysis of selected samples
- A5 Salt concentration (KCl) equivalents, parts per thousand (sediment dry weight)
- A6 Pollen analysis of mangrove history
- A7 Carbonate content of selected samples as percentage of sediment dry weight
- A8 Radiocarbon dates
- A9 Details of depth, elevation with respect to AHD and age of samples used for sea-level plot (Figure 69)

APPENDIX A1: ESTIMATION OF SOUTH ALLIGATOR FLOODWATER DISCHARGES

Floodwater discharges cannot be determined directly for the South Alligator River because there are too few rated gauging stations in the catchment and those which are operating gauge only a small fraction of the total catchment area. Hence, discharge/recurrence interval relationships are estimated by using data from the well-gauged Daly River with appropriate scaling to allow for differences of catchment sizes and geometries. The flood peak discharge/recurrence interval relationship for the Daly is shown by Chappell and Bardsley as a standard log-Pearson plot of a 28 year (annual series) record supplied by the Water Division of the N.T. Department of Transport and Works. Data are normalised to the rated gauge at Mt Nancar, about 8 km upstream of the tide limit (Chappell and Bardsley 1985: Figure 3.3).

The South Alligator and Daly catchments have similar rainfall regimes (Figure 5a) although that of the South Alligator is higher (about 1300 mm average summer rainfall, see Figure 5b, cf. about 1000 mm average for the Daly, see Figure 6.1 of Chappell and Bardsley 1985). Both catchments have similar total relief although the Daly has a smaller percentage of catchment in the Arnhem Plateau. The Daly is somewhat more elongate than the South Alligator catchment, which is roughly square (cf. Figure 2, and Figure 6.1 of Chappell and Bardsley).

The scaling factor for reducing the Daly discharge data to the South Alligator is developed as follows:

- (i) If runoff coefficients and flood concentration times are the same between two catchments, then

$$Q_2 = Q_1 \frac{A_2 P_2}{A_1 P_1} \quad (A1.1)$$

where Q_1 , Q_2 are flood discharges of catchments 1 and 2, A_1 and A_2 are their respective areas, and P_1 and P_2 are their respective rainfalls.

- (ii) When flood concentration times differ, the RHS of (A1.1) is multiplied by C_1/C_2 where these are the respective coefficients related to concentration time. Relationships between C and catchment shape have been investigated in many studies, and a common result is that C is inversely proportional to \sqrt{L} where L is mean length of a simple symmetrical catchment. Alternatively, C is directly proportional to the recession coefficient of the runoff-dominated part of the recession hydrograph. Therefore, the estimating equation used here is:

$$Q_2 = Q_1 A_2 P_2 C_1 / A_1 P_1 C_2, \quad (A1.2)$$

where C_1 and C_2 are derived either from L values or recession data.

The mean length of the Daly catchment is 2.5 X that of the South Alligator, indicating that C (South Alligator) is about 1.6 X C (Daly). Flood recession data are not available for the South Alligator, but comparison with the Daly can be made using the tide gauge at the Arnhem Highway bridge. Using the LWL records from this gauge over the period of wet season flood recessions as a guide, recession times are very similar to those for the Daly described by Chappell and Bardsley (1985). Hence C_1/C_2 is taken as ranging from 1.0 to 1.6. Using these values gives the upper and lower limit estimates of Q_2 shown in Figure 7 (Chapter 1), where Q_1 for each given recurrence interval is read directly from Chappell and Bardsley (1985: Figure 3.3), $A_1 = 48,000 \text{ km}^2$, $A_2 = 9,000 \text{ km}^2$, $P_1 = 1,000$, $P_2 = 1,300$.

The river is modelled as exponentially-diminishing in width, described by

$$b = b_0 \exp(-mx) \quad (A2.1)$$

where b is width at distance x from the mouth, and b_0 is width at the mouth. The general solution of the linearised equations of motion and continuity is

$$\eta = a_0 \exp(mx/2) \cdot \exp(-\mu x) \cdot \cos(\sigma t - kx) \quad (A2.2)$$

where η is tide height relative to M.W.L. at distance x from the mouth, a_0 is tide amplitude at the mouth (i.e. maximum tide height above M.W.L.), m is given in eq. (A2.1), σ is tidal frequency in radians/second, and μ and k are friction-related parameters modifying η and tidal delay, respectively.

If the estuary diminishes in width at more than a critical rate, reflection of the propagating tide should be taken into account. The criterion is

$$mL \ll 1 \quad (A2.3)$$

for reflection not to be significant, where $L=CT$ and C is tidal celerity, T is tidal period (Ippen and Harleman, 1966). This test is applied as follows. For the South Alligator as a whole, $m = 4.4 \times 10^{-5}$. C is evaluated from Table A2, between the mouth and 76 km, as 9.3 m/s (RV data) to 10.5 m/s (C/W data). With $T = 12.5$ hours, $mL = 20$, i.e. $\gg 1$, therefore reflection is significant. Net tidal height $\eta(x,t)$ is the sum of $\eta(\text{primary}) + \eta(\text{reflected})$, where $\eta(\text{reflected})$ is described by eq. (A2.2) with appropriate sign changes for motion in the opposite direction. The explicit solution for μ and k as separate variables, given by Ippen and Harleman (1966), was programmed and the tidal range and delay data from Table A2 used as input. Treating the river as a whole, the resulting values are

$$\mu = 4.5 \times 10^{-5}, \quad k = 1.4 \times 10^{-5}$$

The simplest estimate of discharge is given by the tidal prism method,

$$Q = \frac{4}{T} \int_{x_1}^X b \eta_m dx \quad (A2.4)$$

where Q is mean discharge at point x_1 , X is the tidal limit, T is tidal period, $b(x)$ is described by eq. (A2.1), and maximum tide heights η_m along the river from x_1 to X are provided by observations. This method assumes that the slope of the water surface due to tidal lag has an insignificant effect on the total volume which passes the given point x_1 . The simplest case is where η_m is constant; substituting (A2.1) in (A2.4) gives

$$Q = \frac{4b_0}{mT} (\exp(-mx_1) - \exp(-mX))$$

The tapering coefficient m is not constant along the South Alligator, but changes at each segment (funnel, sinuous, etc.). Tidal range ($2\eta_m$) changes also (Table A2). Discharges calculated using eq. (A2.4) take these facts into account, and are shown as Discharge, model 1, in Table A2.

The tidal prism method becomes increasingly inaccurate as the tidal lag between mouth and tide limit becomes greater. Discharge is given by

$$Q = b \int \frac{\partial \eta}{\partial t} \cdot dx \quad (A2.5)$$

Substituting (A2.1) and (A2.2) in (A2.5) gives

$$Q = \frac{\sigma b_0 a_0}{2} \int_{x_1}^X \exp((m/2 - \mu)x) \cdot \cos(\sigma t - kx) dx$$

The solutions for the comparable equation including the reflection terms was programmed and values of Q computed, with μ and k values given above. Results are shown as Discharge, model 2, in Table A2. In this case a single value of $m = 4.4 \times 10^{-5}$ was used throughout.

Results of both tide models compare closely with observed discharges at 25 and 63 km. Both underestimate the discharge at 47 km, model 2 being more in error than model 1. The error is attributed to the disproportionately greater width of the cusped segment, which provides a tidal basin effect upstream of 47 km thereby enhancing Q at this section. Model 2 is more in error than model 1 because a single value of m is used in model 2, while model 1 takes the changes of m into account.

Non-linear effects are significant in the South Alligator tides, as shown by the upstream slope of MWL (Figure 28, Chapter 3), and also by non-sinusoidal velocity and tidal stage curves (Figure 17, Chapter 2). Detailed analysis is part of the ongoing PhD research of Mr R. Vertessy, Department of Biogeography and Geomorphology, R.S.Pac.S., ANU.

APPENDIX A3: SEASONAL SALINITY MODELLING

During wet-season floods the South Alligator tidal river is largely filled with fresh water, with a salt-wedge mixing zone in the lower estuary. The position of the salt wedge limit depends on the freshwater flood discharge. An example is shown in Figure 22, Chapter 2. As flood-waters recede, seawater mixes progressively upstream. The salt wedge vanishes and waters are well mixed vertically by the turbulent flow caused by tidal currents exceeding 1m/second. As the dry season advances the salinity increases steadily in the upstream direction. The mean flood/ebb two-way movement of tidewater is 10 to 15 km throughout most of the river up to 75 km, i.e. much less than the tidal length. Progressive salinity increase is due to turbulent eddy diffusion. Salinity profiles have been monitored throughout 1984 to 1986, providing an accurate record of the phenomenon. In order to predict the process for this and other rivers in the area, a model has been programmed.

The one-dimensional diffusion equation is

$$\frac{\partial s}{\partial t} + (u-U) \frac{\partial s}{\partial x} = \frac{\partial}{\partial x} \left(D \frac{\partial s}{\partial x} \right) \quad (\text{A3.1})$$

where s is salinity at x , u is instantaneous tidal velocity and U is velocity of net discharge (i.e. freshwater out or mean seawater in), and D is the coefficient of turbulent diffusion. Vertical variation of s is not considered, and eq (A3.1) therefore applies only where mixing is high and stratification is low. These conditions are met throughout the South Alligator once freshwater floods recede. Eq. (A3.1) can be simplified by considering average conditions for a given tide cycle, wherein the time average of u is zero. Ogata and Banks (1961) have solved (A3.1) for constant D and constant U :

$$s = \frac{S_0}{2} e^{Ux/D} \operatorname{erfc}\left(\frac{x+Ut}{2\sqrt{Dt}}\right) + \frac{S_0}{2} \operatorname{erfc}\left(\frac{x-Ut}{2\sqrt{Dt}}\right) \quad (\text{A3.2})$$

where S_0 is seawater salinity. Eq. (A3.2) gives profiles of $s(x,t)$, and was programmed using

$$\operatorname{erfc}(G) = 1 - \frac{2e}{\sqrt{\pi}} e^{-\frac{G^2}{2}} \sum_{n=0}^{\infty} \frac{2^n}{1.3 \dots (2n+1)} G^{2n+1},$$

with truncation at the 0.001 convergence level.

Values for U and D were estimated as follows.

- (i) U is estimated from mean discharge through the river mouth in the dry season. Dry season base flow from all freshwater sources is taken as 5 cumecs maximum, on the basis that the Daly River with a catchment 5X bigger has mean baseflow around 10 to 15 cumecs (Chappell and Bardsley 1985). Opposing the base flow, seawater effectively is flowing into the South Alligator through the dry season as the river is virtually seawater throughout by November. The volume of water in the river at mid-tide is $5.2 \times 10^8 \text{ m}^3$. From the end of the wet to end of the dry is about 240 days, and the inflow reduces to 25 cumecs. This substantially exceeds base flow, and U is therefore in the upstream direction with a velocity around 0.001 m/s at the mouth.

(ii) D is estimated using the steady-state equation

$$D(x) = -U / \left(\frac{d}{dx} (\ln \bar{s}) \right) \quad (A3.3)$$

where \bar{s} is salinity at x averaged through a tide cycle. The river is not in steady state, as we have explained, and an average value of D was calculated using observed salinity profiles to give values of $d/dx(\ln \bar{s})$. The average came to 200m^{-1} .

The model was run using these values of U and D, which were then varied to give a best-fit to the observations. Figure 20 in Chapter 2 shows the results, which are very satisfactory and demonstrate the utility of eq. (A3.2) for modelling other turbulent tidal rivers with a seasonal climate. Best-fit parameter values were $U = 0.007 \text{ m/s}$, $D = 250 \text{ m}^{-1}$. This U-value is significantly higher than the estimate in (i) above which is based on net inflow estimated at the mouth. It is likely that U varies upstream, probably being greatest around 47 km where the 'tidal basin' effect of the cusped region enhances tidal flow (Appendix A2), and the best-fit value probably represents the mean value for the river. The method has been successfully applied to the Adelaide River and Daly Rivers, using D scaled proportionately to mean tidal velocities in each case, showing the general utility of the model.

APPENDIX A4: PARTICLE SIZE ANALYSIS OF SELECTED SAMPLES

Core/ probe	depth (cm)	Strati- graphic/ Morpho- strati- graphic unit*	Percentage by weight ø									
			1	2	3	4	5	6	7	8	9	>9
SAH11	540	LCS	0.1	0.4	1.3	14.4	25	15	5	3	4	32
	600	LCS	0.1	0.3	0.9	13.8	19	16	6	2	3	39
	660	LCS	0.1	0.3	1.0	16.3	23	14	4	3	4	34
SAH12	460	LCS	0.1	0.1	0.4	3.5	18	24	8	3	5	36
	520	LCS	0.1	-	0.4	3.9	21	21	7	4	4	33
	580	LCS		0.1	0.4	4.6	22	22	7	4	4	35
SAH40	700	LCS		0.1	0.5	10.9	23	14	7	4	2	38
	800	LCS	0.1	0.4	1.1	20.6	24	7	6	5	4	33
	900	LCS	0.1	0.3	0.9	9.8	13	15	9	8	3	42
	1000	LCS	0.1	0.2	1.0	8.4	13	17	9	4	4	43
	1100	LCS	0.1	0.7	1.5	13.6	16	15	9	4	2	38
	1200	LCS	0.1	0.4	1.0	14.5	16	14	9	5	2	38
	1300	LCS		0.3	0.9	15.2	21	16	5	5	2	34
	1400	LCS	0.2	0.7	1.5	12.0	21	14	7	3	1	39
SAH43	400	CF						1	4	6	11	78
	450	CF						1	2	5	15	77
	500	CF						1	3	9	28	59
	550	CF					1	1	3	12	21	62
	600	CF					2	1	4	5	5	83
SAH45	900	LCS		0.2	0.4	2.2	14	14	5	6	5	54
	1000	LCS		0.1	0.6	2.4	13	13	7	6	7	52
	1100	LCS		0.1	0.4	1.4	8	9	6	6	5	65
	1200	LCS	0.1	0.2	0.6	3.5	14	12	6	6	7	52
	1300	LCS		0.6	1.6	8.1	18	12	6	5	5	46
	1400	LCS	0.3	0.8	1.4	8.9	16	16	6	4	5	41
SAH17/652	560	MM				0.2	6.8	10.3	21	10	5	46
SAH17/644	400	MM			0.2	0.3	3.7	3.7	11	9	4	68
SAH18/686	420	MM			0.1	0.7	9	14	14	8	4	50
SAH36/911	245	MM				0.1	-	2.0	12	6	6	74
SAH38/921	260	LCS			0.2	18.2	15.2	2.5	2.5	2.5	5	53
SAH38/922	1100	LCS				16.7	20	10	10	3	3	37
SAH47/6	630	MM				0.1	3.5	-	10	3	10	73
SAH51/3	460	MM				1.1	4.9	1.5	10	3	5	74

APPENDIX A4, CONTINUED.

Core/ probe	depth (cm)	Strati- graphic/ Morpho- strati- graphic unit*	Percentage by weight Ø									
			1	2	3	4	5	6	7	8	9	>9
SAH54/5	1585	MM				0.2	3.1	-	10.5	2	6	78
SAH56/2	200	MM				0.1	3.3	10	16	4	7	60
SAH56/6	810	MM			0.1	0.1	1.8	4	5	11	8	69
SAH66/4	550	MM				0.1	1.1	3.2	8.5	11	9	67
SAH66/6	790	MM			0.3	2.6	4.4	7	6	16	12	52
SAH67/6	430	MM			0.1	0.8	4.4	6.1	13	19	15	42
SAH67/10	670	MM			0.1	0.1	1.6	7	15	17	12	46

* LCS Laminated channel sediments
 CF Channel fill (paleochannel unit)
 MM Mangrove mud

APPENDIX 5: SALT CONCENTRATION (KCl EQUIVALENTS), PARTS PER THOUSAND
(SEDIMENT DRY WEIGHT)

Depth (cm)	Coastal Plain		Estuarine funnel/sinuuous		Cuspate			Upstream
	SAH29	SAH30	SAH34	SAH50	SAH40	SAH45	SAH92	SAH71
0	110.8	0.8		4.2			8.7	19.1
10					5.7			
20	35.6	1.0		3.7	4.9		3.5	17.8
30					6.3			
40	50.3	2.9		3.6	7.2		5.3	18.1
50			39.3		8.0			
60	58.3	7.5		4.4	11.4		6.3	21.1
65						8.2		
70					11.0			
80	102.9	5.2		4.6	24.2		7.4	23.1
90					17.2			
100	99.8	3.8	43.8	4.9	13.7		8.8	25.8
110					13.5			
120	72.3	4.2		6.5	17.6		11.7	32.2
130					12.7	13.1		
140	79.0	4.8		8.9	12.4		12.1	36.7
150			52.0		11.4			
160	88.5	6.1		21.4	17.6		13.5	38.8
170			56.6		18.1			
180	91.6	7.2		23.5	25.0		13.6	46.6
190					20.2	22.9		
200	73.6	7.4		20.3	26.8		18.4	44.7
210					30.5			
220	66.9	6.3		19.7	27.5		20.6	39.4
230					24.7			
240	71.2	6.5	64.5	29.1	29.9		25.3	41.7
260	70.6	7.0		14.0		39.5	31.3	37.8
280	59.5	4.2		14.0			33.9	29.6
300	31.5	5.5		18.0			31.8	29.2
310			59.2		46.4			
320				20.1		27.4		
350	34.9							
370					43.8			
375			41.2					
390						25.3		
400	37.7	6.5						25.0
430					38.3			
450	43.6					29.1		
490					36.3			
500	75.8	5.8						21.7
520						30.2		
550	60.8				31.3	26.0		
580						25.8		
600	44.4	4.1			24.6			20.7
640						24.1		
650	41.0				36.7			
700	44.0	6.8				27.3		13.6
720					23.9			
750	39.4							11.5
800	43.1					21.6		
850	29.6							
880					27.4			
900	23.9					24.0		12.9
1000								11.5
1080					24.0			
1100								11.1
1200								12.9
1280					18.4			
1300								10.5
1390					28.7			
1460					2.8			

APPENDIX A6: POLLEN ANALYSIS OF MANGROVE HISTORY

Recent studies have shown that pollen analysis of vertical cores from Holocene intertidal deposits gives good evidence of the general composition of past mangrove communities (Chappell and Grindrod 1984, 1985; Grindrod and Rhodes 1984; Grindrod 1985). There are some reasons for expecting nearshore and intertidal deposits, including mangrove sediments, to be unpromising for pollen analysis. High-resolution pollen analysis of past vegetation classically is applied in bog, swamp, or lake deposits where effects of throughflow of water, turbulence, and bioturbation of the sediment are all small or negligible. These pollen-trapping sediments accumulate in basins which can be regarded as closed systems with minimal sediment mixing. These conditions seemingly are unlikely to apply in mangrove, intertidal, and estuarine floodplain situations where tidal and floodwater flows, often turbulent, apparently provide the means for extensive pollen redistribution and mixing. Bioturbation by crustaceans and molluscs is known to mix sediment to depths of 15-30 cm, particularly in mangroves, potentially confusing the record even further. The proof of any pudding, however, is in the eating. Results of the previous studies in north Queensland showed that pollen analysis of intertidal and supratidal deposits reveal quite faithfully the past plant communities of these environments.

Pollen analyses reported in Chapter 5.3.1 are part of a larger regional program investigating geomorphic controls of Holocene mangrove history by J. Grindrod and J. Chappell. The key to pollen analysis of mangrove, floodplain, and intertidal deposits lies in pollen signatures in modern surface sediments. This is preferable to pollen-rain assessment with pollen traps, as tides, floodwaters, and bioturbation almost certainly mix several years or even decades of sediment deposition, at the ground surface. Grindrod (1985) shows that pollen trap data are a poor guide to pollen signatures in surface sediments across the Princess Charlotte Bay chenier plain. Surface sediment samples from 6 transects across the plain were found to have similar pollen signatures at similar distances from the mangrove fringe. These results were used for interpreting the subsurface deposits, and similar sampling of the surface sediments in different mangrove and coastal environments provided Grindrod and Rhodes (1984) with the key for interpreting transgressive mangrove deposits at Hinchinbrook Island. Surface sediment sampling of transects across mangrove fringes in the South and West Alligator Rivers provides the key for interpreting pollen analysis of cores described in Chapter 5.3.1, as outlined by Chappell and Grindrod (1985).

All pollen analyses are done from extracts of 5 to 10 gm samples taken from surface sediments, cores, and auger holes. Standard extraction techniques are used, in the palynological laboratory in the Dept. of Biogeography and Geomorphology, R.S.Pac.S., ANU. All samples are counted to exceed a minimum of 100 pollen grains. Pollen taxa were identified into the categories shown in Figures 72 and 73, using standard reference collections in the Dept. of Biogeography and Geomorphology. Counting was done by Ms J. Williams and Ms J. Guppy.

APPENDIX A7 CARBONATE CONTENT OF SELECTED SAMPLES AS A PERCENTAGE
OF SEDIMENT DRY WEIGHT

Depth (cm)	Coastal Plain SAH29 SAH30	Sinuuous SAH50	Cusplate SAH40 SAH92	Upstream SAH71
20		nil		
100		nil		
120		8.4		
130	11.2			
140			nil	
160				nil
200		18.0		
230	10.1			
300		17.9	nil	nil trace
330	26.7			
400		16.2		
430	27.2			
500		13.2		
510	23.0			
600		7.0	nil	trace
630	19.8			
700		nil	nil	
720	9.9			
900	nil		3.3 0.3	
1150			trace	
1200				trace

APPENDIX A8: RADIOCARBON DATES

ANU No.	Field No.*	Depth (m)**	Material***	$\delta^{13}\text{C}$	$\delta^{14}\text{C}$	Age (Radiocarbon years B.P.)
S03777	SAH6/292	6.2	MF	-24	-339.0 \pm 20.6	3340 \pm 260
S03778	SAH1/30	4.7	MF	-24	-547.5 \pm 6.9	6390 \pm 130
S037779	SAH8/358	6.4	MF	-24	-228.7 \pm 34.6	2100 \pm 370
S03780	SAH7/323	3.4	MF	-24	-518.5 \pm 13.1	5890 \pm 230
S03781	SAH8/339	2.3	MF	-24	-207.2 \pm 27.9	1880 \pm 290
S03782	SAH7/310	1.8	MF	-24	-548.1 \pm 43.4	6400 \pm 820
S03783	SAH1/32	4.8	MF	-24	-555.6 \pm 36.4	6530 \pm 690
S03784	SAH6/258	2.0	MF	-24	-365.8 \pm 23.0	3680 \pm 300
SW3863B	SAH40/1	5.6	MF	-26.8	-568.1 \pm 6.2	6720 \pm 120
SW3864B	SAH42/1	2.7	MF	-28.9	-282.3 \pm 11.0	2600 \pm 130
SW3865B	SAH46/9	7.25	MF	-25.9	-586.3 \pm 4.7	7070 \pm 90
SW3866B	SAH46/4	3.75	MF	-27.2	-516.5 \pm 6.8	5800 \pm 120
SW3910B	SAH10/414	1.9	MW	-27.4	-164.2 \pm 7.8	1400 \pm 80
SW3911B	SAH37/917	12.6	MW	-26.0	-606.3 \pm 5.7	7470 \pm 120
SW3912B	SAH38/921	2.6	MW	-28.6	-392.8 \pm 7.6	3950 \pm 100
SW3913B	SAH38/922	11.0	MF	-28.9	-499.3 \pm 5.8	5490 \pm 100
SS3914K	SAH40/0	Surface	SM	-9.3	-38.6 \pm 6.9	570 \pm 60
SW3915B	SAH45/1	4.85	MW	-28.1	-322.1 \pm 10.4	3070 \pm 130
SW3916B	SAH19/730	6.1	MW	-27.9	-640.5 \pm 14.8	8170 \pm 340
SW3917B	SAH19/731	6.4	MF	-27.6	-576.4 \pm 10.2	6857 \pm 200
SW3918B	SAH35/907	2.45	MF	-25.1	-382.5 \pm 7.0	3830 \pm 90
SW3919B	SAH35/909	13.2	MF	-28.9	-591.1 \pm 7.5	7120 \pm 150
SP3920B	SAH36/913	13.6	MF	-19.0	-623.9 \pm 6.7	7950 \pm 150
SW3921B	SAH36/911	2.45	MW	-28.9	-4.3 \pm 21.5	99.6 \pm 2.2 \pm M
SW3922B	SAH56/2	2.0	MF	-28.5	-310.8 \pm 14.4	2930 \pm 170
SW3923B	SAH57/1	2.5	MW	-26.9	-534.4 \pm 7.3	6110 \pm 130
SW3924B	SAH58/2	3.7	MW	-24.9	-553.0 \pm 6.0	6470 \pm 110
SW3925B	SAH14/542	2.8	MF	-29.0	-200.0 \pm 15.9	1730 \pm 160
SW3927B	SAH15/585	3.7	MW	-26.6	-36.9 \pm 23.5	104.0 \pm 2.4 \pm M

APPENDIX A8, CONTINUED.

ANU No.	Field No.*	Depth (m)**	Material***	$\delta^{13}\text{C}$	$\delta^{14}\text{C}$	Age (Radiocarbon years B.P.)
SS3928K	SAH24/1	7.60	S	-3.9	-432.4 \pm 10.5	4900 \pm 150
SW3929	SAH28/1	2.45	MW	-25.9	-545.6 \pm 9.7	6320 \pm 170
SW3930B	SAH28/2	3.95	MW	-27.5	-542.6 \pm 7.3	6240 \pm 130
SW3931B	SAH25/1	6.7	MF	-28.2	-568.6 \pm 8.1	6700 \pm 150
SW3932B	SAH29/1	1.5	MW	-25.9	-28.5 \pm 7.5	2200 \pm 60
SW3933B	SAH29/2	8.15	MW	-27.2	-547.3 \pm 8.2	6330 \pm 150
SW3934	SAH13/528	7.2	MW	-26.1	-535.9 \pm 11.5	6150 \pm 200
SS3935K	SAH30/1	6.05	S	-3.5	-475.2 \pm 10.6	5530 \pm 170
SW3936B	80/1	MLW	MW	-27.3	-532.3 \pm 4.9	6070 \pm 90
SI3937K	80/2	MLW	FW	-13.2	-526.5 \pm 4.8	6200 \pm 80
SS3987K	80/4	Surface	SM	-6.6	2.9 \pm 7.5	280 \pm 60
SW3988B	80/3	MLW	MW	-27.1	-94.5 \pm 7.0	760 \pm 70
SP3989B	SAH62/2	4.6	MF	-28.2	-491.7 \pm 14.0	5390 \pm 230
SP3990B	SAH61/2	2.45	MF	-25.4	-522.9 \pm 5.4	5940 \pm 90
SS3991K	SAH61/1	0.3	S	-8.7	-384.5 \pm 7.5	4170 \pm 100
SS3992K	SAH61/0	Surface	SM	-10.8	-419.3 \pm 5.6	4600 \pm 80
SS3993K	SAH49/0	Surface	SM	-10.3	-357.4 \pm 5.5	3790 \pm 70
SS3994K	SAH54/0	Surface	SM	-9.7	-203.7 \pm 6.5	2080 \pm 70
SP3995B	SAH18/686	4.2	MF	-28.3	-313.2 \pm 16.5	2970 \pm 200
SP3996B	SAH20/806	2.1	MF	-24	-535.4 \pm 14.8	6170 \pm 260
SP3997B	SAH26/1	7.3	MF	-24	-566.0 \pm 18.2	6720 \pm 350
SP3998	SAH27/1	6.7	MF	-27.2	-556.4 \pm 10.8	6550 \pm 200
SP3999B	SAH48/2	1.9	MF	-27	-404.6 \pm 25.5	4170 \pm 350
SP4000B	SAH47/6	6.3	MF	-24	-500.5 \pm 12.5	5600 \pm 210
SP4001B	SAH47/15	11.7	MF	-24	-556.5 \pm 12.6	6540 \pm 240
SP4002	SAH51/3	4.6	MF	-27.2	-289.4 \pm 10.4	2710 \pm 120
SP4003	SAH52/2	2.4	MF	-27.0	-554.6 \pm 6.9	6470 \pm 130
SP4004	SAH60/4	7.3	MF	-25.7	-564.2 \pm 5.1	6660 \pm 100
SP4005	SAH60/2	4.6	MF	-25.9	-518.1 \pm 6.0	5850 \pm 100

APPENDIX A8, CONTINUED.

ANU No.	Field No.*	Depth (m)**	Material***	δ13C	δ14C	Age (Radiocarbon years B.P.)
SW4006	SAH60A/1	MLW	MW	-25.1	-507.5±5.1	5690±90
SP4007B	SAH32/900	2.45	MF	-27	-439.3±15.7	4620±240
SP4008B	SAH32/902	9.15	MF	-27.9	-573.3±7.8	6800±150
SP4009B	SAH52/3	3.65	MW	-28.9	-557.2±5.7	6480±90
SP4010B	SAH56/6	8.1	MF	-28.0	-571.6±4.4	6760±90
SP4011B	SAH59/2	4.6	MF	-27.1	-221.7±9.9	1980±110
SP4041	80/13	Surface	SM	-7.1	-238.7±6.7	2480±70
SS4042	80/11	Surface	SM	-8.5	-63.8±8.0	800±70
SS4043	80/10	Surface	SM	-2.4	-7.8±8.0	430±70
SS4044K	80/9	Surface	SM	-4.0	-21.4±7.3	520±60
SS4045	80/8	Surface	SM	-12.4	-298.3±6.2	3050±70
SS4046	80/7	Surface	SM	-10.4	-50.1±7.6	650±70
SS4047	80/6	Surface	SM	-10.2	-191.7±9.5	1950±100
SS4048	80/5	Surface	SM	-4.4	-43.4±7.8	690±70
SP4049B	SAH67/10	6.7	MF	-28.9	-573.5±5.2	6780±100
SP4050B	SAH67/6	4.3	MF	-27.5	-524.4±6.4	5930±110
SP4051B	SAH66/4	5.5	MF	-27.2	-543.2±5.7	6260±100
SP4052B	SAH65/4	2.45	MF	-27.6	-528.1±7.2	5990±130
SP4053B	SAH64/6	5.5	MF	-27.9	-540.7±7.7	7150±140
SP4054B	SAH63/12	10.7	MF	-27.5	-597.2±4.9	7260±100
SP4055B	SAH66/6	7.9	MF	-28.9	-569.7±7.3	6710±140
SP4056K	SAH44/4	3.7	SrCO ₃	-29.3	-224.2±20.5	1970±220
SP4057K	SAH37/917	12.6	SrCO ₃	-34.0	-528.7±14.0	5900±240
SP4058K	SAH37/916	3.5	SrCO ₃	-29	-462.0±13.5	4920±230
SP4059B	SAH17/652	5.6	MF	-27.9	-565.2±5.6	6640±110
SP4060B	SAH17/644	4.0	MF	-26.5	-487.9±11.2	5350±180
SP4061	SAH17/636	2.35	MF	-26.0	-461.2±5.3	4950±80
SP4062	SAH12/499	6.75	SrCO ₃	-18.1	-365.4±13.7	3770±180
SP4063	SAH12/498	6.75	MF	-16.6	-375.3±7.9	3920±110

Appendix A8, continued.

ANU No.	Field No.*	Depth (m)**	Material***	$\delta^{13}\text{C}$	$\delta^{14}\text{C}$	Age (Radiocarbon years B.P.)
SS4064K	SAH14/530	2.8	MF	-2.0	-194.4 \pm 8.8	2120 \pm 90
SC4065B	SAH67/3	2.5	MW	-26	-497.1 \pm 17.7	5510 \pm 300
SW4066B	SAH40/2	14.3	MW	-26.4	-568.4 \pm 4.6	6730 \pm 90
SS4067K	80/12	Surface	SM	-11.9	-264.5 \pm 6.1	2680 \pm 70
SP4113K	SAH41/6	14.0	MF	-23.7	-482.5 \pm 12.6	5310 \pm 200
SP4114K	SAH40/1	5.6	SrCO ₃	-5.6	-353.2 \pm 13.7	3460 \pm 170
SP4115K	SAH32/901	3.95	MF	-23.2	-515.3 \pm 16.4	5850 \pm 280
SP4116K	SAH13/516	4.7	SrCO ₃	-30.1	-525.6 \pm 11.2	5910 \pm 190
SP4117K	SAH11/460	3.0	SrCO ₃	-28.8	-301.8 \pm 13.2	2820 \pm 160
4121	SAH71/1	11.75	MF	-24	-147.0 \pm 14.2	1290 \pm 140
SW4122B	SAH69/1	2.1	MW	-26.9	-534.4 \pm 5.7	6110 \pm 100
SP4123K	SAH54/5	15.85	MF	-25.1	-626.8 \pm 15.7	7920 \pm 350
SP4124K	SAH21/833	4.0	MF	-25	-486.9 \pm 14.4	5360 \pm 230
SC4125B	SAH50/1	3.65	MW	-27.4	-506.0 \pm 6.9	5630 \pm 120
4126	SAH33/905	4.25	MF	-24	-360.6 \pm 40.7	3610 \pm 530
SP4128B	SAH75/4	4.6	MF	-26.8	-530.1 \pm 9.5	6040 \pm 170
SP4129B	SAH73/5	3.0	MF	-28.4	-560.6 \pm 7.7	6550 \pm 140
SP4130B	SAH73/3	1.5	MF	-28.7	-520.5 \pm 5.1	5850 \pm 90
SS4243K	SAH14/533	1.0	SH	-2.2	-180.5 \pm 6.4	1970 \pm 70
SP4244B	SAH22/1	8.5	MF	-28.4	-561.1 \pm 14.2	6560 \pm 270
SS4245K	SAH24/2	3.0	MF	-1	-295.3 \pm 12.5	3210 \pm 160
SP4246B	SAH24/3	7.7	MF	-25	-494.6 \pm 15.4	5480 \pm 250
SP4248	SAH25/3	6.7	MF	-25	-559.2 \pm 14.7	6580 \pm 280
SW4249B	SAH29/3	8.15	MW	-30.8	-551.4 \pm 14.0	6350 \pm 260
SS4250K	SAH30/2	4.10	SH	-3.4	-367.0 \pm 8.9	4030 \pm 120
SP4251B	SAH34/1	14.6	MF	-28.3	-576.7 \pm 6.0	6850 \pm 120
SP4252B	SAH44/11	25.0	MF	-28	-427.1 \pm 10.5	4430 \pm 150
SP4253K	SAH44/12	25.6	SrCC ₃	-19.1	-313.5 \pm 13.7	3120 \pm 160
SP4254K	SAH48/2	1.9	SrCO ₃	-27.7	-499.8 \pm 9.0	5520 \pm 150

Appendix A8, continued.

ANU No.	Field No.*	Depth (m)**	Material***	$\delta^{13}\text{C}$	$\delta^{14}\text{C}$	Age (Radiocarbon years B.P.)
SP4255K	SAH49/1	2.7	SrCO ₃	-28.5	-456.0 \pm 16.3	4840 \pm 250
SP4256K	SAH49/2	3.8	SrCO ₃	-29.8	-330.6 \pm 20.8	3150 \pm 260
SP4257B	SAH68/3	7.4	MF	-24.9	-604.3 \pm 4.7	7450 \pm 100
SW4259B	80/14	MLW	MW	-28.0	-490.8 \pm 5.0	5370 \pm 80
SW4260B	80/15	MLW	MW	-24.0	-115.7 \pm 6.9	1000 \pm 70
4622	BT10		MW	-24	-107.0 \pm 5.6	930 \pm 60
4623	BT7B		MW	-25.7	-563.1 \pm 5.1	6640 \pm 100
4624	BT7A		MW	-24	-482.7 \pm 6.8	5310 \pm 110
4625	BT3B		MW	-26.5	-494.8 \pm 5.3	5460 \pm 90
4626	BT3A		MW	-24.5	-499.0 \pm 4.9	5560 \pm 80
4627	BT3C		S	-12.2	-510.6 \pm 6.1	5950 \pm 100
4628	BT2		MW	-27.5	-220.6 \pm 7.6	1960 \pm 80
4629	BT1		MW	-28.1	-103.3 \pm 7.0	830 \pm 70
4630	EW6		MW	-24	-104.4 \pm 8.5	900 \pm 90
4631	EW5D		S	-10.1	-512.5 \pm 5.4	6010 \pm 90
4632	EW5		L			6550 \pm 100
4634	EW3		MW	-24	-103.9 \pm 5.1	900 \pm 60
4635	SAH128/15	11.2	SH	-3.5	-359.1 \pm 9.2	3930 \pm 120
4636	SAH122/3	2.65	MF			2280 \pm 270
4637	SAH117/7	9.5	MF			5110 \pm 120
4638	SAH114/6	9.6	MF			2880 \pm 100
4639	SAH109/3	2.6	MF			1790 \pm 190
4640	SAH101/9	6.5	MF			4390 \pm 130
4641	SAH100/3	2.9	MF			5580 \pm 200
4642	SAH87/4	1.6	MF			1170 \pm 390
4643	SAH85/5	2.7	MF			5990 \pm 120
4644	SAH83/14	5.0	MF			6490 \pm 250
4645	SAH83/9	2.7	MF			5000 \pm 370
4646	SAH109/6	7.0	MF			2350 \pm 100

Appendix A8, continued.

ANU No.	Field No.*	Depth (m)**	Material***	$\delta^{13}C$	$\delta^{14}C$	Age (Radiocarbon years B.P.)
4913	120/1	2.8	MF			4550 \pm 190
4914	120/2	5.3	MF			5870 \pm 110
4915	80/16	3.0	SM			6240 \pm 100
4916	120/3	7.0	MF			6870 \pm 150

* For location of cores see Figure 39; for location of other samples see table overleaf

** MLW - Mean low water

*** Material

MF - Mangrove fragments
 MW - Mangrove wood
 SM - Shell midden
 S - Shell
 SH - Shell hash
 SrCO₃ - Strontium carbonate
 L - Lobster

APPENDIX A8

Field No.	Location	Grid Reference
80/1	Stump at LWL	KG 297007
80/2	Stump at LWL	KG 297007
80/3	Stump on river bank, 0.1m AHD	KG 203121
80/4	Surface Shell	KG 213273
80/5	On chenier, surface	KG 245558
80/6	At SAH 9, surface	KG 193095
80/7	At SAH 11, surface	KG 217083
80/8	Midden on plains surface	KF 280983
80/9	At SAH 12, surface	KG 217083
80/10	On chenier, surface	KG 283570
80/11	At SAH 17, surface	KG 287526
80/12	Beside SAH 13, surface	KG 199090
80/13	On salt mudflat, surface	KG 160387
80/14	Stump, c. mean sea level	KG 262010
80/15	Stump exposed by erosion, southern end of island	KG 150470
80/16	Fossil shell midden at stump site, 0.6 m AHD	KG 214055
BT1	Log in laminated channel sediments, mid tide level	KG 198153
BT2	Log in laminated channel sediments, mid tide level	KG 183251
BT3A	Stump on river bank, LWL, west bank	KG 180139
BT3B	Log lying in river bank, 1 m above LWL	KG 180139
BT3C	Shells <u>in situ</u> at fossil site	KG 180139
BT7A	Stump, east bank, 2 m above LWL	KG 234101
BT7B	Stump, east bank, LWL	KG 234101
BT10	Stump, east bank, 1 m above LWL	KG 223077
EW3	Large stump at LWL, west bank	KG 167413
EW5C	Lobster at fossil site, west bank	KG 144314
EW5D	Shell at fossil site, west bank	KG 144314
EW6	Short core 16, mid tide level	KG 199207

APPENDIX A9: DETAILS OF DEPTH, ELEVATION w.r.t. AHD AND AGE OF SAMPLES
USED FOR SEA-LEVEL PLOT (FIGURE 69)

Field No.	Lab No.	Grid reference	Radiocarbon age + standard deviation C14 years B.P.	Elevation of sample w.r.t. A.H.D. + error (m)	Depth below ground surface (m)	Material
SAH 15/585	3927	KG 283575	Modern	-0.91±0.2	3.7	MW
SAH 14/542	3925	KG 283570	1730±160	+0.95±0.1	2.8	MW
SAH 8/339	3781	KG 216203	1880±290	+0.7*±0.4	2.3	FMF
SAH 8/358	3779	KG 216203	2100±370	-3.4*±0.4	6.4	FMF
SAH 29/1	3932	KG 283573	2200±60	+1.41±0.1	1.5	MW
SAH 42/1	3863	KG 088203	2600±130	+0.4±0.3	2.7	FMF
SAH 51/3	4002	KG 216206	2710±120	-0.66±0.2	4.0	FMF
SAH 56/2	3922	KG 158338	2930±170	+1.16±0.2	2.0	FMF
SAH 18/686	3995	KG 198345	2970±200	-1.31±0.2	4.2	VFMF
SAH 24/2	4245	KG 283567	3210±160	+0.82±0.3	4.0	FMF
SAH 33/905	4126	KG 212349	3610±530	-1.25±0.3	4.25	FMF
SAH 38/921	3912	KG 204088	3950±100	+0.30±0.3	2.7	MW
SAH 32/900	4007	KG 217350	4620±240	+0.30±0.2	2.45	FMF
SAH 1/32	3783	KG 215046	6530±90	-2.4±0.3	4.8	FMF
SAH 1/30	3778	KG 215046	6390±130	-2.3±0.3	4.7	FMF
SAH 7/313	3782	KG 141306	6400±820	+1.2*±0.3	1.8	FMF
SAH 7/323	3780	KG 141306	5890±230	-0.4*±0.3	3.4	FMF
SAH 13/516	4116	KG 199090	5910±190	-1.35±0.3	4.7	FMF
SAH 13/528	3934	KG 199090	6150±200	-3.85±0.2	7.2	MW
SAH 17/644	4060	KG 287526	6350±180	+0.11±0.3	3.9	FMF
SAH 17/652	4059	KG 287526	6640±110	-1.49±0.3	5.5	FMF
SAH 20/806	3996	KF 319792	6170±260	+1.1*±0.4	6.1	FMF
SAH 21/833	4124	KF 309936	5360±230	+0.82±0.3	4.0	FMF
SAH 25/1	3931	KG 285558	6700±150	-3.97±0.3	6.7	FMF
SAH 25/3	4248	KG 285558	6580±280	-3.97±0.3	6.7	FMF
SAH 26/1	3997	KG 285546	6720±350	-4.37±0.3	7.3	FMF
SAH 27/1	3998	KG 287527	6550±200	-3.70±0.3	6.7	FMF
SAH 28/1	3929	KG 289525	6320±170	+0.05±0.2	2.45	MW
SAH 28/2	3930	KG 289525	6240±130	-1.45±0.2	3.95	MW
SAH 29/2	3933	KG 283573	6330±150	-5.24±0.1	8.15	MW
SAH 32/901	4115	KG 217350	5850±280	-1.20±0.2	3.95	FMF
SAH 40/1	3863	KG 215085	6720±120	-2.40±0.2	5.6	FMF
SAH 46/4	3866	KG 136213	5800±120	-1.04±0.2	3.75	FMF
SAH 46/9	3865	KG 136213	7070±90	-4.54±0.2	7.25	FMF
SAH 47/6	4000	KG 185214	5600±210	-3.20*±0.3	6.3	FMF
SAH 50/1	4125	KG 137214	5630±120	-0.94±0.2	3.65	MW
SAH 52/2	4003	KG 220204	6470±130	+0.95±0.2	2.4	FMF
SAH 52/3	4009	KG 220204	6480±90	-0.35±0.2	3.7	MW
SAH 56/6	4010	KG 158338	6760±90	-4.94±0.2	8.1	FMF
SAH 57/1	3923	KG 149337	6110±130	+0.62±0.2	2.3	MW
SAH 58/2	3924	KG 139337	6470±110	-1.43±0.2	3.7	MW
SAH 60/2	4005	KG 178142	5850±100	-1.40±0.2	4.6	FMF
SAH 60/4	4004	KG 178142	6660±100	-3.80±0.2	7.0	FMF
SAH 61/2	3990	KG 165138	5940±90	+0.62±0.2	2.4	FMF
SAH 65/4	4052	KF 313987	5990±130	+1.06±0.2	2.45	MW/FMF
SAH 66/4	4051	KF 306986	6260±100	-1.94±0.2	5.5	FMF
SAH 66/6	4055	KF 306986	6710±140	-4.34±0.2	7.9	FMF
SAH 67/6	4050	KF 288926	5930±110	-1.32±0.2	4.3	FMF
SAH 67/10	4049	KF 288926	6780±100	-3.72±0.2	6.7	FMF
SAH 67/3a	4065	KF 288926	5510±300	+0.58±0.2	2.4	MW
SAH 68/3	4257	KF 293933	7450±100	-4.04±0.1	7.4	FMF
SAH 69/4	4122	KF 275970	6110±100	+0.9*±0.5	2.1	MW
SAH 73/3	4130	KF 270979	5850±90	+1.30±0.2	1.5	FMF
SAH 73/5	4129	KF 270979	6550±140	-0.30±0.2	3.1	FMF
SAH 75/4	4128	KF 294986	6040±170	+0.05±0.3	4.25	FMF
SAH 32/902	4008	KG 217350	6800±150	-6.40±0.2	9.15	FMF
SAH 63/12	4054	KF 303934	7260±100	-7.15±0.2	10.7	FMF
SAH 47/15	4001	KG 185214	6540±240	-8.6*±0.3	11.5	FMF
SAH 37/917	3911	KG 197088	7470±120	-9.35±0.3	12.6	MW
SAH 35/909	3919	KG 203181	7120±150	-10.0*±0.6	13.0	FMF
SAH 36/913	3920	KG 202277	7950±150	-11.0*±0.7	13.7	FMF
SAH 54/5	4123	KG 211197	7920±350	-12.8*±0.6	15.9	FMF
SAH 120/1	4913	KG 214055	4550±190	+0.84±0.1	2.8	FMF
SAH 120/2	4914	KG 214055	5870±110	-1.66±0.1	5.3	FMF
SAH 120/3	4916	KG 214055	6870±150	-3.36±0.1	7.0	FMF

* Estimated

MW - Mangrove wood
FMF - Fine mangrove fragments
VFMF - Very fine mangrove fragments

ANU NARU

Mangrove Monographs:

1. Coasts and Tidal Wetlands of the Australian Monsoon Region
edited by K.N. Bardsley, J.D.S. Davie & C.D. Woodroffe (1985).
2. Coastal Management in Northern Australia
edited by J.D.S. Davie, J.R. Hanley & B.C. Russell (1985)
3. Geomorphological Dynamics and Evolution of the South Alligator Tidal River and Plains, Northern Territory
C.D. Woodroffe, J.M.A. Chappell, B.G. Thom & E. Wallensky (1986)